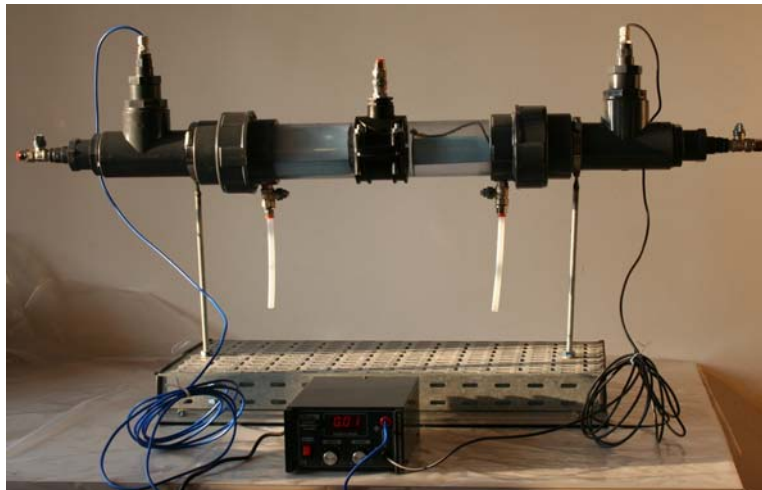


---

# Electrochemical Oxidation of Soils Contaminated with Organic Pollutants

Elisa Ferrarese



UNIVERSITÀ DEGLI STUDI DI TRENTO  
Dipartimento di Ingegneria Civile  
e Ambientale

2008

**Based on the Doctoral thesis in Environmental Engineering (XX cycle) defended in February 2008 at the Faculty of Engineering of the University of Trento.**

**Academic year 2006/2007**

**Supervisor: prof. Gianni Andreottola**

**On the cover: one of the experimental setups used in the study.**

**© Elisa Ferrarese (text and images, unless otherwise specified)**

**Direttore della collana: Alberto Bellin**

**Segreteria di redazione: Laura Martuscelli**

**Dipartimento di Ingegneria Civile e Ambientale**

**Università degli Studi di Trento, Italia**

**Aprile 2008**

**ISBN: 978-88-8443-245-2**

# Acknowledgments

Many people helped me to complete this research, directly or indirectly, and I am really grateful to all of them.

First of all, I would like to thank my supervisor Prof. Gianni Andreottola, who gave me the opportunity to have this valuable experience. His ideas and advices gave essential contributions to this work. I also wish to thank my co-supervisor Prof. Aldo Muntoni, who helped to assess this thesis and provided many kind and useful comments.

My thanks to my students and colleagues, particularly to those who shared a part of the work with me: Irina, Giorgio, Devendra and Elisa, for their collaboration, help and kindness. I have met many exceptional people in these years. Their friendly attitude always provided me good times and their brilliant skills were a great source of motivation for me.

Apart from my colleagues, I would like to thank my mother and my great friends, for being very patient with me during these years! I am particularly grateful to Mr. Martino Godenzi, who taught me that it is possible to build everything with very few tools! And, above all, I wish to thank Mr. Claudio Godenzi, who has always encouraged me, for his precious suggestions and great ideas, and for always being ready to help me when I was in need. This work would not have been possible without their special support.



# Table of Contents

<b>ABSTRACT.....</b>	<b>3</b>
<b>1 INTRODUCTION.....</b>	<b>7</b>
<b>2 ELECTROCHEMICAL REMEDIATION TECHNIQUES: THEORETICAL ASPECTS AND TECHNOLOGY STATUS.....</b>	<b>11</b>
2.1 DIRECT CURRENT TECHNOLOGIES.....	11
2.2 ELECTRICAL PROPERTIES OF FINE-GRAIN SOILS .....	13
2.2.1 <i>Clay mineralogy</i> .....	13
2.2.2 <i>Surface charge and double layer</i> .....	15
2.3 ELECTROCHEMICAL PROCESSES IN SOILS.....	20
2.3.1 <i>Transport phenomena</i> .....	21
2.3.1.1 Electroosmosis.....	21
2.3.1.2 Electromigration .....	25
2.3.1.3 Electrophoresis .....	26
2.3.1.4 Chemical diffusion.....	27
2.3.1.5 Electrokinetic transport.....	28
2.3.2 <i>Water electrolysis and changes in soil pH</i> .....	28
2.3.3 <i>Geochemical reactions in soils</i> .....	30
2.3.3.1 Redox reactions in soils .....	30
2.3.3.1.1 Electrochemically induced oxidation in aqueous systems.....	31
2.3.3.1.2 Electrochemically induced oxidation in soils.....	32
2.3.3.2 Other geochemical reactions.....	33
2.3.4 <i>The microconductor principle</i> .....	34
2.3.5 <i>Soil electrical conductivity</i> .....	39
2.4 APPLICATION OF DCTs FOR SOIL REMEDIATION.....	40

2.4.1	<i>Electrokinetic remediation</i> .....	40
2.4.1.1	Contaminant transport.....	41
2.4.1.2	Applicability and influence factors.....	43
2.4.1.3	Enhanced electrokinetic remediation.....	46
2.4.1.4	Benefits and limitations.....	52
2.4.1.5	Electrokinetic barriers.....	54
2.4.1.6	Different applications of the electrokinetic techniques.....	55
2.4.1.6.1	EK-PRB systems.....	55
2.4.1.6.2	Bioelectrokinetic remediation.....	56
2.4.2	<i>Electrokinetic-Fenton process</i> .....	57
2.4.2.1	Chemical oxidation.....	57
2.4.2.1.1	Hydrogen peroxide and Fenton's reagent.....	58
2.4.2.1.2	Ozone.....	60
2.4.2.1.3	Permanganate.....	61
2.4.2.1.4	Persulfate.....	62
2.4.2.1.5	In situ chemical oxidation.....	62
2.4.2.2	Electrokinetic-Fenton processes.....	63
2.4.3	<i>Electrochemical oxidation</i> .....	66
2.4.4	<i>Practical aspects of soil remediation by DCTs</i> .....	69
2.4.4.1	Electrode configuration and operating conditions.....	69
2.4.4.2	Cost analysis.....	72
2.4.5	<i>Current technology status and perspectives</i> .....	73
<b>3</b>	<b>MATERIALS AND METHODS.....</b>	<b>75</b>
3.1	RESEARCH SCHEME.....	75
3.2	EXPERIMENTAL SETUPS.....	76
3.2.1	<i>Setup 1</i> .....	78
3.2.2	<i>Setup 2</i> .....	81
3.3	EXPERIMENTAL PROCEDURES.....	85
3.4	ANALYTICAL METHODS.....	87
<b>4</b>	<b>ELECTROOXIDATION OF DIESEL FUEL-CONTAMINATED SOILS.....</b>	<b>93</b>
4.1	CONTAMINANTS.....	93

4.1.1	<i>Diesel fuel</i> .....	93
4.1.2	<i>Environmental behavior of diesel fuel</i> .....	95
4.1.3	<i>Diesel fuel remediation</i> .....	96
4.1.3.1	Biological methods .....	97
4.1.3.2	Physical and chemical methods .....	100
4.2	EXPERIMENTAL INVESTIGATION .....	103
4.2.1	<i>Research scheme</i> .....	103
4.2.2	<i>Materials</i> .....	105
4.2.2.1	Soils .....	105
4.2.2.2	Diesel fuel .....	108
4.3	RESULTS .....	109
4.3.1	<i>Tests on diesel-contaminated kaolin</i> .....	109
4.3.1.1	Test KAO.1 .....	109
4.3.1.2	Test KAO.2 .....	116
4.3.1.3	Test KAO.3 .....	123
4.3.1.4	Test KAO.4 .....	129
4.3.1.5	Test KAO.5 .....	135
4.3.1.6	Test KAO.6 .....	140
4.3.1.7	EK-Fenton test .....	141
4.3.2	<i>Tests on diesel-contaminated bentonite</i> .....	148
4.3.2.1	Test BEN.1 .....	148
4.3.2.2	Test BEN.2 .....	154
4.4	DISCUSSION .....	160
4.4.1	<i>Diesel Fuel Remediation</i> .....	160
4.4.1.1	Contaminant removal efficiencies .....	160
4.4.1.2	Influence of the applied voltage.....	162
4.4.1.3	Influence of the treatment duration.....	163
4.4.1.4	Influence of the soil mineralogy .....	165
4.4.2	<i>Electroosmotic flow</i> .....	166
4.4.3	<i>Contaminant transport</i> .....	167
4.4.4	<i>Soil pH profiles</i> .....	168
4.4.5	<i>Soil humidity and temperature</i> .....	171
4.4.6	<i>Electric current intensities</i> .....	173

4.4.7	<i>Energy consumption</i> .....	174
4.5	CONCLUSIONS .....	176
<b>5</b>	<b>FEASIBILITY STUDIES .....</b>	<b>179</b>
5.1	PAH-CONTAMINATED SEDIMENTS .....	179
5.1.1	<i>Contaminants</i> .....	180
5.1.1.1	Polycyclic aromatic hydrocarbons .....	180
5.1.1.2	PAH remediation.....	189
5.1.1.3	Contaminated site .....	191
5.1.2	<i>Experimental investigation</i> .....	195
5.1.2.1	Materials .....	195
5.1.2.2	Research scheme.....	196
5.1.3	<i>Results and Discussion</i> .....	197
5.1.3.1	Contaminant removal.....	197
5.1.3.1.1	Test PAH.1 .....	197
5.1.3.1.2	Tests PAH.2 and PAH.3 .....	200
5.1.3.2	Contaminant hydrophobicity and removal efficiency.....	207
5.1.3.3	Contaminant distribution and transport .....	211
5.1.3.4	pH profiles .....	216
5.1.3.5	Electroosmotic flow .....	217
5.1.3.6	Contaminant volatilization.....	218
5.1.3.7	By product formation.....	218
5.1.4	<i>Conclusions</i> .....	219
5.2	SILTY SOILS CONTAMINATED BY ORGANOLEAD COMPOUNDS .....	221
5.2.1	<i>Contaminants</i> .....	221
5.2.1.1	Tetraethyl lead and organolead compounds.....	221
5.2.1.2	Contaminated site .....	224
5.2.2	<i>Experimental investigation</i> .....	228
5.2.3	<i>Results and discussion</i> .....	229
5.2.4	<i>Conclusions</i> .....	238
5.3	CLAY CONTAMINATED BY LANDFILL LEACHATE .....	240
5.3.1	<i>Contaminants</i> .....	240
5.3.2	<i>Experimental investigation</i> .....	241



5.3.2.1	Research objectives.....	241
5.3.2.2	Materials .....	242
5.3.2.3	Experimental setup and procedures .....	243
5.3.3	<i>Results and discussion</i> .....	244
5.3.4	<i>Conclusions</i> .....	250
<b>6</b>	<b>CONCLUSIONS AND PERSPECTIVES.....</b>	<b>253</b>
	<b>REFERENCES.....</b>	<b>263</b>
	<b>PUBLICATIONS.....</b>	<b>281</b>



# List of Figures

Figure 2.1 – Schematic diagram of DCT application for soil remediation. ....	12
Figure 2.2 – Basic unit structures of phyllosilicates: silica tetrahedron and alumina octahedron (Mitchell, 1993).....	14
Figure 2.3 – Basic structural patterns of clay minerals (Mitchell, 1993). ....	14
Figure 2.4 – Schematic diagram of ions and potential distribution in the double layer near a clay particle surface (Mitchell, 1993; Alshawabkeh, 2001). ....	17
Figure 2.5 – Effect of the pore water pH on the surface charge of montmorillonite and kaolinite (Alshawabkeh, 2001).....	20
Figure 2.6 – Schematic representation of the electroosmosis phenomenon in soils (Coletta et al., 1997).....	22
Figure 2.7 – Schematic diagram of the electroosmotic flow across a soil under the influence of an electric field (Acar et al., 1995). ....	22
Figure 2.8 – Schematic representation of the electromigration phenomenon in soils.....	25
Figure 2.9 – Schematic representation of the electrophoresis phenomenon in soils.....	27
Figure 2.10 – Electrical circuit schematic model of soil current conduction in the presence of electrolyte solution and microconductors (Rahner et al., 2002). $R_p$ is the polarization resistance, $R_{MC}$ is the microconductor resistance, $R_E$ is the electrode resistance (usually negligible) and $R_{soil}$ is the resistance of the soil-pore water system.....	36
Figure 2.11 – Dependence of the soil electrolyte resistance ( $R_{soil}$ ) on the amount and type of added microconductors, with and without the addition of Fe(III) ions. The values were experimentally determined under aerated condition in presence of a base electrolyte ( $Fe_2(SO_4)_3$ ) at a pH of 3 (Rahner et al., 2002). ....	37
Figure 2.12 – Schematic diagram of an enhanced-electrokinetic remediation system. ....	51
Figure 2.13 – Schematic diagram of an electrokinetic barrier to prevent underground pollutant spreading. ....	54

---

Figure 2.14 – Schematic diagram of Lasagna™ EK-PRB systems: vertical configuration (on the left) and horizontal configuration on the right) (Ho et al., 1997). .....	56
Figure 2.15 – Schematic diagram of an in situ EK-Fenton process. ....	64
Figure 2.16 – Examples of possible electrode distribution for electrochemical soil treatment (Alshawabkeh, 2001). Each configuration generates an area of effective electric field and an area of ineffective electric field. ....	71
Figure 3.1 – Scheme of the test setup used in the experimental investigation. ....	77
Figure 3.2 – DC generator Stab AR50 used in the experimental investigation (providing a stabilized DC up to 15 V and up to 5 A). ....	77
Figure 3.3 – Two DC generators Mitek MICP 3005S-2 used in the experimental investigation (each one providing a stabilized DC up to 60 V and up to 5 A). ....	78
Figure 3.4 – Schematic diagram of Setup 1 used in the experimental investigation. ....	79
Figure 3.5 – Picture of the test device “Setup 1” used in the experimental investigation, here with DC generator Stab AR50. ....	79
Figure 3.6 – Components of the test device “Setup 1” used in the experimental investigation. ....	80
Figure 3.7 – Detail of Setup 1: reaction cell. The cell was provided with vents at the electrode compartment to allow gases to escape and fluid to flow out of the cell. Another valve was inserted above the soil cell to allow the dosage of process fluid, if necessary. ....	80
Figure 3.8 – Stainless steel holed electrode used in Setup 1. ....	80
Figure 3.9 – Schematic diagram of Setup 2 used in the experimental investigation. ....	82
Figure 3.10 – Three-dimensional diagram of Setup 2. In order to perform the experiments, the electrodes were placed in the reactor grooves, then the space across them was filled with the contaminated soil. The cell was provided with gas and liquid vents. ....	82
Figure 3.11 – Picture of the test device “Setup 2” used in the experimental investigation. ....	83
Figure 3.12 – Detail of Setup 2: reaction cell. ....	84
Figure 3.13 – Detail of the test Setup 2, including the reaction cell, tanks for the pore fluid collection at cathode compartments and the scale at the cathode side for the electroosmotic flow monitoring. ....	84
Figure 3.14 – Stainless steel electrodes used in Setup 2. ....	84
Figure 3.15 – Detail of the test Setup 2: soil specimen being treated with Setup 2. ....	85

---

Figure 3.16 – Digital multimeter ISO-Tech IDM 207 for continuous current monitoring.....	85
Figure 3.17 – Scheme of the treated specimen sectioning for sample analysis: a half of the treated specimen was sliced into 5 segments which were separately analyzed for contaminant concentrations, while the remaining part of the specimen was mixed to produce a homogenized sample.....	86
Figure 4.1 – Sample of kaolin used for the experimental investigation.....	106
Figure 4.2 – Sample of bentonite used for the experimental investigation.....	106
Figure 4.3 – XRD spectrum of the kaolin clay.....	108
Figure 4.4 – XRD spectrum of the bentonite clay.....	108
Figure 4.5 – Electric current recorded during test KAO.1.....	111
Figure 4.6 – Electroosmotic flow recorded during test KAO.1.....	111
Figure 4.7 – Soil pH profile recorded during test KAO.1.....	113
Figure 4.8 – Soil pH profile recorded at the beginning and at the end of test KAO.....	113
Figure 4.9 – Contaminant concentrations in the soil samples achieved during test KAO.1.....	114
Figure 4.10 – Contaminant removals achieved during test KAO.1.....	115
Figure 4.11 – Contaminant distribution along the soil specimen at the end of test KAO.1.....	116
Figure 4.12 – Soil humidity distribution along the soil specimen at the end of test KAO.1.....	116
Figure 4.13 – Electric current recorded during test KAO.2.....	118
Figure 4.14 – Electroosmotic flow recorded during test KAO.2.....	119
Figure 4.15 – Soil pH profile recorded during test KAO.2.....	120
Figure 4.16 – Soil pH profile recorded at the beginning and end of test KAO.2.....	120
Figure 4.17 – Contaminant concentrations in the soil samples achieved during test KAO.2.....	121
Figure 4.18 – Contaminant removals achieved during test KAO.2.....	121
Figure 4.19 – Contaminant distribution along the soil specimen at the end of test KAO.2.....	122
Figure 4.20 – Soil humidity distribution along the soil specimen at the end of test KAO.2.....	122
Figure 4.21 – Electric current recorded during test KAO.3.....	124

Figure 4.22 – Electroosmotic flow recorded during test KAO.3. ....	125
Figure 4.23 – Soil pH profile recorded during test KAO.3. ....	126
Figure 4.24 – Soil pH profile recorded at the beginning and at the end of test KAO.3. ....	126
Figure 4.25 – Contaminant concentrations recorded during test KAO.3. ....	127
Figure 4.26 – Contaminant removals achieved during test KAO.3: concentrations (a) and removal efficiencies (b). ....	127
Figure 4.27 – Contaminant distribution along the soil specimen at the end of test KAO.3. ....	128
Figure 4.28 – Soil humidity distribution along the soil specimen at the end of test KAO.3. ....	128
Figure 4.29 – Electric current recorded during test KAO.4. ....	130
Figure 4.30 – Electroosmotic flow recorded during test KAO.4. ....	131
Figure 4.31 – Soil pH profile recorded during test KAO.4. ....	131
Figure 4.32 – Soil pH profile recorded at the beginning and at the end of test KAO.4. ....	132
Figure 4.33 – Contaminant concentrations recorded during test KAO.4. ....	133
Figure 4.34 – Contaminant removals achieved during test KAO.4. ....	133
Figure 4.35 – Contaminant distribution along the soil specimen at the end of test KAO.4. ....	134
Figure 4.36 – Soil humidity distribution along the soil specimen at the end of test KAO.4. ....	134
Figure 4.37 – Electric current recorded during test KAO.5. ....	136
Figure 4.38 – Electroosmotic flow recorded during test KAO.5. ....	136
Figure 4.39 – Soil pH profile recorded at the beginning and at the end of test KAO.5. ....	137
Figure 4.40 – Contaminant concentrations recorded during test KAO.5. ....	138
Figure 4.41 – Contaminant removals achieved during test KAO.5. ....	138
Figure 4.42 – TOC distribution along the soil specimen at the end of test KAO.5. ....	139
Figure 4.43 – TPH distribution along the soil specimen at the end of test KAO.5. ....	139
Figure 4.44 – Electric current recorded during test KAO.HP. ....	143
Figure 4.45 – Soil pH profile recorded during test KAO.HP. ....	144
Figure 4.46 – Soil pH profile recorded at the beginning and at the end of test	

KAO.HP .....	144
Figure 4.47 – Contaminant concentrations recorded during test KAO.HP .....	145
Figure 4.48 – Contaminant removals achieved during test KAO.HP.....	146
Figure 4.49 – Comparison of the contaminant removal efficiencies achieved during tests KAO.2 (performed with a voltage gradient of 1 V/cm) and KAO.HP (performed with a voltage gradient of 1 V/cm and 3% hydrogen peroxide as anolyte solution).....	146
Figure 4.50 – TOC distribution along the soil specimen at the beginning and at the end of test KAO.HP.....	147
Figure 4.51 – TPH distribution along the soil specimen at the beginning and at the end of test KAO.HP.....	148
Figure 4.52 – Electric current recorded during test BEN.1.....	150
Figure 4.53 – Soil pH profile recorded during test BEN.1.....	151
Figure 4.54 – Soil pH profile at the beginning and at the end of test BEN.1.....	151
Figure 4.55 – Contaminant concentrations recorded during test BEN.1.....	152
Figure 4.56 – Contaminant removals achieved during test BEN.1.....	153
Figure 4.57 – Contaminant distribution along the soil specimen at the end of test BEN.1.....	154
Figure 4.58 – Soil humidity distribution along the soil specimen at the end of test BEN.1.....	154
Figure 4.59 – Electric current recorded during test BEN.2.....	156
Figure 4.60 – Soil pH profile recorded during test BEN.2.....	157
Figure 4.61 – Soil pH profile at the beginning and at the end of test BEN.2.....	157
Figure 4.62 – Contaminant removals achieved during test BEN.2: concentrations (a) and removal efficiencies (b).....	158
Figure 4.63 – Contaminant removals achieved during test BEN.2: concentrations (a) and removal efficiencies (b).....	158
Figure 4.64 – Contaminant distribution along the soil specimen at the end of test BEN.2.....	159
Figure 4.65 – Soil humidity distribution along the soil specimen at the end of test BEN.2.....	159
Figure 4.66 – Comparison of the TOC and TPH removal efficiencies achieved during the tests performed on diesel contaminated kaolin (a) and bentonite (b): influence of the applied voltage. ....	163

---

Figure 4.67 – Comparison of the TOC (a) and TPH (b) removal efficiencies achieved during tests KAO.1, KAO.2 and KAO.3, performed on diesel contaminated kaolin: influence of the treatment duration. ....	164
Figure 4.68 – Comparison of the TOC (a) and TPH (b) removal efficiencies achieved during tests BEN.1 and BEN.2, performed on diesel contaminated bentonite: influence of the treatment duration. ....	165
Figure 4.69 – Comparison of the TOC (a) and TPH (b) removals during the performed on diesel-contaminated soils: influence of the soil type. ....	166
Figure 4.70 – Distribution of the residual contaminant content (ratio of the final contaminant concentration $C$ and the initial contaminant concentration $C_0$ ) along the soil specimen for the tests performed on 10 cm long specimen of kaolin (a) and bentonite (b). ....	168
Figure 4.71 – pH profiles achieved at the beginning and at the end (28 days) of the tests performed on 10 cm long soil specimen of kaolin (a) and bentonite (b). ....	170
Figure 4.72 – Comparison of the residual contaminant distribution ( $C_0$ initial TPH concentration, $C$ final TPH concentration) and the soil pH profiles measured at the end (28 days) of tests KAO.1 (a), KAO.2 (b), KAO.3 (c) and KAO.4 (d) performed on diesel-contaminated kaolin. ....	171
Figure 4.73 – Comparison of the residual contaminant distribution ( $C_0$ initial TPH concentration, $C$ final TPH concentration) and the soil pH profiles measured at the end (28 days) of tests BEN.1 (a) and BEN.2 (b) performed on diesel-contaminated bentonite. ....	171
Figure 4.74 – Kaolin sample being treated with Setup 2: the anode can be seen on the right side of the sample, where the soil was compacted and changed to a yellow-orange color because of the formation of iron hydroxides from the soil natural iron content and from the electrode corrosion. ....	172
Figure 4.75 – Current intensities measured during the first hours in the tests performed on 10 cm long specimen of diesel-contaminated kaolin (a) (i.e. tests KAO.1, KAO.2, KAO.3, KAO.4) and bentonite (b) (i.e. tests BEN.1 and BEN.2) ....	174
Figure 5.1 – Polycyclic aromatic hydrocarbons. ....	181
Figure 5.2 – Contaminated sites in the northern suburbs of Trento (Italy): the picture indicates the Carbochimica site, location of a former coal tar production, now contaminated by PAHs and BTEX, and the rivers contaminated by PAHs. ....	193
Figure 5.3 – Picture of the “Roggia Campotrentino” or “Fossa Campotrentino” canal, in the northern suburbs of Trento (Italy), heavily contaminated by	

---



PAHs.....	193
Figure 5.4 – Map of the former industrial poles and of ditches, streams and rivers in the northern suburbs of Trento (Collins et al., 2005).....	194
Figure 5.5 – pH variations in the PAH-contaminated sediment samples after acid or base additions. The pH increase was obtained by adding 1 M NaOH to a sediment sample of 20 g having a volume of 50 mL; the pH decrease was obtained in the same way by adding 1 M HCl.....	196
Figure 5.6 – Results of test PAH.1: contaminant concentrations (a) and removal efficiencies (b).....	200
Figure 5.7 – Results of tests PAH.2: contaminant concentrations (a) and removal efficiencies (b).....	204
Figure 5.8 – Results of tests PAH.3: contaminant concentrations (a) and removal efficiencies (b).....	207
Figure 5.9 – Results of test PAH.1: removal efficiencies achieved as a function of PAH species (a) and of PAH octanol-water partition coefficient ( $K_{ow}$ ) (b). Since benzo(a)pyrene and benzo(k)fluoranthene are characterized by the same value of $K_{ow}$ , as well as phenanthrene and anthracene, in the plots only the results for benzo(a)pyrene and for phenanthrene are presented.....	209
Figure 5.10 – Results of tests PAH.2: removal efficiencies achieved as a function of PAH species (a) and of PAH octanol-water partition coefficient ( $K_{ow}$ ) (b). Since benzo(a)pyrene and benzo(k)fluoranthene are characterized by the same value of $K_{ow}$ , as well as phenanthrene and anthracene, in the plots only the results for benzo(a)pyrene and for phenanthrene are presented.....	210
Figure 5.11 – Results of tests PAH.3: removal efficiencies achieved as a function of PAH species (a) and of PAH octanol-water partition coefficient ( $K_{ow}$ ) (b). Since benzo(a)pyrene and benzo(k)fluoranthene are characterized by the same value of $K_{ow}$ , as well as phenanthrene and anthracene, in the plots only the results for benzo(a)pyrene and for phenanthrene are presented.....	211
Figure 5.12 – Concentrations of PAHs along the treated sample at different distances from the electrodes at the end of test PAH.1.....	212
Figure 5.13 – Concentrations of PAHs (a) and TOC (b) along the treated sample at different distances from the electrodes at the end of test PAH.2.....	214
Figure 5.14 – Concentrations of PAHs (a) and TOC (b) along the treated sample at different distances from the electrodes at the end of test PAH.3.....	216
Figure 5.15 – pH profile across the sediment specimen at the beginning and at the end of test PAH.1.....	217

---

Figure 5.16 – Electrodes (covered with filter papers) at the end of test PAH.1, lasting for 14 days. The cathode (on the right) showed a brown color due to the contact with the sediments, while the anode (on the left) showed an orange color because of the formation of iron hydroxides from the sediment natural iron content and from the anode corrosion. ....	217
Figure 5.17 – Molecular structure of tetraethyl lead (Collins et al., 2005). ....	222
Figure 5.18 – Overview of the northern suburbs of Trento and locations of the local contaminated sites: the SLOI site (61000 m <sup>2</sup> ), contaminated by organolead compounds, and the Carbochimica site (43000 m <sup>2</sup> ), contaminated by PAHs. ....	225
Figure 5.19 – Production process of TEL implemented at the SLOI factory (Collins et al., 2005). ....	227
Figure 5.20 – Layout of the SLOI production plant (Collins et al., 2005). ....	228
Figure 5.21 – Experimental setup used for the tests performed on the samples of soil contaminated by organolead compounds. ....	229
Figure 5.22 – Results of test TEL.1: pH profile along the soil specimen at the beginning and at the end of the electrochemical treatment. ....	231
Figure 5.23 – Results of test TEL.1: distribution of TEL (a), TREL (b), DEL (c), TOL (d) along the soil specimen at the end of the electrochemical treatment. ....	232
Figure 5.24 – Results of test TEL.1: distribution of total lead along the soil specimen at the end of the electrochemical treatment. ....	232
Figure 5.25 – Results of test TEL.2: pH profile along the soil specimen at the beginning and at the end of the electrochemical treatment. ....	234
Figure 5.26 – Results of test TEL.2: TOC distribution along the soil specimen at the end of the electrochemical treatment. ....	235
Figure 5.27 – Results of test TEL.2: distribution of TEL (a), TREL (b), DEL (c), TOL (d) along the soil specimen at the end of the electrochemical treatment. ....	235
Figure 5.28 – Results of test TEL.2: distribution of total lead along the soil specimen at the end of the electrochemical treatment. ....	236
Figure 5.29 – Possible application of electrooxidation as an innovative engineering solution for landfill bottom barrier. ....	242
Figure 5.30 – Results of tests LEA.1, LEA.2, LEA.3 and LEA.4: contaminant concentrations in original and final samples for ammonia nitrogen (a) and total nitrogen (b). ....	246
Figure 5.31 – Results of tests LEA.1, LEA.2, LEA.3 and LEA.4: TOC concentrations in original and final samples. ....	246

Figure 5.32 – Results of tests LEA.1, LEA.2, LEA.3 and LEA.4: removal efficiencies achieved for total nitrogen, ammonia and TOC during the tests performed. .... 247

Figure 5.33 – Results of test LEA.5: concentration of contaminant species (TOC, ammonia nitrogen and total nitrogen) measured during the process. .... 248

Figure 5.34 – pH profile along the soil specimen achieved at the end of test LEA.5. .... 249

Figure 5.35 – Ammonia nitrogen (a) and total nitrogen (b) concentrations along the soil specimen achieved at the end of test LEA.5. .... 249

Figure 5.36 – TOC concentrations along the soil specimen achieved at the end of test LEA.5. .... 250



# List of Tables

Table 2.1 – Case studies of electrooxidation for soil and sediment remediation. ....	68
Table 3.1 – List of the laboratory tests performed.....	76
Table 4.1 – List of the laboratory tests performed on diesel fuel-contaminated soils.....	104
Table 4.2 – Main features of the kaolin used for the experimental investigation: grain size, chemical compositions and main chemical parameters. ....	106
Table 4.3 – Main features of the bentonite used for the experimental investigation: grain size, mineralogical and chemical compositions and main chemical parameters. ....	107
Table 4.4 – Main features of test KAO.1.....	110
Table 4.5 – Results of the electric current and electroosmotic flow monitoring during test KAO.1.....	111
Table 4.6 – Soil pH profile during test KAO.1.....	112
Table 4.7 – Contaminant removals achieved during test KAO.1. ....	114
Table 4.8 – Contaminant and soil humidity distribution along the soil specimen at the end of test KAO.1.....	115
Table 4.9 – Main features of test KAO.2.....	117
Table 4.10 – Results of the electric current and electroosmotic flow monitoring during test KAO.2. ....	118
Table 4.11 – Soil pH profile during test KAO.2.....	119
Table 4.12 – Contaminant removals achieved during test KAO.2. ....	121
Table 4.13 – Contaminant and soil humidity distribution along the soil specimen at the end of test KAO.2.....	122
Table 4.14 – Main features of test KAO.3.....	123
Table 4.15 – Results of the electric current and electroosmotic flow monitoring during test KAO.3. ....	124
Table 4.16 – Soil pH profile during test KAO.3.....	125

---

Table 4.17 – Contaminant removals achieved during test KAO.3.....	127
Table 4.18 – Contaminant and soil humidity distribution along the soil specimen at the end of test KAO.3. ....	128
Table 4.19 – Main features of test KAO.4. ....	129
Table 4.20 – Results of the electric current and electroosmotic flow monitoring during test KAO.4.....	130
Table 4.21 – Soil pH profile during test KAO.4. ....	131
Table 4.22 – Contaminant removals achieved during test KAO.4.....	132
Table 4.23 – Contaminant and soil humidity distribution along the soil specimen at the end of test KAO.4. ....	134
Table 4.24 – Main features of test KAO.5. ....	135
Table 4.25 – Results of the electric current and electroosmotic flow monitoring during test KAO.5.....	135
Table 4.26 – Soil pH at the beginning and at the end of test KAO.5. ....	137
Table 4.27 – Contaminant concentration and removals achieved during test KAO.5. ....	137
Table 4.28 – Contaminant and soil humidity distributions along the soil specimen at the end of test KAO.5. ....	138
Table 4.29 – Contaminant and soil humidity distribution along the soil specimen at the end of test KAO.5. ....	140
Table 4.30 – Main features of test KAO.6. ....	140
Table 4.31 – Contaminant concentrations and losses during test KAO.6.....	141
Table 4.32 – Main features of test KAO.HP.....	142
Table 4.33 – Results of the electric current monitoring during test KAO.HP.....	143
Table 4.34 – Soil pH profile during test KAO.HP.....	144
Table 4.35 – Contaminant removals achieved during test KAO.HP. ....	145
Table 4.36 – Contaminant distribution along the soil specimen at the end of test KAO.HP. ....	147
Table 4.37 – Main features of test BEN.1. ....	149
Table 4.38 – Results of the electric current and electroosmotic flow monitoring during test BEN.1.....	150
Table 4.39 – Soil pH profile during test BEN.1. ....	151
Table 4.40 – Contaminant removals achieved during test BEN.1.....	152
Table 4.41 – Contaminant and soil humidity distribution along the soil specimen at	

---

the end of test BEN.1. ....	153
Table 4.42 – Main features of test BEN.2. ....	155
Table 4.43 – Results of the electric current and electroosmotic flow monitoring during test BEN.2. ....	155
Table 4.44 – Soil pH profile during test BEN.2. ....	156
Table 4.45 – Contaminant removals achieved during test BEN.2. ....	157
Table 4.46 – Contaminant and soil humidity distribution along the soil specimen at the end of test BEN.2. ....	159
Table 4.47 – Results of the tests performed on diesel-contaminated soils: TOC and TPH removals. ....	161
Table 4.48 – Estimated parameters for current function modelling during the tests performed. The current was modelled as an exponential function with a steady state component. In the table, $i_0$ is the initial current, $i_{ss}$ is the current at the steady state, $t$ is time and $\tau$ is a time constant. ....	175
Table 5.1 – Summary of the main physical and chemical properties of the PAHs considered in this study (Wild and Jones, 1995; Muller, 2002). ....	183
Table 5.2 – Physico-chemical properties of different PAH species (Wild and Jones, 1995; Muller, 2002). ....	184
Table 5.3 – Main features of the sediments of concern. ....	196
Table 5.4 – List of the laboratory tests performed on PAH-contaminated sediments. ....	197
Table 5.5 – Main features of test PAH.1. ....	198
Table 5.6 – Results of test PAH.1: contaminant concentrations and removal efficiencies. ....	199
Table 5.7 – Main features of test PAH.2. ....	201
Table 5.8 – Main features of test PAH.3. ....	201
Table 5.9 – Results of test PAH.2: contaminant concentrations in the original sample and 7, 14, 21 and 28 days after the beginning of the test. ....	202
Table 5.10 – Results of test PAH.2: contaminant removal efficiencies achieved 7, 14, 21 and 28 days after the beginning of the test. ....	203
Table 5.11 – Results of test PAH.3: contaminant concentrations in the original sample and 7, 14, 21 and 28 days after the beginning of the test. ....	205
Table 5.12 – Results of test PAH.3: contaminant removal efficiencies achieved 7, 14, 21 and 28 days after the beginning of the test. ....	206
Table 5.13 – Results of test PAH.1: contaminant concentrations and pH profile along	

---

the treated sample at different distances from the electrodes. ....	212
Table 5.14 – Results of test PAH.2: contaminant concentrations along the treated sample at different distances from the electrodes. ....	213
Table 5.15 – Results of test PAH.3: contaminant concentrations along the treated sample at different distances from the electrodes. ....	215
Table 5.16 – Main chemical and physical data of the organolead compounds considered in this stud (Collins et al., 2005). ....	223
Table 5.17 – Main features of test TEL.1. ....	229
Table 5.18 – Results of test TEL.1: contaminant concentrations in the soil samples and removal efficiencies. ....	230
Table 5.19 – Results of test TEL.1: contaminant and pH distribution along the soil specimen at the end of the experiment. ....	231
Table 5.20 – Main features of test TEL.2. ....	233
Table 5.21 – Results of test TEL.2: contaminant concentrations in the soil samples and removal efficiencies. ....	233
Table 5.22 – Results of test TEL.2: contaminant and pH distribution along the soil specimen at the end of the experiment. ....	234
Table 5.23 – Characteristics of the clay used in the experiments on leachate-contaminated soils. ....	243
Table 5.24 – List of the tests performed on the leachate-contaminated clay. Each test was performed on a soil specimen having length of 10 cm and a mass about 1 kg. ....	244
Table 5.25 – Main results of the one-day tests performed on the leachate-contaminated clay: concentration of TOC and nitrogen species in the original soil samples and in the final treated samples. ....	245
Table 5.26 – Current flowing across the soil specimen during test LEA.5. ....	247
Table 5.27 – Results of test LEA.5: concentration of contaminant species and removal efficiencies achieved during the process. ....	248



**Electrochemical Oxidation of Soils Contaminated  
with Organic Pollutants**



# Abstract

Electrochemical oxidation, or electrooxidation, is a branch of Direct Current Technologies (DCTs), which are innovative techniques for contaminated soil remediation, in which electrical fields are created in the polluted media by applying low-voltage direct currents (DC) to electrodes placed in the ground.

In recent years, DCTs have proven to be effective for the remediation of many organic and inorganic pollutants from soils and sediments. The main electrochemically induced phenomena include water electrolysis, electroosmosis, electromigration, electrophoresis, changes in soil pH and geochemical reactions. In particular, the electric fields can enhance oxidation and reduction reactions, able to mineralize the organic pollutants occurring in the target media. Moreover, in soils the presence of microconductors can promote redox reactions diffusively in the treated matrix and the production of hydrogen peroxide. Once hydrogen peroxide has been created, the soil natural iron content can catalyze the production of hydroxyl radicals, which are strong non-selective oxidant agents, capable of degrading most of organic pollutants. These recovery techniques seem particularly effective in saturated low permeability soils (like clays and silts), which are often very difficult to treat with conventional methods, because of their low permeability and their high sorption capacity. However, it is still not clear what processes play the most important roles in organic mineralization, and what factors can affect the treatment results.

The main objectives of this study were to evaluate the effectiveness of electrochemical oxidation for the remediation of different organic contaminants from various types of fine-grain soils and sediments. The research also aimed at assessing the best design parameters and the most important factors that can influence the system efficiency, as the applied voltage, the treatment duration and the soil mineralogy. A better knowledge of these processes will help to design more efficient and more effective remediation actions.

For these purposes, two one-dimensional experimental setups for bench-scale testing were assembled and several laboratory tests were performed. Each experimental device included a PVC electrochemical cell, a pair of plate stainless steel electrodes, a stabilized DC power supply, a multimeter for voltage and current monitoring and tanks for the pore

fluid collection at the electrode compartments. During each experiment, the contaminant removal was evaluated under a constant voltage gradient, ranging from 0.5 to 6 V/cm, for a fixed period of time, which arrived up to 4 weeks. No conditioning fluids were dosed to improve the soil conductivity or to enhance the contaminant transport (unenhanced electroremediation). Several parameters were investigated, including contaminant concentrations, changes in soil pH, electroosmotic flux, soil humidity and soil mineralogy. Moreover, at the end of each trial, the contaminant content in the soil sample was evaluated at different distances from the electrodes.

A systematic study was performed to assess the effectiveness of electrooxidation on fine-grain soils contaminated with diesel fuel. Diesel fuel is a mixture of aliphatic and aromatic hydrocarbons and was chosen to represent the environmental pollution due to spills of oil and other petroleum products, which are a frequent source of soil contamination and pose important environmental concerns. Two types of soils were considered in the study: a silty clay, mainly composed of kaolin, and a bentonite clay, mainly composed of montmorillonite, in order to assess the influence of different soil mineralogical compositions on the electrochemical processes. In addition, different feasibility studies were conducted to assess the applicability of electrooxidation for the remediation of river sediments contaminated by polycyclic aromatic hydrocarbons (PAHs), silty soils contaminated by organolead compounds, and clayey soils contaminated by landfill leachate.

According to the results achieved, electrochemical oxidation proved to be effective for the remediation of various types of aliphatic and aromatic hydrocarbons, as well as for ammonia and leachate organic contaminants, while a limited removal was encountered for the target organolead compounds. The tests performed on diesel-contaminated soils resulted in about 46-69% TOC (Total Organic Carbon) removal and in 66-87% TPH (Total Petroleum Hydrocarbons) removal after four-week treatments. Significant degradations of both TOC and ammonia (about 60%) were achieved in the leachate-contaminated clay after electrochemical processes of a few days. The results also showed that a very efficient remediation of PAH-contaminated sediments could be attained via electrochemical methods, with total PAH removals above 90%. These contaminant degradation efficiencies can be considered very satisfactory, since the remediation of fine-grain soils and sediments contaminated with hydrophobic and sorbed organic pollutants is very difficult to attain and represents up to now a challenging technical task.

Among the main influence factors, the applied voltage seems not to considerably affect the system efficiency, good results being achieved with specific voltages as low as 1 V/cm. Contaminant removals proved to significantly increase with process duration, with higher removal efficiencies being attained for treatments lasting for a few weeks, rather than for a few days. Final contaminant concentrations were found to be evenly distributed

across the treated sample. This indicated that the oxidation reactions occurred homogeneously within all the treated volume and not only close to the electrodes. Moreover, the electrokinetic transport of the target pollutants was negligible during the tests performed. The occurrence of the electroosmotic flux does not seem to be necessary to attain the pollutant mineralization and the processes seem to require low energy expenditures, being the current densities applied very low, about 0.01-1 mA/cm<sup>2</sup>. The buffer capacity of the soil affected the soil pH changes, by determining the tendency of the treated medium towards acidification or basification, though the remediation efficiency did not seem to be influenced by changes in the soil pH. On the opposite, the soil mineralogy, and in particular the iron content, seems to significantly affect the degradation process, the best results being achieved for soils with high metal concentrations. In this framework, the diffuse indirect oxidation is assumed to be the main mineralization pathway. The process occurs at the pore scale and includes the electrochemical production of hydrogen peroxide and the subsequent generation of hydroxyl radicals through Fenton-like reactions.

On the whole, electrochemical oxidation seems to be effectively and amenably applicable for the mineralization of many organics with low energy expenditures, especially in finest soils, like silts and clays, with significant iron contents.

*Keywords: remediation, electrochemical oxidation, electrooxidation, electro-Fenton, EK-Fenton, direct current technologies, soil, sediments, diesel, polycyclic aromatic hydrocarbons, tetraethyl lead, leachate.*



# Chapter 1

## Introduction

The remediation of fine-grain soils contaminated by sorbed organic pollutants is as far as today a challenging task. Despite the fact that many techniques have been developed for the recovery of soils, sediments and groundwater, it is still difficult to remove hydrophobic organic compounds (HOCs), which are often strongly sorbed onto soil particles. In particular, *in situ* remediation techniques deserve ever-growing attention in soil remediation, as they can offer important advantages, with no need to handle hazardous materials, low costs, and effortless management, in comparison with *ex situ* treatments.

Nevertheless, many *in situ* processes can hardly be applied to fine-grain and low-permeability soils, like silts and clays. In fact, the mobility of apolar organic pollutants is commonly limited in the subsurface, while the restricted mass transfer of chemical reactants, oxygen, water, and nutrients in fine-grain soils constrains the chemical and biological degradation processes. Moreover, many organics are recalcitrant to biological degradation, while the low permeability and high sorption capacity of silts and clays hinder the applicability of a number of chemical and physical remediation techniques, like soil flushing and chemical oxidation. On the other hand, conventional *ex situ* methods, as the disposal in sanitary landfill or incineration are discouraged, because they are very expensive and may represent a source of air pollution.

The same problems are encountered when treating contaminated sediments, which are commonly characterized by the presence of many different pollutants and by very high percentages of fine-grain particles, with a significant sorption capacity. As in industrialized countries huge amounts of sediments have been contaminated and are potentially dangerous to human health and to aquatic environment, the individuation of successful and cost-effective remediation techniques for such matrices is of a great practical interest.

For all these reasons, the selection of effective and efficient recovery methods for fine-grain soils and sediments is a complex technical issue, which may require the application of innovative remediation methods.

Electrochemical treatments are emerging technologies for the in situ or ex situ remediation of environmental matrices. Among the different electrochemical processes, Direct Current Technologies (DCTs) are remediation techniques that use low-voltage direct currents (DC) to degrade or remove pollutants.

At first, DCTs were used mainly for geotechnical purposes, as for soil and sediment dewatering and for slope stabilization. More recently, DCTs have been successfully applied for the recovery of metals, radionuclides, and polar organic pollutants from soils and sediments, the process being named as electrokinetic remediation. Furthermore, recent studies suggested that DCTs can be effectively used for the mineralization of many organics, including apolar and immobile compounds, with lower energy expenditures, if compared to traditional electrokinetic remediation methods. When the electric currents are used to degrade organic pollutants, the process is commonly named as electrochemical oxidation or electrooxidation. Empirical evidence indicated that the reaction rates are inversely proportional to grain size, thus these remediation techniques seem particularly effective in fine-grain matrices, like silts and clays, which are often the most difficult to recover with conventional methods.

The application of an electrical field to a soil has several complex physical and chemical effects that involve soil particles, pore water, and contaminants. The most important electrochemical phenomena are electrolysis, electroosmosis, electromigration, electrophoresis, changes in soil pH and geochemical reactions. During an electrochemical treatment, the soil-pore water system works as an electrochemical cell, in which oxidation and reduction reactions occur, water electrolysis providing the partners for redox reactions. Moreover, in soils the presence of microconductors allows the redox reactions to occur not only close the electrodes as in traditional electrochemical cells, but also simultaneously at all interfaces between the soil particles and the pore water, thus leading to a contaminant removal within the entire treated medium. In particular, during the electrochemical processes, hydrogen peroxide ( $H_2O_2$ ) can be produced as a result of redox reactions. Since soils commonly contain significant amounts of iron, once hydrogen peroxide has been created, hydroxyl radicals ( $\bullet OH$ ) can be produced, according to the catalytic Fenton's reaction. Hydroxyl radicals are strong non-selective oxidant agents, they are considered able to react with most of organic pollutants and they are regarded as the main responsible of the organic matter mineralization during the electrochemical processes.

To date there are several examples of application of electrochemical techniques to real cases of contamination in Europe and North America, but a good knowledge of the phenomena ruling the remediation processes has not been achieved yet. In particular, it is not clear what processes play the most important roles in organic mineralization, and what factors can affect the results of these techniques. Therefore, at the moment the calibration of the remediation actions is mainly based on empirical data and on the results of



preliminary field tests.

This study aimed at evaluating the effectiveness of electrochemical oxidation for the remediation of different organic pollutants from fine-grain soils and sediments, in case of unenhanced electroremediation, i.e. when the application of the electric field is not supported by the addition of conditioning fluid to adjust the soil pH, help the contaminant transport or to promote the soil conductivity.

Other objectives of this research were to assess the most important design parameters that can affect the system efficiency (as the applied voltage and the treatment duration) and to understand any link between contaminant removal efficiencies and macroscopic electrochemical phenomena, like the electroosmotic flux and the changes in soil pH. The influence of the soil type and mineralogical composition was also investigated.

To conduct the investigation, two one-dimensional experimental setups for bench scale testing were developed and several laboratory tests were performed. Each experimental setup included a PVC electrochemical cell, a pair of plate stainless steel electrodes, a stabilized DC power supply, a multimeter for voltage and current monitoring and tanks for the pore fluid collection at the electrode compartments. In each trial, a contaminated soil sample, having a mass ranging from one to several kilograms, was tested under a constant voltage gradient, ranging from 0.5 V/cm to 6 V/cm, for a fixed time, which arrived up to 4 weeks. All the tests performed were unenhanced, thus no conditioning fluid was dosed to improve soil conductivity or to promote contaminant migration. Several parameters were monitored during the tests, including the contaminant content, the electric current and voltage values, the evolution of the soil pH profiles, the occurrence of the electroosmotic flow and the soil moisture. At the end of each trial, the contaminant content in the soil sample was evaluated at different distances from the electrodes, in order to assess the extent of electrochemical reactions along the soil specimen and the possible contribution of the electrokinetic transport.

During the first phase of this experimental investigation, a systematic study was performed to assess the effects of electrooxidation on clayey soils contaminated with petroleum hydrocarbons, the ultimate goals being to assess the removal efficiencies attainable by the electrochemical methods and to individuate some guidelines for the most important design parameters.

The attention was focused on such pollutants because, among different environmental contaminants, oil is one of the most commonly occurring and threatening to the ecological balance of the affected areas. In fact, oil spills are a frequent source of pollution, which can endanger human health, devastate natural resources and affect the economy. Due to the high occurrence of these events, petroleum spills have contaminated many large areas and they are widely recognized as posing important environmental concerns.

Diesel fuel was chosen as a typical contaminant that can derive from spills of petroleum products. In order to evaluate the influence of the soil type and mineralogical composition on the effectiveness of the electrochemical processes, two types of soils were considered in the study: a silty clay, mainly composed of kaolin and a bentonite clay, mainly composed of montmorillonite.

During the second phase of the research, three feasibility studies were carried out to assess the applicability of electrochemical oxidation for the recovery of different environmental matrices, including rivers sediments contaminated by polycyclic aromatic hydrocarbons (PAHs), silty soils polluted by organolead pollutants, and clayey soils contaminated by landfill leachate. The first two cases regarded the “Trento Nord” contaminated site, one of the major contaminated sites in Italy, which was caused by the improper management of industrial activities carried out last century, and which still poses important environmental concerns. The third investigation focused on the application of electrooxidation for the recovery of a landfill clay barrier that has been contaminated by leachate. This technique could be of interest either for the recovery of old landfills, in case of a failure of the liner systems, or as an innovative engineering solution for new landfill plants.

This thesis describes the main results achieved during the experimental research and explains the conclusions that have arisen from the empirical evidence. The state of the art of the electrochemical remediation techniques is outlined in Chapter 2. The procedures used to conduct the research work are illustrated in Chapter 3, while the experimental investigations about the diesel fuel-contaminated soils and the other environmental matrices are described in Chapter 4 and Chapter 5 respectively. In conclusion, the main results and the evidence achieved during the investigation are summarized in Chapter 6.

## **Chapter 2**

# **Electrochemical remediation**

# **techniques: theoretical aspects and technology status**

## **2.1 Direct current technologies**

The base method for the current research, the electrochemical oxidation, is a branch of Direct Current Technologies (DCTs), which are remediation techniques for contaminated soils, in which an electrical field is created in the polluted medium by applying a low-voltage direct current (DC) to electrodes placed in the ground (Figure 2.1).

Electroosmotic technologies have been in use since the 1930s in construction sites, such as for soil, sediment, and sludge dewatering, and as slope stabilization techniques (Segall et al., 1980; Mitchell, 1993; Zorn et al., 2005b). In 1980, the water collected from electroosmotic flow was reported to contain high concentrations of metals organics and dissolved solids (Segall et al., 1980). This discovery promoted the application of the electrochemical techniques for soil remediation.

Among the environmental applications, at first DCTs were used mainly for the remediation of polar organic and inorganic pollutants from soil and groundwater, the method being named electrokinetic remediation. Many researches demonstrated the feasibility of electrokinetic remediation for many hazardous inorganic pollutants, as metals

and radionuclides (Acar and Alshwabkeh, 1993; Probst and Hicks, 1993; Acar et al., 1995; Wong et al., 1997; Puppala et al., 1997; Virkutyte et al., 2002; Chung and Kamon, 2005; Zhou et al., 2005; Reddy et al., 2006).

In recent years, researches have been developed about DCTs and their effectiveness in the removal of apolar organic pollutants, such as PAHs and chlorinated solvents, from soils and sediments (Doering et al., 2001a,b; Röhrs et al., 2002; Chung and Kamon, 2005; Reddy et al., 2006; Isosaari et al., 2007; Szpyrkowicz et al., 2007; Zheng et al., 2007). These studies seem to suggest that DCTs can be effectively used for the mineralization of many organics, with lower energy expenditures if compared to traditional electrokinetic methods (Acar et al., 1995).

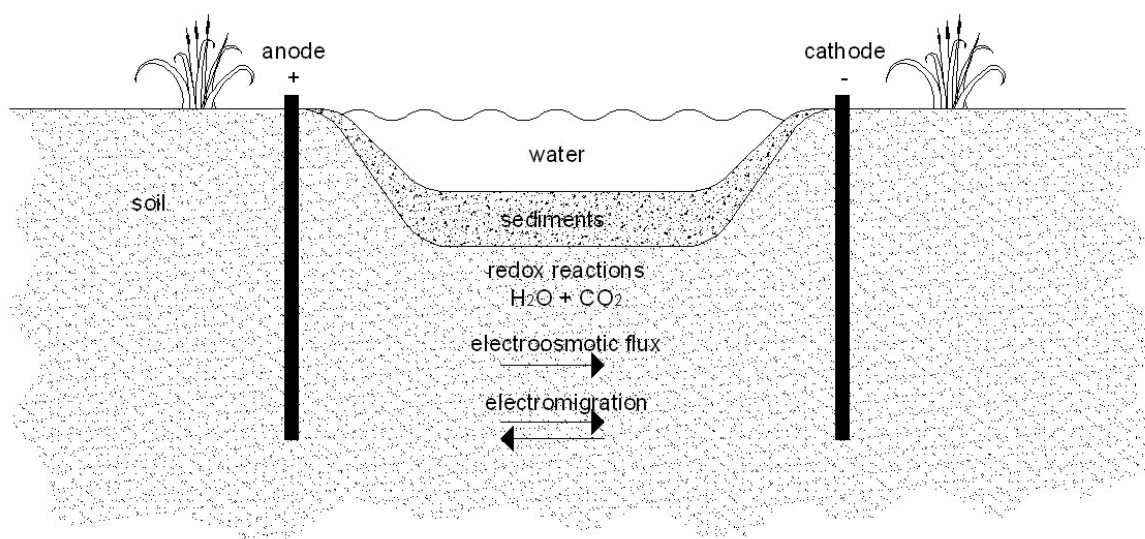


**Figure 2.1 – Schematic diagram of DCT application for soil remediation.**

Usually, for real scale in situ DCT applications, the applied electric current density is of the order of milliamperes per square centimeter ( $1 \text{ mA/cm}^2$ ) and the electric potential difference is on the order of a few volts per centimeter across the electrodes ( $1 \text{ V/cm}$ ) (Van Cauwenberghe, 1997; U.S. AEC, 2000; Chung and Kamon, 2005; Reddy et al., 2006).

Empirical evidence indicates that the reaction rates are inversely proportional to grain size (Acar et al., 1995), thus these remediation techniques are particularly effective in saturated low permeability soils (like clays and silts), which commonly pose the most important technical difficulties in contaminant remediation.

## 2.2 Electrical properties of fine-grain soils

### 2.2.1 Clay mineralogy

Clay minerals are common weathering products of rocks and soils, characterized by small-size particles with very high specific surfaces. They are composed of a layer structures, named as phyllosilicates. Each phyllosilicate is composed of unit cells which bond to each other form sheets and layers. Two different basic units can be found in phyllosilicates (Mitchell, 1993):

- A silica tetrahedron cell, where a silicon ion ( $\text{Si}^{4+}$ ) is tetrahedrally coordinated with four oxygen atoms to form a silica crystal. Each unit consists of a central four-coordinated atom (Si) surrounded by four oxygen atoms that, in turn, are linked with other nearby Si atoms.
- An octahedron cell, where aluminum ( $\text{Al}^{3+}$ ), iron or manganese ions are octahedrally coordinated with six oxygens or hydroxyl groups ( $\text{OH}^-$ ). Each unit consists of a central six-coordinated metallic atom (e.g.  $\text{Al}^{3+}$ ), surrounded by six hydroxyl groups that, in turn, are linked with other nearby metal atoms. In most of clay minerals, two-thirds of the octahedron cells are occupied by Al ions, thus forming alumina crystals; the other minerals contain Fe or Mg.

Silica tetrahedra (chemical composition  $\text{SiO}_4$ ) coordinate to each other to form tetrahedral sheets whose structure is characterized by the presence of planes of basal oxygen atoms at the boundaries of the sheets. Similarly, the alumina octahedra (chemical composition of  $\text{Al}_3(\text{OH})_6$ ) form octahedral layers whose structure is called gibbsite.

The basic structures of these clay minerals are shown in Figure 2.2.

In each clay particle, the sheets of tetrahedral (T) and octahedral (O) cells are stacked on each other to form layers. The silicon and aluminum layers are held together by share chemical bonds. The oxygen atoms and the hydroxyl groups serve as inter-unit linkages to hold the tetrahedral and octahedral sheets together. The tetrahedral and octahedral sheets can be organized under different conditions (Figure 2.3) (Mitchell, 1993):

- Two-sheet structure (T-O): kaolinite is the only mineral having this 1:1 structure, i.e. where one layer of tetrahedral cells is alternated with one layer of octahedral cells, with a repetitive T-O structure.
- Three-sheet structure (T-O-T): these minerals, including montmorillonite, which belongs to the smectite group, are characterized by a 2:1 structure,

where each mineral layer is composed by two sheets of tetrahedral cells divided by one sheet of octahedral cells. Thus, this structure is constituted by the repetition of Tetrahedron – Octahedron – Tetrahedron (TOT) layer. Under these conditions, water and exchangeable cations are commonly present in the interlayer.

- Four-sheet structure (T-O-T-O): as chlorites, which are similar to smectites, except of the presence of octahedral interlayers, which, unlike other sheets, do not have inter-unit linkages to bond them to the nearby tetrahedral sheets.

The most common clay types are kaolinite, illite and bentonite, which is a mixture of different clay minerals, mainly composed of montmorillonite (Mitchell, 1993).

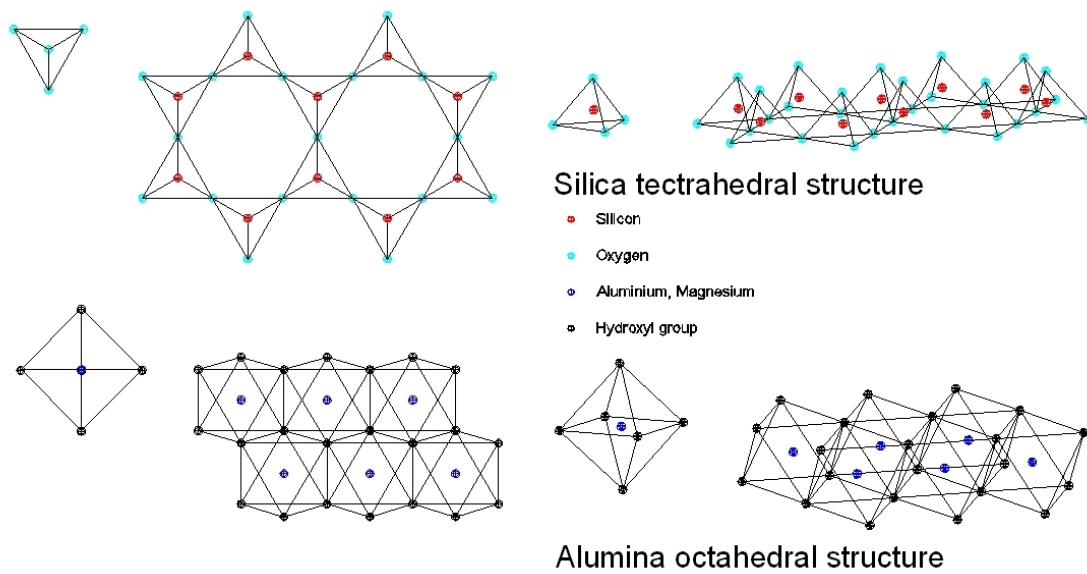


**Figure 2.2 – Basic unit structures of phyllosilicates: silica tetrahedron and alumina octahedron (Mitchell, 1993).**

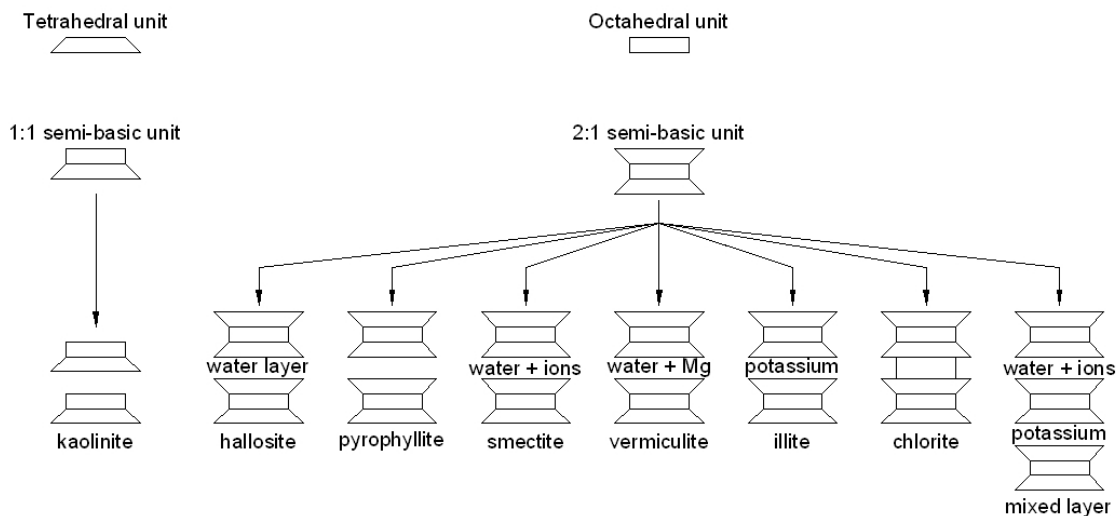


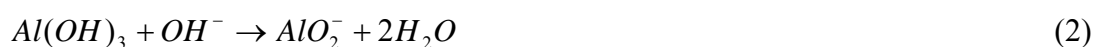
**Figure 2.3 – Basic structural patterns of clay minerals (Mitchell, 1993).**

### 2.2.2 Surface charge and double layer

Clay particles are generally characterized by negative surface charges, which are caused by the conditions occurring during the formation of the minerals themselves. The surface charge is mainly due to two phenomena: isomorphous substitution and broken bonds at the mineral boundaries (Mitchell, 1993; Acar et al., 1995).

The isomorphous substitution consists in the replacement of one ion by another of similar size in the crystal lattice of the mineral. Because of the isomorphous substitution, the ion in the middle of the tetrahedral or octahedral cell can be replaced by another having a lower valence, e.g.  $\text{Si}^{4+}$  in the tetrahedral cell can be replaced by  $\text{Al}^{3+}$ , or  $\text{Al}^{3+}$  in the tetrahedral cell can be replaced by Fe or Mg ions.

Broken bonds can occur as a result of surface imperfections, which are common especially at the boundaries of the clay minerals. In particular, at mineral boundaries ions like  $\text{Al}^{3+}$  and  $\text{Si}^{4+}$  can be exposed and the broken bonds cause them to interfere with the ions in the surrounding aqueous phase.  $\text{Al}^{3+}$  ions can complexate with  $\text{H}^+$  and  $\text{OH}^-$ , thus forming the following aluminol groups (Mitchell, 1993):



While  $\text{Si}^{4+}$  can complexate with  $\text{OH}^-$ , forming silanol groups.

Because of broken bonds and isomorphous substitution, all soil particles are characterized by an excess of negative surface charge. The total electrical charge per unit area (called surface charge density) increases as the specific surface (particles total surface area per unit weight) increases. Therefore, since the specific surface increases from gravel to sand, and then to silt and to clays, also the surface charge density increases in the following order (Acar et al., 1995):

gravel < sand < silt < clay

Furthermore, among different types of clays, the specific surface and the surface charge density increase from kaolinite to illite and then to montmorillonite, which is the clay mineral with the greatest specific surface.

This negative surface charge of soil particles results in attraction of cations close to particle surface, while anions remain in the pore fluid. The conjunction of the negative charged zone in soil particles surface and of the zone with excess of cations is called electrical double layer (Acar et al., 1995; Alshwabkeh, 2001).

Helmoltz introduced the earliest model of the electrical double layer, which was described as two parallel layers for charges (negative charge on the soil particle surface

and positive charges of cations in the pore fluid) at a certain distance, similarly to a condenser.

This model was then improved into the Gouy-Chapman theory of the diffuse double layer. According to this model, the cations near the soil particle surface are distributed in the pore water therefore their concentration is exponentially decreasing with distance from the particle, as a result of the counterbalancing effects of the electric forces that generate the double layer, and of the osmotic forces that tend to maintain an homogeneous charge distribution in the pore fluid.

Afterwards, Stern proposed an intermediate model, including two components:

- A rigid double layer (also named as Stern layer), including cations with a specific affinity towards the soil particle surface, which are adsorbed into the surface;
- A diffuse double layer, including cations in the pore water whose concentration exponentially decrease with distance from the particle surface.

According to this model, the excess of negative surface charge of the soil particle ( $\sigma_0$ ) is balanced by the excess of positive charge of both the Stern layer ( $\sigma_s$ ) and of the diffuse double layer ( $\sigma_d$ ):

$$\sigma_0 = \sigma_s + \sigma_d \quad (3)$$

A schematic diagram of the ions and potential distribution in the double layer is provided in Figure 2.4.



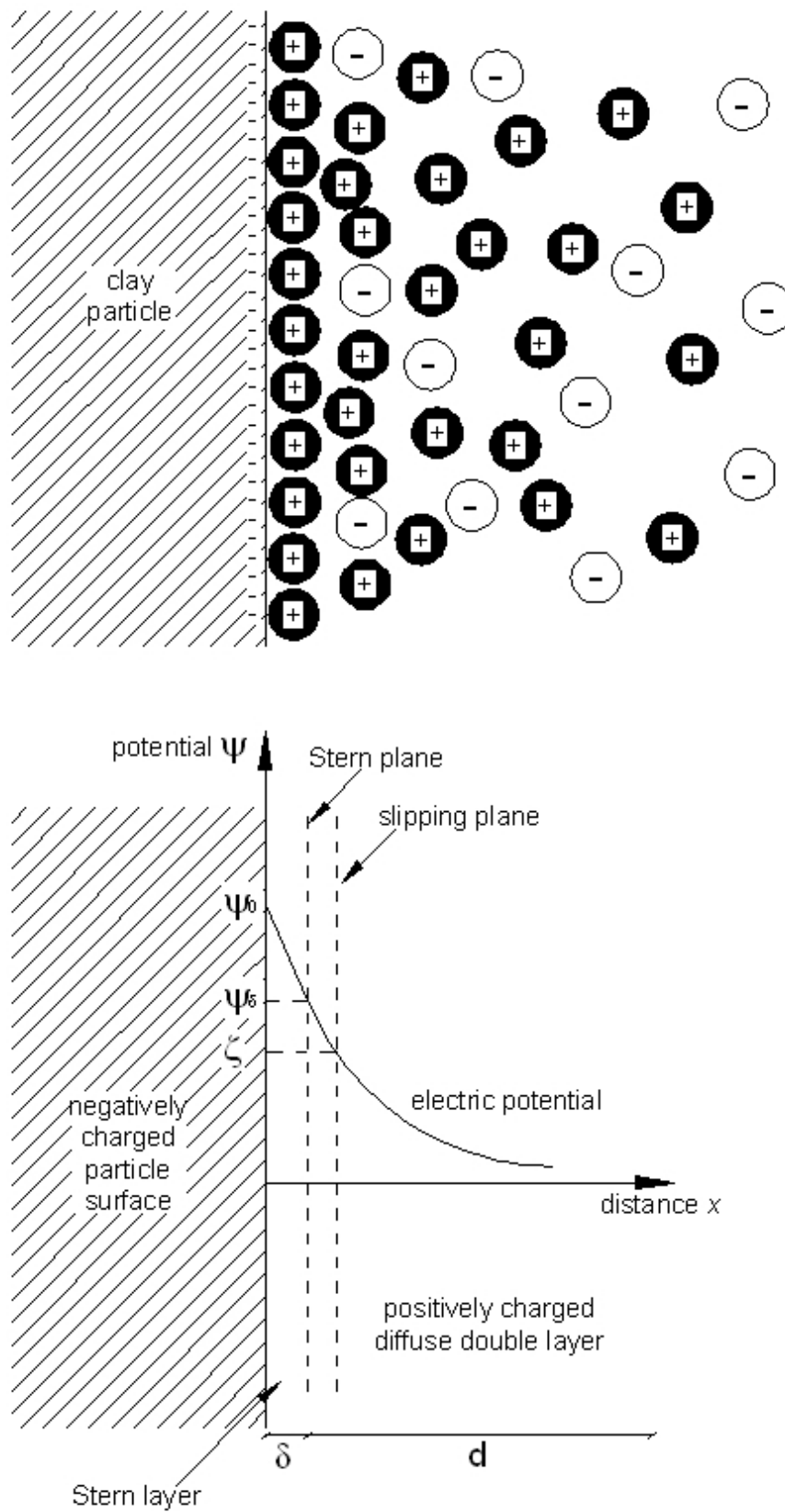


Figure 2.4 – Schematic diagram of ions and potential distribution in the double layer near a clay particle surface (Mitchell, 1993; Alshwabkeh, 2001).

The double layer is often expressed in terms of electrokinetic potential. In fact, the electric double layer causes a voltage difference (electrokinetic potential, usually of the order of millivolts) between the soil particle surface and the nearby pore fluid (Alshawabkeh, 2001).

The potential curve indicates the strength of the electrical force between the soil particle and the cations in the pore fluid at a certain distance from the soil particle surface.

The potential drop is almost linear in the Stern layer and exponential in the diffuse layer, following this function:

$$\begin{cases} \psi = \psi_{\delta} e^{-K(x-\delta)} \\ \psi_{\delta} < \psi_0 \end{cases} \quad (4)$$

Where:

$\psi_0$  is the potential on the surface of the soil particle;

$\psi_{\delta}$  is the potential on the Stern plane;

$1/K$  is the thickness of the diffuse double layer;

$x$  is the distance from the particle surface;

$\delta$  is the thickness of the Stern layer.

As can be seen from equation (4), the potential tends to zero as  $x \rightarrow \infty$ , i.e. where the pore fluid is not affected by the presence of the soil particle.

If the pore water is flowing in relation to the soil particle, a slip occurs between the inner part of the double layer, which moves jointly to the solid particle, and the external part of the double layer.

The value of the potential at the slip plane is known as the “zeta potential” ( $\zeta$ ). The zeta potential is used to quantify the magnitude of the electrical charge at the double layer; it is less than the surface potential of the particle, and it is often assumed to be nearly equal to the value of the potential at the Stern plane.

For saturated silts and clays, the zeta potential is typically negative, with values measured in the range of 10-100 mV (Virkutyte et al., 2002). However, depending on the chemical composition of the pore fluid, the zeta potential can change and under certain conditions it can be reverted and can become positive (Mitchell, 1993).

Because of the occurrence of the double layer, the clay particle-water-electrolyte system is usually considered to consist of three different zones (Alshawabkeh, 2001):

- The clay particle, with negatively charged surface;
- The double layer pore fluid, with excess positive charge;
- The free pore fluid, with zero net charge.

The thickness of the double layer depends on the charge density of the soil surface, on the ion concentration in the pore fluid, on the valence of the cations and on the

dielectric properties of the pore fluid (Acar et al., 1995). In particular, the thickness of the double layer increases if (Alshawabkeh, 2001):

- the cation valence decreases;
- the cation concentration of the pore fluid (electrolyte solution) increases;
- the pH increases;
- the cation size increases.

The amount of the exchangeable cations contained in the double layer required constitutes the cation exchange capacity (CEC) of the soil, which is expressed in milliequivalents (meq) per 100 grams of dry soil (Alshawabkeh, 2001).

The presence of the ionic double layer also affects the behavior of the pore fluid. In fact, when an ion is inserted in water, the water molecules near it tend to rotate and reorient themselves to face the ion with the pole having opposite charge, this resulting in the formation of a hydration shell. In sum, the negative surface charge of soil particles attracts cations close to particle surface, producing a double layer, and these cations cause the formation of a hydration shell.

The surface charge of the clay particles can highly affect the soil geochemical behavior. However, the density of the surface charge varies from mineral to mineral and is affected by the pore fluid environment and mainly by the pH of the pore water (Alshawabkeh, 2001).

For example, amorphous materials can coat the soil particles, thus modifying the feature of the surface. Amorphous materials (e.g. amorphous iron, alumina, etc.) include a core, mainly composed of silica tetrahedra, and a coating mainly composed by octahedral structures with Al and Fe ions. The surface of these materials is amphoteric, i.e. it can change its surface charge as a function of pH. In particular, when acid conditions (low pH) are created, an acid washing occurs on the amorphous materials, thus leading to a negative surface charge. On the other hand, under basic conditions (high pH) the amorphous materials exhibit positive surface charge.

Therefore, the soil surface charge may change as a result of pH changes. In particular, decreasing the pH reduces the value of the negative surface charge and may also cause surface charge reversal (Alshawabkeh, 2001), as shown in Figure 2.5.

In a similar way, also the organic matter that exists in soils often has functional groups, e.g. hydroxyl, carboxyl and phenolic. These functional groups have the ability to protonate or deprotonate, depending on the pH of the pore water, which makes the organic matter to change the electric charge according to the pH conditions (Yu and Neretnieks, 1997).

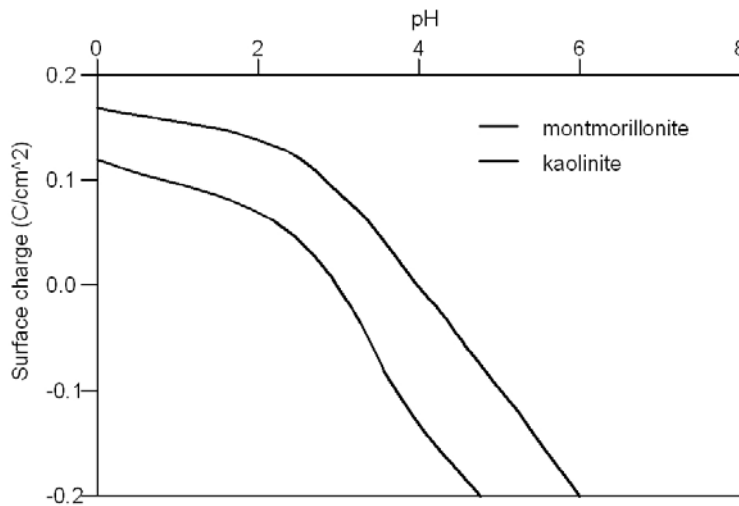


Figure 2.5 – Effect of the pore water pH on the surface charge of montmorillonite and kaolinite (Alshawabkeh, 2001).

## 2.3 Electrochemical processes in soils

The application of an electrical field to a soil environment involves a number of complex physical and chemical effects. The most important electrochemical phenomena are (Probstein and Hicks, 1993; Acar et al., 1995; Puppala et al., 1997; U.S. AEC, 2000; Rahner et al., 2002; Alshawabkeh et al., 2004; Chung and Kamon, 2005; Reddy et al., 2006):

- Electrolysis;
- Electroosmosis;
- Electromigration;
- Electrophoresis;
- Changes in soil pH;
- Geochemical reactions.

From the soil remediation point of view, the processes induced by electric field can be distinguished into two categories: electrokinetic transport (including electroosmosis, electromigration and electrophoresis), and electrochemically induced chemical reactions within the soil matrix, responsible for the destruction of immobile organic contaminants. All these processes occur concurrently and each one can influence the others. For example, water electrolysis causes important changes in soil pH, which affects the dissolution equilibrium of metals and salts, which can migrate under the influence of the electric field, while the ionic concentration of the pore fluid determines the rate of the electroosmotic flow.

The main processes involved in the electrokinetic remediation are described in detail as follows.

### **2.3.1 Transport phenomena**

When an electric field is created across a soil volume, it provides a driving force that may induce a mass movement of particles, similar to the effect of other driving forces, such as pressure gradient, concentration gradient and thermal gradient. In particular, the application of an electric field causes three main transport phenomena in soils (Acar and Alshawabkeh, 1993; Probstein and Hicks, 1993; Acar et al., 1995; Li et al., 1996; Yu and Neretnieks, 1996; Wong et al., 1997):

- Electroosmosis;
- Electromigration;
- Electrophoresis.

All these electrokinetic phenomena are highly influenced by the surface charge densities of the soil particles, and therefore by the soil mineralogical composition.

#### *2.3.1.1 Electroosmosis*

Electroosmosis is a bulk transport of water, which flows through the soil as a result of the applied electrical field (Probstein and Hicks, 1993; Acar et al., 1995; Yu and Neretnieks, 1996; Wong et al., 1997; Coletta et al., 1997; U.S. AEC, 2000; Virkutyte et al., 2002; Chung and Kamon, 2005; Reddy et al., 2006; Lynch et al., 2007).

The fluid migration occurs mostly from the anode to the cathode, due to the predominance of a negative charge on the soil particle surfaces. In fact, the electroosmotic flow is caused by the fact that when an electric field is applied to a soil, the excess of cations close to soil particles surface (double layer) tend to move towards the cathode. The movement of these ions, and of the water molecules associated with these species (hydration shells), imparts a net strain on the pore fluid surrounding the hydrations shell. This strain is transformed into a shear force because of the viscosity of the pore fluid. In sum, as there is usually an excess of cations close to soil particles, the electric fields leads to a net force towards the cathode which results in a pore fluid flux in this direction (Acar et al., 1995).

Hence, the electric field causes the pore fluid to flow from the anode compartment to the cathode, producing a flux and forcing the water table to arise in the cathode compartment (Acar et al., 1995).

The electroosmotic flow ceases when the counteracting flow, due to the hydraulic gradient between the anode and the cathode compartments, equals the electroosmotic force, or when the soil surface potential approaches to zero as a result of changes in the pore fluid composition (Acar et al., 1995)

The electroosmotic flow phenomenon is conceptualized in Figure 2.6 and Figure 2.7.

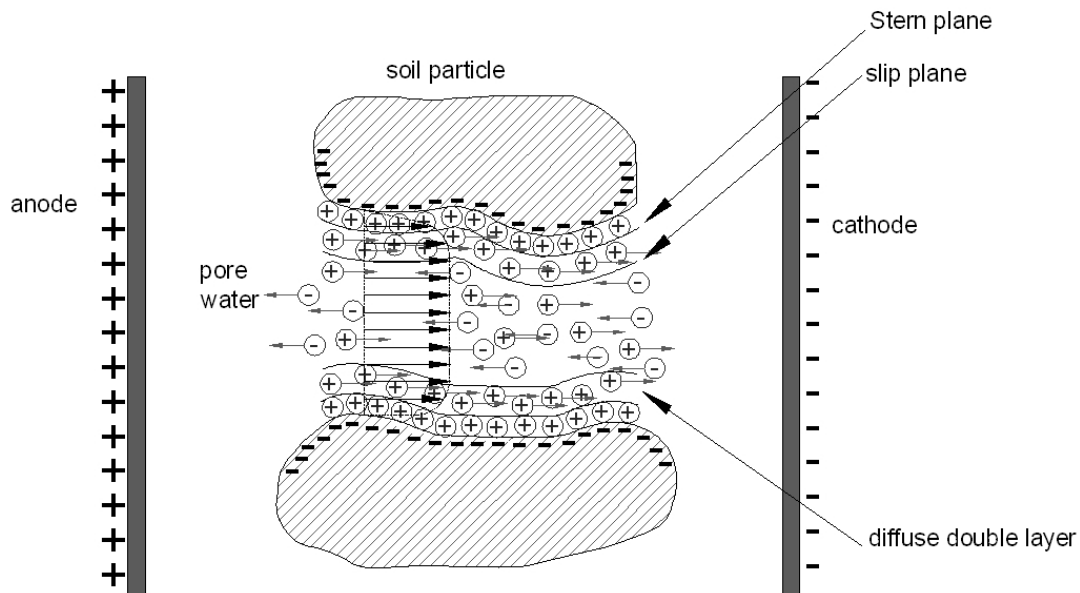


Figure 2.6 – Schematic representation of the electroosmosis phenomenon in soils (Coletta et al., 1997).

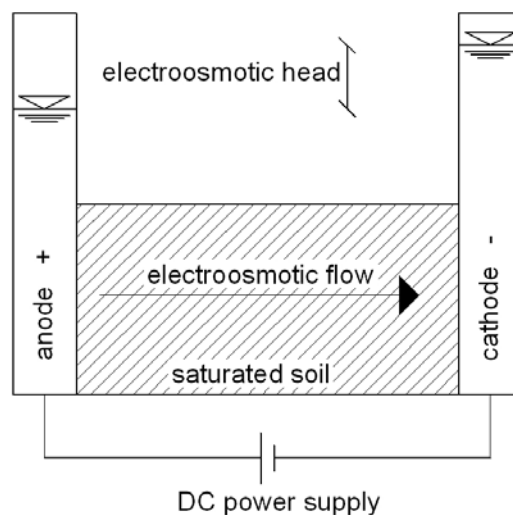


Figure 2.7 – Schematic diagram of the electroosmotic flow across a soil under the influence of an electric field (Acar et al., 1995).

Usually, the electroosmotic flow can be appreciated only in very fine-grain soils,

like clays and silts, with rates about 10 cm/day (Wong et al., 1997), depending on the electric field and on the soil features. In fact, the electroosmotic flow rate increases with the strength of the electric field (Alshwabkeh, 2001; Kim et al., 2006). Moreover, since the electroosmotic flow is determined by the occurrence of an excess of cations in the double layer, it will be influenced by its characteristics, and primarily by its thickness. A wider diffuse double layer will cause a more strong and more uniform strain field, which, in turn, will cause more electroosmotic flow. In other words, the electroosmotic flow rate increases with the increase of negative zeta potential (Acar et al., 1995; Alshwabkeh, 2001; Kim et al., 2006).

Furthermore, as previously discusses, the thickness of the double layer depends on the charge density of the soil surface, on the ions concentration in the pore fluid, on the valence of the cations and on the dielectric properties of the pore fluid (Acar et al., 1995). Therefore, when the ionic concentration in the pore fluid increases, the thickness of the diffuse double layer decreases, and consequently the extent of the strain filed (causing the pore fluid flow) decreases too. As a result, the electroosmotic flux decreases too (Acar et al., 1995; Alshwabkeh, 2001).

In general, the electroosmotic flux will be maximized (approximately about  $10^{-4}$  cm/s under an electric gradient of 1 V/cm) (Acar et al., 1995; Virkutyte et al., 2002):

- In low activity clays (clays activity is defined as the plasticity index divided by the percent of particles under the 2  $\mu\text{m}$  size).
- At high water contents and low electrolyte concentrations, since the thickness of the diffuse double layer is maximum when the pore fluid conductivity is minimized (order of magnitude of 100  $\mu\text{S}/\text{cm}$  or less).

The electroosmotic flow is also significantly affected by the soil pH. In fact, it is known that when the electrolyte concentration is high and the pH of the pore fluid is low, the surface charge of the soil particles may be reverted, e.g. because of the effect of amphoteric materials. This can cause the electroosmotic flux to start flowing towards the anode (Eykholt and Daniel, 1991; Acar et al., 1995; Yang and Lin, 1998; Alshwabkeh, 2001). Therefore, a decrease in the pH of the pore fluid during an electrochemical treatment causes a decrease in the electroosmotic flow rate, due to a decrease in the zeta potential. An isoelectric point (or point of zero charge, PZC) can be individuated, corresponding to a zeta potential equal to zero (i.e. to zero net surface charge of the soil particles) and to the occurrence of no electroosmotic flow. If the pH undergoes a further decrease, a net positive surface charge can be created on soil particle, and the electroosmotic flow can be reverted, thus starting to flow towards the anode.

In fluid dynamics, a generic flux of a fluid through a porous medium, caused by a hydraulic gradient, is given by the Darcy's Law:

$$Q_h = k_h \cdot i_h \cdot S \quad (5)$$

Where:

$Q_h$  (m<sup>3</sup>/s) is the hydraulic flux;

$k_h$  (m/s) is the coefficient of hydraulic conductivity of the soil;

$i_h$  is the hydraulic gradient (m/m);

$S$  (m<sup>2</sup>) is the cross-sectional area to flow.

Similarly, the electroosmotic flow caused by the application of a voltage gradient is given by (Chung and Kang, 1999; Alshawabkeh, 2001; Virkutyte et al., 2002; De Battisti, 2006; Lynch et al., 2007):

$$Q_e = k_e \cdot i_e \cdot A \quad (6)$$

Where:

$Q_e$  (m<sup>3</sup>/s) is the electroosmotic flux;

$k_e$  (m<sup>2</sup>/Vs) is the coefficient of electroosmotic conductivity of the soil;

$i_e$  (V/m) is the applied voltage gradient;

$A$  (m<sup>2</sup>) is the cross-section of the treated volume (i.e. where the electric field is established).

Therefore, the rate of electroosmotic flow is mainly defined by the coefficient of electroosmotic conductivity of the soil ( $k_e$ ), which is a measure of the fluid flux per unit area of the soil per unit electric gradient. According to the Helmholtz-Smoluchowski theory, the value of  $k_e$  is a function of the zeta potential of the soil-pore fluid interface, of the viscosity of the pore fluid, of the soil porosity and tortuosity, and soil electrical permittivity (Casagrande, 1949; Probstein and Hicks, 1993, Alshawabkeh, 2001; De Battisti et al., 2006):

$$k_e = -\frac{\varepsilon_0 \cdot D_k \cdot \zeta}{\eta} \cdot n \cdot \tau \quad (7)$$

Where:

$\zeta$  (V) is the zeta potential of the soil-pore fluid interface;

$\eta$  (Ns/m<sup>2</sup>) is the viscosity of the pore fluid;

$n$  (-) is the soil porosity;

$\varepsilon_0$  (F/m) is the vacuum electrical permittivity;

$D_k$  (-) is the dielectric constant of the pore fluid;

$\tau$  (-) is the soil tortuosity.

Moreover, the electroosmotic flow rate can be also expressed as follows (Chung and Kang, 1999):

$$Q_e = k_i \cdot I \quad (8)$$

Where:

$k_i$  (m<sup>3</sup>/As) is the coefficient of the water transport efficiency;



I (A) is the current flowing.

It must be noted that  $k_e$  is time-dependent, as it is affected by the chemistry of the pore water (Alshawabkeh, 2001). However, generally the coefficients of electroosmotic conductivity are in the range of  $10^{-9}$ - $10^{-10}$   $m^2/Vs$  (Mitchell, 1993; Alshawabkeh, 2001).

### 2.3.1.2 Electromigration

The second transport mechanism generated by the voltage gradient, electromigration, is the movement of ions in the pore solution under the influence of an electric field. Positive ions (cations) migrate towards the cathode while negative ions (anions) are transported towards the anode because of Lorentz force (Figure 2.8). Because of electromigration ions tend to concentrate near the opposite charged electrode (Acar et al., 1995; Yu and Neretnieks, 1996; Chung and Kang, 1999; Alshawabkeh et al., 2004; U.S. AEC, 2000; Virkutyte et al., 2002; Chung and Kamon, 2005; Reddy et al., 2006).

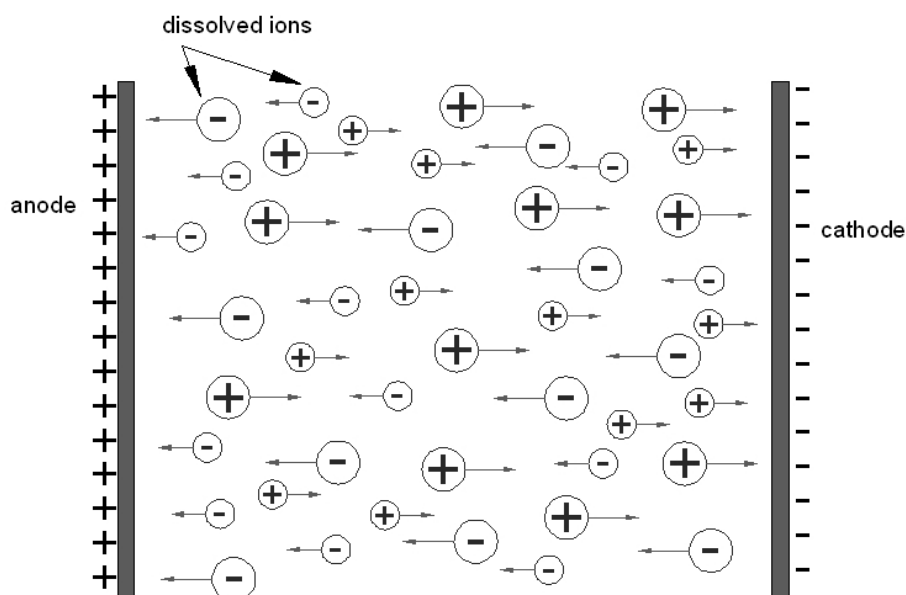


**Figure 2.8 – Schematic representation of the electromigration phenomenon in soils.**

The electromigration of cations and anions towards the electrode opposite in charge is proportional to the ion concentration in the pore water solution and to the electric field strength (Kim et al., 2005a).

The ionic mobility is a term used to describe the rate of migration of a specific ion specie under a unit electric field. In soils, the rate of ionic migration can be better defined by the effective ionic mobility, which also accounts for soil porosity and tortuosity, which can significantly affect ion migration (Alshawabkeh, 2001). The electromigrational mass

flux can be represented by the following Nernst-Einstein equation (Acar and Alshawabkeh, 1993; Probstein and Hicks, 1993; Chung and Kang, 1999; Alshawabkeh, 2001; De Battisti et al., 2006; Lynch et al., 2007):

$$u_i = \frac{D_i^* \cdot z_i \cdot F}{R \cdot T} \quad (9)$$

Where:

$u_i$  (sC/kg) is the electromigration flux;

$D_i^*$  ( $m^2/s$ ) is the effective diffusion coefficient of the  $i^{\text{th}}$  ionic specie;

$z_i$  (-) is the ionic valence of the  $i^{\text{th}}$  ionic specie;

$F$  (96.487 C/mol) is the Faraday constant;

$R$  (8.314 J/Kmol) is the universal gas constant;

$T$  (K) is the absolute temperature.

The effective diffusion coefficient can be calculated as:

$$D_i^* = D_i \cdot n \cdot \tau$$

Moreover, the effective ionic mobility can be calculated as:

$$u_i^* = u_i \cdot n \cdot \tau \quad (10)$$

Where, as already indicated for the electroosmotic flow:

$n$  (-) is the soil porosity;

$\tau$  (-) is the soil tortuosity.

Overall, the effective ionic mobility of heavy metals is usually in the range of  $10^{-8}$ - $10^{-9}$   $m^2/Vs$  (Alshawabkeh, 2001), which cause a migration rate of a few centimeters per day under a unit voltage gradient (1 V/cm).

### 2.3.1.3 Electrophoresis

Electrophoresis consists in a movement of charged particles and colloids under the influence of an electrical field (Figure 2.9). When a DC electric field is applied across a colloidal suspension, charged particles and colloids that are suspended in the pore fluid are electrostatically attracted to one of the electrodes and repelled from the other. Similarly to the electromigration process, positively charged particles tend to move towards the cathode and negatively charged particles tend to move towards the anode. For example, negatively charged clay particles tend to move towards anode (Yu and Neretnieks, 1996; Alshawabkeh, 2001; Virkutyte et al., 2002; Ahmad, 2004).

Usually, for environmental applications, electrophoresis is less important than

electroosmosis and electromigration in terms of mass flux; although in some cases electrophoresis may play a role in decontamination, e.g. if the migrating colloids have the contaminants adsorbed on them (Li et al., 1996).

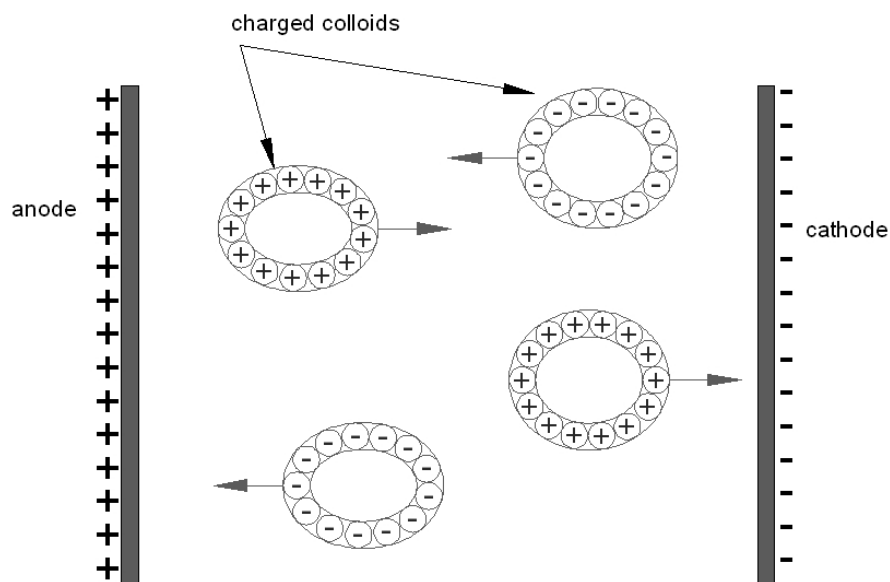


**Figure 2.9 – Schematic representation of the electrophoresis phenomenon in soils.**

#### 2.3.1.4 Chemical diffusion

Chemical diffusion is a flow of solutes driven by a concentration gradient. At the steady state, chemical diffusion can be described by the Fick's Law:

$$Q = -D \frac{\partial \phi}{\partial x} u_i^* = n \cdot \tau \cdot u_i \quad (11)$$

Where:

Q (mol/m<sup>2</sup>s) is the diffusion flux;

D (m<sup>2</sup>/s) is the diffusion coefficient, also called diffusivity;

Φ (mol/m<sup>3</sup>) is the solution concentration;

x (m) is the position.

Unlike electroosmosis, electromigration and electrophoresis, chemical diffusion tends to recreate a homogeneous distribution of the solutes in the pore water; therefore, it opposes to all the particles fluxes generated by the electrochemical processes.

In electrochemical applications for soil remediation, the role of chemical diffusion is commonly neglected (Acar and Alshwabkeh, 1993; Ahmad, 2004).

### 2.3.1.5 Electrokinetic transport

In sum, the overall movement of pollutants in the subsurface under a DC electric field is given by the combined effects of these components:

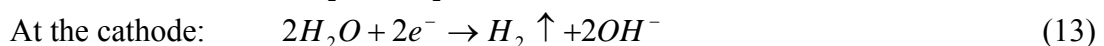
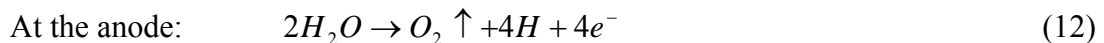
- Advection due to the hydrodynamic flow, driven by the pressure gradient;
- Advection due to the electroosmotic flow, due to interaction of the double layer with the DC field;
- Electromigration, due to the electrical forces on ionic species;
- Electrophoretic flow, due to the electrostatic attraction of charged particles and colloids by the electrodes;
- Chemical diffusion, driven by the concentration gradient.

As a consequence, the resulting pollutant transport rate depends on soil moisture content, soil grain size, ionic mobility, pore water amount and concentration, current density and contaminant concentration (Virukyte et al., 2002).

### 2.3.2 Water electrolysis and changes in soil pH

Under the influence of electrical fields, water electrolysis reactions occur at the electrodes, also resulting in pH changes.

Oxidation of water occurs at the anode and generates hydrogen ions ( $H^+$ ). On the opposite, reduction of water occurs at the cathode and generates hydroxyls ions ( $OH^-$ ), according to the following reactions (Acar and Alshawabkeh, 1993; Yu and Neretnieks, 1996; Wong et al., 1997; Chung and Kang, 1999; Alshawabkeh, 2001):



Consequently, during the electrochemical treatment, gas evolution occurs at the electrodes, with the production of hydrogen at the cathode and oxygen at the anode.

Furthermore, the hydrogen ions  $H^+$  generated at the anode create an acid front that moves towards the cathode, while hydroxyls ions  $OH^-$  generated at the cathode create a base front, which moves towards the anode (Acar et al., 1995; Yu and Neretnieks, 1996; Alshawabkeh, 2001; U.S. EPA, 2004; Chung and Kamon, 2005; Reddy et al., 2006; Lynch et al., 2007).

As a result of water electrolysis, the soil pH can drop to below 2 at the anode and increase to above 10 at the cathode within a few days of processing, depending on the soil buffer capacity and on the current applied (Alshawabkeh, 2001).

Both the acid and base fronts advance along the soil by electromigration, chemical diffusion and advection (i.e. electroosmotic advection, caused by the electroosmotic flow)

(Li et al., 1996; Virkutyte et al., 2002; Kim et al., 2005a). However they are differently affected by these phenomena. In fact, under usual conditions (i.e. when the electroosmotic flux flows from the anode towards the cathode), the acid front advances by:

- Electroosmotic transport;
- Electromigration;
- Chemical diffusion.

Differently, the base front advances only by:

- Electromigration;
- Chemical diffusion.

While it can be retarded by the electroosmotic flow.

Moreover, the transport of  $H^+$  is faster than the transport of  $OH^-$  (approximately 1.8 times faster) (Acar et al., 1995; Li et al., 1996; Alshawabkeh, 2001)

As a consequence, the acid front usually moves faster than the base front. Unless the  $H^+$  transport is not retarded by the soil buffering capacity, this difference in front moving rates lead to an acidification of the soil between the electrodes (Acar et al., 1995; Li et al., 1996; Puppala et al., 1997; U.S. AEC, 2000; Alshawabkeh, 2001; Kim et al., 2005a).

When the acid and base fronts meet each other, the soil between the anode and the cathode can be divided into two zones: a low-pH zone and a high-pH zone, with a sharp pH change in between. Where the acid and base fronts meet, a pH-change zone is created, where a transition from acid to basic conditions occurs. The location of the pH-change zone depends on several factors, both linked with the electric field and with the soil chemical properties, even though it is usually located closer to the cathode because of the larger advance rate of the acid front (Li et al., 1996). An increase in the applied voltage was observed to be able to promote the migration of the acidic front along the specimen (De Gioannis et al., 2007c), but on the other hand it may result in an increase in the energy expenditure.

This sweep of the acid from across the soil can assist the desorption of the ionic species, thus promoting their mobilization and enhancing their removal by the electrokinetic process. If strong enough, this process can also act as a sort of acid flushing of the soil, which promotes the contaminant dissolution and mobilization (Acar et al., 1995; Yang and Lin, 1998; U.S. ACE, 2000).

The migration of the acid and base front is however affected by the buffering capacity of the soil, which may neutralize  $H^+$  or  $OH^-$  ions, as well as by the soil initial pH. In particular, low soil buffer capacities can promote the migration of the acid front and the consequent acidification of the soil volume (Kim et al., 2006; Reddy et al., 2006).

The pH-change zone is commonly characterized by metal precipitation and by a

consequent low ionic conductivity. This phenomenon has important practical consequences that may affect the electrokinetic remediation process. In fact, most of heavy metals can complex into negatively charged species at high pH. These compounds can be then transported towards the anode under the electric field. In unenhanced electrokinetic remediation, the rise in the soil pH at the cathode compartment may result in a negative complexation of heavy metals within the zone of pH change, where they can ultimately precipitate as insoluble compounds (e.g. hydroxides). Metal precipitation also affects the ionic conductivity of the pH-change zone, which may be significantly decreased. The formation of this low conductivity zone, where metals tend to precipitate, can be avoided by using containing agents, like acid solutions to depolarize the cathode. The resulting process is named as enhanced electrokinetic remediation (see Chapter 2.4.1.3).

### **2.3.3 Geochemical reactions in soils**

As far as the geochemical reactions are concerned, during the electrochemical treatment of a contaminated soil, the soil-pore water system can be considered as an electrochemical cell, where oxidation and reduction reactions occur, water electrolysis providing the partners for redox reactions (Acar et al., 1995; Alshawabkeh, 2001; Rahner et al., 2002). Geochemical reactions include both homogeneous and heterogeneous reactions, i.e. reactions occurring among species in the aqueous phase or among species in the aqueous phase and solid particles (Yu and Neretnieks, 1996).

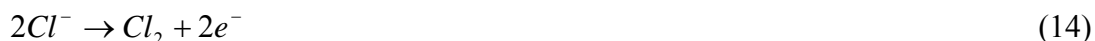
Furthermore, numerous reactions occur concurrently, including electrolysis, redox reactions, sorption and desorption of organic and inorganic compounds, acidification and basification of the soil, precipitation and dissolution of inorganic species. All these chemical processes can significantly influence the transport phenomena and affect the pollutant remediation.

#### *2.3.3.1 Redox reactions in soils*

So far, the mechanisms of the electrochemically promoted redox reactions has been extensively studied as far as aqueous systems are concerned, and electrochemical methods have been applied for water and wastewater treatment. Conversely, the knowledge of electrooxidation reactions pathways in soils is currently still limited.

### 2.3.3.1.1 *Electrochemically induced oxidation in aqueous systems*

In aqueous systems, electrochemical processes have proven to be able to generate active oxidant agents in presence of an oxidizing solution. For example, reactive chloride species, as chlorine ( $Cl_2$ ), hypochloric acid ( $HOCl$ ) and hypochlorite ions ( $ClO^-$ ), can be electrochemically generated from a solution containing chloride, e.g. NaCl used as electrolyte solution, due to the NaCl electrolysis:



The formation of the reactive chloride species causes an increase in the redox potential of the solution, and can allow the oxidation of the organic substances in the treated medium (Meinero and Zerbinati, 2006; Szpyrkowicz et al., 2007; Wang et al., 2007).

Moreover, oxidation reactions can occur also when oxidizing solutions are not added to the treated medium. The electrochemically induced oxidation processes in aqueous systems include (Brillas and Casado, 2002; Meinero and Zerbinati, 2006; Pazos et al., 2007; Wang et al., 2007):

- Direct anodic oxidation;
- Indirect oxidation, with the production of hydrogen peroxide.

In the direct anodic oxidation, adsorbed hydroxyl radicals ( $\bullet OH$ ) are produced at the anode from water oxidation, according to the following reaction:



Different electrode materials have been investigated to improve these degradation processes, like Pt,  $PbO_2$ , doped  $SnO_2$ , platinum, gold, titanium compounds or boron-doped diamond (BDD), and including two- and three-dimensional electrodes (Iniesta et al. 2001; Sopchak et al., 2002; Brillas and Casado, 2002; Meinero and Zerbinati, 2006; Panizza and Cerisola, 2007; Wang et al., 2007).

The indirect electrochemical oxidation, i.e. the electrochemical production of hydrogen peroxide, has recently gained a significant attention as an innovative technology for water and wastewater treatment. This process is based on the production of hydrogen peroxide in an electrochemical cell, as a result of redox reactions, in particular by the reduction of atmospheric oxygen from air at the cathode (Panizza and Cerisola, 2001; Ventura et al., 2002; Da Pozzo et al., 2005; Meinero and Zerbinati, 2006; Laine and Cheng, 2007; Liu et al., 2007), according to the following reaction:



This treatment, named as Electro-Fenton process, has been successfully applied for the removal of different organics from water, including pesticides (Ventura et al., 2002). Air is commonly bubbled at the cathode to enhance the hydrogen peroxide production. While being generated at the cathode, hydrogen peroxide can be decomposed at the anode (Meinero and Zerbinati, 2006).

For the electrochemical production of hydrogen peroxide, carbon or graphite cathodes are commonly preferred, because they exhibit a significant activity towards oxygen reduction and hydrogen evolution, and low catalytic activity for hydrogen peroxide decomposition (Panizza and Cerisola, 2001; Meinero and Zerbinati, 2006).

The oxidative action of hydrogen peroxide can be improved by the addition of ferrous ions or other catalysts (Panizza and Cerisola, 2001), which can enhance the production of hydroxyl radicals according to the Fenton's reaction:



This catalytic reaction is propagated by the  $Fe^{3+}$  reduction, which leads to the  $Fe^{2+}$  regeneration, this reaction being enhanced by the electrochemical process itself (Meinero and Zerbinati, 2006). Moreover, in the electrochemical cells, the Fenton's reaction can be enhanced by electrochemical regeneration of Fe(II) ions on the cathode surface (Meinero and Zerbinati, 2006).

The direct electro-generation of hydroxyl radicals from water at the electrodes has also been reported, with the following mechanism (Wang et al., 2007):



These water treatment methods are particularly appreciated, as they are able to produce hydrogen peroxide and hydroxyl radicals on-site continuously when needed, thus eliminating the needs for acquisition, shipment and storage of reactants, in comparison to traditional chemical oxidation. Furthermore, these processes have proven to be able to degrade the organic matter in aqueous systems and to be efficient in terms of energy consumption if compared to direct anodic oxidation (Meinero and Zerbinati, 2006; Wang et al., 2007).

#### 2.3.3.1.2 *Electrochemically induced oxidation in soils*

As far as the soil treatment is concerned, the generation of oxidant agents near the electrodes, as  $OH^-$ ,  $Cl_2$ ,  $ClO^-$ ,  $HClO$ ,  $O_3$  at the anode, and  $\bullet OH$  at the cathode, and their subsequent diffusion within the soil matrix has been regarded as a possible oxidation pathway (Sanromán et al., 2005), although the mobility of these oxidant agents is known to be very limited in fine-grain soils, both because of the low permeability of such soils



and of the short lives of these chemicals (ITRC, 2005).

A number of redox reactions occur close to the electrodes, electron transfers taking place between the electrodes and the species in the pore solution. Primarily, anode reactions involve oxidation of the species, in which the species lose electrons to the anode. Cathode reactions involve reduction of the species, in which the species gain electrons from the cathode (Yu and Neretnieks, 1996).

Furthermore, according to the “microconductor principle” (Rahner et al., 2002), in soils redox reactions are supposed to occur not only close to the electrodes as in a traditional electrochemical cell, but also simultaneously at any and all interfaces between soil and pore water, thus leading to a contaminant removal within all the treated medium. This effect is exposed in detail in Section 2.3.4.

Since soils commonly contain significant amounts of iron, once hydrogen peroxide has been created (reaction 18), hydroxyl radical ( $\bullet\text{OH}$ ) can be produced, according to the Fenton reaction (reaction 19).

Iron may be present in soils in different forms, including:

- Exchangeable and bound to carbonate;
- Bound to Fe/Mn oxides;
- Bound to organic matter and sulfides;
- Residual fraction.

Generally, the first three fractions are the soluble and amorphous solid representing more readily available sources of iron for the Fenton-like reactions. Conversely, the iron in residual fractions is mainly characterized by a crystalline structure and is sparingly available for chemical reactions (Kim et al., 2005a).

Hydroxyl radicals are strong non-selective oxidant agents (standard oxidation potential about versus the standard hydrogen electrode 2.8 V), able to react with most of organic pollutants (Watts et al., 2002; ITRC, 2005; Rivas, 2006), and they are considered the main responsible of the organic matter mineralization. In fact, this radical-based redox process (also addressed as indirect oxidation) seem the most probable mineralization mechanism for electrooxidation, as the alternative pathway (i.e. the direct oxidation or reduction at the soil microconductor surface) may be effective on mobile contaminants, but seems unlikely for immobile organic pollutants, due to its very high activation energies of the reactions involved (Rahner et al., 2002).

### *2.3.3.2 Other geochemical reactions*

Besides water electrolysis and redox reaction, other important geochemical

reactions can occur in the soil-pore water system, including (Yu and Neretnieks, 1996; Wong et al., 1997; Alshawabkeh, 2001):

- Sorption/desorption reactions;
- Dissolution/precipitation reactions;
- Metal complexation reactions.

These geochemical reactions are very important for soil remediation, since they can significantly affect the availability of the target contaminant and can enhance or constrain their mobilization and transport. For example, precipitation and sorption of heavy metals prevent their transport and thus limit extraction, while complexation could reverse the charge of the ion and might reverse the direction of migration. All these reactions are highly dependent on the soil pH, which, as previously discussed, depends on the electrochemical processes themselves. In particular, The acid front sweeping causes low pH conditions, favorable for the dissolution of most metal precipitates, while the pH-change zone, where the base and acid fronts meet, is commonly characterized by metal precipitation (see Section 2.3.2) (Chung and Kang, 1999). Moreover, soils with significant contents of carbonates, sulfides and sulfates can reduce metal solubility and promote precipitation (Wong et al., 1997; Virkutyte et al., 2002).

On the whole, at the anode oxidizing conditions are created, with oxygen gas evolution and production of protons ( $H^+$ ), which generate an acid front that starts moving towards the opposite electrode, also promoting metal dissolution. At the cathode, reducing conditions are created, with hydrogen gas evolution and the production of hydroxyl ions ( $OH^-$ ). The hydroxyl ions generate a base front that starts moving towards the anode and that favors metal precipitation, thus constraining metal mobility.

### **2.3.4 The microconductor principle**

The “microconductor principle” was introduced by Rahner et al. (2002) to explain the fact that the degradation of immobile, mostly organic, contaminants was sometimes observed during the electrokinetic tests on polluted soils.

According to this theory, electrochemical reactions can be induced within the soil matrix if the soil contains particles of films with electronic conducting properties (named as microconductors). In the presence of microconductors, the electric fields can induce the wet soil to act as a diluted electrochemical solid bed reactor, thus allowing the occurrence of the redox processes within the soil volume.

The concept underlying this theory is that, during an electrochemical soil treatment, immobile organic pollutants can be removed only as a result of reduction or oxidation reactions, the main reaction pathways being oxidation for aromatic and aliphatic

hydrocarbons, and reduction for chlorinated solvents. However, these reactions are known to have high activation energies, and to require high overpotentials to occur in aqueous media. Therefore, it was supposed that such reactions could occur only in the presence of a substrate with sufficient electronically conducting properties, i.e. only in the presence of proper microconductors.

The microconductors existing in soils are mainly weathering products of rocks and minerals, such as fine particles or films of iron, manganese or titanium compounds, carbonaceous particles and certain humic substances. They can be often doped by catalytically active transition metals. Their occurrence, abundance and distribution depend on the soil type and origins. The composition, size, electronic conductivity and electrochemical activity of microconductors may vary from type to type. Even similar minerals can show different electronic properties. For example, among iron minerals, hematite is known to be an insulator (i.e. it is electrochemically inactive as microconductor), while magnetite and graphite are microconductors with important electronic conductivities (i.e. they are electrochemically active as microconductors) (Rahner et al., 2002).

Microconductors possess a large number of electrochemical micro-reaction places. When an electric field is applied to a soil, the microconductors are polarized and may act as microelectrodes (either monopolar or bipolar microelectrodes), able to induce redox reactions in their vicinity (Rahner et al., 2002).

In sum, the electrical conduction in soils is given by the different contributions of these particle species:

- Inactive particles, with no conducting properties;
- Particles with electronic conducting properties (microconductors);
- Ionic species (deriving from dissolved salts) and charged colloids, with surface covered of charged particles.

The electrical scheme of a conductive soil in the presence of microconductors can be schematized as in Figure 2.10.

According to this model, the electric conductivity of a wet soil is given by the different contribution of:

- The ionic conductivity of the pore-water system;
- The conductivity of the microconductors.

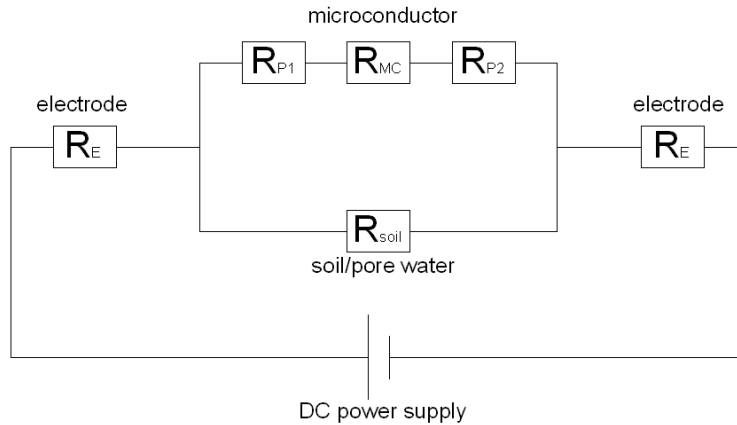
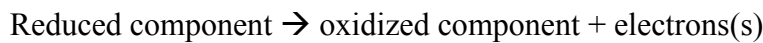


**Figure 2.10 – Electrical circuit schematic model of soil current conduction in the presence of electrolyte solution and microconductors (Rahner et al., 2002).  $R_p$  is the polarization resistance,  $R_{MC}$  is the microconductor resistance,  $R_E$  is the electrode resistance (usually negligible) and  $R_{soil}$  is the resistance of the soil-pore water system.**

The ionic conductivity of the pore-water system is due to the presence of ions and charged colloids and salts dissolved in the pore water. The electrical resistance due to these contributions can be indicated as  $R_{soil}$ . Under DC electric fields, and unless the pore water composition is not maintained by the addition of conditioning fluids, the resistance due to this contribution increases with time because of the electrochemically induced geochemical reactions.

The conductivity due to the presence of microconductors shows a certain resistance that can be indicated as  $R_{MC}$ . Moreover, a polarization resistance  $R_p$  should be added to  $R_{MC}$ . The polarization resistance is due to the fact that at the surface of the active microconductors, a transfer proceeds from ionic to electronic charge carriers and vice versa according to the schematic reaction pathway:



Normally, the polarization resistances  $R_p$  cannot be neglected, as they are much higher than the electronic resistances of the microconductors  $R_{MC}$ . The polarization resistance is a measure for the electrochemical reactivity of the microconductors, i.e. the lower the value of  $R_p$  the higher the electrochemical reactivity. If the polarization resistance is too high, no electric current flows through the microconductor and no electrochemical reactions can occur.

Based on this model of soil current conduction, the total current flowing across the soil can be modeled according to Ohm's and Kirchhoff's Laws:

$$I = I_{MC} + I_{soil} \quad (21)$$

$$I_{MC} = \frac{V}{R_{P1} + R_{MC} + R_{P2}} \quad (22)$$

$$I_{soil} = \frac{V}{R_{soil}} \quad (23)$$

where:

$I_{MC}$  (A) is the current flowing across the microconductor particle

$I_{soil}$  (A) is the current flowing across the pore water

$V$  (V) is the applied voltage gradient

Rahner et al. (2002) experimentally demonstrated the validity of the microconductor principle by simulating the effect a microconductor particle by a platinum wire embedded in an insulating epoxy resin, in presence of an electrolyte solution with the eventual presence of  $H_2SO_4$ , iron sulphates and complexing agents.

It was also found that the addition of microconductors can lower the electrolyte resistance due to an enhancement of the surface conductivity of the particles. Usually, a microconductor content of 1-2% in a soil may significantly decrease the electrical resistance (Figure 2.11).

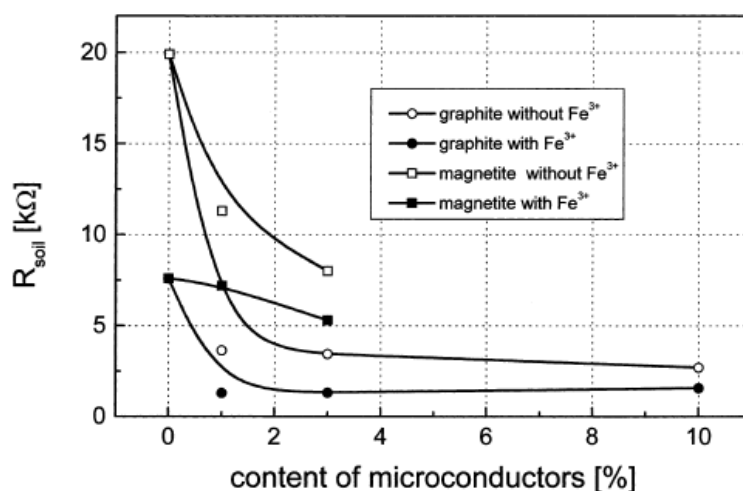


**Figure 2.11 – Dependence of the soil electrolyte resistance ( $R_{soil}$ ) on the amount and type of added microconductors, with and without the addition of Fe(III) ions. The values were experimentally determined under aerated condition in presence of a base electrolyte ( $Fe_2(SO_4)_3$ ) at a pH of 3 (Rahner et al., 2002).**

Three different reaction pathways can be individuated for contaminant degradation due to the microconductor effect. These phenomena can be summarized as follows (Rahner et al., 2002):

- Direct oxidation and reduction at the microconductor surface;
- Indirect oxidation and reduction by induced radicals;
- Acceleration of microbiological activity induced by the electrochemical processes.

The direct redox reactions at the microconductor surface seem quite unlikely to

occur for immobile organic contaminants due to their very high activation energies. On the other hand, it was shown that they could occur for soluble and mobile inorganic contaminants when they are adsorbed at the microconductor surface

Indirect redox reactions are assumed to be the primary degradation pathway for contaminant removal. According to the indirect oxidation processes already described in Section 2.3.3.1, oxygen can be reduced on the surface of the microconductor to produce hydrogen peroxide (reaction 18, page 31), while the presence of  $\text{Fe}^{2+}/\text{Fe}^{3+}$  redox couple can enhance the production of hydroxyl radicals according to the Fenton's process (reaction 19, page 32). Oxygen can be generated by the electrochemical process itself (reaction 12, page 28). Hydroxyl radicals could also migrate and oxidize organic compounds at a certain distance from the microconductor.

The biologic activity of degrading bacteria could be improved by the electrochemical generation of oxygen and by the transfer of oxygen and nutrients by the electrokinetic transport processes. Of course, the occurrence of strongly acidic or alkaline conditions due the electrochemical processes could also reduce the biologic activity of certain bacteria, but usually microorganisms are able to adapt to such conditions.

On the whole, the direct oxidation pathway is supposed be valid for mobile contaminants, while the indirect pathway is considered the most probable for immobile organic contaminants.

Rahner et al. (2002) also suggested that electrochemical reactions at the microconductor surfaces can occur when the electric field (E) applied to the soil is higher than a critical electric field ( $E_{\text{crit}}$ ). The value of this critical electric field depends on the soil characteristics (mainly by the features of the microconductors contained in the soil) and must be experimentally evaluated case to case.

In order the electrochemically generated redox reactions to occur, the presence of microconductors in an active state is necessary.

The electrochemical and catalytic activity of these micro-reaction sites depends on the nature and the chemical composition of the microconductor and on the redox systems in the vicinity of the microconductor particle (i.e. on the pore water). In other words, the reactions that are induced by the microconductors depend on the nature of the contaminant, on the nature of the microconductor itself, and on the characteristics of the electrolyte solution. For example, the solution pH may enhance or constrain the redox reactions, while the addition of  $\text{Fe}^{3+}$  ions can improve the microconductor activity. Also the prediction of the degradation products is difficult, since they can include a large number of by-products and reaction intermediates, some of which may be mobile and be influenced by the electrokinetic processes, besides the geochemical reactions.

Therefore, the occurrence of proper conditions must be evaluated under site-specific

conditions, as the degradation of organic contaminants depends on the occurrence of the suitable microconductors in combination with a proper redox system (Rahner et al., 2002).

### **2.3.5 Soil electrical conductivity**

Soils are conductive materials, i.e. they show significant electrical conductivities. However, the soil electrical resistivity is affected by several factors, including water content, clay content, soil mineralogy and texture, the presence of soluble salts in the pore fluid, organic matter content, cracks and temperature (Corwin and Lesch, 2005; Samouëlian et al., 2005). For example, clayey, silty and sandy soils show different electrical resistivities. Moreover, the soil water content is determinant in the electrical conduction processes, therefore the electric resistance in dry soils are usually very high (Nor and Ramli, 2007).

Soil resistivity is commonly expressed as  $\Omega\text{m}$ , while soil conductivity is expressed as  $\text{mS/m}$ . Typical values of soil resistivity are about 5-30  $\Omega\text{m}$  for clays and about 500-1000  $\Omega\text{m}$  for sands (up to 10000  $\Omega\text{m}$  for gravels); these correspond to electrical conductivities of about 10-500  $\text{mS/m}$  for clays and of 0.1-5  $\text{mS/m}$  for sand and gravels (Fauri et al., 1999; Samouëlian et al., 2005).

Commonly, when a voltage gradient is applied to a soil, the resulting current flowing is found to be decreasing with time after an initial period of increase, which may last for several hours (Virkiute et al., 2002; Kim et al., 2005a; Lynch et al., 2007).

In fact, the initial current increase is due to an increase in the salt concentration in the soil pore water, due to the salt dissolution from soil particles (Mitchell, 1993). As time elapses, the pore water ionic concentration decreases due to the gradual depletion of solutes, to the precipitation of non-conductive solids from the pore water salts and the polarization of the electrodes, (Acar and Alshwabkeh, 1993; Acar et al., 1995; Yu and Neretnieks, 1997; Virkiute et al., 2002; Reddy and Chinthamreddy, 2004; De Giannis et al., 2007c; Lynch et al., 2007). In particular, during the unenhanced electrochemical treatment, the current flowing is gradually decreased because of the formation of high electric resistivity zone near the cathode, due to the precipitation of metal hydroxides under the local basic conditions (Acar et al., 1995; Amrate et al., 2005; Kim et al., 2006). Therefore, it is common for the current to reduce with time, unless amendments, such as ionic solutions, are supplied to provide new charge carriers in the soil-solution system (Reddy and Chinthamreddy, 2004). Usually, in bench-scale electrokinetic tests, the electrical currents are found to increase rapidly after the application of the voltage gradient, to reach a peak value within 1-24 h, and then to decrease and stabilized at a nearly constant steady state value (Reddy and Chinthamreddy, 2004; Kim et al., 2005a).

Various salts can contribute to the ionic conductivity of the pore water solution.  $\text{HCO}_3^-$  and  $\text{CO}_3^{2-}$  may be released from soil. The addition of ionic solutions (e.g. NaCl,  $\text{H}_2\text{SO}_4$ ) can allow an additional salt release and improve the soil conductivity. Also the addition of hydrogen peroxide could enhance the ionic conductivity, by providing anions deriving from its decomposition, such as  $\text{O}_2^{\bullet-}$  and  $\text{HO}_2^-$  (Kim et al., 2006).

In the electrokinetic processes, the decrease in the current flowing may be counterbalanced by the addition of proper ionic solutions as the electrolyte, to compensate the exhaustion rate of the electrolyte solution by electromigration (Park et al., 2005). These processes are designed in order to balance the ionic extraction rate due to electromigration and the supplementation of salts in the electrolyte solution, therefore the resulting current may be constant.

## 2.4 Application of DCTs for soil remediation

So far, DCTs have been successfully applied for the recovery of soils and sediments contaminated by mainly mobile inorganic pollutants, in electrokinetic remediation actions (U.S. AEC, 2000; U.S. EPA, 2002a; U.S. EPA, 2004). Bench-scale and pilot-scale tests indicated that the technology can be successful in clayey to fine sandy soils (Acar et al., 1995; Alshawabkeh, 2001). The practical aspects of these remediation techniques are discussed in Chapter 2.4.1.

Moreover, recently the use of DCTs for the removal of immobile organic pollutants has gained growing attention, with the employ of surfactant-enhanced electrokinesis, bioelectrokinesis, Electrokinetic-Fenton remediation (described in Chapter 2.4.2) and of electrooxidation processes (Chapter 2.4.3).

### 2.4.1 Electrokinetic remediation

Electrokinetic remediation is a physico-chemical treatment that relies upon the application of a direct current electric field through pairs of electrodes. The process aims at transporting charged pollutants towards the electrodes, where they can be concentrated and removed. Cations, including most of metals, ammonium ions and positively charged organic compounds, tend to move toward the cathode. Anions, like chlorides, cyanides, fluorides, nitrates, and negatively charged organic compounds, tend to move toward the



anode.

Once the target pollutants have been transported toward the electrode opposite in charge along the soil, various reactions involving ions can occur close to of the electrodes. Such reactions can be used to remove the target pollutants from the soil or from the purging solution dosed at the electrodes if necessary. For example, metals can be plated onto the electrodes (electrodeposition), or can precipitate or co-precipitate near the electrodes (e.g. near the cathode for the positive ionic species), while gaseous compounds can be liberated. Alternatively, the contaminants can be carried out from the soil by a flushing fluid and then separated from the flushing fluid by a purification process (Acar et al., 1995; Yu and Neretnieks, 1997; U.S. AEC, 2000; FRTR, 2002; Virkutyte et al., 2002). Adsorption onto the electrode may also be feasible, especially when the electrodes are coated with specific materials (Virkutyte et al., 2002).

During the past few years, electrokinetic remediation has been successfully applied for the removal of a number of mobile pollutants from soils and sediments, including:

- Metals, like arsenic, cadmium, chromium, cobalt, copper, mercury, nickel, lead and zinc (Acar et al., 1995; Li et al., 1996; Haran et al., 1997; Wong et al., 1997; Yang and Lin, 1998; U.S. ACE 2000; Alshawabkeh, 2001; Reddy and Chaparro, 2001; Virkutyte et al., 2002; De Gioannis et al., 2007a,c; Szpyrkowicz et al., 2007).
- Radionuclides, like cesium, plutonium, radium, thorium, uranium and strontium (Acar et al., 1995; Yu and Neretnieks, 1997; Alshawabkeh, 2001).
- Soluble and polar organic pollutants, like phenols, polychlorinated biphenyls (PCBs), acetic acid and industrial dyes (Acar et al., 1995; Alshawabkeh, 2001; Virkutyte et al., 2002; Kim et al., 2005a; Sanromán et al., 2005; Pazos et al., 2007).

Electrokinetics belongs to the class of separation remediation technologies, i.e. this process only aims at separating the target pollutants from the contaminated matrix, without destroying them.

#### *2.4.1.1 Contaminant transport*

Under the influence of the electric fields, the transport phenomena in soils consist in mass fluxes generated by the different contributions of chemical diffusion, electromigration, electroosmotic advection and electrophoresis. Among these contributions, electromigration and electroosmotic advection are generally regarded as the major causes of the electrokinetic transport (Acar et al., 1995; Haran et al., 1997; Chung

and Kang, 1999; Alshawabkeh, 2001; Zorn et al., 2005a; De Gioannis et al., 2007c).

However, a significant metal transport has been observed also when no electroosmotic flow was encountered, due to sole the effect of electromigration (Acar et al., 1995). This situation can be encountered when the ionic concentration of the pore water is high, or when the pH has reached the isoelectric point. Therefore, electromigration mass flux can transport ionic species even when the electroosmotic flux has ceased or is not present. Moreover, while electromigration occurs in all soils, the electroosmotic flow occurs only in very fine-grain soils, like clays and silts, while electromigration exists in all soils (Wong et al., 1997).

Some Authors (Chung and Kang, 1999) suggested electroosmosis and electromigration to be superposed on decontamination of heavy metals from low contaminated soils, and electromigration to be the primary removal mechanism in highly contaminated soils, as well as when the soil zeta potential is small (Haran et al., 1997).

The complementary contributions of electroosmotic advection and of electromigration can however affect ionic species in different ways. In fact, electroosmosis, like any other hydraulic flow (e.g. hydraulic flow generated by hydraulic gradients) will usually carry all types of solute in the flow direction. However, electromigration separates negatively and positively charged ions and cause their migration on opposite directions (Alshawabkeh, 2001). Consequently, the electroosmotic flow might enhance the migration of certain ions, but retard migration of other ions (with opposite charge).

Once the species are solubilized, the transport by electromigration is on the order of 1-80 cm/day, under an electric field of 1 V/cm (Acar et al., 1995). The ionic mobility of hydrogen ions ( $H^+$ ), which determines the rate of the acid front migration, is about 80 cm/day under an electric field of 1 V/cm. However, this rate can significantly decrease because of sorption, dissolution and other geochemical reactions. For example, in kaolinite it has been reported to be about 1-8 cm/day (Acar et al., 1995).

Most of metals occur in cationic forms under environmental conditions. Therefore, during an electrochemical treatment, such complexes will tend to migrated towards the cathode. However, even under environmental and even under acidic conditions, negatively charged aqueous metal complexes can be formed including hydroxo complexes like  $Me(OH)_3^-$  and  $Me(OH)_4^{2-}$  (Wong et al., 1997; De Gioannis et al., 2007a,c), according to the reaction:



When dissolved in the pore water, these compounds will tend to migrate towards the anode. Moreover, besides the metal hydroxide formation, certain metals occur in

different anionic forms under environmental conditions. For example Cr(VI), which is regarded as the most hazardous form of chromium, due to its high toxicity and important mobility, mostly exists as chromate ( $\text{CrO}_4^{2-}$ ), monochromate ( $\text{HCrO}_4^-$ ), or dichromate ( $\text{Cr}_2\text{O}_7^{2-}$ ) anions, depending on the pH of the solution (Haran et al., 1997). The electrokinetic removal of such pollutant species could be achieved by transporting them toward the anode.

#### *2.4.1.2 Applicability and influence factors*

Electrokinesis is most applicable to fine-grain soils, which are usually saturated and partially saturated clays and silt-clay mixtures, typically characterized by low hydraulic permeability (Alshwabkeh, 2001; Virkutyte et al., 2002). Besides soils, electrokinesis can be applied to sediments, sludge and mud, which are similarly fine grain materials with low hydraulic permeability (FRTR, 2002). Moreover, electrokinetic methods have recently been applied to other materials for environmental purposes. For example municipal solid waste incinerators (MSI) fly ashes were treated with electrokinetic methods to remove heavy metals, through the “electrodialytic process”, if necessary improved by the use of enhancing agents, like chlorides, surfactants and acid solutions. The main aim of such treatments was to remove dangerous pollutants from MSI fly ashes in order to allow their valorization and reuse (Lima et al., 2005; Traina et al., 2005).

Among inorganic compounds, electrokinetic remediation showed different effectiveness towards different pollutants, mainly depending on the mobility of the target species. For example, among metals, mercury is often difficult to be removed, as in soils it is frequently bound to soil particles or organic matter (Szpyrkowicz et al., 2007), while lead tends to precipitate as hydroxides, with very low water solubility, and may be removed only when a very aggressive acid conditioning is performed (Acar et al., 1995; De Gioannis et al., 2007a,c). Hence, the target pollutant specie may pose significant limitations on this technology, if they exist in immobile forms, e.g., sorbed on the soil particle surface or precipitated in the soil pore.

Among organic pollutants, phenol is one of the easiest pollutants to remove by electrokinesis, because it is water miscible and it protonates in an acid, this production a positive charged compound (Acar et al., 1995). Conversely, it is particularly difficult to treat contaminants with low water solubility and high octanol-water partition coefficients, as HOCs (Kim et al., 2005a; Park et al., 2007), since these compounds are commonly sorbed onto soil particles and characterized by very limited mass transfers.

Sorption can affect the remediation processes in two ways: firstly, it retards the rate

of transport of apolar contaminants and decreases the transfer rate from the solid to the liquid phase. Secondly, it constrains the contact between the pollutants and the reactants dosed to chemically degrade them (as for oxidant agents) or to enhance their transport (as for surfactants or solvents) (Kim et al., 2005a). Hence, soils with significant sorption capacities usually result in slower recovery processes (Yu and Neretnieks, 1997).

A certain degree of electrokinetic transport of BTEX (benzene, toluene, ethylene and xylene) and trichloroethylene (TCE) was demonstrated, at concentrations below the solubility limit of these compounds (Alshawabkeh, 2001). Mitchell (1991) stated that the transport of apolar organic pollutants could be possible if they were present as emulsions that could be swept along with the electroosmotic flow. However, HOCs proved to be effectively removed only by surfactant-enhanced electrokinesis, i.e. when surfactants are used to solubilize them. Conversely, the electrokinetic transport of such species under unenhanced conditions (i.e. where no surfactants were used) showed to be very limited (Acar et al., 1995; Alshawabkeh, 2001; Lee et al., 2005a; Wick et al., 2005; Oonnittan et al., 2007).

During the electrokinetic process, sorption/desorption, precipitation/dissolution and complexation reactions can significantly affect the contaminant transport and therefore the efficacy of the remediation treatment. In particular, since all these processes are highly influenced by the soil pH, the effectiveness of the electrokinetic remediation is highly dependent on the occurrence of proper acidic conditions, which favor the dissolution processes (Wong et al., 1997; De Gioannis et al., 2007a,c; Szpyrkowicz et al., 2007). However, the low pH required for successful contaminant recovery may be difficult to achieve, because of the soil buffer capacity, and the migration of the acid front may be insufficient to promote the dissolution of the target pollutants.

Also high calcium concentration in the treated soils can significantly hinder the metal transport, because the migration and precipitation of calcium as bicarbonates and hydroxides can clog soil pores and increase the soil buffer capacity, constraining the advance of the acid front (Acar et al., 1995; Alshawabkeh, 2001; Reddy et al., 2006; De Gioannis et al. 2007c).

Several methods have been tested to overcome the problem of metal precipitation near the cathode due to the alkaline conditions. Most of them rely upon the dosage of acid solution to condition the soil pH, and are described in detail in Chapter 2.4.1.3. Tests have also been conducted with the “polarity exchange” technique, i.e. operating by inverting the electrode polarity at short time intervals, in order to periodically generate hydrogen ions in the alkaline zone, favoring the metal dissolution (Pazos et al., 2006).

For metals, besides the soil pH and buffer capacity, the remediation efficiency can be significantly affected by partitioning and speciation of the target species, the more

mobile fractions (e.g. exchangeable, bound to carbonate and bound to Fe/Mn oxides fraction) being more available for transport and removal, while the less mobile fractions (e.g. the residual fraction) being more recalcitrant to recovery (De Gioannis et al., 2007c).

Electrokinetic remediation has been reported to be effective in both saturated and unsaturated soils (Virkiute et al., 2002). However, it must be point out that, since the pore fluid plays a very important role in all electrochemical processes, in order the electrochemical remediation to be effective, the presence of a pore fluid in soil pores is required, both to conduct the electric field and to transport target species across the soil mass (Acar et al., 1995). Moreover, the soil must be wet to keep the resistance low and provide significant currents flowing (Röhrs et al., 2002). Theoretically, it may be possible to saturate a partially saturated soil by electroosmotic flux of the pore fluid, but this process must be carefully engineered and controlled (Acar et al., 1995).

On the whole, electrokinetic phenomena are governed both by electroosmosis and electromigration and by the electrolysis reactions occurring at the electrodes (Kim et al., 2005a). Hence, the electrokinetic transport rates depend on many parameters, including the soil pH, the zeta potential, the soil activity coefficient and the ionic concentration (Alshawabkeh, 2001; Lynch et al., 2007). The most favorable conditions for contaminant transport (including both the contribution of electroosmotic advection and of electromigration) involve (Alshawabkeh, 2001; Virkiute et al., 2002):

- High soil water content (i.e. high degree of saturation);
- Low ionic strength of the pore water (i.e. low electrolyte concentration);
- Low soil activity;
- Limited soil buffer capacity.

In particular, the pH changes, regulated by water electrolysis and by the soil buffer capacity, play an important role in contaminant migration, since they can influence metal solubility and mobility in the soil. Since acid conditions may favor the metal migration and prevent metal precipitation, the electrokinetic remediation is usually enhanced by the addition of conditioning agents to adjust the soil pH, in order to control system chemistry and to promote contaminant solubilization and transport.

On the whole, 85-95% metal removal efficiencies were reported for electrokinesis, but with the success of the remediation process strongly depending on (Acar and Alshawabkeh, 1993; Alshawabkeh, 2001; Virkiute et al., 2002):

- Soil type;
- Types and amount of contaminant present;
- Soil pH and buffer capacity;
- Organic matter content;
- Pore water composition.

### 2.4.1.3 Enhanced electrokinetic remediation

The injection of proper conditioning fluids, or simply of clean water, can improve the efficiency of the electrokinetic remediation process, the technique being named as “enhanced electrokinesis”.

Commonly, when the remediation of heavy metals and radionuclides is performed, the electrokinetic transport is enhanced by flushing the soil with acid solutions, chelating agents, complexing agents or other conditioning fluids, to adjust soil pH to promote metal solubilization and transport (Li et al., 1996; Puppala et al., 1997; Alshwabkeh, 2001; Virkutyte et al., 2002; Reddy and Chinthamreddy, 2004; Zhou et al., 2005; De Gioannis et al., 2007a,c). Solvents, surfactants or cyclodextrins can also be used to enhance the mobilization and flushing of apolar organic pollutants (Reddy et al., 2006; Isosaari et al., 2007; Park et al., 2007).

On the whole, a number of chemical conditioners can be used as processing fluids to enhance the electrokinetic process. The most common include (Puppala et al., 1997; Alshwabkeh, 2001; Yang and Lin, 1998; Reddy and Chaparro, 2001; Reddy and Chinthamreddy, 2004; De Gioannis et al., 2007a,c; Park et al., 2007):

- Acid solutions (e.g. acetic acid, nitric acid, sulphuric acid, hydrochloric acid);
- Chelating agents (e.g. citric acid, EDTA);
- Surfactants, cosolvents and cyclodextrins;
- Electrolyte solutions (e.g. potassium iodine KI, sodium chloride NaCl):

All these chemicals aim at improving the solubility of the target pollutants, by adjusting the soil pH to low values, in order to avoid metal precipitation, or by creating soluble complexes by the use of chelating agents, surfactants and complexing agents. In sum, the most common ways to enhance the electrokinetic transport include (Acar et al., 1995; Puppala et al., 1997; Alshwabkeh, 2001):

- Dosage of acid solutions at the cathode to depolarize the electrode (i.e. to prevent the formation of high pH conditions near the cathode due to water electrolysis reactions);
- Dosage of acid solutions at the anode to promote the acid front sweeping;
- Dosage of chelating agents, surfactants or complexing agents to promote the contaminant solubilization.

The conditioning fluids used for enhanced electroremediation are commonly added at one or all electrode wells, from where can be diffused through the soil both by electroosmosis and, if ionized, by electromigration (Wong et al., 1997).

Acid conditioning, either at the cathode or at the anode side, is the probably the

most common type of enhancement of the electrokinetic processes. For example, the injection of acids at the cathode aims at neutralizing the strong alkaline conditions that are commonly created in this area due to the production of hydroxyl ions ( $\text{OH}^-$ ) by water electrolysis. This is very important for the pollutant removal, as, unless neutralized, these conditions favor metal precipitation close to the cathode and hinder their recovery (Li et al., 1996; Wong et al., 1997; Reddy and Chinthamreddy, 2004).

Otherwise, acids can be added in the anolyte solution, to improve the acid sweeping due to the electroosmotic transport (Li et al., 1996). This could be useful especially in case the treated soil showed a strong buffer capacity, and therefore the sole electrochemical generation of the hydrogen ions ( $\text{H}^+$ ) was unable to lower the soil pH. Acid conditioning proved also to be capable of promoting the migration of organic pollutants, in comparison to unenhanced electrokinetic transport (Pazos et al., 2007).

Acetic acid and nitric acid are most commonly used for environmental applications, while the use of hydrochloric acid is discouraged because of the possible evolution of chlorine gas and of the possible increase the chloride concentration in groundwater (Li et al., 1996; Alshawabkeh, 2001). Acetic acid is particularly appreciated for environmental applications, as it is an environmentally safe chemical, biodegradable and does not create a health hazard for in situ applications. Moreover, most of metal acetates are highly soluble in water (Puppala et al., 1997; Giannis et al., 2007). Nevertheless, nitric acid may be preferred for the conditioning of soils with strong buffer capacity (De Gioannis et al., 2007a,c).

Alternatively to acids, buffer solutions, e.g. sodium acetate, can be used as conditioning agents to keep the soil pH constant (Mohamed, 1996; Park et al., 2007). Ion-selective membranes have also been applied, and have been reported to be effective in preventing hydroxyl ions (or even hydrogen ions, if necessary) to advance across the treated soil, though their application is less common than the acid conditioning (Li et al., 1996; Puppala et al., 1997; Alshawabkeh, 2001; Virkutyte et al., 2002; Kim et al., 2005c).

Both the addition of acids in the anolyte and in the catholyte solutions aim at creating acidic conditions along all the volume to be treated, to promote metal dissolution. In fact, if proper acid conditions are not created, the pollutant transport along the soil could be incomplete and may lead to an accumulation of metals in the central part of the treated soil (Wong et al., 1997).

Some metals are amphoteric and can exist either in positive or negative ion forms, e.g.  $\text{Pb}^{2+}/\text{PbO}_2\text{H}^-$  and  $\text{Cr}^{3+}/\text{Cr}(\text{OH})_4^-$ , depending on local pH conditions (Puppala et al., 1997). The species mobilized near the anode, as a result of the desorption occurring under low pH conditions, tend to migrate towards the cathode, as under such conditions they generally exist in the cationic form. However, when they reach the pH-change zone (where

the acid and base fronts meet), such metal complexes can be converted into anionic compounds, due to the excess of hydroxyl ions (OH<sup>-</sup>). These anionic compounds can start to migrate backwards towards the anode, until they reach the low pH zone, where they can speciate back to cationic forms. This result of such mechanisms is a sort of pulsing movement, which can reduce the efficiency of the electroremediation process (De Gioannis et al., 2007c).

Furthermore, neutralizing the alkaline conditions that are generated at the cathode by electrolysis reactions can assist in the extraction of positively charged species into the cathode compartment, once they have been transported along the soil (Puppala et al., 1997).

In case the target compounds exist in soils as precipitates and the soil exhibits a significant buffer capacity, only an aggressive acid conditioning can allow them to be dissolved, transported and removed (De Gioannis et al., 2007c). However, it must be observed that the acid conditioning can increase electrolyte concentration, thus constraining the electroosmotic flow rate. This could hinder the electroosmotic transport to a certain extent (Alshawabkeh, 2001).

Chelating agents can be used to convert the soil-bounded heavy metals into soluble metal complexes (Wong et al., 1997; Yang and Lin, 1998; Amrate et al., 2005). Chelating agents contain two or more ligands (L) that bond with metal to form stable, ring-like coordination complexes, called chelates. Chelating agents can be particularly effective for the remediation of strongly buffered alkaline soils, in which the pH cannot be easily lowered by the addition of acid solutions (Wong et al., 1997; Amrate et al., 2005).

Among different chelating agents, ethylenediaminetetraacetic acid (EDTA) has shown to be very effective for metal solubilization in soils, and it has been extensively applied also for soil washing and soil flushing (Polettini et al., 2006; Di Palma and Mecozzi, 2007), being a widely available non-toxic chemical. EDTA is generally available as the acid H<sub>4</sub>L or the disodium acid salt Na<sub>2</sub>H<sub>2</sub>L, where L represents the EDTA ligand, (NCH<sub>2</sub>)<sub>2</sub>(CH<sub>2</sub>COO<sup>-</sup>)<sub>4</sub>. EDTA is soluble at pH above about 3.5 and its speciation, i.e. the degree of protonation ("n" for the chemical compound being H<sub>n</sub>L<sup>(4-n)-</sup>), depends on the pH (Wong et al., 1997; Amrate et al., 2005). In particular, to ensure the stability of the EDTA-metal complexes, the pH should be maintained slightly alkaline, e.g. about 8-10, e.g. by the addition of base solutions. On the other hand, a too high pH should be avoided, as they might favor metal precipitation and hinder EDTA complexation (Amrate et al., 2005).

Since the EDTA metal complexes are typically negatively charged (ML<sup>2-</sup>), these species tend to migrate towards the anode (Wong et al., 1997; Amrate et al., 2005; Reddy and Chinthamreddy, 2004; De Gioannis et al., 2007c). Therefore, in EDTA-enhanced electrokinetic remediation, EDTA is commonly added to the catholyte solution, in order to



be transported across the soil to solubilize the precipitated metals and transport them towards the anode.

In addition to provide a ligand to solubilize metals, the EDTA can help to moderate the elevation of the pH in the vicinity of the cathode, because of the generated hydrogen ions from the dissociation of this acid salt (Wong et al., 1997):



Other chelating agents, such as citric acid, were tested for the electrokinesis enhancement, but with poorer results than EDTA (Reddy and Chinthamreddy, 2004; De Giannis et al., 2007a,c). Similarly to chelating agents, complexing agents (such as ethylenediamine, EDA) can be used to prevent metal precipitation (Wong et al., 1997).

Since chelating and complexing agents are commonly expensive, the recovery of the conditioning solutions and their reuse is encouraged, in order to reduce the remediation costs. Certain Authors (Amrate et al., 2005) suggested the possible in situ recovery of the EDTA solution by the use of cation exchange membranes at the anode compartments. This could also avoid the loss of the chelating agent due to anodic oxidation.

Surfactant-enhanced electrokinesis can be used to remove hydrophobic contaminants that are not soluble in water, i.e. HOCs, like PAHs (Reddy et al., 2006; Giannis et al., 2007; Park et al., 2007).

Surfactants are chemical compounds with both hydrophobic and hydrophilic groups. Indeed, surfactants tend to form micelles when their concentration in water is greater than the critical micelle concentration (CMC). When surfactants exist in an aqueous solution, HOCs can accommodate to the interior of micelles where the hydrophobic groups are present, the process being named as micellar solubilization. This allows the HOCs to be transported together with the water solution. A surfactant-enhanced electrokinetic process hence relies on two steps: the dissolution of HOCs into the surfactant micelles, and the transport of micelles containing HOCs in electric field, e.g. by electroosmotic advection (U.S. EPA, 2000; Reddy et al., 2006; Giannis et al., 2007; Park et al., 2007).

Different types of surfactants have been used in electrokinetic remediation, including Tween 80, APG (alkyl polyglucoside), Brij30 (polyoxyethylene-4-lauryl ether), SDS (sodium dodecyl sulfate) and humic acids. The process resulted in good recovery efficiencies for hydrophobic contaminant, like PAHs, and in an improvement of metal mobility (Reddy et al., 2006; Giannis et al., 2007; Park et al., 2007). In many cases, surfactants are used in combination with complexing agents, like acetic acids, as their combination has proven to enhance the capability extracting heavy metals from contaminated soil by electrokinesis (Giannis et al., 2007; Park et al., 2007).

In the same way as surfactants, also cosolvents (n-Butylamine) and cyclodextrins (e.g. hydroxypropyl- $\beta$ -cyclodextrin or HPCD) can be used in flushing solutions, as solubilizing agents, to enhance the removal of hydrophobic pollutants, like PAHs, from soils (Maturi and Reddy, 2006; Reddy et al., 2006).

Sometimes, the addition of a flushing solution can influence the electrochemical process parameters. For example, the use of cosolvents as conditioning agents was reported to cause an increase in the soil pH and to improve the electroosmotic flow rate (Reddy et al., 2006). The addition of EDTA was observed to produce an increase in the current intensity, resulting from the increased ionic strength of the circulating solution, if compared to the use of deionized water as circulating solution. Moreover, it was also found to promote the migration of the acidic front across the specimen, especially when used in combination with acid solutions (De Gioannis et al., 2007c).

Saline solutions can be used as electrolyte fluids to improve soil conductivities (Park et al., 2007). Furthermore, salts can be used to form soluble metal complexes, like KI, which can form a highly soluble iodide complex with mercury ( $\text{HgI}_4^{2-}$ ), and NaCl, which can form a chlorine complex with mercury ( $\text{HgCl}_4^{2-}$ ) (Reddy and Chaparro, 2001; Reddy and Chinthamreddy, 2004).

In certain cases, a hydraulic gradient is applied to the treated soil to improve contaminant transport due to advection (Mohamed, 1996; Virkutyte et al., 2002; Reddy et al., 2006; De Gioannis, 2007c).

Typical concentrations of the extracting solutions injected in the electrode chambers range from 0.1 M to more than 1 M for acid conditioners (Puppala et al., 1997; Reddy and Chaparro, 2001; Reddy and Chinthamreddy, 2004; Pazos et al., 2007), while lower concentrations are commonly used for chelating agents, like EDTA (below 0.2 M) (Wong et al., 1997; Reddy and Chinthamreddy, 2004; Amrate et al., 2005).

The extracting agents can also help to improve the contaminant removal at the electrode compartments, once they have been transported along the soil (Puppala et al., 1996; Reddy and Chaparro, 2001).

In enhanced-electrokinetic remediation, purging solutions that are circulated at the electrodes must be extracted to remove (or concentrate) the collected pollutants, or can be regenerated by using proper membranes. Therefore, besides the power supply system, the complete enhanced-electrokinetic remediation process includes (Figure 2.12):

- The application of an electric field;
- The injection of the purging solution at one or all electrodes;
- The recovery of the solution at the electrodes;
- Extraction or exchange system to treat (and in case recycle) the process solutions.

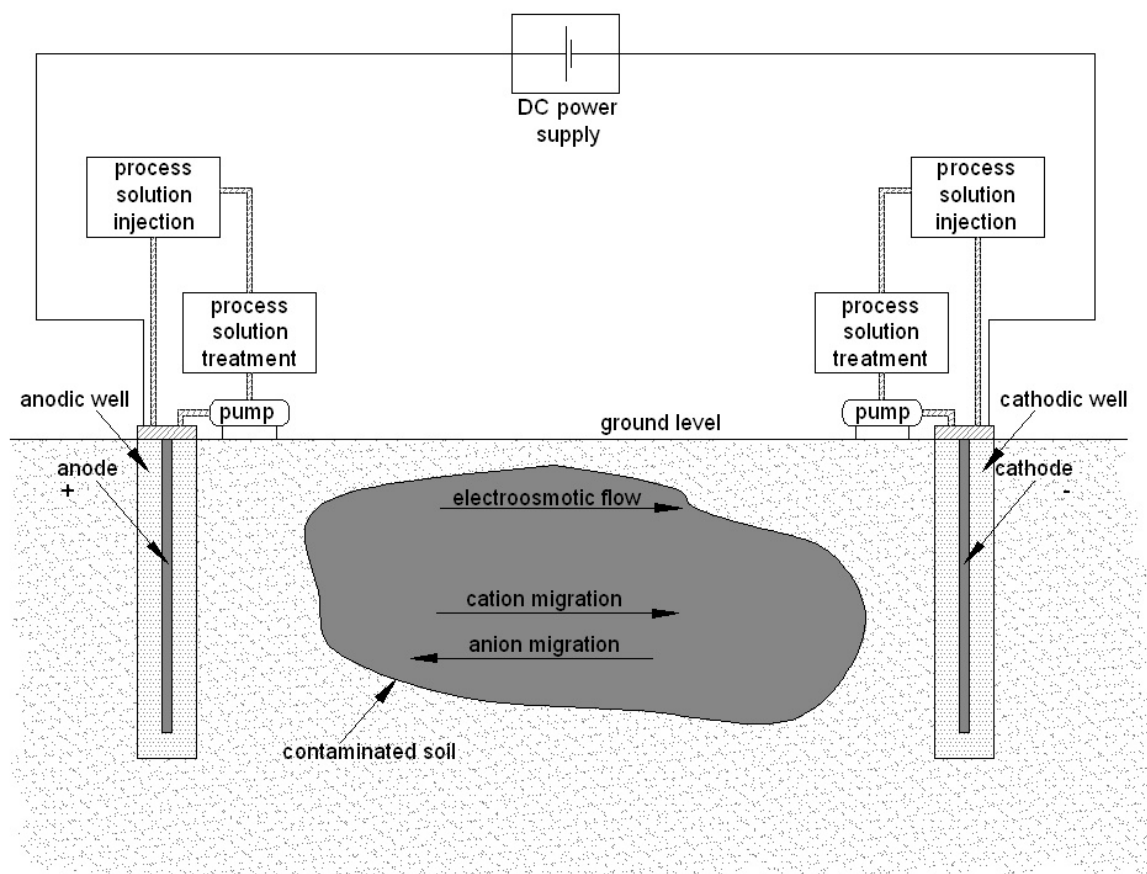


**Figure 2.12 – Schematic diagram of an enhanced-electrokinetic remediation system.**

The use of conditioning agents was sometimes reported to reduce the electric power consumption of the electrochemical process (Pazos et al., 2007), even though the use of conditioning fluid commonly contributes to increasing the overall remediation cost, due to the more complex treatment setup and operations required (Virikutyte et al., 2002).

Acid solutions, surfactants, cosolvents, cyclodextrins and chelating agents can help to improve the effectiveness of electrokinesis significantly, especially for the removal of organic compounds otherwise difficult to remove. However, the use of such chemicals for in situ applications must be carefully evaluated, as the surfactants remained in soil after a remediation treatment may be another contaminant themselves and/or can cause a secondary contamination by improving the mobility of the residual pollutants (Park et al., 2007). Therefore, the chemical to be used for environmental applications should fulfill the following requirements (Wong et al., 1997; Park et al., 2007):

- They must be non-toxic and environmentally compatible;
- High biodegradability;
- Small sorption (to avoid losses of the injected chemicals due to sorption on soil surface, which would result in a clogging of the soil pores and reduce

- the effectiveness of the electrokinetic process);
- They should react with the target pollutants in short times;
- The chelating agents should have a great affinity for the target pollutants, rather than for other species that may be naturally present in soils;
- The surfactants must have high mobility, to transport HOCs, and low CMC (to achieve high removal rates with small amount of surfactants);
- Cost-effectiveness.

#### *2.4.1.4 Benefits and limitations*

If effective, electrokinetic remediation can provide important advantages for the recovery of metals and other mobile pollutants in comparison to other remediation techniques. First of all, electrokinesis can be applied both in ex situ and in situ applications (Acar et al., 1995; Li et al., 1996; Yu and Neretnieks, 1997; Rahner et al., 2002; De Battisti et al., 2006; De Gioannis et al., 2007a,c). In particular, it can be easily and successfully applied for the treatment of fine-grain soils and sediments (like soils with significant clay and silt contents), which are very difficult to treat with in situ conventional methods, because their low permeability and high sorption capacity constrain the applicability of most chemical and physical remediation techniques. In situ electrokinetic remediation can also be applied for the treatment of soils that are difficult to access with other methods (Lynch et al., 2007).

Moreover, this technique was often reported to be cost-effective for soil remediation, and the treatment costs due to the energy expenditures can be limited by a proper selection of low current/voltage values (Acar et al., 1995; Yu and Neretnieks, 1997; Rahner et al., 2002; Virkutyte et al., 2002).

Another important advantage of electrokinetic remediation is that it seems to be capable of achieving a quite homogeneous cleanup even in case of heterogeneous media. In fact, while the hydraulic conductivity of fine-grain and coarse soils can vary of several orders of magnitude, the electric conductivities of these soils are within an order of magnitude. As a result, when a voltage gradient is applied across an heterogeneous deposit, the electric field in different soil layers will be similar, and the resulting electromigration transport rates will be similar as well (Li et al., 1996; Yu and Neretnieks, 1997; Alshawabkeh, 2001; Virkutyte et al., 2002).

However, the drawbacks of such remediation technique must be taken into account. Firstly, in order to be effective, the process may require the addition of conducting fluids to improve soil conductivity; alternatively, the process may require an acid conditioning to

solubilize the target compounds. If a proper solubilization cannot be achieved, the treatment may fail in attaining a good contaminant removal. The need for soil conditioning may significantly increase the overall treatment cost. The effectiveness of this method can be hindered by side reactions, competition between ionic species, insufficient soil moisture content, and detrimental effects on the electrodes. Above all, precipitation reactions can affect the success of the electrokinetic removal. The precipitation/dissolution equilibrium is influenced by soil pH, which also affects the negative surface charge of clay particles, which determines the electroosmotic flow rate. If suitable pH conditions are not created, the process may fail in achieve a complete pollutant removal, and this can lead to the necessity of applying enhancing solution, thus rising the technical difficulty and the costs of the system implementation (Acar et al., 1995; Alshawabkeh, 2001; FRTR, 2002; Virkutyte et al., 2002; De Gioannis et al., 2007a,c).

The rate of pollutant removal may depend on the contaminant type and on the distribution. For example, dense, localized deposits of pollutants, with low surface area to mass ratios and relatively few active sites, will be more difficult to solubilize. Certain contaminants are less amenable recovered than others are, while the effects of aging and interactions with soil chemicals might make remediation in the field more difficult than is reported here for spiked laboratory samples (Wong et al., 1997). In metal electrokinetic remediation, the contemporaneous presence of different species could reduce the overall recovery efficiency (Turer and Genc, 2005), as the remediation efficiency can be constrained by ionic competition, especially in case of low target ion concentrations and high nontarget ion concentrations (Virkutyte et al., 2002).

Moreover, the presence of buried metallic or insulating material can induce variability in the electrical conductivity of the soil; in particular, deposits that exhibit very high electrical conductivity can cause the technique to be inefficient. Metallic electrodes may dissolve as a result of electrolysis and introduce corrosive products into the soil mass (FRTR, 2002).

On the whole, the contaminant transport rates and the efficiency of the process depend heavily on the soil type, mineralogical composition and on the pore water composition. Therefore, even in homogenous and saturated conditions, the complex geochemical reactions make it difficult to predict transport rates (Alshawabkeh, 2001; Virkutyte et al., 2002). Thus, the effectiveness of the electrolysis must be evaluated under site-specific conditions, in order to assess the reactions involving the target pollutants and to individuate the best operating conditions, as voltage, treatment duration and conditioning fluid.

### 2.4.1.5 Electrokinetic barriers

A particular application of the electrokinetic processes involves the creation of an electrokinetic barrier, also named as electro-fencing, whose aim is to prevent the spreading of pollutants in the environment into uncontaminated soils (Narasimhan and Sri Ranjan, 2000; Lynch et al., 2007).

In these systems, the electroosmotic and electromigration flows generated by the electric fields are used to counteract the effect of natural hydraulic gradients or chemical diffusion. These phenomena are used as a barrier to prevent spontaneous contaminant migration (Figure 2.13).

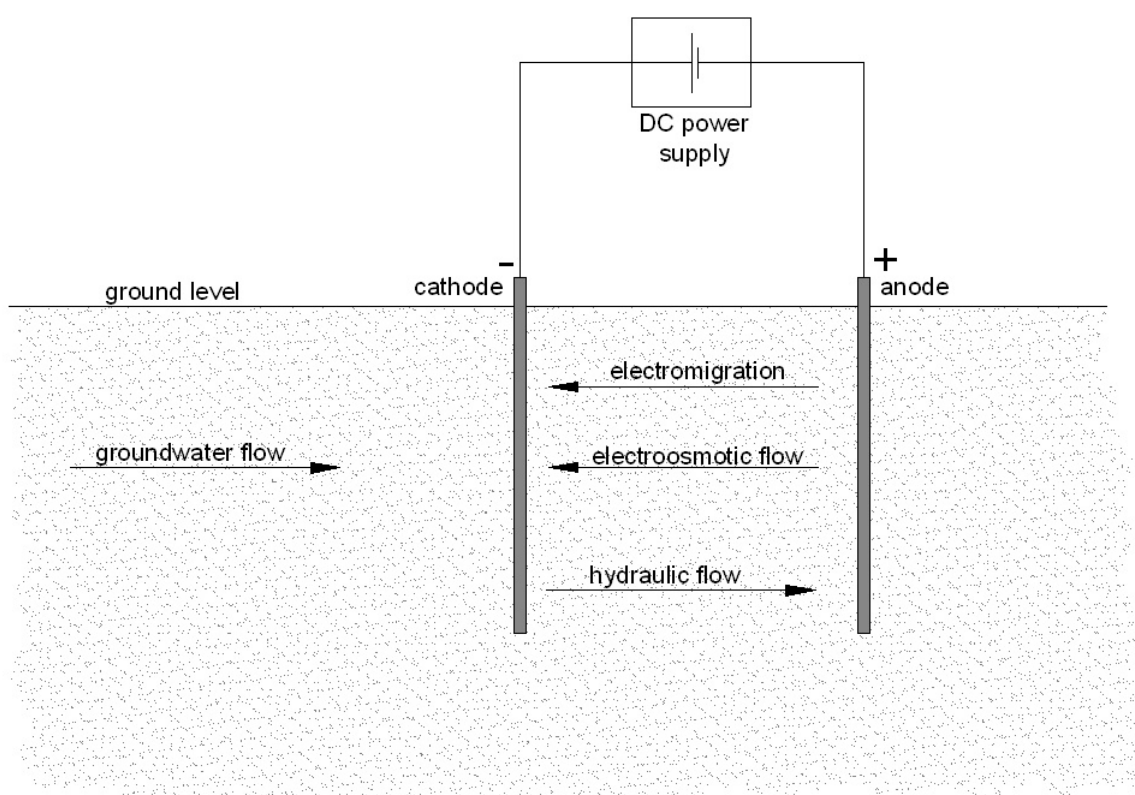


**Figure 2.13 – Schematic diagram of an electrokinetic barrier to prevent underground pollutant spreading.**

In electrokinetic barriers, the optimum voltage is the one at which the target pollutants are just stopped from moving downstream with groundwater, while greater voltages would lead to a waste of power (Lynch et al., 2007). Since electrokinetic barriers do not aim at removing pollutants but only at containing them, they usually operate at lower voltage values than traditional electrokinetic applications, in order to reduce the energy expenditures and therefore the operating costs of the barrier. Alternatively, the barrier can be operated by pulsed power, i.e. alternating periods of applied voltage gradient

and of no voltage gradient (Lynch et al., 2007).

The barrier implementation depends on the target pollutant to be constrained. For example, if both cations and anions must be arrested, a triple row of anodes and cathodes may be necessary for the barrier effectiveness (Narasimhan and Sri Ranjan, 2000). As for traditional electrokinetic methods, the operating parameters (e.g voltage gradient and power timing) must be evaluated under site-specific conditions, as the type of pollutant and the soil characteristics may affect the system efficiency (Lynch et al., 2007).

#### *2.4.1.6 Different applications of the electrokinetic techniques*

Electrokinesis has proven to be able to remove polar organic compounds or partially dissociated organic species, such as acetic acid and phenols. However, because of their low solubilities and slow desorption rates, many apolar organic pollutants, like HOCs, are difficult to remove with traditional electrokinetic methods. For this reason, electrokinesis has been combined with other remediation technologies, as bioremediation (electro-bioremediation), and permeable reactive barrier (EK-PRB systems). These remediation techniques are described as follows.

Electrokinetic methods could be used also to promote the delivery of reactant in fine-grain soils, in order to degrade immobile pollutants. For example, these methods have been applied for the delivery of nanoscale iron particles (NIPs) which can be used to achieve the reductive degradation of chlorinated compounds (Reddy et al., 2007).

The same enhanced electrokinetic process, with the use of surfactants, chelating agents or complexing agents, described in Chapter 2.4.1.3, can be considered as a combination of electrokinesis and of soil flushing.

Another important and innovative technology for the remediation of organic pollutants relies on the integrated use of electrokinetic transport and chemical oxidation. Since this method is deeply related to the topic of this research, its features are outlined in detail in Chapter 2.4.2.

##### *2.4.1.6.1 EK-PRB systems*

Electrokinetic remediation has been applied in combination with permeable reactive barriers (PRB), the process being sometimes indicated as EK-PRB systems. In such systems, the electric fields are used to improve the contaminant flow across the reactive materials, where they can be degraded or absorbed (Van Cauwenberghe, 1997; Chung, 2005; Chung and Lee, 2007; De Gioannis et al., 2007b). PRB can be filled with different

reactant materials, as adsorbant agents, zeolites, activated carbons, iron powders, atomizing slag, etc. The coupling of these two remediation techniques proved to be particularly effective for the in situ treatment of contaminated groundwater.

A particular combination of electrokinetic methods and reactive barriers is used in the Lasagna<sup>TM</sup> process (Ho et al., 1997; Van Cauwenberghe, 1997; Virkutyte et al., 2002). This application includes the presence of several permeable “treatment” zones, created by mixing the soil with adsorbent agents (e.g. activated carbons), catalytic reagents, buffering solutions, oxidizing agents, etc. (Figure 2.14). When an electric field is applied to this system, the electrokinetic phenomena promote the contaminant transport into the treatment zones, where they can be degraded or immobilized. This scheme can be applied either in an horizontal or in a vertical configuration, depending on the site conditions (Ho et al., 1997).

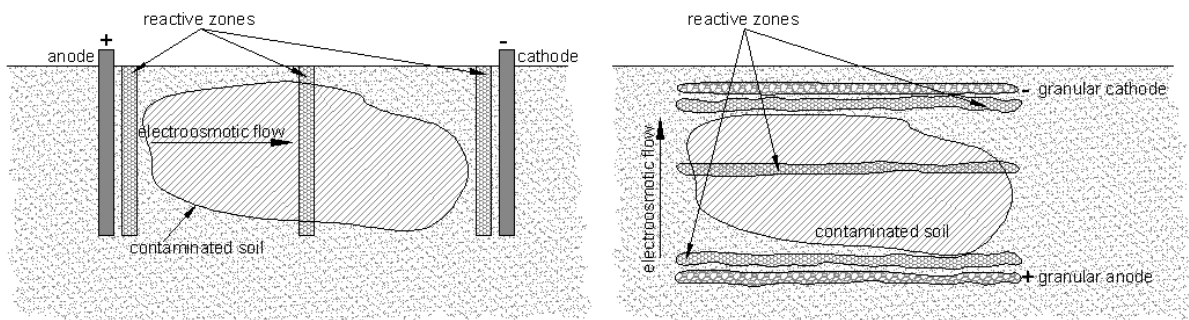


**Figure 2.14 – Schematic diagram of Lasagna<sup>TM</sup> EK-PRB systems: vertical configuration (on the left) and horizontal configuration on the right) (Ho et al., 1997).**

#### 2.4.1.6.2 *Bioelectrokinetic remediation*

Studies have been conducted to investigate the application of DCTs to achieve the transport of nutrients, electron acceptors and other additives to enhance the in situ bioremediation processes, the method being named as bioelectrokinetic remediation, electro-bioremediation or electro-biofence (Acar et al., 1995; Van Cauwenberghe, 1997; Carter et al., 2005; Godschalk and Lageman, 2005; Lee et al., 2005b; Suni and Romantschuk, 2005; Luo et al., 2006).

This remediation technique plays on the fact that nutrients, like nitrogen, phosphorus, oxygen donors, organic compounds and other micronutrients required for biodegradation, once dissolved in the groundwater, occur almost always as electrically charged compounds, and can hence be electrokinetically dispersed through the soil (Godschalk and Lageman, 2005). Also bacterial cells can be transported during the electrokinetic treatment (De Flaun and Condee, 1997; Wick et al., 2005), while the



electrochemical generation of hydrogen and oxygen can favor the microbial degradation (Tiehm et al., 2005). Moreover, the electrical methods can be used to increase the soil temperature and therefore to improve the rate of biological activity (Lageman and Godschalk, 2005; Kim et al., 2005b). Empirical evidence has shown that nutrients can be effectively be transported by electrokinetic methods, the biologic activity can be improved and contaminants, including chlorinated VOCs and phenols, can be degraded (Godschalk and Lageman, 2005; Luo et al., 2006), provided that the current intensities are low enough not to inhibit degrading bacteria activity (Lohner and Tiehm, 2005). However, the applicability of such techniques must be evaluated case to case, as the changes in the soil chemical conditions (e.g. soil acidification) could hinder bacteria activity (Lear et al., 2007).

## **2.4.2 Electrokinetic-Fenton process**

In some recent studies traditional chemical oxidation was used in combination with electrochemical methods. Different reactants were tested for this purpose, including hydrogen peroxide, Fenton's reagent, chlorine species or persulphate, good results attained on different organic contaminants, as chlorinated solvents and PAHs (Yang and Liu, 2001; Kim et al., 2005a; Park et al., 2005; Kim et al., 2006; Isosaari et al., 2007; Szpyrkowicz et al., 2007, Zheng et al., 2007). Significant benefits seem to be possible by integrating electrokinetic remediation with in situ chemical oxidation, because the electrokinetic treatment is supposed to facilitate the oxidant delivery and to promote the production of radicals (Isosaari et al., 2007).

In particular, the combination of electrokinesis and chemical oxidation with Fenton's reagent has recently gained attention from various Authors (Yang and Liu, 2001; Kim et al., 2005a) for the removal of immobile organic compounds, the process being names as electrokinetic Fenton (EK-Fenton). The degradation mechanisms of the EK-Fenton processes depend on both the mineralization pathways of chemical oxidation (hereby described in detail in Section 2.4.2.1) and of the electrokinetic transport (Section 2.4.2.2).

### *2.4.2.1 Chemical oxidation*

Chemical oxidation is a common technique for contaminated soil remediation. In the past years it has been extensively applied for the degradation of organic pollutants, including many recalcitrant compounds (ITRC, 2005).

The oxidants most commonly used for environmental purposes are ozone, hydrogen peroxide, permanganate and persulfate, while in advanced oxidation processes (AOPs) various combinations of reactants are used to enhance the formation of highly reactive radicals, which may attack and mineralize even the most recalcitrant organic compounds. Among AOPs, the Fenton's reagent, activated persulfate and perozone (i.e. a combination of ozone and hydrogen peroxide) are the techniques most extensively applied for soil treatment.

#### 2.4.2.1.1 *Hydrogen peroxide and Fenton's reagent*

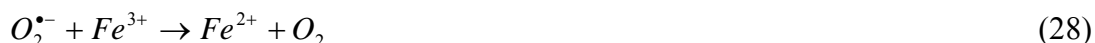
Hydrogen peroxide (H<sub>2</sub>O<sub>2</sub>) is a liquid oxidant widely used in environmental applications, commonly at concentrations ranging from 3% to 35% (ITRC, 2005; Rivas, 2006). The dosage of hydrogen peroxide leads to the production of hydroxyl radicals (<sup>•</sup>OH), which are very strong non-selective oxidizing agents (with a standard oxidation potential, versus the standard hydrogen electrode (SHE), of about 2.8 V), able to react both with alkanes and aromatic compounds (Watts et al., 2002; ITRC, 2005; Rivas, 2006). Hydrogen peroxide can be used alone, but it is considered not kinetically fast enough to degrade most of organic contaminants before its decomposition occurs (ITRC, 2005).

In Fenton's reagent, hydrogen peroxide is dosed together with a solution of a transition metal (typically iron) to enhance the radical formation. The catalyst addition dramatically increases the peroxide oxidative strength (Watts and Dilly, 1996; Kong et al., 1998; Nam et al., 2001; Kakarla et al., 2002; Watts et al., 2002; Bogan and Trbovic, 2003; Flotron et al., 2005; Watts et al., 2005; ITRC, 2005; Bissey et al., 2006; Huling and Pivetz, 2006; Rivas, 2006; Sun et al., 2007b).

The typical Fenton's reaction is based on the hydrogen peroxide decomposition into hydroxyl radicals in the presence of ferrous iron, according to the reaction:



This catalytic reaction is propagated by the Fe(III) reduction, which leads to the Fe(II) regeneration:



Since in environmental conditions iron is mainly found as Fe(III), low pH (optimal range about 3.5-5) or chelating agents (like citric acid, cyclodextrins, EDTA, catechol, etc.) can be used to increase the availability of iron(II), to enhance the Fenton's reactions (ITRC, 2005; Sun et al., 2007).

Once hydroxyl radicals have been created, the degradation can be due either to

hydrogen abstraction (reaction 29) or to hydroxyl addition (reaction 30) (Flotron et al., 2005):



In modified Fenton's system, the radical formation is enhanced by the addition of chemicals (e.g. chelating agents) and/or by high peroxide concentrations.

When high oxidant concentrations are used, many complex reactions are involved in the Fenton's system, and numerous reacting species can be generated in addition to hydroxyl radical, including hydroperoxide radicals ( $HO_2\cdot$ ), superoxide anions ( $O_2^{\cdot-}$ ) and hydroperoxide anions ( $HO_2^-$ ) (Watts and Dilly, 1996; Kakarla et al., 2002; Watts et al., 2002; ITRC, 2005; watts et al., 2005; Bissey et al., 2006):



These radicals are highly reactive and seem to be able to degrade even most recalcitrant compounds or contaminants in the sorbed form (Dadkhah and Akgerman, 2002; Watts et al., 2002; Kronholm et al., 2003; ITRC, 2005; Flotron et al., 2005). Therefore, vigorous oxidation condition can improve the remediation efficiency, by attacking even the most refractory compounds. On the other hand, too high peroxide concentrations must be avoided, as they can enhance the oxidant self-consumption (Kakarla et al., 2002; Flotron et al., 2005), leading to a poorer oxidant efficiency.

In soils and sediments, the presence of natural occurring iron minerals can enable the Fenton's reactions to proceed without any iron addition, if large amounts of hydrogen peroxide are dosed. Thus, the iron addition is not always required for the remediation of contaminated environmental solids, as the presence of natural iron can catalyze the formation of radicals and promote Fenton-like reactions (Kong et al., 1998; Watts et al., 2002; Flotron et al., 2005; Bissey et al., 2006; Rivas, 2006). Sometimes, co-solvents or surfactants are used in combination with the Fenton's reagent, in order to improve the effectiveness of the process (Rivas, 2006).

As the peroxide oxidation is exothermic, it can enhance the desorption and dissolution of sorbed pollutants, making them more available for the oxidation treatment. On the other hand, the temperature increase can cause the contaminant to migrate or volatilize, diffusing them into the environment (ITRC, 2005; Rivas, 2006); this must be taken into account when designing a remediation action by chemical oxidation.

So far, hydrogen peroxide and Fenton's reagent have been used to degrade a number of organic contaminants, including many types of petroleum hydrocarbons. Laboratory experiments have shown that spiked hydrocarbons can be more easily oxidized

than native pollutants, which are usually more sorbed onto solid matrices (Kong et al., 1998). It has also been noticed that in case of low contamination levels, a large amount of oxidant is required in order to allow the oxidation of sorbed hydrocarbons due to strong matrix-hydrocarbon interactions, which may reduce the cost-efficiency of the remediation process (Kong et al., 1998; Sun et al., 2007b). Therefore, the oxidation treatment seems to be more dedicated to highly contaminated environmental matrices, as the sources of contamination of industrial sites (U.S. EPA, 1998).

The main factors influencing the pollutant removal efficiencies in bench scale laboratory experiments with modified Fenton's reagent (conducted in solid-liquid suspension form, i.e. in soil slurries) seem to be the level and nature of the contamination (as contaminant concentration and contaminant availability, correlated to the date and level itself of contamination) and the solid matrix characteristics (as the organic matter content of the matrix) (Kong et al., 1998; Sun et al., 2007). In particular, contaminant availability can highly influence the treatment efficiency, the least sorbed pollutants (i.e. the species that are less hydrophobic) being the most available for oxidation, while the most hydrophobic and most sorbed molecules proved to be the most resistant to oxidation (Kong et al., 1998; Sun et al., 2007b). The effects of sorption on contaminant degradability can be minimized with high oxidant dosages, which seem to be able to oxidize also contaminants in the sorbed form (Bogan and Trbovic, 2003). The contaminant availability also depends on the solid matrix characteristic, and in particular on the content of natural organic matter. Usually, the organic matter is considered as a scavenger of active oxidant species (Kong et al., 1998; Kim and Choi, 2002; Bogan and Trbovic, 2003; Rivas, 2006), as it tends to compete with pollutants for reactant consumption. Nevertheless, recent studies showed that for soils containing less than 5% organic matter, the pollutants were adsorbed in the micropores, being less available than for soils with higher organic matter content, where pollutants are mainly sorbed onto the organic matter (Bogan and Trbovic, 2003).

#### 2.4.2.1.2 Ozone

Ozone ( $O_3$ ) is a highly reactive and powerful oxidant that has been widely used both in chemical industry and for oxidation or disinfection in the treatment of drinking water and wastewaters. In the last years, ozone has gained a considerable interest in the remediation of contaminated soils, especially sites containing low or non-volatile organic compounds that cannot be easily removed through biological methods (Masten and Davies, 1997; ITRC, 2005; O'Mahony et al., 2006; Kulik et al., 2006; Rivas, 2006).

Ozone can be used in either the gas or aqueous phase, depending on site conditions,

and it can oxidize organic compounds by direct oxidation, by indirect oxidation, through generation of hydroxyl radicals, or by both mechanisms (Kulik et al., 2006).

The direct ozone reaction with a generic organic compound with a carbon-carbon double bond can be described as follows:



The indirect oxidation mechanism involves the production of hydroxyl radicals ( $\bullet OH$ ), which may be formed due to the reaction of ozone with the hydroxide ion at neutral or basic pH (ITRC, 2005):



In AOPs, the hydroxyl radical formation can be enhanced by the combined use of ozone and UV radiation (e.g. for ex situ groundwater treatment) or by the combined use of ozone and hydrogen peroxide (perozone process).

The use of ozone in soil remediation has several benefits. First of all, after a short period of time unreacted ozone reverts back to oxygen, and therefore no toxic residues of the oxidant remain in the soil; moreover, the overall cost involved is often reported to be competitive when compared to other chemical soil remediation techniques (Masten and Davies, 1997; O'Mahony et al., 2006; Kulik et al., 2006).

The efficiency of ozonation is strongly dependent on the physical properties of soil, including the soil water and the soil composition (e.g. sand and clay content) (Kulik et al., 2006; O'Mahony et al., 2006). In particular, the soil water content can affect the transport of gaseous ozone in the subsurface and can constrain the reactions with organic pollutants (Choi et al., 2007).

Ozonation has been recently applied for the remediation of different subsurface pollutants contamination, including chlorinated compounds, PAHs and petroleum hydrocarbons (Masten and Davies, 1997; Choi et al., 2001; Choi et al., 2002; ITRC, 2005; Kulik et al., 2006; O'Mahony et al., 2006). Organic compounds treated with ozone are transformed to oxygenated intermediates which are more soluble and, thus, more biodegradable and bioavailable than the original pollutants (Kulik et al., 2006). This may lead to the potential use of a combined ozonation and biological treatment for hydrocarbon contaminated soils (O'Mahony et al., 2006).

#### 2.4.2.1.3 Permanganate

Permanganate is an oxidant agent with a standard oxidation potential about 1.7 V. It

was reported to be effective in the remediation of many petroleum hydrocarbons and it has been applied for in situ and ex situ remediation actions in the last years (Brown et al., 2003; ITRC, 2005; Huling and Pivetz, 2006). In an aqueous system the permanganate salts generate permanganate ions ( $MnO_4^-$ ), which undergoes this decomposition reaction:



Both potassium permanganate ( $KMnO_4$ ) and sodium permanganate ( $NaMnO_4$ ) can be used for environmental applications, with similar results. Despite the relatively low standard oxidation potential, permanganate salts are considered strong oxidizing agents, able to break organic molecules containing carbon-carbon double bonds, aldehyde groups, or hydroxyl groups (Brown et al., 2003; ITRC, 2005). Permanganate oxidation mechanisms at contaminated sites are quite complex, as there are numerous reactions in which manganese can participate due to its multiple valence states and mineral forms (ITRC, 2005; Huling and Pivetz, 2006).

#### 2.4.2.1.4 *Persulfate*

Persulfate is the most recent form of oxidant agent being used for environmental applications. Sodium persulfate ( $Na_2S_2O_8$ ) is the most commonly used form of persulfate salt, as the low solubility of potassium persulfate ( $K_2S_2O_8$ ) limits its application as remediation agent (ITRC, 2005; Huling and Pivetz, 2006). Persulfate salts dissociate in water to persulfate anions ( $S_2O_8^{2-}$ ), which, although strong oxidants (standard oxidation potential about 2.0 V), are kinetically slow in destroying most of organic contaminants. Like in the case of modified Fenton's reagent, the addition of transition metal ions (as ferrous ions) could activate the persulfate anion ( $S_2O_8^{2-}$ ) to produce a powerful oxidant known as the sulfate free radical ( $SO_4^{\bullet-}$ ):



Sulfate free radicals have a standard redox potential of 2.6 V and may be able to oxidize many organic pollutants (ITRC, 2005; Huling and Pivetz, 2006; Liang et al., 2004a; Liang et al., 2004b).

#### 2.4.2.1.5 *In situ chemical oxidation*

When applicable, in situ remediation technologies are preferred over ex situ techniques, as they offer many advantages in terms of cost-effectiveness and technical

difficulties.

The most critical parameters for in situ chemical oxidation are linked with the efficiency distribution of the oxidant agents (oxidant delivery) in the contaminated volume and the reactivity of the target pollutants, which may be constrained by a difficult contact between contaminants and reactants. In particular, the oxidant delivery can be highly affected by subsurface heterogeneities and by the occurrence of preferential flow pathways (ITRC, 2005; Huling and Pivetz, 2006; Rivas, 2006).

These difficulties can be overcome using ex situ chemical oxidation, which, on the other hand, requires the soil excavation, which may pose a complex technical task and usually results in a significant increase in the recovery costs.

#### *2.4.2.2 Electrokinetic-Fenton processes*

In EK-Fenton processes, the electrokinetic treatment of contaminated soil is combined with the addition of hydrogen peroxide in the anode chamber, as anolyte solution (Yang and Long, 1999; Yang and Liu, 2001; Kim et al., 2005a; Park et al., 2005; Kim et al., 2006).

A typical installation for the EK-Fenton treatment of a contaminated soil thus includes the presence of electrodes to create a voltage gradient across the soil and at least one injection well for the dosage of the oxidant solution, as shown in Figure 2.15.

So far, EK-Fenton has proven to be effective for the remediation of soils contaminated by PAHs and chlorinated solvents (Yang and Liu, 2001; Kim et al., 2005a; Kim et al., 2006).

During an EK-Fenton treatment, the migration of hydrogen peroxide, which is commonly difficult to be achieved in low permeability soils, is assumed to be enhanced by the electrokinetic transport phenomena, as electromigration and electroosmosis. Hydrogen peroxide can therefore advance towards the cathode by the electroosmotic flow (through chemical diffusion and advective transport), but it also undergoes a catalytic decomposition on the soil surface during this movement (Yang and Liu, 2001; Kim et al., 2005a; Park et al., 2005). Hence, when hydrogen peroxide is injected as anolyte solution, its residual concentration usually decreases along the treated soil from the anode to the cathode (Kim et al., 2005a; Park et al., 2005). The anions resulting from hydrogen peroxide decomposition (i.e.  $\text{O}_2^{\bullet-}$ ,  $\text{HO}^{2-}$ ) may also move toward the anode due to electromigration (Kim et al., 2005a).

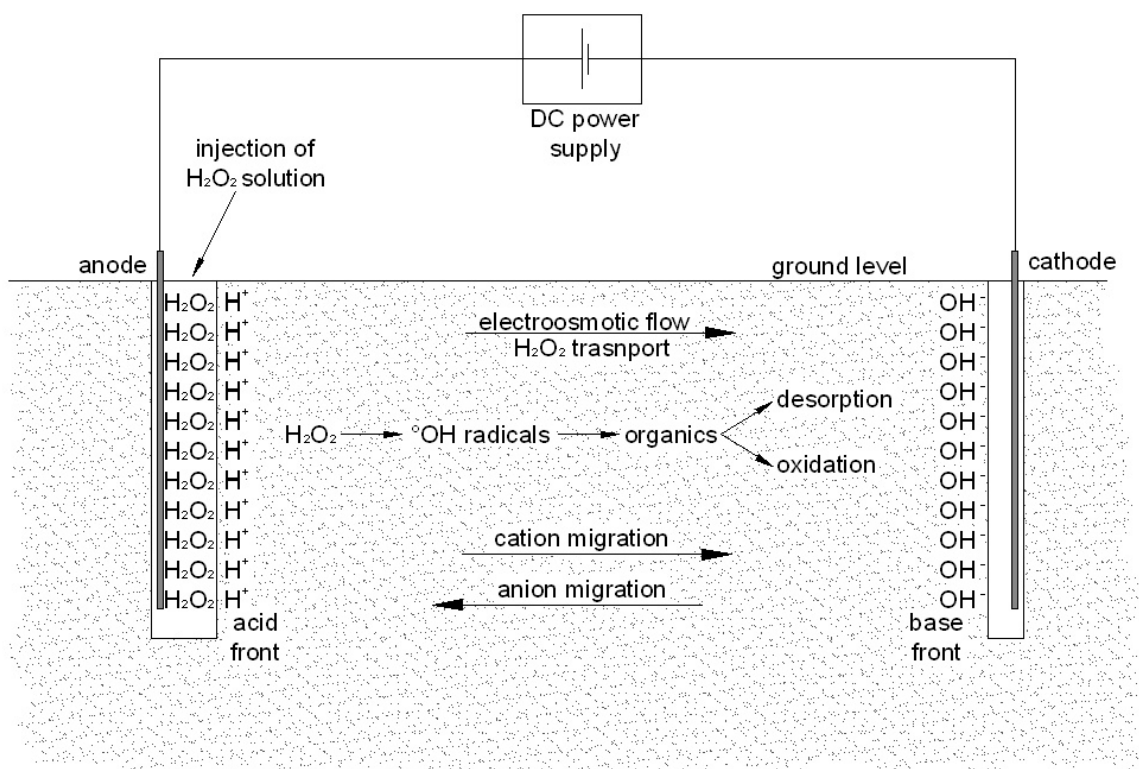


Figure 2.15 – Schematic diagram of an in situ EK-Fenton process.

In most of the EK-Fenton applications, a 3-7% hydrogen peroxide solution was used as anolyte solution, while deionized water was used as cathode reservoir fluid (Yang and Liu, 2001; Kim et al., 2005a; Kim et al., 2006). Bench-scale experiments of EK-Fenton treatment proved that hydrogen peroxide could be transported along the treated soil within a 10 cm long soil specimen under voltage gradients of 1-1.5 V/cm, under a proper acid conditioning at the anode chamber (Yang and Liu, 2001; Kim et al., 2006),

Under these conditions, the contaminant degradation is often more effective near the anode, because of the high hydrogen peroxide concentrations.

During the enhanced EK-Fenton processes, two pollutants remediation mechanisms occur concurrently:

- Contaminant migration due to the electrokinetic transport;
- Contaminant degradation due to the mineralization processes.

Either mechanism can be predominant, depending on the treatment conditions, i.e. strength of the electroosmotic flow and the amount of hydroxyl radicals generated. In most of the EK-tests that have been performed so far, the major mechanism of pollutant removal was thought not to be removal by electrokinetic transport but degradation by chemical oxidation (Kim et al., 2005a).

In sum, EK-Fenton technique is a complex process, which relies on different



phenomena, including (Kim et al., 2005a):

- Electroosmotic transport;
- Electromigration;
- Electrolysis reactions;
- Fenton-like reactions (hydrogen peroxide decomposition into hydroxyl radicals);
- Reactions with organic contaminants (pollutant degradation) and naturally occurring organic matter.

All these phenomena are affected both by the treatment options (e.g, voltage, electrical current, acid conditioning, oxidant dose) and by the characteristics of treated soils and of the target contaminants.

The electroosmotic flow rate is known to be dependent on many factors, including voltage, current and characteristics of the electrolyte solution. In particular, the electroosmotic flow was reported to increase significantly as the current flowing increases (Hamed and Bhadra, 1997; Kim et al., 2005a). Moreover, the use of hydrogen peroxide as anolyte solution was shown to result in an increase in the electric current flowing, compared to the used of deionized water, the electric current increasing as the hydrogen peroxide concentration increased (Kim et al., 2005a). This is due to the fact that the dosage of hydrogen peroxide results in the generation of ions in the pore water, which may improve the soil conductivity. Increasing the current density may also reduce the time needed for the acid front generated at the anode to reach the cathode (Kim et al., 2005a).

In certain studies, an acid conditioning was used to enhance the electrokinetic transport and to improve the degradation efficiency (Kim et al., 2005a; Kim et al., 2006). In fact, experiments showed that the use of acid conditioners (e.g. H<sub>2</sub>SO<sub>4</sub>) in addition to hydrogen peroxide in the anolyte solution could significantly improve the electroosmotic flow rate (Kim et al., 2006). The acid conditioning was also reported to be capable of reducing the hydrogen peroxide decomposition rate, and therefore to improve the hydrogen peroxide stability, which is a key factor in the effectiveness of the Fenton-like processes. In sum, for the EK-Fenton process to be effective, an injection of acid seems to be necessary, but to an extent that doses not decrease the electroosmotic flow rate (Kim et al., 2005a).

During acid-enhanced EK-Fenton processes (with hydrogen peroxide addition and strong acid conditioning), certain desorption of transportation of apolar compounds was occasionally observed (Kim et al., 2006). This is thought to be due to a combination of a release mechanism, caused by the radical species as O<sub>2</sub><sup>•-</sup> and HO<sub>2</sub><sup>-</sup>, and of the electroosmotic transport due to the enhanced electrokinetic process (Watts et al., 1999).

Recent studies investigated the effectiveness of integrated chemical oxidation-electrokinetic treatment with the dosage of different oxidant agents, like persulphate

(Isosaari et al., 2007). This reactant was reported to be even more effective than hydrogen peroxide in PAH degradation, probably because of its higher stability in comparison to hydrogen peroxide.

Sometimes, iron powders are added at the electrode compartments to improve the hydrogen peroxide decomposition into hydroxyl radicals (Kim et al., 2005a), and a few studies investigated the influence of different forms of iron were tested as catalysts for Fenton reactions, including (Yang and Liu, 2001; Kim et al., 2005a; Kim et al., 2006):

- FeSO<sub>4</sub> solution.
- Scrap iron powder (SIP), which is a granular material and may be used in the form of a permeable reactive barrier in the treated sample. SIP-PRBs have gained attention mainly for the removal of chlorinated solvents, like TCE, which could be detoxified by the zero-valent iron in the barrier (Yang and Liu, 2001).

The addition of iron can improve the hydrogen peroxide catalytic decomposition, but may also lead to the production of Fe(OH)<sub>3</sub> precipitates (Yang and Liu, 2000), which can clog soil pores and constrain soil permeability.

When oxidizing conditions are created in the soil, they can affect the metal equilibrium and the electrokinetic phenomena. In fact, the oxidation processes can mineralize the organic matter, which often adsorb metal to a significant extent, thus making metals more available for the electrokinetic recovery. On the other hand, metals that usually occur in soils in the reduced forms may be oxidized; this can affect their solubility equilibrium, which is also highly dependent in the soil pH (Szpyrkowicz et al., 2007).

The effectiveness of the EK-Fenton process is also known to be dependent on the stability of the hydrogen peroxide solution, with the best contaminant removals being achieved when the stabilization of hydrogen peroxide was improved (Kim et al., 2006).

In the same way as chemical oxidation, soils with higher contents of naturally occurring organic matter were reported to result in worse contaminant destruction efficiencies, as the organic matter can act as an oxidant scavenger, consuming the hydroxyl radicals produced by the electrochemical processes, and competing with contaminant for the mineralization (Yang and Liu, 2001). Moreover, organic matter can also absorb target pollutants, preventing them to come in contact with the degrading agents.

### **2.4.3 Electrochemical oxidation**

So far, the electrooxidation processes, and in particular the methods based on the electrochemical production of hydrogen peroxide (Electro-Fenton processes), have been

successfully applied for the degradation of various pollutants from water, wastewater, and sludge. The target pollutants included chlorinated solvents, aromatic compounds, PAHs and refractory wastes (Panizza and Cerisola, 2001; Iniesta et al. 2001; Sopchak et al., 2002; Meinero and Zerbinati, 2006; Szpyrkowicz et al., 2007; Zheng et al., 2007). In wastewater treatments, good COD removals proved to be attained within one or a few hours with current densities of 100-200 mA/cm<sup>2</sup> (Meinero and Zerbinati, 2006; Wang et al., 2007).

Theoretically, the same electrochemical oxidation processes that occur in aqueous systems could also occur in soils. These include:

- The direct electro-generation of radicals species, e.g.  $\bullet\text{OH}$  and  $\text{O}_2\bullet^-$ , from water at the electrodes (cathodes) (see reaction 17 on page 31) and their subsequent diffusion within the soil matrix, due to the combined effect of chemical diffusion, electroosmotic advection and electromigration (Sanromán et al., 2005; Wang et al., 2007).
- The indirect electrochemical oxidation, i.e. the electrochemical production of hydrogen peroxide ( $\text{H}_2\text{O}_2$ ) from oxygen reduction (Sanromán et al., 2005) (see reaction 18 on page 31). Since soils commonly contain significant amounts of iron, once hydrogen peroxide has been created, hydroxyl radicals ( $\bullet\text{OH}$ ) can be produced, according to the catalytic Fenton's reaction (reaction 19 on page 32).

Moreover, according to the microconductor principle (Rahner et al., 2002) (see Chapter 2.3.4.), in soils these redox reactions can occur simultaneously at the interfaces between microconductor particles and pore water, thus leading to the diffused production of hydrogen peroxide and radicals, which allows the oxidation processes to occur within all the treated volume.

The degradation of organic pollutants from soils by electrochemical treatments with the addition of a chlorine-enhanced leaching solution has also been investigated (Szpyrkowicz et al., 2005), in order to produce the same chlorine-based oxidant agents that are sometimes used for water treatment (reactions 14, 15 and 16, on page 31).

Until now, a few studies have investigated the use of unenhanced electrochemical treatments for soil recovery, proving these methods to be effective for the degradation of indigo, an aromatic compound being used as textile dye (Sanromán et al., 2005) and of PAHs (Doering et al., 2001a,b) from contaminated soils, both in laboratory-scale experiments and in real-scale applications.

However, the examples of application of such techniques to soil recovery are currently very limited, and there is a general lack of knowledge about their capabilities in pollutant degradation in soils. In particular, the application of such remediation techniques for the recovery of aliphatic hydrocarbons and petroleum products is still very limited.

Some real-scale and pilot-scale case studies of electrooxidation applications are reported in Table 2.1.

**Table 2.1 – Case studies of electrooxidation for soil and sediment remediation.**

Case	Remediation Action	Scale	Material	Target contaminants	Results	Year	Reference
Enns (Austria)	Electrooxidation	Real scale	Pile of excavated soil	PAHs	500 t of soil were treated; PAHs were reduced from above 1000 mg/kg to 55 mg/kg in 70 days	-	(Doering et al., 2001a,b)
Lake Superior, Minnesota (USA)	Electrooxidation, Electrokinetics	Pilot scale (field test)	Lake sediments	PAHs, Hg	Reduction of Hg, PAH and phenol contents (removal efficiencies unavailable)	2002	(U.S. EPA, 2002a)
TPH Remediation in Northern Denmark	Electrooxidation	Real scale	Soil	Petroleum hydrocarbons (TPH) (Accidental oil spill)	Removal of about 1400-2400 L of oil. Complete removal of TPH from above 2000 mg/kg. Treatment duration: 2 years, with stop during tourism season	1997	(ECP, 2003)
VOCs Remediation Georgia (USA)	Electrooxidation	Real scale	Soil	Chlorinated solvents	Contaminant removal in about 210 days. TCE was reduced from 15500 µg/kg to less than 500 µg/kg	2004	(ECP, 2003)
Remediation of a Tank Farm in Greater Stockholm, Sweden	Electrooxidation	Real scale	Soil (thick clay)	Petroleum hydrocarbons (TPH)	76200 t of hydrocarbon-saturated soil were treated; the TPH concentration was reduced to less than 500 pm in about 10 days (removal efficiencies unavailable)	2003	(ECP, 2003)

Röhrs et al. (2002) investigated the occurrence of the electrochemically generated reactions that could lead to the organic pollutant degradation. According to these studies, redox reactions induced by the presence of microconductors may be regarded as the main degradation pathway for chlorinated hydrocarbons.

Electrochemically generated redox reactions were observed to start shortly after the application of the electric field (Röhrs et al., 2002). Moreover, the use of DC lead to better results than the use of AC in terms of organic mineralization. Two explanations have been given for this effect (Röhrs et al., 2002):

- The changes of the polarization in AC systems cause every time a change of the double layer. This results in the consumption of a relatively high capacitive part of the current due to the double layer discharging or recharging. Therefore, the current flow through the conducting particles is too low to induce redox reactions.
- The transport phenomena (electromigration and electroosmotic advection) induced by the DC processes may help the transport of reactive species, thus enhancing the mineralization processes. If the electrode polarity is reverted, the transport mechanisms are reverted too.

While the time required to complete an electrokinetic remediation process is highly dependent on the features of the material to be treated, electrooxidation has been reported to work rapidly, on the order of months, at costs competitive with excavation and disposal (Doering et al., 2002).

In the same ways as for the electrokinetic processes, a rise in the strength of the electric field did not result in improvements of the mineralization processes (Acar et al., 1995; Röhrs et al., 2002).

Besides this important empirical evidence, so far a complete explanation of the electrochemically induced degradation mechanisms has not been given. Hence, further studies are needed to understand the phenomena ruling the degradation process and to assess the efficacy of the electrochemical treatment towards different organic pollutants.

## **2.4.4 Practical aspects of soil remediation by DCTs**

### *2.4.4.1 Electrode configuration and operating conditions*

Most of the experience gained so far about real-scale outdoor implementations of DCTs concerned the use of electrokinesis for the removal of metals from soils and sediments. Different configurations can be used for these applications. For example, the

electrodes can be made of different materials, as stainless steel, carbon or noble metals, and they can be placed in the soil either in a vertical or horizontal array, at various distances.

A significant interest in the effectiveness of different electrode materials has recently arisen for the application of electrochemical remediation techniques, especially in aqueous systems, as for groundwater and wastewater treatment, with the use of platinum,  $\text{PbO}_2$ , titanium, boron doped diamond, gold, silver, and ceramics (Röhrs et al., 2002; Meniero and Zerbinati, 2006; Laine and Cheng, 2007; Lee et al., 2007). Nevertheless, since in soil remediation all electrodes undergo corrosion, fouling and passivation, the use of low cost materials, as stainless steel, titanium or graphite, is commonly preferred for real-scale applications (Acar et al., 1995; Virkutyte et al., 2002; Lohner and Tiehm, 2005; Kim et al., 2005c). The use of higher grade carbon or inert materials may be preferred for anodes, which may undergo important corrosion processes, while low grade carbons may be used for cathodes (Acar et al., 1995; Röhrs et al., 2002; Lee et al., 2007). Graphite electrodes were sometimes reported to be superior to stainless steel electrodes in terms of pollutant degradation in EK-Fenton processes (Yang and Liu, 2001).

Sometimes, open electrodes (i.e. perforated electrodes or electrodes made up to porous materials) are used. These electrodes allow the dosage of processing fluids, like electrolyte solutions, acid solution, surfactants, or other conditioning agents.

For in situ enhanced electrokinetic applications, the electrodes are usually placed in wells with permeable walls and filled with processing fluid to promote the pollutant extraction (Röhrs et al., 2002), while when the electrooxidation is used, the contaminant recovery systems are not necessary.

Different possible electrode distributions can be used for the electrochemical soil treatment, including both linear configurations (with arrays of cathodes and anodes) and polar configurations, e.g. with a central cathode and radially-distributed anodes (Alshwabkeh, 2001; Kim et al., 2005c). This latter configuration is especially useful in electrokinetic processes, as it can concentrate the target pollutants near the central cathode and it can enhance the acid to proceed towards the cathode, while constraining the migration of the base front. Each electrode distribution generates an area of effective electric field and an area of ineffective electric field. Thus, the electrode distribution must be carefully designed to be capable of treating the target volume, as the presence of inactive areas could affect the treatment success (Turer and Gneć, 2005). Some examples of electrode distribution are shown in Figure 2.16.

How to place the electrode in the soil has also been discussed, in order to define a reliable and efficient electrode configuration (Virkutyte et al., 2002). Certain Authors recommend placing the electrodes directly into the wet soil (Acar and Alshwabkeh, 1993;

Reddy et al., 1999; Virkutyte et al., 2002), while other Authors suggest to place the electrodes not directly into the wet soil mass, but into an electrolyte solution, attached to the contaminated soil, or else to use different membranes and other materials (Van Cauwenberghe, 1997; Virkutyte et al., 2002).

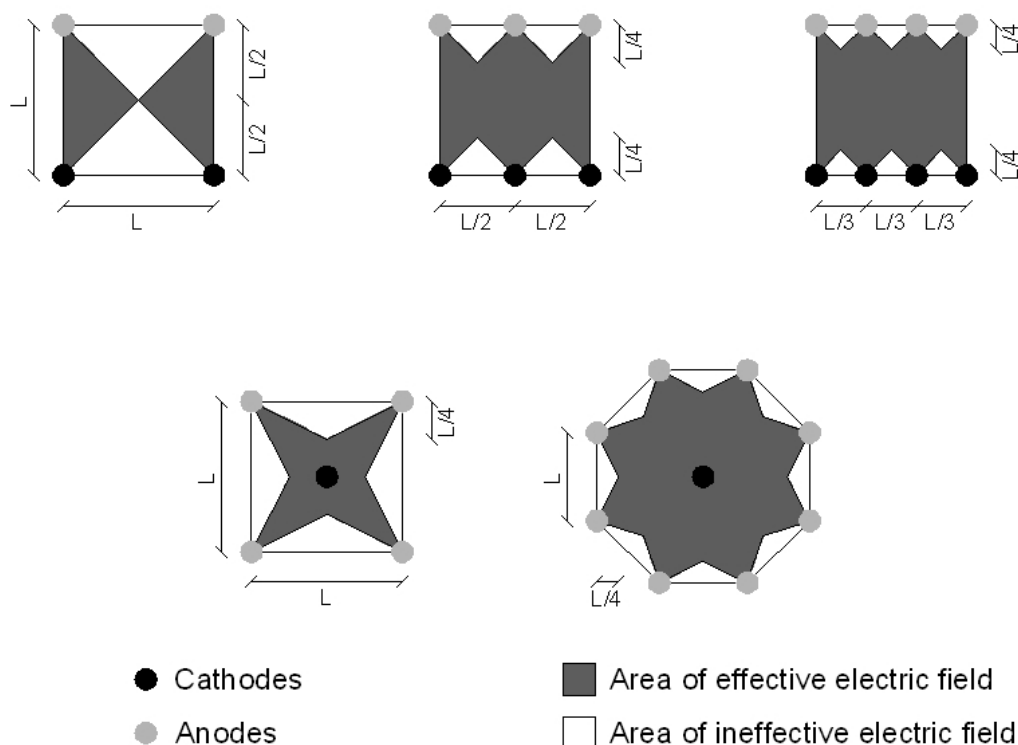


**Figure 2.16 – Examples of possible electrode distribution for electrochemical soil treatment (Alshawabkeh, 2001). Each configuration generates an area of effective electric field and an area of ineffective electric field.**

Usually, for real scale in situ DCT applications, distances across cathodes and anodes ranging from one to few meters are used (Alshawabkeh, 2001; Virkutyte et al., 2002). Common applied voltage gradients range from 0.5 V/cm to more than 1 V/cm, with electric current densities of the order of 1-10 A/m<sup>2</sup> (Acar et al., 1995; Van Cauwenberghe, 1997; U.S. AEC, 2000; Alshawabkeh, 2001; FRTR, 2002 Chung and Kamon, 2005; Reddy et al., 2006). Laboratory tests showed that increasing the current density did not always result in an improvement in the contaminant removal efficiency, but increased the energy expenditures (Acar et al., 1995).

Because of their rather simple setup, electrochemical systems are often considered less environmentally intrusive than many traditional chemical remediation methods (Laine and Cheng, 2007).

#### 2.4.4.2 Cost analysis

When selecting the best remediation option for a contaminated site, several parameters must be taken into account, including the effectiveness towards the target contaminants, the development status of the technology, the availability of the technique, the time needed for the cleanup. Among these parameters, the overall treatment cost is a key-factor in evaluating the feasibility of a recovery method.

The overall cost of DCTs includes a capital cost for the technology implementation (including designing of the remediation action, testing, equipment, utility installation, etc.) and the operation and maintenance (O&M) costs (including materials, energy expenditures, analysis, etc.) (U.S. AEC, 2000).

Most of data available about the cost and performance of such techniques regard electrokinesis, which has received the widest attention among electrochemical remediation techniques so far.

Usually, electrokinetic remediation is reported to be a cost-effective technology. Nevertheless, the overall remediation cost is highly site-dependent and varies with many parameters, like the amount of soil to be treated, the conductivity of the soil, the type and concentration of contaminants, the need for chemical conditioners, the spacing of electrodes, and the type of process design employed (Alshawabkeh, 2001; FRTR, 2002)

Bench-scale studies suggested energy expenditures of about 10-220 kWh/m<sup>3</sup> (Acar et al., 1995; Alshawabkeh, 2001), while more reliable pilot-scale tests indicated that the energy expenditures may rise up to 500 kWh/m<sup>3</sup> or more (FRTR, 2002; Virkutyte et al., 2002). Nevertheless, a few Authors reported much higher energy expenditures (e.g. about 2000-9000 kWh/m<sup>3</sup>) for the removal of HOCs by surfactant-enhanced electrokinesis (Park et al., 2007).

The resulting cost may range from about 10 €/m<sup>3</sup> to 100 €/m<sup>3</sup> (FRTR, 2002). However, based on the site-specific conditions, the overall cost can arrive to 1200 €/m<sup>3</sup> (U.S. AEC, 2000), mainly depending on (FRTR, 2002; Virkutyte et al., 2002):

- Soil properties (e.g. moisture, texture);
- Dept of contamination;
- The cost of chemical enhancement (including the cost of conditioning fluids, if necessary, and the cost for the treatment of the process fluid, if necessary);
- The cost of system implementation (including electrodes, electrode accommodation, power supply system, etc);
- Clean-up time;
- Cost of labor;
- Energy expenses.



A possible distribution of the overall remediation expenses can be the following (Virkytyte et al., 2002):

- 40% for electrode construction;
- 10-15% for electricity;
- 17% for labor;
- 17% for materials;
- Up to 16% for licenses and other fixed costs.

Similarly to electrokinesis, the cost of EK-Fenton processes mainly depends on:

- The cost of electricity;
- The cost of the chemicals required;
- The cost of materials for treatment implementation.

For EK-Fenton processes, unit operating costs of about 1-6 \$/m<sup>3</sup> have been estimated from bench-scale tests (Yang and Liu, 2001), thus indicating that, if successful, this remediation technique can be considered highly cost-effective for soil recovery. However, to be considered reliable, these values should be confirmed by real-scale application data.

To date, no official data are available for the application of unenhanced electrooxidation for soil remediation.

## **2.4.5 Current technology status and perspectives**

So far, electrokinesis has proven to be an effective and viable technology for the remediation of a number of metals and polar pollutants from environmental matrices, including both soils and sediments. Even so, its application must be evaluated case to case by preliminary studies, since the chemistry of the target pollutants and the features of the treated matrix (like the pH, the buffer capacity, the natural organic matter content, and the occurrence of competitor ions) may determine the best remediation conditions, as the optimal voltage, the treatment duration and the need for electrolyte solutions and conditioning fluids.

Surfactant-enhanced electrokinesis and EK-Fenton are innovative methods for the remediation of organic pollutants from fine-grain soils. Such techniques are very interesting, as they can allow the recovery of contaminated matrices that are usually difficult to treat. Being quite new remediation technologies, further studies are needed to define their effectiveness towards different pollutants and their applicability in various media.

Electrooxidation has recently been reported to be capable of degrading organic pollutants in soils. However, its effectiveness must be confirmed by proper scientific

studies. Moreover, the base mechanisms of this technique are not fully understood and need to be investigated. If effective, this technology could be of a considerable practical interest, as it could allow to conduct remediation actions that would otherwise be hardly feasible, like the mineralization of immobile organics from fine-grain soils and sediments, low permeability media, matrices difficult to access or thick clays.

# Chapter 3

## Materials and Methods

In order to conduct this study, two one-dimensional experimental setups for bench-scale testing were assembled, including a preliminary test apparatus and an improved experimental device.

The main features of the experimental setups, the test procedures and the analytical methods used are shown as follows.

### 3.1 Research scheme

The research presented here was divided into two parts:

- A systematic study conducted on diesel fuel-contaminated soils, the ultimate goals being to assess the effectiveness of the electrochemical methods and to individuate the most important influence factors that can affect the remediation effectiveness.
- Feasibility studies which aimed at assessing the applicability of electrochemical oxidation for the recovery of different contaminated matrices. These studies focused on:
  - River sediments contaminated by PAHs;
  - Silty soils polluted by organolead pollutants;
  - Clayey soils contaminated by landfill leachate.

A list of all the experiments performed is provided in Table 3.1, which also indicates the main operating parameters of the tests performed, as voltages applied, test durations and specimen dimensions.

The tests carried out during this research included seven trials performed on diesel fuel-contaminated kaolin, two trials performed on diesel fuel-contaminated bentonite, three

tests performed on PAH-contaminated sediments, two tests performed on silty soils with organolead compounds and five tests performed on a clayey soil contaminated by landfill leachate.

**Table 3.1 – List of the laboratory tests performed.**

Test	Matrix	Contaminant	Sample length [cm]	Applied voltage [V]	Specific voltage [V/cm]	Duration [d]
KAO.1	kaolin	diesel fuel	10	5	0.5	28
KAO.2	kaolin	diesel fuel	10	10	1	28
KAO.3	kaolin	diesel fuel	10	30	3	28
KAO.4	kaolin	diesel fuel	10	60	6	28
KAO.5	kaolin	diesel fuel	50	50	1	28
KAO.6	kaolin	diesel fuel	10	0	0	28
KAO.HP	kaolin	diesel fuel	10	10	1	28
BEN.1	bentonite	diesel fuel	10	5	0.5	28
BEN.2	bentonite	diesel fuel	10	10	1	28
PAH.1	river sediments	PAHs	10	15	1.5	14
PAH.2	river sediments	PAHs	10	10	1	28
PAH.3	river sediments	PAHs	10	20	2	28
TEL.1	silt	oganolead compounds	10	15	1.5	14
TEL.2	silt	oganolead compounds	10	15	1.5	14
LEA.1	clay	landfill leachate	10	10	1	1
LEA.2	clay	landfill leachate	10	20	2	1
LEA.3	clay	landfill leachate	10	30	3	1
LEA.4	clay	landfill leachate	10	60	6	1
LEA.5	clay	landfill leachate	10	30	3	7

## 3.2 Experimental setups

As already noted, two one-dimensional experimental setups for bench-scale testing were developed during this study. Each experimental setup included the following elements:

- An electrochemical cell, where the soil specimen was inserted during the tests;
- A pair of plate sinless steel electrodes;
- A stabilized direct current generator, connected to the electrodes by 2.5 mm copper wires;
- Two tanks for the collection of the pore fluid potentially transported by the electroosmotic flow at the electrode compartments;

- Gas vents at the electrode compartments to allow the gases produced by the electrochemical reactions (mainly oxygen and hydrogen) to escape. All the vents were provided of valves and could be open or closed during the tests.

A scheme of this experimental setup is provided in Figure 3.1.

Two types of DC generators were used according to the experimental needs:

- A Stab AR50 by Stab, Italy, which could provide up to 15 V and up to 5 A (Figure 3.2);
- A Mitek MICP 3005S-2, which could provide up to 60 V and up to 5 A (Figure 3.3).

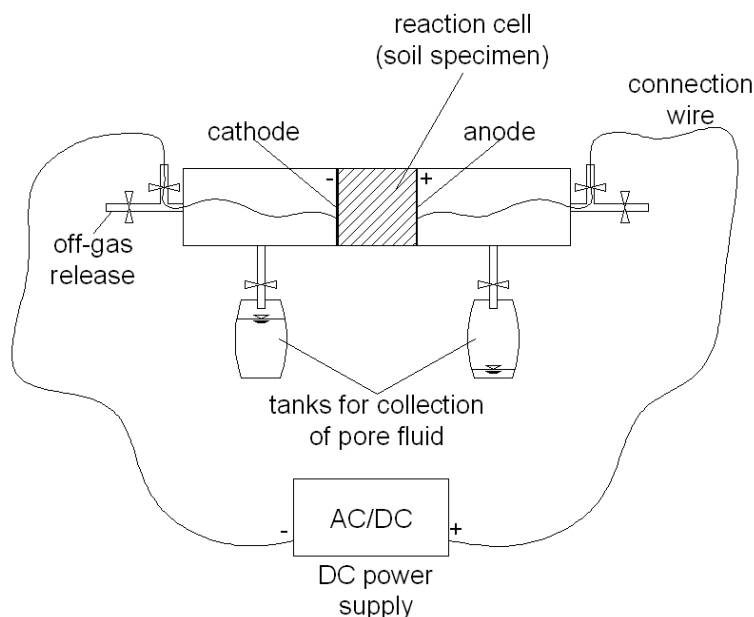


**Figure 3.1 – Scheme of the test setup used in the experimental investigation.**



**Figure 3.2 – DC generator Stab AR50 used in the experimental investigation (providing a stabilized DC up to 15 V and up to 5 A).**



**Figure 3.3 – Two DC generators Mitek MICP 3005S-2 used in the experimental investigation (each one providing a stabilized DC up to 60 V and up to 5 A).**

### 3.2.1 Setup 1

The first test setup that was assembled, named as “Setup 1”, is shown in Figure 3.5 and Figure 3.6. A schematic diagram of this experimental setup is provided in Figure 3.4.

The device included the following components:

- A cylindrical electrochemical cell (internal diameter 9 cm, length 60 cm) made up of 2 mm-thick transparent PVC (Figure 3.7);
- A pair of plate electrodes. The electrodes were made up of stainless steel and had 3 mm-wide holes to allow water to flow across them (Figure 3.8);
- A stabilized DC power supply;
- Two tanks for the pore fluid collection at the electrode compartments.

In the reaction cell, the anode and cathode were placed vertically and parallel to each other. They were kept in the proper location by plastic spacers (Figure 3.8).

To perform each test, the soil specimen was inserted and compacted in the cylindrical cell, the electrodes being kept in contact with the soil sample except for filter papers. The specimen length can be changed by varying the distance between the electrodes, ranging from 10 cm to 50 cm.

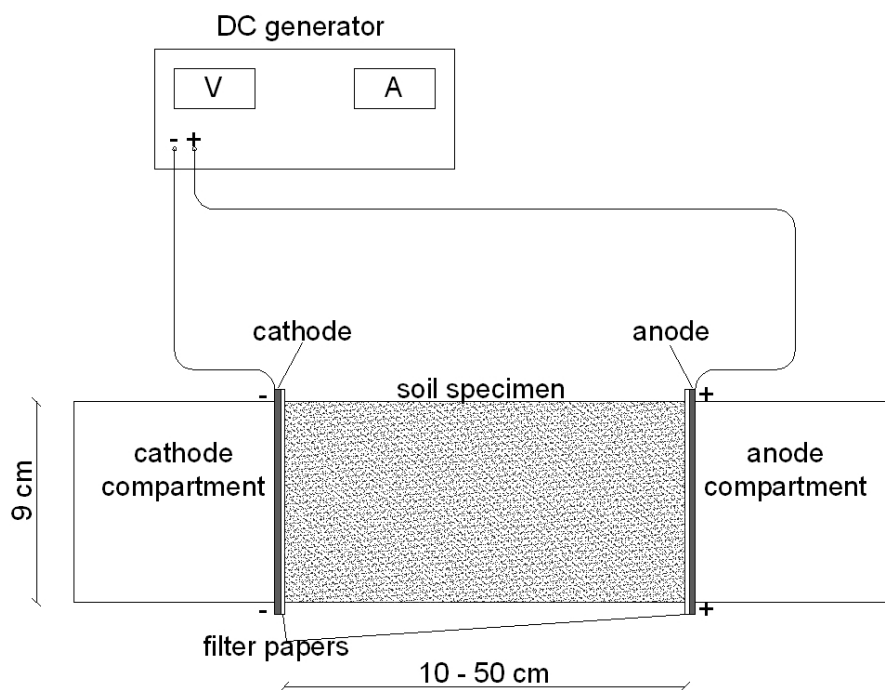


Figure 3.4 – Schematic diagram of Setup 1 used in the experimental investigation.

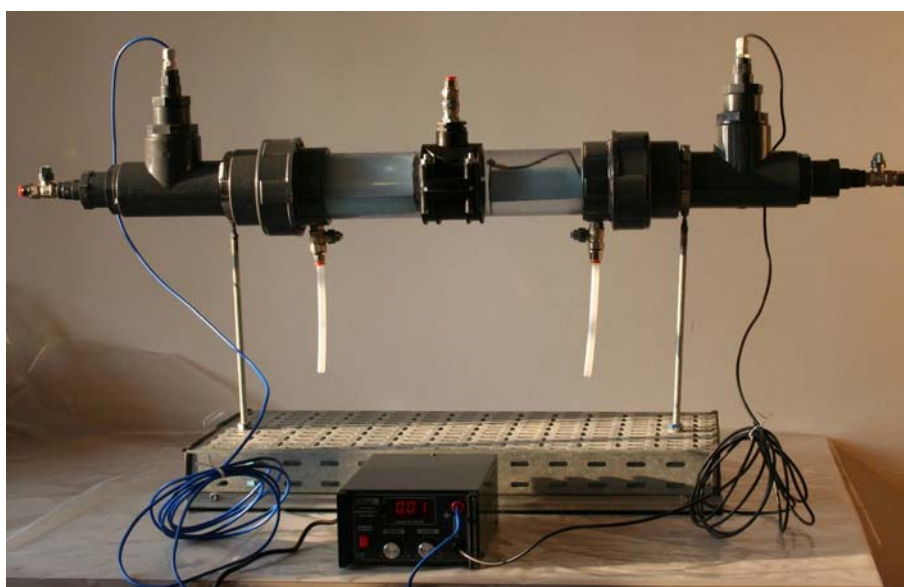
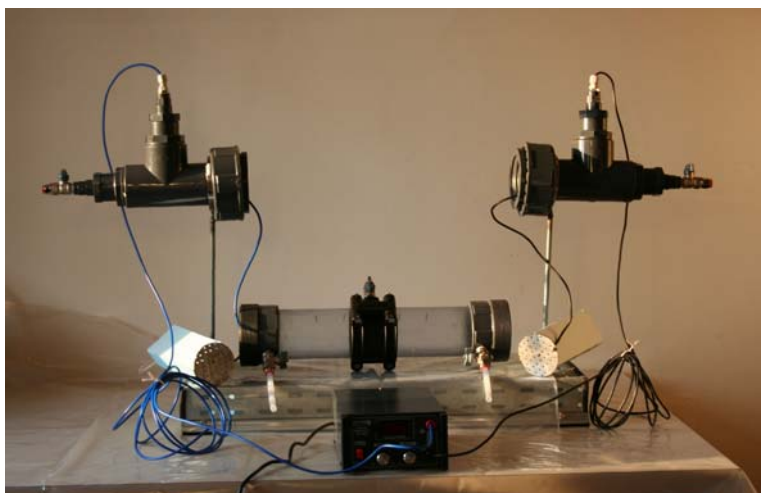
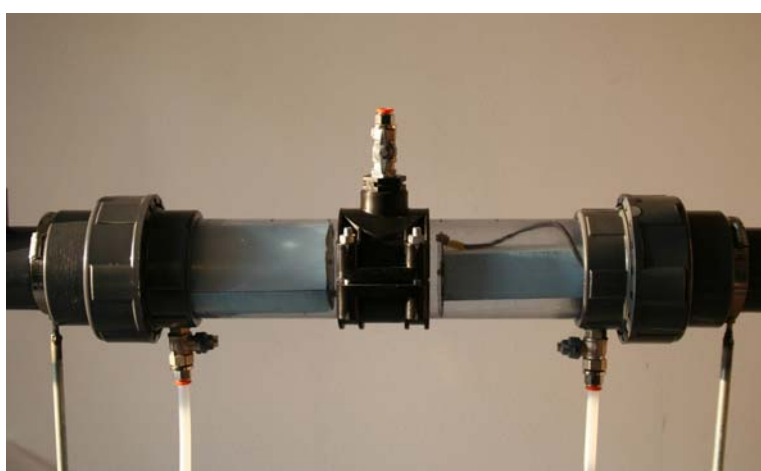


Figure 3.5 – Picture of the test device “Setup 1” used in the experimental investigation, here with DC generator Stab AR50.



**Figure 3.6 – Components of the test device “Setup 1” used in the experimental investigation.**



**Figure 3.7 – Detail of Setup 1: reaction cell. The cell was provided with vents at the electrode compartment to allow gases to escape and fluid to flow out of the cell. Another valve was inserted above the soil cell to allow the dosage of process fluid, if necessary.**

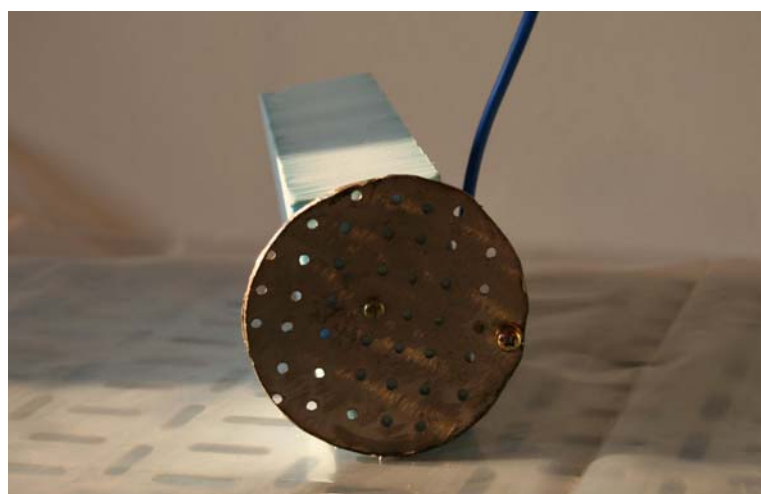


**Figure 3.8 – Stainless steel holed electrode used in Setup 1.**



Setup 1 was used to perform a number of preliminary tests (not shown here) which allowed to evaluate the behavior of soils spiked with metals (lead and cadmium) and aromatic pollutants (benzene, xylene) under unenhanced electrochemical treatment. It was also used to perform:

- Test PAH.1, on PAH-contaminated river sediments, when it allowed to estimate the contaminant volatilization;
- Tests TEL.1 and TEL.2, on samples of silty soils contaminated by organolead compounds;
- Test KAO.5, which was performed on a 50 cm long kaolin specimen.

### **3.2.2 Setup 2**

After some preliminary tests performed with Setup 1, two new improved setups were developed, named as “Setup 2” (shown in Figure 3.9, Figure 3.10 and Figure 3.11). The whole apparatus included two identical devices, each one including the following components:

- A rectangular reactor (10 cm wide, 10 cm high and 60 cm long, made up of 10 mm thick transparent PVC) (Figure 3.12);
- A pair of plate electrodes. The electrodes were rectangular plates (10 cm by 10 cm) made up of stainless steel with holes to allow the pore fluid to flow across them (Figure 3.14);
- A stabilized DC power supply;
- Two tanks for the pore fluid collection at both electrode compartments.

In this system, the soil specimen was 10 cm wide, 10 cm high and its length could be varied from 2 cm to 50 cm by changing the position of the electrodes, which were supported in the reaction cell by vertical grooves in the reactor’s walls. As for the previous setup, the electrodes were covered with filter papers and kept in contact with the soil sample during the tests.

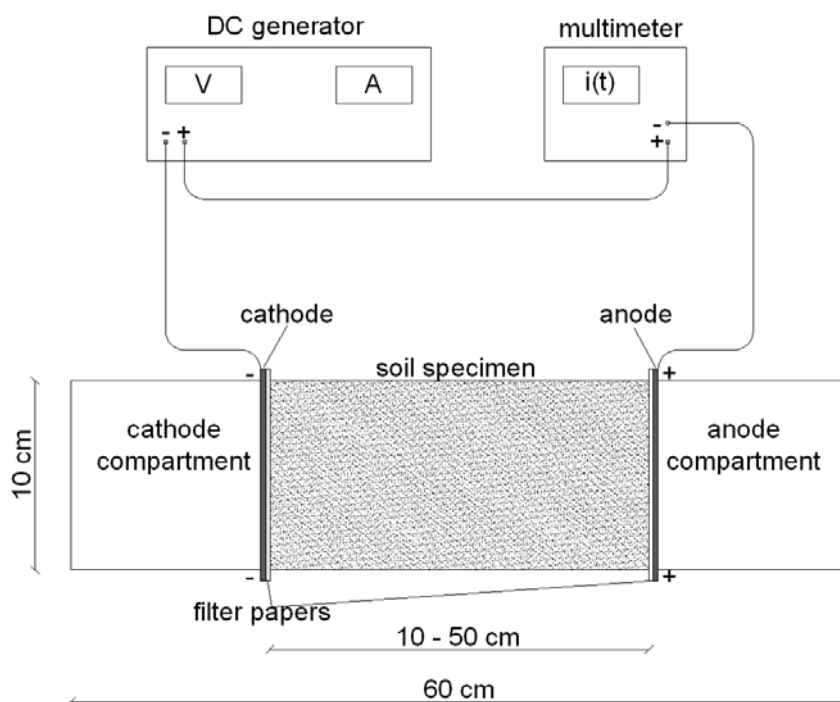


Figure 3.9 – Schematic diagram of Setup 2 used in the experimental investigation.

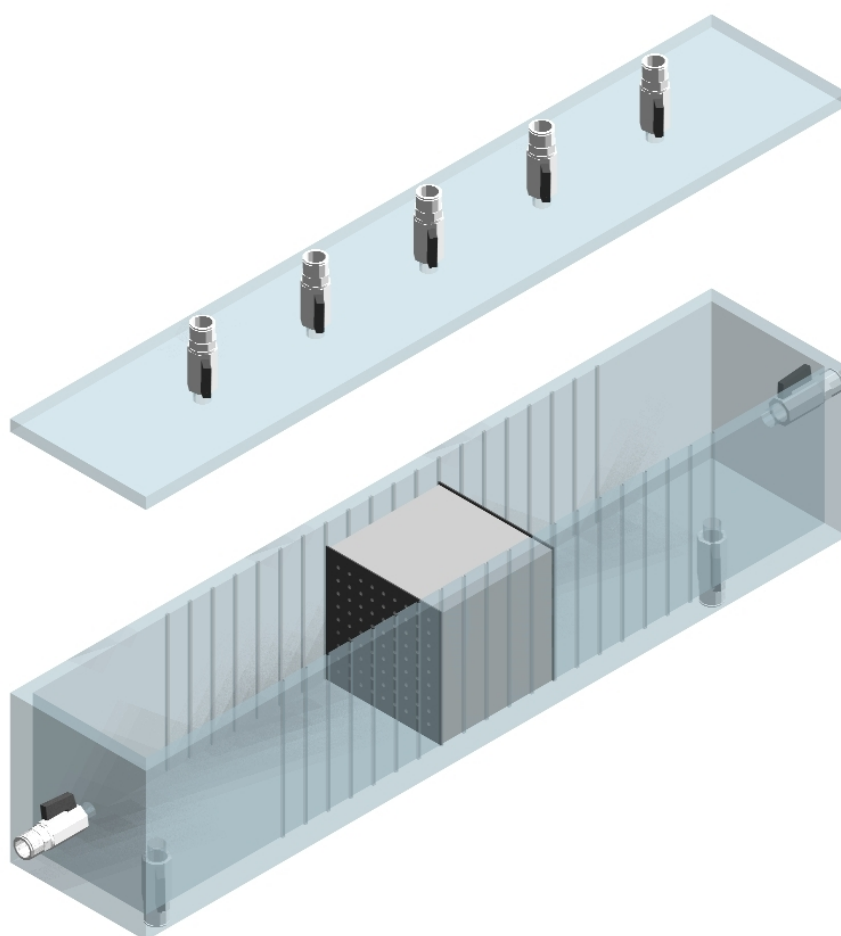


Figure 3.10 – Three-dimensional diagram of Setup 2. In order to perform the experiments, the electrodes were placed in the reactor grooves, then the space across them was filled with the contaminated soil. The cell was provided with gas and liquid vents.

To perform the experimental trials with this setup, the electrodes were at first placed in the reactor grooves, then the space across them was filled with the contaminated soil (Figure 3.15). The soil was manually compacted to achieve the same density of natural soils (e.g. about 2 kg/L) and trying to avoid leaving cavities in the specimen. Filter papers were inserted between the electrodes and the soil to prevent or limit their corrosion.

To perform the tests on diesel fuel-contaminated soils (see Chapter 4), the experimental apparatus was also equipped with:

- A digital multimeter (ISO-Tech IDM 207, with the data logging software ISO-Tech 300 Virtual DMM) for continuous current monitoring (Figure 3.16);
- A scale (Sartorius GW6206 Gold Scale) which allowed the monitoring of the electroosmotic flux;
- A pc for data logging.

Setup 2 allowed opening the reaction cell to measure soil pH and to collect samples while the tests were in progress.

Setup 2 was used to carry out all the tests on diesel fuel contaminated soils, except for test KAO.5. Tests PAH.2 and PAH.3 with PAH-contaminated river sediments were also conducted with this setup.

To perform the tests on the clayey soils contaminated by landfill leachate a very similar setup was used, with a smaller electrochemical cell, which was 10 cm long, 9 cm wide and 7 cm high. The setup and the methods used in this study are described in detail in Chapter 5.3.

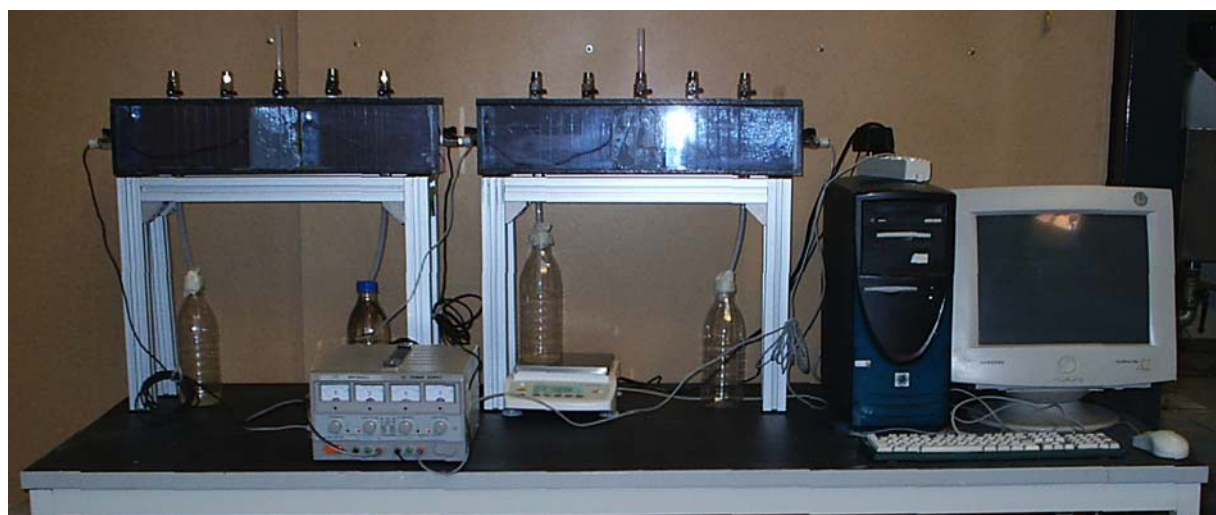


**Figure 3.11 – Picture of the test device “Setup 2” used in the experimental investigation.**

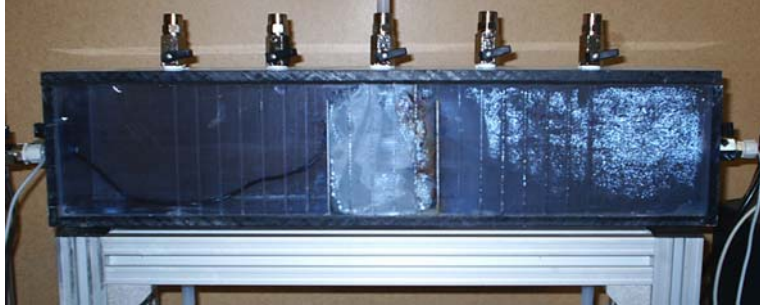


**Figure 3.12 – Detail of Setup 2: reaction cell.**

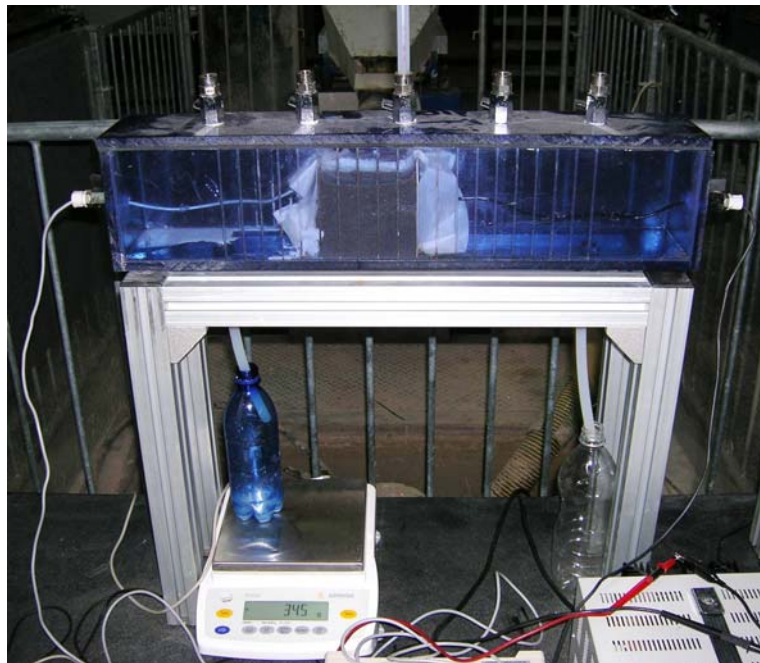


**Figure 3.13 – Detail of the test Setup 2, including the reaction cell, tanks for the pore fluid collection at cathode compartments and the scale at the cathode side for the electroosmotic flow monitoring.**

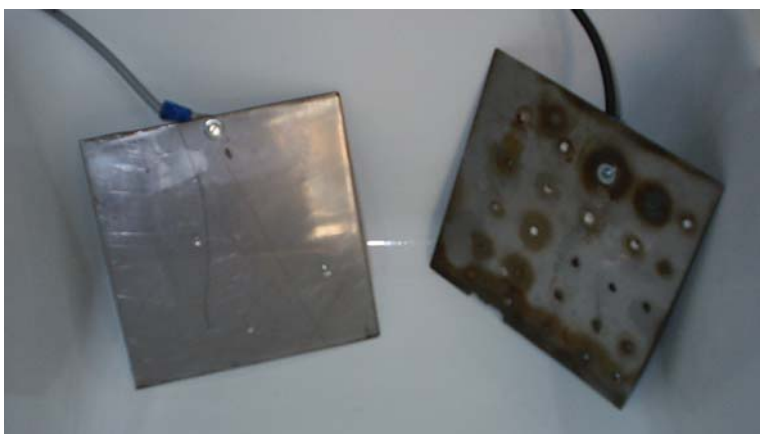


**Figure 3.14 – Stainless steel electrodes used in Setup 2.**

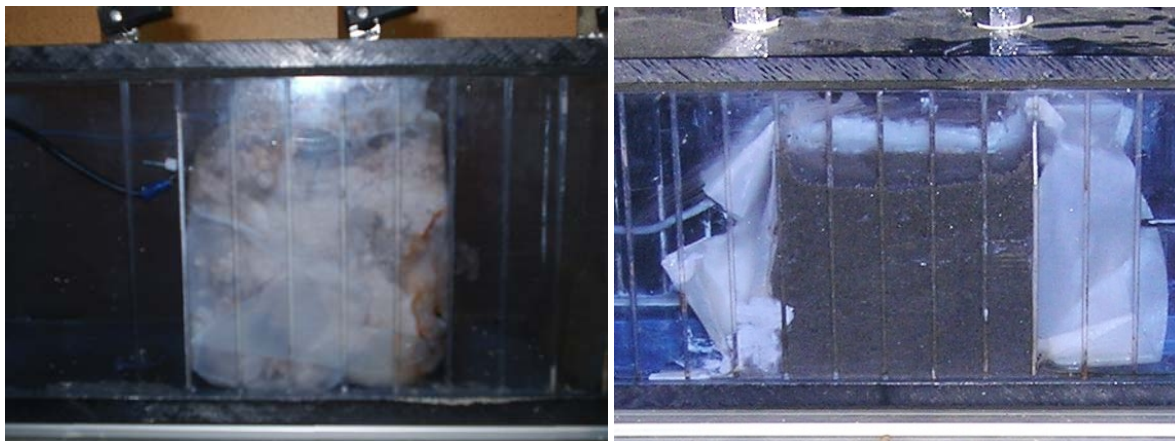


Figure 3.15 – Detail of the test Setup 2: soil specimen being treated with Setup 2.



Figure 3.16 – Digital multimeter ISO-Tech IDM 207 for continuous current monitoring.

### 3.3 Experimental procedures

During each experimental run, a soil sample, having a mass from one to several kilograms, was placed in the experimental setup, compacted to achieve a proper density (about 1.5-2 kg/L), and a constant electric potential (from 5 V to 60 V) was applied across it for a fixed period of time, which ranged from 1 to 28 days.

At the end of the trial, the soil specimen was removed from the test setup and analyzed. After the runs, a part of the specimen was transversally sliced into a certain number of segments (i.e. five 2 cm long segments for a 10 cm long specimen, and five 10 cm long segments for a 50 cm long specimen). Each segment was analyzed for pH and contaminant concentrations, in order to assess the extent of electrochemical reactions at different distances from the electrodes, and the potential contribution of electromigration.

The residual part of the specimen was mixed to produce the final homogeneous sample, representing the whole specimen. A scheme of the specimen subdivision is shown in Figure 3.17.

Besides the contaminant concentrations, during the tests, several parameters were monitored, including voltage and current, evolution of the soil pH profiles, electroosmotic flow, soil humidity, soil temperature and soil mineralogy.

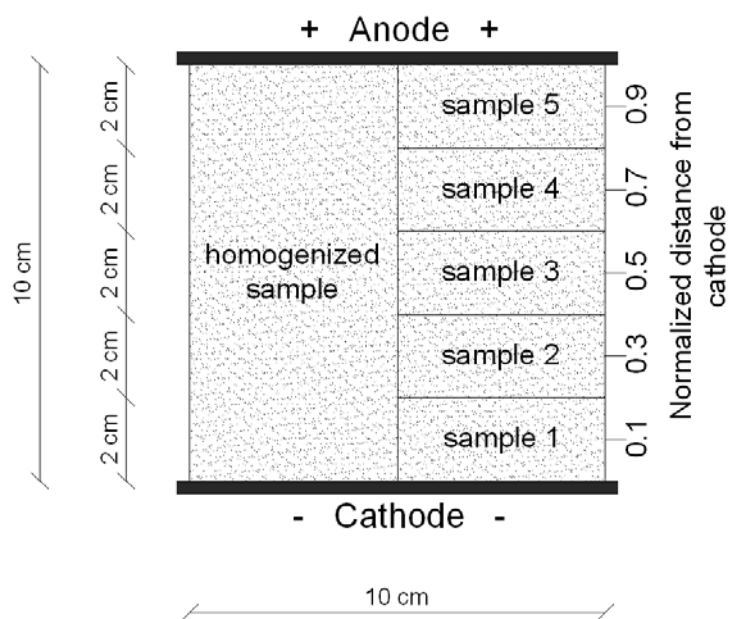


**Figure 3.17 – Scheme of the treated specimen sectioning for sample analysis: a half of the treated specimen was sliced into 5 segments which were separately analyzed for contaminant concentrations, while the remaining part of the specimen was mixed to produce a homogenized sample.**

Since Setup 2 also allowed to open the reaction cell to measure soil pH and to collect samples while the tests were in progress, samples were also collected at regular time intervals (e.g. once a week) from the upper part of the soil specimen, to assess the evolution of the mineralization process during the runs.

During the tests performed on the PAH-contaminated sediments, the ecotoxicity of the initial and treated samples were also investigated, as well as the volatilization of the target pollutants.

Since the objective of this study was to evaluate the efficiency of the electrochemical remediation in the simplest configuration, all the tests were performed at room temperature and were unenhanced, i.e. no hydraulic gradient was applied across the electrodes and no conditioning fluids were dosed at the electrode compartments to improve the soil conductivity, to adjust the soil pH or to promote the contaminant migration.

## 3.4 Analytical methods

Several parameters were investigated during this study, both to determine the contaminant content and to characterize the main features of the investigated soils and sediments.

In particular, in order to perform the study about the diesel fuel-contaminated soils, the following parameters were measured:

- pH;
- TOC;
- TPH;
- Total iron content;
- Total manganese content;
- Cation exchange capacity (CEC);
- Soil humidity;
- Soil mineralogical composition.

During the study on the PAH-contaminated river sediments, the following parameters were determined:

- pH;
- TOC;
- PAHs (including: naphthalene, acenaphthylene, acenaftene, fluorene, phenanthrene, anthracene, fluoranthene, pyrene, chrysene, benzo(a)anthracene, benzo(b)fluoranthene, benzo(k)fluoranthene, benzo(a)pyrene, dibenzo(a,h)anthracene, benzo(g,h,i)perylene, indeno(1,2,3-cd)pyrene);
- Total iron content;
- Total manganese content;
- CEC;
- Sediment humidity;
- Ecotoxicity.

During the study on the silty soils contaminated by organolead compounds, these parameters were considered:

- pH;
- TOC;
- Tetraethyl lead;
- Triethyl lead;
- Diethyl lead;
- Total organic lead content;

- Total lead content;
- Inorganic lead content;
- Soil humidity.

Finally, the study about the clay contaminated by landfill leachate included the monitoring of these parameters:

- pH;
- TOC;
- Ammonia nitrogen;
- Organic nitrogen;
- Total Kjehldahl Nitrogen (TKN);
- Nitrates;
- Nitrites;
- Total nitrogen;
- Total iron;
- Total manganese;
- CEC;
- Soil humidity.

To detect the contaminant content in the soil and sediment samples, the solid and liquid phases were extracted together, to take into account all pollutants in the samples.

The analytical procedures used to detect the parameters of concern are described as follows:

- The TOC content was determined by IR analysis of thermal induced carbon dioxide with a TOC Analyzer Shimadzu TOC-V CSH, after heating the sample at 900°C with a Shimadzu Solid Sample Module.
- The TPH content was determined by gravimetric method after pollutant extraction by sonication and solvent addition. In order to perform the analysis, a soil sample (mass about 5 g) was carefully weighted and mixed with anhydrous sodium sulphate to eliminate soil humidity. The sample was extracted by sonication for 15 min, then 10 mL of solvent (HPLC grade n-hexane) were added to it. About 5 mL of the obtained solvent were collected and cleaned-up on a Florisil tube. The solvent sample was transferred into a pre-weighted vial, it was allowed to evaporate and then the vial was weighted. The TPH content was determined from the difference between the initial and final weight of the vial.
- The pH was taken in a soil/water suspension using a pH-meter HI 99121 by Hanna Instruments, with HI 1292D electrode for soil pH measurement. The same instrument was also used to measure soil and water temperature.
- The cation exchange capacity (CEC) was measured by barium replacement



method, according to the prescriptions of the Italian Ministry of Agriculture (D.M. 13/09/1999, “Approvazione dei metodi ufficiali di analisi chimica del suolo”, “Metodo XIII.2 - Determinazione della capacità di scambio cationico con bario cloruro e trietanolamina”). In order to perform the analysis, a pre-weighted soil sample was saturated with a barium chloride (BaCl) solution buffered at pH of 8.2. After stirring, a solution of magnesium sulphate, MgSO<sub>4</sub>, having a known concentration, was gradually added to the sample. This caused the production of insoluble barium sulphate, and the exchange between Mg and Ba. The residual Mg concentration dissolved in the aqueous phase was determined by titration. The amount of absorbed Mg allowed to calculate the amount of Ba exchanged and hence the CEC of the soil.

- For the kaolin and bentonite soils considered in the study about diesel fuel contamination, the mineralogical composition was determined by X-ray powder diffraction (XRD), in particular in order to identify the main iron minerals existing in the soils samples. The analysis were conducted on samples of dry soils having an approximate volume of 1.5 cm by 1.0 cm by 1 μm, using a vertical diffractometer (model X'Tra Thermo ARL) with Bragg-Brentano geometry and molybdenum wavelength. The phase identification was performed by using the software MDI Jade 5.0 and the spectrum database ICDD PDF2-47.
- Metal (iron and manganese) contents were determined by inductively coupled plasma (ICP): the samples were at first mineralized according to method EPA 3051: a sample of soil having a mass about 1 g (carefully weighted) was mixed with 10 mL of demineralized water and 8 mL of nitric acid in a closed Teflon bottle. The sample was then mineralized in a microwave oven at 180°C for 20 minutes and allowed to cool. A certain volume of demineralized water was added, therefore the final sample volume was exactly 100 mL and the sample was passed through a 0.45 μm filter. Then the sample was analyzed according to the method APAT IRSA-CNR 3020 using a VARIAN ICP-OES VISTA. Before the analysis, the setup was calibrated using five external standards and one internal standard.
- As for PAH detection in sediment samples, in order to achieve a good resolution both for light and for heavy PAH species, light PAH concentrations in sediments samples were determined with analysis by gaschromatography (GC) and heavy PAH concentrations were detected by high performance liquid chromatography (HPLC). As for light PAH detection by GC, the pollutants were at first extracted by sonication and

solvent addition (HPLC grade acetonitrile, CH<sub>3</sub>CN), then a sample of solvent was injected into the gas-chromatograph and analyzed using a Varian 4000 GC/MS. As for heavy PAH detection, the samples were at first extracted by solvent addition (HPLC grade dichloromethane) and filtered on a 0.45 μm filter. The solvent was allowed to evaporate, then an acetonitrile solution (70% HPLC grade acetonitrile and 30% water) was added to the sample. A sample of the obtained solution was injected into the HPLC and analyzed. The HPLC included: auto-sampler Gilson ASPEC XL (solid base extraction), Dionex P680 HPLC Pump, Dionex STH 585 Column Oven, HPLC detector Dionex UVD 340U (diode array). A Supelco-SIL LC-PAH column (520 mm × 4.6 mm i.d., 5 μm particle size) was used for PAH detection. The setups were tested before analyzing the samples; external standards were used for HPLC calibration, while internal standards were used for GC calibration. The extraction efficiencies were about 85% both for HPLC and for GC.

- BTEX concentrations were determined through purge&trap extraction followed by gaschromatographic analysis with VARIAN 4000 GC/MS.
- The ecotoxicity tests were performed according to the international standard methods ISO 113348-3:1998(E) “Water quality – determination of the inhibitory effect of water samples on the light emission of *Vibrio fischeri* (Luminescent bacteria test)”, using a Microbics Microtox 500. Each test was conducted on a soil sample having a mass of 7 g diluted with 35 mL of demineralized water. After stirring the sample for 10 minutes, sub-samples were collected to evaluate the sediment toxicity at different dilution rates.
- As for the detection of the organic lead compounds, the tetraethyl lead (TEL) content was determined by purge&trap extraction followed by gas-chromatographic detection, using a AGILENT 5973 INERT gaschromatograph. In order to determine the concentrations of the ionic alkyl lead species (TREL and DEL), the soil samples were at first buffered at pH 8.5 with a EDTA, NaDDTC (sodium diethyldithio carbamate) and ammonia solution, then extracted into n-hexane, derivatized with Grignard reagent (pentile and magnesium chloride MgCl<sub>2</sub>), and then detected by GC-MS, using a VARIAN 4000 GC/MS.
- The total lead concentrations, including both the organic lead content and the inorganic Pb content, were determined by inductively coupled plasma (ICP), using the same procedure described above for the iron and manganese detection.
- The inorganic lead content (i.e. the metallic lead concentration) was determined as difference between the total lead content and the total organic

lead content.

- In the study about the landfill leachate contaminated clay, the ammonia, nitrite and nitrate contents in the soil samples were determined by water solubilization followed by ion-chromatographic detection. During the analysis, a soil sample was mixed with demineralized water to solubilize  $\text{NH}_4^+$ ,  $\text{NO}_3^{2-}$  and  $\text{NH}_2^-$ , which are highly soluble species. Ammonia content in the liquid phase was determined according to the method APAT CNR-IRSA 3030 with a Dionex ICS-1500 ion chromatograph. Nitrites and nitrates contents in the liquid phase were determined according to the method APAT CNR-IRSA 4020 with a Dionex DX-500 ion chromatograph.
- The total nitrogen content was detected according to the Standard Method “4500-N Nitrogen”, with persulfate digestion and oxidation. Accordingly, during the analysis the soil sample was at first digested in autoclave at  $120^\circ\text{C}$  for 30 min, with a oxidant mixture of potassium persulfate ( $\text{K}_2\text{S}_2\text{O}_8$ ) and soda ( $\text{NaOH}$ ). Under these conditions, all nitrogen forms are converted into nitrates, which can be determined by ion chromatography according to the method APAT CNR-IRSA 4020 as discussed above.
- The Total Kjehldahl Nitrogen (TKN) and the organic nitrogen contents were determined as difference from total nitrogen and nitrates, nitrites and ammonia.



## Chapter 4

# Electrooxidation of diesel fuel-contaminated soils

This chapter presents the results of the systematic study that was conducted to assess the effectiveness of using electrooxidation for the remediation of petroleum hydrocarbons from different types of fine-grain clayey soils.

Several laboratory tests were performed on soil samples spiked with diesel fuel, which was chosen as a model hydrocarbon mixture to represent the soil pollution due to spills of oil and various petroleum products.

The main aims of this study were to evaluate the effectiveness and the efficiency of electrooxidation for hydrocarbon removal, to understand the role of different geochemical phenomena, to assess the most important design parameters in system efficiency (as applied voltage, treatment duration and soil mineralogy) and to evaluate any link between removal efficiency and macroscopic electrochemical phenomena, as electroosmotic flux and changes in soil pH.

## 4.1 Contaminants

### 4.1.1 Diesel fuel

Diesel fuel is a mixture of hydrocarbons produced from crude oil. It is composed of about 75-80% saturated hydrocarbons (mainly straight-chain alkanes, paraffins) and 20-25% aromatic hydrocarbons.

Diesel is widely used as a fuel in automobiles, trains, ships, trucks and industrial

machinery, as well as for domestic and industrial heating and as a cleaning solvent for industrial machines (U.S. EPA; 1999; Yu et al., 2007).

Diesel fuel combustion in vehicle engines is considered responsible for important atmospheric pollution phenomena, which involve both particulate and vapor emissions (e.g. CO, CO<sub>2</sub>, NO<sub>x</sub>, SO<sub>x</sub>). In particular, diesel combustion processes and vehicle emissions are now accounted as the primary source of particulate in the atmosphere (Searle and Mitchell, 2006). Diesel particulate is commonly described as combustion-generated carbon soot, with adsorbed and/or condensed hydrocarbons and some inorganic species. It consists mainly of spherical particles with an approximate diameter of 10-20 nm which agglomerate together to form larger structures (Searle and Mitchell, 2006).

Besides the atmospheric pollution problems, oil spills are a frequent source of environmental contamination that may derive from fuel spills from underground tanks, storage facilities, illegal dumping, industrial activities, oil refinery, gas stations, pipeline leaks, and oil transport accidents (U.S. EPA, 1999). The period during the transport of oil is normally the most vulnerable, and most of the world's major spills have occurred as a result of accidental damages to oil tankers. Oil spills can involve both coastal areas, due to offshore facilities and to the frequent transport of oil cargoes by sea, and inland areas. The scale of marine disasters can be enormous as there is very little way to control the spillage of oil into the sea. Inland spills typically have a more direct impact on human populations, because they usually occur closer to areas where people live and work, and they can directly affect drinking water sources, metropolitan areas, recreational waterways, industries and facilities. In addition, the species affected by coastal and inland spills are likely to differ because freshwater and marine ecosystems are different (U.S. EPA, 1999).

In sum, oil spills are of great environmental concern, since they can endanger public health, devastate natural resources, and affect the economy. Moreover, in industrialized countries, the used of oil-based products is so widespread that during the manufacture, transportation, storage, use, and disposal of petroleum products, releases to the environment of petroleum hydrocarbons are frequent and almost unavoidable. Due to the high occurrence of these events, petroleum spills have contaminated many large areas and they are widely recognized as posing important environmental threats (Saner et al., 1996; Watts and Dilly, 1996; Curtis and Lammey, 1998; U.S. EPA, 1999; Rivera-Espinoza and Dendooven, 2004; Iturbe et al., 2005; Powell et al., 2007; Yu et al., 2007).

This type of contamination is known to be hazardous to the health of plants, animals and humans (Sarkar et al., 2005). Nevertheless, the environmental risks due to releases of mixtures of hydrocarbons are very difficult to assess because the mobility and toxicity of petroleum products strongly depends on the relative amounts of individual constituents within the hydrocarbon mixture (Iturbe et al., 2005). Typical diesel fuel concentrations in contaminated soils have been reported to range from 5000 mg to 15000 mg of total

petroleum hydrocarbons (TPH) per kilogram of dry soil weight (Yu et al., 2007).

Hence, the remediation of large areas of soil contaminated with hydrocarbons have become a problem of high priority in industrialized countries (Saner et al., 1996; U.S. EPA, 1999) and many efforts have been made to identify proper remediation technologies.

#### **4.1.2 Environmental behavior of diesel fuel**

When diesel fuel is split over the ground, it can percolate into the subsurface, where it can exist at three different phases (Suthersan, 1997; Yu et al., 2007):

- Aqueous phase;
- Gaseous phase;
- Non-aqueous phase liquids (NAPLs).

NAPLs are commonly divided into two categories (U.S. EPA, 2000):

- Dense non-aqueous phase liquids (DNAPLs), which are heavier than water and exist below the water table. In general, DNAPLs are often a complex mixture of contaminants, which may include both halogenated solvents, like trichloroethylene (TCE) and tetrachloroethylene (PCE), and nonhalogenated compounds, like polycyclic aromatic hydrocarbons (PAHs).
- Light non-aqueous phase liquids (LNAPLs), whose density is lower than that of water and that occur above the water table. LNAPLs include gasoline, jet fuel and heating oils.

The movement of NAPLs in the subsurface is quite complex and it differs for heavy and light compounds (U.S. EPA, 2000).

DNAPLs tend to flow downward through the vadose zone with relatively little spreading. Moreover, due to capillary forces, a small amount of DNAPL is often retained in each soil pore, accumulating what is commonly called residual DNAPL. Below the water table, the migration of DNAPL is highly irregular and dependent on factors such as geologic distribution and entry pressures, resulting from capillary forces between the DNAPL and the water that exists in the saturated zone. These forces result in the lateral migration of DNAPL forming large horizontal layers referred to as pools. There is also a tendency for the DNAPL to follow preferential pathways in the subsurface, resulting in highly heterogeneous distributions. On the whole, DNAPL distribution in the saturated zone usually consists of a series of horizontal pools connected by narrow vertical pathways (U.S. EPA, 2000).

LNAPL flow through the subsurface is similar to that of DNAPL, except in the area of the watertable. In fact, the lighter density of LNAPL causes them to float on the watertable and to create significant pools at this level (U.S. EPA, 2000).

As a result of this behavior, the contamination due to immiscible contaminants, like

petroleum hydrocarbons, is usually characterized by an strongly heterogeneous spatial distribution (Kechavarzi et al., 2007), which constrains the amenability of all the remediation actions that involve a reactant flow in the subsurface, as soil flushing or in situ chemical oxidation.

In particular, diesel fuel can occur in soils in different forms (Suthersan, 1997; Yu et al., 2007):

- Adsorbed NAPLs in the form of thin liquid film on soil particles, colloidal materials and natural organic matter (NOM);
- Residual NAPLs in the form of small ganglia in soil pores;
- Free product, which tend to float on the groundwater surface, being diesel fuel a LNAPL.

In sum, diesel fuel, like most of organic contaminants deriving from petroleum products, in soils is usually sorbed or present as NAPL (Watts and Dilly, 1996); although some diesel fuel fractions would also dissolve into water and other would volatilize and thereby would be isolated in soil pores (Yu et al., 2007).

Once petroleum hydrocarbons have been released into the subsurface, their fate and behavior depends on both biotic and abiotic processes, which include transport (dispersion, mainly determined by floating and transport in the groundwater flow), sorption onto soil particles and organic matter, and physical, chemical and biological degradation (Saner et al., 1996; Powell et al., 2007; Yu et al., 2007).

### **4.1.3 Diesel fuel remediation**

Two major steps are involved to control the environmental damages due to oil spills: containment and recovery. In fact, when an oil spill has occurred, it is critical to contain it by proper barrier systems as quickly as possible, in order to minimize danger and potential damage to persons, property, and natural resources (U.S. EPA, 1999). Once the containment measures have been established, the remediation efforts to remove the oil from the contaminated media (soil, water, groundwater or sediments) can begin. This process may be conducted by different methods, and may take several years to gain a complete environmental recovery. The specific measures taken to respond to an oil spill depend on the type of oil discharged, the location of the discharge, the proximity of the spill to sensitive environments, and other environmental factors (U.S. EPA, 1999).

The remediation of diesel fuel and other petroleum hydrocarbons from soil, sediments and groundwater has been extensively studied by several Authors (Saner et al., 1996; Curtis and Lammey, 1998; Höhener et al., 1998; Watts et al., 2002; Sarkar et al., 2005; Delille et al., 2007; Powell et al., 2007; Yu et al., 2007) and a number of remediation techniques, including chemical, biological and physical methods, have been tested for the



recovery of these pollutants from the environmental media.

#### *4.1.3.1 Biological methods*

So far, bioremediation is the recovery technique that has gained the widest attention for petroleum hydrocarbon remediation. The biological degradation of many types of hydrocarbons has been well documented by several Authors (Luthy et al., 1994; Saner et al., 1996; Curtis and Lamme, 1998; Höhener et al., 1998; Hunkeler et al., 1998; Taylor and Jones, 2001; Namkoong et al., 2002; McCarthy et al., 2004; Sarkar et al., 2005; Delille et al., 2007), and many researches have been developed to assess the feasibility of using various biological methods, including bioremediation, bioaugmentation, biostimulation and ladfarming, for the removal of such pollutants from the environmental media.

Bioremediation may be defined as the use of living organisms to remove environmental pollutants from soils, water, and gases. In biodegradation processes, the pollutant destruction occurs as a result of bacteria oxidizing reduced materials (e.g. hydrocarbons) to obtain energy (Curtis and Lamme, 1998; Sarkar et al., 2005; Delille et al., 2007). The bacteria metabolism removes electrons from the hydrocarbons (which act as electron donors) via a number of enzyme-catalyzed steps to the final electron receptor, i.e. oxygen for aerobic biodegradation and other electron acceptors (as nitrites, ferrous iron, sulphates) for anaerobic biodegradation. The transformation of the hydrocarbons ends up as the growth of new cell mass and new microbes, the final by-products being carbon dioxide and water.

Bioremediation can be conducted with soil indigenous bacteria or with the addition of external selected bacterial strains (bioaugmentation) (Saner et al., 1996; Taylor and Jones, 2001; Delille et al., 2004; Sarkar et al., 2005; Powell et al., 2007). Usually, soils possess a great number and a diversity of microorganisms that may be enough to degrade a variety of pollutants (Saner et al., 1996; Curtis and Lamme 1998; Höhener et al., 1998; Delille et al., 2007). Moreover, in contaminated soils local microbial communities have proven to be capable of adapting to utilize hydrocarbons from fuel and oil spills as a source of energy (Milcic-Terzic et al., 2001; Powell et al., 2007).

Bioremediation can be conducted either in aerobic or anaerobic conditions (Curtis and Lamme, 1998; Hunkeler et al., 1998). During a remediation action, nutrients and water are commonly added to the soil to enhance the degradation rates (Taylor and Jones, 2001; Rayner et al., 2007). Oxygen has also usually to be added in case of aerobic bioremediation (the process being named as bioventing), being oxygen the most common limiting factor in aerobic biologic remediation methods. Alternatively, to enhance anaerobic bioremediation, nitrates ( $\text{NO}_3^{2-}$ ) or other electron acceptor can be dosed (Höhener et al., 1998; Hunkeler et al., 1998). Some recent studies also aimed at evaluating the extent

of hydrocarbon mineralization in absence of both oxygen and nitrates, under reducing (Fe-reducing, Mn-reducing and  $\text{SO}_4^{2-}$ -reducing) conditions or methanogenic conditions (Hunkeler et al., 1998).

Usually, organic and/or inorganic fertilizers are used as nutrient supplementation to provide nitrogen (N) and phosphorous (P), as contaminated soils are often characterized by low nitrogen and phosphorus content and require nutrient additions to allow a sufficient increase in biomass growth and a significant hydrocarbon degradation to occur (Ferguson et al., 2003; Sarkar et al., 2005). Moreover, recently the role of carbon (C) supplementation, with the addition of glucose, biosolids, sewage sludge or compost, has been investigated, proving to be able to allow a significant improvement of the degradation rates (Namkoong et al., 2002; Rivera-Espinoza and Dendooven, 2004; Sarkar et al., 2005).

Bioremediation can be enhanced by different methods. Bioaugmentation involves the introduction into the contaminated medium of microorganisms that have been cultured in laboratory to degrade the target pollutants. The cultures may be derived from the contaminated soil or they may be obtained from a commercial stock of microbes that have been previously proven to degrade the pollutants of concern. Once introduced into the system, the cultured microorganisms are supposed to selectively consume the target contaminants (Sarkar et al., 2005).

Biostimulation involves the addition of nutrients into a contaminated system to increase the population of the indigenous microorganisms (Delille et al., 2004; Sarkar et al., 2005). The indigenous microorganisms may or may not primarily target the hydrocarbons as a food source. However, the hydrocarbons are assumed to be degraded more quickly in comparison to natural attenuation due to the increased numbers of microorganisms caused by increased levels of nutrients (Sarkar et al., 2005).

Landfarming involves the enhancement of biological degradation by the addition of nutrients and water and periodic tilling to mix and aerate the soil. Additional amendments (as bulking agents to increase aeration, lime to adjust pH, or bacterial inoculations) can also be added to improve the recovery rate (McCarthy et al., 2004).

Attempts have also been made to increase the contact between sorbed organic pollutants and degrading bacteria, to enhance the biodegradation rates, such as the use of solvents or surfactants that can disperse sorbed pollutants and enhance their contact with degrading bacteria (Taylor and Jones, 2001; Gong et al., 2005; Gong et al., 2006; Okuda et al., 2007).

In certain cases, the bioremediation process is conducted *ex situ* (e.g. in bioslurry reactors or in biopiles) to improve the degradation processes by controlling the main influence factors, as temperature, to increase the contact between pollutants and degrading bacteria, to overcome the problem of pollutant bioavailability or to enhance to use of surfactants and solvents (Saner et al., 1996; Filler et al., 2001; Okuda et al., 2007). Usually,

the ex situ biological treatment allows a more rapid soil recovery than the in situ processes.

Bioremediation is currently considered as a viable technology for the remediation of petroleum products. When effective, it can have important benefits, such as the conversion of toxic wastes to non-toxic or less-toxic end products, reduced health and ecological effects and long-term liabilities associated with non-destructive treatment methods, and the ability to perform the treatment in situ without disturbing native ecosystems, a low or negligible need for material disposal (Sarkar et al., 2005).

However, for bioremediation to be amenable applicable for in situ remediation, a number of requisites must be fulfilled. Firstly, the soil must be permeable enough to allow the delivery of nutrients and of electron acceptors, the presence of recalcitrant toxic compounds (as heavy metals) must be limited, and the soil pH, temperature, water content and sorption capacity must not be limiting factors for biologic activity (Höhener et al., 1998; Delille et al., 2004). Secondly, for the clean-up criteria to be met, the contaminants must be completely mineralized (i.e. turned into carbon dioxide and water) or successfully detoxified (Höhener et al., 1998).

Monitored Natural Attenuation (MNA) is the unenhanced, naturally occurring process which reduces the contaminant content in soils and groundwater (Curtis and Lammey, 1998; U.S. EPA, 2002b; Delille et al., 2002; Sarkar et al., 2005). Although MNA relies on biological, physical and chemical processes, the biological phenomena are often addresses as the most important degradation pathways, as chemical attenuation mechanisms are rare in hydrocarbon contaminated sites, while physical attenuation mechanisms do not result in the destruction of the hydrocarbons (Curtis and Lammey, 1998; U.S. EPA, 2002b). Natural biological processes may consist in both aerobic and anaerobic biodegradation; while physical processes include dispersion, diffusion, dilution, volatilization, and chemical processes include sorption, oxidation, reduction and other chemical or abiotic reactions (Curtis and Lammey, 1998; Sarkar et al., 2005).

If effective, MNA provides many more benefits in terms of costs and efforts than many other remediation techniques (Sarkar et al., 2005; U.S. EPA, 2002b). In certain cases, MNA was reported to have the same contaminant removal performances as bioremediation (Sarkar et al., 2005) and some studies indicated that natural attenuation occurs at fuel plumes, as a result of biologic degradation, denitrification, ferrous iron reduction and sulphate reduction (Curtis and Lammey, 1998). However, its applicability must be evaluated under site-specific conditions, in order to assess the presence of suitable conditions for MNA to be effective. In fact, certain soils may be poor candidates for MNA while others can result in excellent recoveries. Therefore, the occurrence of proper conditions must be carefully evaluated as they may vary from site to site and may involve only the most degradable hydrocarbons, as BTEX (Curtis and Lammey, 1998; Sarkar et al., 2005).

Phytoremediation, i.e. the remediation process that uses plant to remove and degrade pollutants, has also been studied for the recovery of contaminated soils (Kechavarzi et al., 2007). The primary mechanism involved in the phytoremediation is considered to be biodegradation through the stimulation of microorganism growth in the plant rhizosphere. Despite the fact that petroleum hydrocarbon are phytotoxic, a certain root growth has been documented when no immediate uncontaminated soil is available. However, the plant cover may be problematic too achieve if the concentration of diesel in the soil is too high to effectively support germination. Moreover, the effectiveness of phytoremediation did not significantly differ from the hydrocarbon recovery due to natural attenuation (Kechavarzi et al., 2007).

Many hydrocarbons showed to be effectively removed by biological methods, while other organic pollutants proved to be more recalcitrant to biological degradation (Sarkat et al., 2006; Powell et al., 2007). However, the degradation rates of organic pollutants are often considered too slow for bioremediation to be amenably applied to real scale remediation actions (Delille et al., 2007). In fact, the grow of soil microorganisms and the rates of microbial degradation are strongly affected by many factors, including the availability of the organic substrate (nutrients), soil moisture, oxygen, contaminant content and bioavailability, microorganism type, pH and temperature (Saner et al., 1996; Höhener et al., 1998; Filler et al., 2001; Ferguson et al., 2003; Delille et al., 2004; Molina-Barahona et al., 2004; Delille et al., 2007). Moreover, many hydrocarbons are strongly sorbed onto soil particles and show a limited mass transfer, which reduces their bioavailability and results in low degradation rates, especially for xenobiotics (Luthy et al., 1994; Saner et al., 1996; Taylor Jones, 2001). Overall, biological methods can be considered amenably applicable for hydrocarbon recovery from moderately contaminated soils only (McCarthy et al., 2004).

For these reasons, the use of full-scale in situ remediation of diesel-contaminated soils is often discouraged (Delille et al., 2007) and the use of chemical techniques has gained much interest for hydrocarbon remediation, since these methods can offer a rapid and aggressive alternative that is not so sensitive to the type and concentration of contaminant as the biological processes are.

#### *4.1.3.2 Physical and chemical methods*

Among physical remediation techniques, the application of pump and treat to soil and groundwater remediation has proven to be hardly able to meet a complete recovery, often failing to meet the clean-up criteria (Curtis and Lammey, 1998). The disposal in sanitary landfill and the incineration represent a reliable and rapid way to solve the contamination problem, but they are often discouraged as they are very expensive and may

represent a source of direct or indirect air pollution (Sarkar et al., 2005).

Both air stripping (AS) and soil vapor extraction (SVE) are remediation techniques that aim at evaporating the target pollutants from soils, in order to collect them in the form of vapors, which can be extracted by applying a vacuum to extraction wells to be properly treated (U.S. EPA, 2001a,b).

AS consists in forcing an air flow through groundwater to cause chemicals to evaporate, and it is used for the recovery of polluted groundwater and saturated soils. In the same way, SVE is used for soil recovery above the water table, and it consists in forcing an air flow in the unsaturated zone. Since they work in similar ways, AS and SVE can also be applied together. Alternatively, a vacuum can be applied to the vadose soil to enhance the evaporation of volatile compounds (Halmemies et al., 2003). The main techniques for off-gas treatment include thermal treatment adsorption on activated carbons or other materials (e.g. zeolites or polymers), biofiltration, membrane separation and vapor condensation (U.S. EPA, 2006).

Both AS and SVE are considered particularly effective for the removal of organic pollutants that can be easily evaporate, like certain solvents and fuels, e.g. gasoline (U.S. EPA, 2001a; U.S. EPA, 2001b; Halmemies et al., 2003). These compounds, named volatile organic compounds (VOCs) are characterized by quite high values of vapor pressure (i.e. above 5.35 bar at 25°C). Conversely, SVE and AS are commonly not effective for the removal of semi-volatile organic compounds (SVOCs), which are characterized by a vapor pressure below 5.35 bar at 25°C. Even though, SVE can be thermally enhanced by raising the soil temperature (e.g. to 50-150°C) by in situ soil heating (Poppendieck et al., 1999; Lageman and Godschalk, 2007). The heating can be achieved by radio frequency, electrical resistance heating, hot air injection, steam injection and it allows to improve both the rate of pollutant removal and the range of compounds that can be removed (Poppendieck et al., 1999).

Petroleum hydrocarbons are mostly composed of apolar molecules, with low water solubilities and that tend to sorb onto soil particles, i.e. they are mostly composed of NAPL compounds. For this reason, the use of solvent and surfactants has been applied for their removal from environmental matrices.

Both soil flushing and soil washing aim at using solvent to separate contaminants from soil particles (U.S. EPA, 2000; U.S. EPA, 2001c,d; Moloson et al., 2002; Lee et al., 2005a). In soil flushing, the solvents or surfactants are used for the in situ recovery of soil and groundwater, while soil washing is an ex situ remediation technique.

The in situ flushing process involves the injection of an aqueous solution with surfactants or solvents, commonly through vertical wells, into a contaminated zone. The solution then flows through the polluted soil and the resulting effluent is extracted downgradient where it is treated and subsequently discharged or re-injected (U.S. EPA,

2000). The process can be applied into the vadose zone, in the saturated soil or in both of them. During an *ex situ* soil washing, the contaminated soil must be excavated and mixed with the detergent solution in a scrubbing unit, which separates the clean soil from the most polluted matrix (U.S. EPA, 1991; U.S. EPA, 2001d).

To be effective, these techniques should both transfer the contaminants to the solvent/surfactant fluid and treat the effluent solution to prevent further environmental contamination (U.S. EPA, 1991; Lee et al., 2005a). The separation of the contaminants from the solvent/surfactant solution may be technically difficult to be performed and highly expensive, thus increasing the overall remediation costs (Lee et al., 2005a). For this reason, the use of soil flushing and washing is commonly devoted only to the recovery of highly contaminated soils, as they may be not cost-effective for low pollutant contents (U.S. EPA, 2001c,d; Silva et al., 2005). The effectiveness of soil flushing may be constrained by subsurface heterogeneity and by soil low permeability. Furthermore, the distributions of NAPL contaminants may significantly affect the clean-up success (Lee et al., 2005a). For this reason, a good site characterization is required to apply this remediation technique, in order to avoid a failure of the remediation process or an uncontrolled mobilization of hazardous pollutants. Moreover, since fine grain soils, as silts and clays, usually have higher sorption capacities than coarser soils (e.g. sand and gravel), their presence in the soils to be treated may affect the effectiveness of these techniques (U.S. EPA, 2000; U.S. EPA, 2001c, Silva et al., 2005).

Surfactants and solvents have shown excellent effectiveness in hydrocarbon remediation, due to their high solubilization potential. Various studies (Molson et al., 2002; Lee et al., 2005a; Silva et al., 2005) proved both soil flushing and soil washing to be able to remove high quantities of petroleum hydrocarbons from diesel fuel-contaminated soils. However, some surfactants and solvents can be toxic to the indigenous microbes and may have potential negative environmental impacts (Molson et al., 2002; Silva et al., 2005). In alternative, natural organic matter, like humic acids, can be used to enhance the NAPL dissolution and remediation (Molson et al., 2002). Recently, also the use of sonochemical treatment has been investigated as an alternative solution for hydrocarbon desorption to enhance diesel fuel remediation (Feng and Aldrich, 2000).

Chemical oxidation seems to be effective in the remediation of various organic pollutants (ITRC, 2005), the oxidants most commonly used for environmental purposes being ozone, hydrogen peroxide, Fenton's reagent, permanganate and persulfate. This technique has been described in detail in Chapter 2.4.2.1.

So far, among the different available oxidant, Fenton's reagent and ozone have received most of the attention in scientific literature and have been applied for the remediation of different organic pollutants, including petroleum hydrocarbons (Watts and Dilly, 1996; Kong et al., 1998; Choi et al., 2002; Ferguson et al., 2007; Yu et al., 2007).

Most of these studies suggested chemical oxidation to be an effective technology for the recovery of diesel fuel-contaminated soils (Watts and Dilly, 1996; Kong et al., 1998; Yu et al., 2007), with very high contaminant removal achieved even for the non-volatile, sorbed and recalcitrant compounds, which are not easily biodegradable.

Nevertheless, while several Authors (Nam et al., 2001; Haapea and Tuhkanen, 2006; Kulik et al., 2006; Rivas, 2006; Sun et al., 2007b) suggested that chemical oxidation can effectively be applied in combination with bioremediation, by enhancing the biodegradability of the most recalcitrant compounds, other studies (Ferguson et al., 2007) reported that strong in situ chemical oxidation can lead to a near complete destruction of subsurface microbiota, thus hindering the soil bioremediation potential.

Overall, despite that many remediation techniques have been applied for diesel fuel remediation, a unique solution has not been identified, and the choice of the most appropriate treatment must be carefully evaluated case to case.

## **4.2 Experimental investigation**

### **4.2.1 Research scheme**

Two types of uncontaminated fine-grain soils were used to carry out the experimental investigation on diesel fuel remediation. The first soil was a silty clay mainly composed of kaolin, while the second soil was a bentonite clay mainly composed of montmorillonite. In order to perform the tests, the soil samples were spiked with diesel fuel to simulate the contamination due to petroleum product spills.

A list of the tests performed during this experimental investigation is given in Table 4.1. All the trials were performed with Setup 2, except for test KAO.5, which was conducted with Setup 1 (see Chapter 3.1 for details about the experimental devices).

As already observed in Chapter 3.3, during each experiment, a contaminated soil sample was placed in the experimental setup, and a constant electric potential was applied across it for a fixed period of time. At the end of the trial, the soil specimen was removed from the test setup. At the end of each test, a part of the specimen was transversally sliced into five segments. Each segment was analyzed for soil moisture content, pH and contaminant concentrations, in order to assess the extent of electrochemical reactions at different distances from the electrodes and the potential contribution of electromigration. The residual part of the specimen was carefully mixed to produce a final homogeneous sample, representing the whole soil specimen. The physical parameters monitored during the experiments included voltage, current, and electroosmotic flow.

Since Setup 2 allowed to open the electrochemical cell while the tests were in progress, during tests KAO.1, KAO.2, KAO.3, KAO.HC, BEN.1 and BEN.2, samples were collected once a week from the upper part of the soil specimen (i.e. on the 7<sup>th</sup>, 14<sup>th</sup> and 21<sup>st</sup> day after the beginning of the trial) while the experiment was in progress, to assess the extent of the electrochemical processes with time.

All the tests were performed at room temperature and were unenhanced, i.e. no conditioning fluid was dosed at the electrode compartments to improve the soil conductivity, to adjust the soil pH or to promote contaminant migration. Moreover, no hydraulic gradient was applied across the electrodes.

**Table 4.1 – List of the laboratory tests performed on diesel fuel-contaminated soils.**

Test	Matrix	Sample length [cm]	Applied voltage [V]	Specific voltage [V/cm]	Oxidant agent	Duration [d]
KAO.1	kaolin	10	5	0.5	-	28
KAO.2	kaolin	10	10	1	-	28
KAO.3	kaolin	10	30	3	-	28
KAO.4	kaolin	10	60	6	-	28
KAO.5	kaolin	50	50	1	-	28
KAO.6	kaolin	10	0	0	-	28
KAO.HP	kaolin	10	10	1	3% H <sub>2</sub> O <sub>2</sub>	28
BEN.1	bentonite	10	5	0.5	-	28
BEN.2	bentonite	10	10	1	-	28

As can be seen from Table 4.1, four trials (tests KAO.1, KAO.2, KAO.3 and KAO.4) were performed on contaminated kaolin samples (the specimens being 2 kg in weight, 10 cm long, 10 cm high and 10 cm wide), with test duration of 4 weeks (28 days), and constant voltages of 5, 10, 30 and 60 V respectively (corresponding to specific voltages of 0.5, 1, 3 and 6 V/cm). Another test (test KAO.5) was performed on contaminated kaolin to assess the treatment efficiency in case of a larger soil specimen. In this test, the soil specimen had a length of 50 cm and it was tested under a constant voltage gradient of 50 V, corresponding to a specific voltage gradient of 1 V/cm, for 4 weeks. Test KAO.6 was performed on a diesel-contaminated kaolin sample without the application of any voltage gradient: this experiment was conducted as a reference test to assess any loss of pollutants due to chemical, physical, or biological processes not linked with the electrochemical treatment.

Another experiment (KAO.HP) was conducted to evaluate the effects of a combined treatment of chemical oxidation and electrochemical process (EK-Fenton process). During the test, a constant voltage gradient of 1 V/cm was applied and at the same time 3% hydrogen peroxide was dosed at the anode compartment.



Two tests were performed on diesel contaminated bentonite (named as tests BEN.1 and BEN.2), each one on a soil specimen having dimensions of 10 cm by 10 cm by 10 cm. Both tests lasted for 4 weeks (28 days) and the voltages applied were 5 V and 10 V respectively (0.5 and 1 V/cm).

## **4.2.2 Materials**

### *4.2.2.1 Soils*

Two types of soils were considered in this experimental research.

The first soil (speswhite kaolin, Figure 4.1) could be classified as a silty clay (BSI, 1999), being mainly composed by particles having dimensions ranging between 2  $\mu\text{m}$  and 75  $\mu\text{m}$  (40%) or lower than 2  $\mu\text{m}$  (60%). From a chemical point of view, it was mainly composed of  $\text{SiO}_2$  (47%) and  $\text{Al}_2\text{O}_3$  (38%), its Cation Exchange Capacity (CEC) was 8.3  $\text{m}_{\text{eq}}/100\text{g}$  and its pH was about 6.0.

The second soil (Figure 4.2) was essentially composed of montmorillonite (65%), the remaining part being quartz (12%), mica (12%) and kaolin (11%). The granulometric analysis led to the following results: 2-10  $\mu\text{m}$  33%, 0.5-2  $\mu\text{m}$  16%, <0.5  $\mu\text{m}$  42%, thus the soil could be classified as clay according to BSI (1999). Also this soil was mainly composed of  $\text{SiO}_2$  (59%) and  $\text{Al}_2\text{O}_3$  (24%); its CEC was 34.2  $\text{m}_{\text{eq}}/100\text{g}$  and its pH was about 10.0.

The main features of the target soils are listed in Table 4.2 and Table 4.3



Figure 4.1 – Sample of kaolin used for the experimental investigation.



Figure 4.2 – Sample of bentonite used for the experimental investigation.

Table 4.2 – Main features of the kaolin used for the experimental investigation: grain size, chemical compositions and main chemical parameters.

Grain size	< 2 $\mu\text{m}$	60%
	2 ÷ 75 $\mu\text{m}$	40%
Chemical composition	$\text{SiO}_2$	47%
	$\text{Al}_2\text{O}_3$	38%
pH	6.0	
CEC	8.3	$\text{m}_{\text{eq}}/\text{100g}$
Fe	2794	$\text{mg}/\text{kg}_{\text{DW}}$
Mn	34	$\text{mg}/\text{kg}_{\text{DW}}$
TOC	0.01	$\text{mg}/\text{kg}_{\text{DW}}$

**Table 4.3 – Main features of the bentonite used for the experimental investigation: grain size, mineralogical and chemical compositions and main chemical parameters.**

Grain size	< 0.5 $\mu\text{m}$	42%
	0.5 ÷ 2 $\mu\text{m}$	16%
	2 ÷ 10 $\mu\text{m}$	33%
Chemical composition	$\text{SiO}_2$	59%
	$\text{Al}_2\text{O}_3$	24%
	$\text{Fe}_2\text{O}_3$	1.46%
	$\text{CaO}$	2.02%
	$\text{MgO}$	3.53%
	$\text{Na}_2\text{O}$	1.20%
	$\text{K}_2\text{O}$	1.28%
	$\text{TiO}_2$	0.25%
Mineralogical composition	montmorillonite	65%
	quartz	12%
	mica	12%
	kaolin	11%
pH	10.0	
CEC	34.2	$\text{m}_{\text{eq}}/100\text{g}$
Fe	10180	$\text{mg}/\text{kg}_{\text{DW}}$
Mn	44	$\text{mg}/\text{kg}_{\text{DW}}$
TOC	0.12	$\text{mg}/\text{kg}_{\text{DW}}$

Different iron minerals that exist in soils can have different electric properties, certain metals acting as microconductors (e.g magnetite, goethite) while certain others do not (e.g. hematite). For this reason, the soil samples were analyzed by X-ray powder diffraction (XRD), in order to identify the content of the different mineral structures. The spectra achieved for the kaolin and for the bentonite are reported in Figure 4.3 and Figure 4.4.

In both soil spectra, a peak appears about the  $14^\circ\text{C}$ , which can be considered due to the presence of magnetite, which is know to be a microconductor (Rahner et al., 2002). However, it was not possible to quantify the amount of the different iron minerals in the soil samples, due their low content in comparison with the other minerals existing in the soils (mainly kaolinite for the kaolin and montmorillonite for the bentonite), which confounded the overall spectra of the soils, especially in the case of the bentonite sample. Moreover, a peak of maghemite appears in both soils very close to the magnetite peak, thus hindering its identification.

Overall, certain fractions of the iron minerals in the soils seem to be attributed to magnetite, thus suggesting a certain content of microconductors in the soils samples, though itsr quantification was not possible.

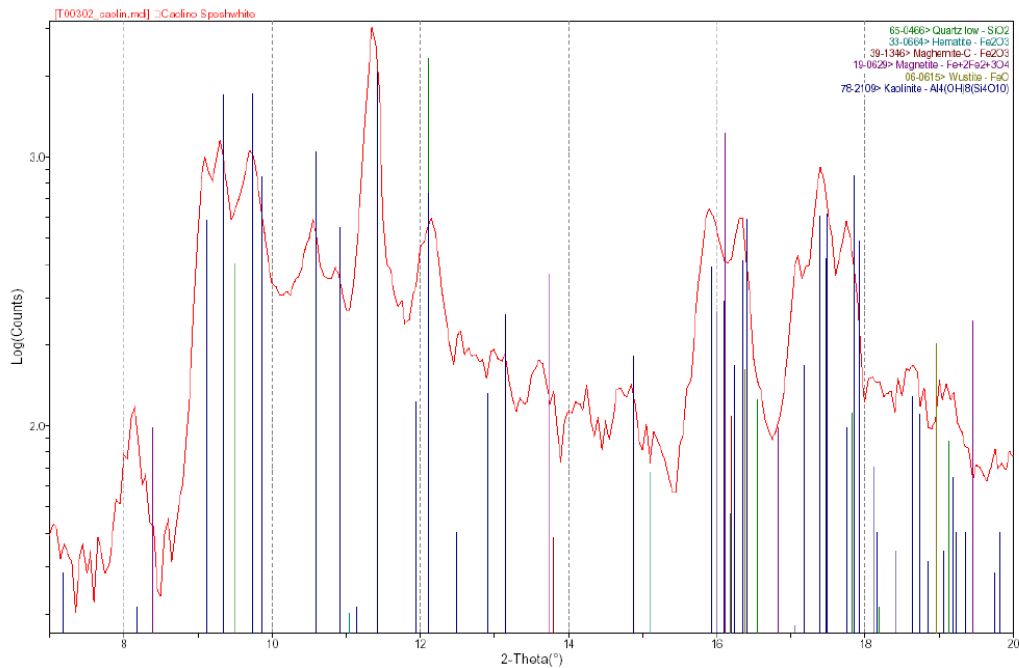


Figure 4.3 – XRD spectrum of the kaolin clay.

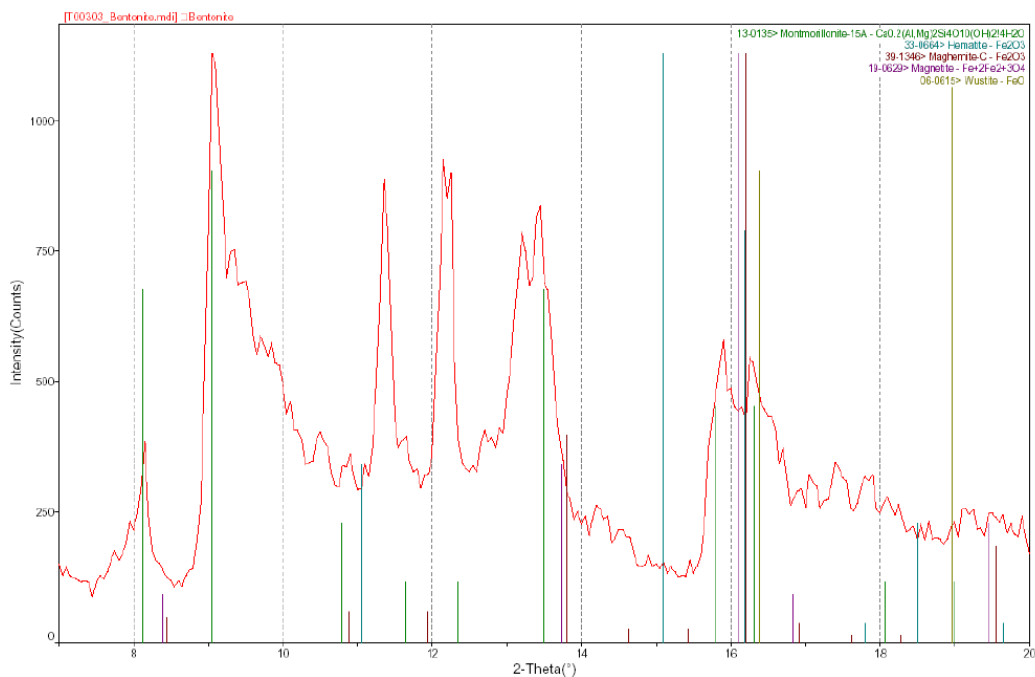


Figure 4.4 – XRD spectrum of the bentonite clay.

#### 4.2.2.2 Diesel fuel

The diesel fuel used in this study was commercially available and was purchased from a gasoline pump at a typical refuel station.

To prepare the diesel-contaminated soil samples, the soil was at first dried at 105°C for more than 24 hours, and then spiked with diesel fuel. One kilogram of dry soil was mixed with about 100 mL of diesel fuel, then the sample was stirred with stainless steel

spoons in a glass backer, to ensure the contaminants to be evenly distributed through the soil. After mixing, the sample was allowed to evaporate for about two weeks.

Two parameters were used to consider the contaminant content in the soil samples:

- TPH (total petroleum hydrocarbons), which refers to a family of many petroleum-based hydrocarbons;
- TOC (total organic carbon), which represents the whole content of organic substances in the soil samples.

The initial TOC concentration in the spiked soil samples ranged from 185.0 g/kg<sub>DW</sub> to 264.8 g/kg<sub>DW</sub>, while the TPH concentration ranged from 131.0 g/kg<sub>DW</sub> to 185.3 g/kg<sub>DW</sub>. These are very high contaminant concentrations, which may represent the soil pollution in the hot spots of an underground contamination due to oil spills and fuel leakages.

Before the tests, the spiked samples were saturated with demineralized water, carefully mixed, and inserted in the experimental setup cell. Then they were allowed to evaporate and drain overnight at room temperature before the test begun.

## 4.3 Results

The results of the tests performed on the diesel-contaminated soils are presented in discussed as follows, distinguished for the kaolin and for the bentonite clay.

### 4.3.1 Tests on diesel-contaminated kaolin

#### 4.3.1.1 Test KAO.1

Test KAO.1 was performed on a 2 kg sample of diesel-contaminated kaolin for 28 days, with an applied constant voltage of 5 V, corresponding to a specific voltage gradient of 0.5 V/cm (Table 4.4). The soil sample used for the tests showed an initial TOC concentration of 208.1 g/kg<sub>DW</sub> and a TPH content about 131.0 g/kg<sub>DW</sub>. The soil humidity was about 39.5% and the pH was 6.0.

At the beginning of the trial, an electric current of about 16 mA was measured; then the current rapidly decreased, and reached a steady state value of about 1.0 mA (see Table 4.5 and Figure 4.5). During the electrochemical treatment, the electric current decreases because of the condenser effect and because of the induced geochemical reactions that involve soil particles, that lead to the formation of high electric resistivity zones, due to the gradual depletion of solutes and to the precipitation of insoluble compounds, as metal hydroxides (Acar and Alshwabkeh, 1993; Acar et al., 1995; Yu and Neretnieks, 1997;

Virkutyte et al., 2002; Reddy and Chinthamreddy, 2004). The electric currents measured at the steady state here were quite low because the experiment was unenhanced, i.e. no solution was dosed to provide new charge carriers and to improve the soil conductivity.

As a result of the current flowing, an electroosmotic flux was encountered during the tests, from the anode toward the cathode (Figure 4.6). Thus, during the treatment a certain volume of water was accumulated at the cathode compartment. The electroosmotic flow started to be appreciable about 1 day after the application of the voltage gradient, and it was significant during the first 10 days of the test, then it became negligible. This period corresponds to the highest values of the electric current, i.e. above 1.5 mA. Furthermore, the highest electroosmotic flow was encountered mainly during the first two days of the tests, when the current was above 5 mA.

**Table 4.4 – Main features of test KAO.1.**

Test name	KAO.1	
Matrix	kaolin	
Contaminant	diesel fuel	
Sample weight	2	[kg]
Sample length	10	[cm]
Sample volume	1.0	[L]
Sample density	2.0	[kg/L]
Test duration	28	[d]
Voltage (constant)	5	[V]
Specific voltage	0.5	[V/cm]

**Table 4.5 – Results of the electric current and electroosmotic flow monitoring during test KAO.1.**

Time [h]	Time [d]	Current [mA]	Water collected at cathode compartment [mL]
0	0.0	16	0.0
4	0.2	9	0.5
8	0.3	9	1.8
25	1	7	3.7
50	2	5	4.7
216	9	1.4	6.7
312	13	1.3	6.8
336	14	1.3	6.8
360	15	1.2	6.8
504	21	1.2	6.8
528	22	1.0	6.8
672	28	1.0	6.8

**Test KAO.1 - 0.5 V/cm**

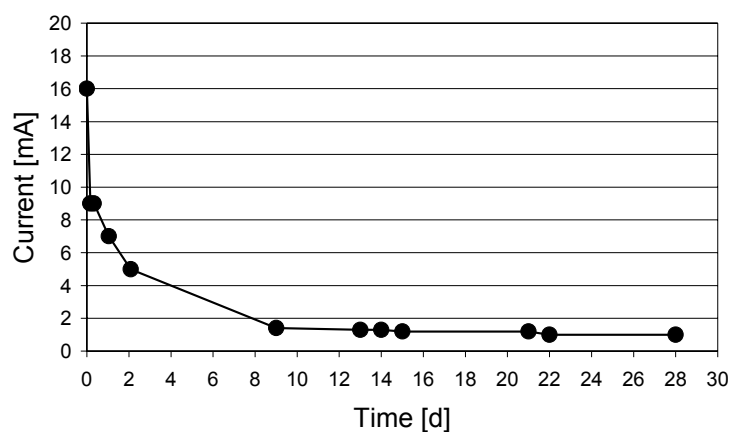


**Figure 4.5 – Electric current recorded during test KAO.1.**

**Test KAO.1 - 0.5 V/cm**

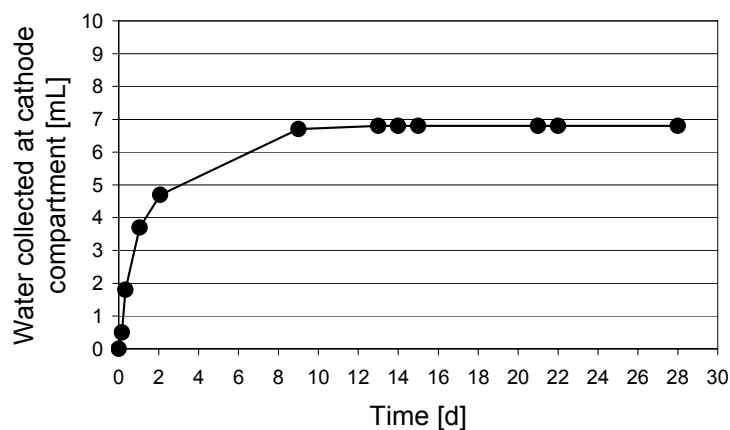


**Figure 4.6 – Electroosmotic flow recorded during test KAO.1.**

The pH profile of the soil specimen was monitored at the beginning and at the end of the trial, as well as several times during the test (see Table 4.6, Figure 4.7 and Figure 4.8). The soil pH changed during the electrochemical treatment because of water electrolysis near the electrodes and of the formation of the acid and base fronts. Significant pH changes occurred in the soil during the electrochemical treatment. In particular, the soil pH tended to increase significantly at the cathode side and decreased at the anode side, with important pH changes already being encountered 1 or 2 days after the beginning of the test. As the treatment continued, the pH decreases near the anode and the pH increases near the cathode went on. Besides this, the sweeping of the acid front from the anode to the cathode and the sweeping of the base front from the cathode towards the anode could also be appreciated.

The migration of the acid front was overall predominant over the migration of the base front, which was unable to be transported over the second section on the cathode side, corresponding to a normalized distance from the cathode of 0.3. Consequently, the process resulted in the acidification of the soil in all sections except that nearest to the cathode, where strongly alkaline conditions were created. Moreover, by the last week of the test (i.e. between the 21<sup>st</sup> and the 28<sup>th</sup> day of the test), the acid front reached the cathode side; this caused the pH in this area to decrease from 10.6 to 9.0 during this period.

As a result of water electrolysis, the soil pH increased up to about 10.6 near the cathode (maximum value measured 21 days after the beginning of the test) and decreased down to 2.8 at the anode side (maximum value measured at the end of the test, i.e. 28 days after the beginning of the treatment).

**Table 4.6 – Soil pH profile during test KAO.1.**

Normalized distance from cathode	Time [d]							
	0	1	2	7	14	21	28	
0.1	6.0	8.4	8.5	9.6	9.9	10.6	9.0	
0.3	6.0	5.9	8.2	5.5	5.5	6.7	5.1	
0.5	6.0	5.5	5.9	5.1	4.8	5.4	4.1	
0.7	6.0	5.2	4.2	4.2	3.7	4.1	3.8	
0.9	6.0	3.9	3.6	3.3	3.2	2.9	2.8	



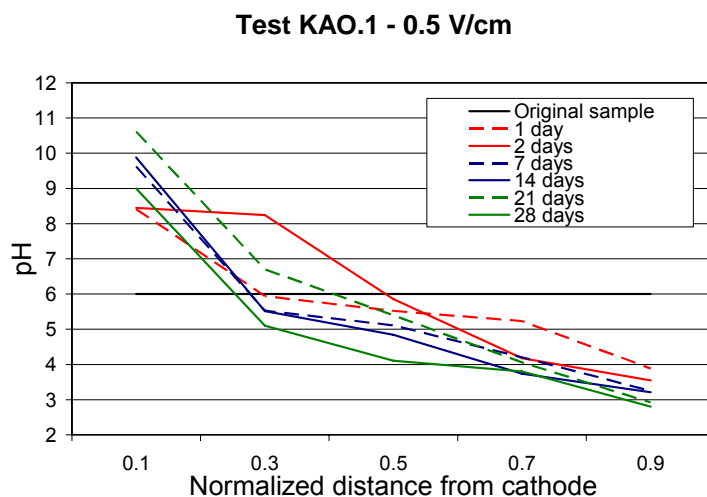


**Figure 4.7 – Soil pH profile recorded during test KAO.1.**

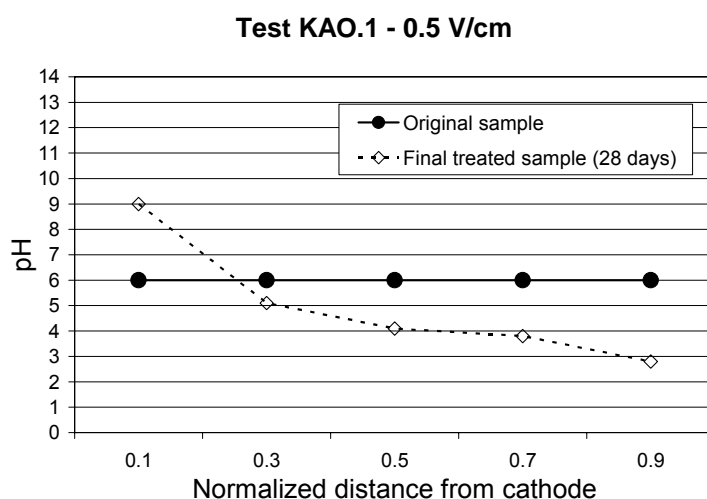


**Figure 4.8 – Soil pH profile recorded at the beginning and at the end of test KAO.**

As can be seen from Table 4.7, an important contaminant removal was encountered during the tests, which resulted in a final TOC removal about 46% and in a TPH removal of 66%. The contaminant removal significantly increased with treatment duration (Table 4.7, Figure 4.10 and Figure 4.10) In fact, the TOC removal after a one-week treatment was about 9%, but it increased to 12% after 2 weeks, to 39% after 3 weeks, and finally to 46% at the end of the test (four weeks). In the meanwhile, TPH removals of 28%, 36%, 46% and 66% were encountered.

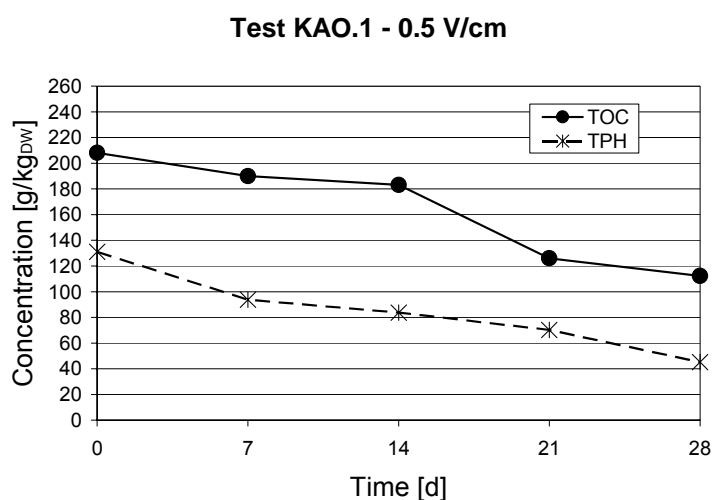
As expected, the TOC removal was lower than TPH removal, due to the fact that TOC represents all the organic matter in a soil sample, and therefore it accounts also for all the degradation by products, which may not appear in the TPH content. A decrease in the TOC concentration indicates that a certain fraction of the organic matter has been completely mineralized and turned into carbon dioxide ( $\text{CO}_2$ ) and water ( $\text{H}_2\text{O}$ ).

Figure 4.10 also indicates that the TPH removal efficiency significantly increased

with time since the beginning of the test, as an almost-linear function. Differently, the TOC removal significantly improved between the 14<sup>th</sup> and the 21<sup>st</sup> day of the process (i.e. during the third week of the experiment). This may suggest that, despite the oxidation process started soon after the application of the voltage gradient, a quite long time, of the order of a few weeks, can be required to achieve a complete mineralization of the organic pollutants.

**Table 4.7 – Contaminant removals achieved during test KAO.1.**

Elapsed time [d]	TOC [g/kg <sub>DW</sub> ]	TPH [g/kg <sub>DW</sub> ]	TOC Removal	TPH Removal
0	208.1	131.0	-	-
7	189.9	93.8	9%	28%
14	183.1	83.7	12%	36%
21	126.0	70.3	39%	46%
28	112.3	45.2	46%	66%



**Figure 4.9 – Contaminant concentrations in the soil samples achieved during test KAO.1.**

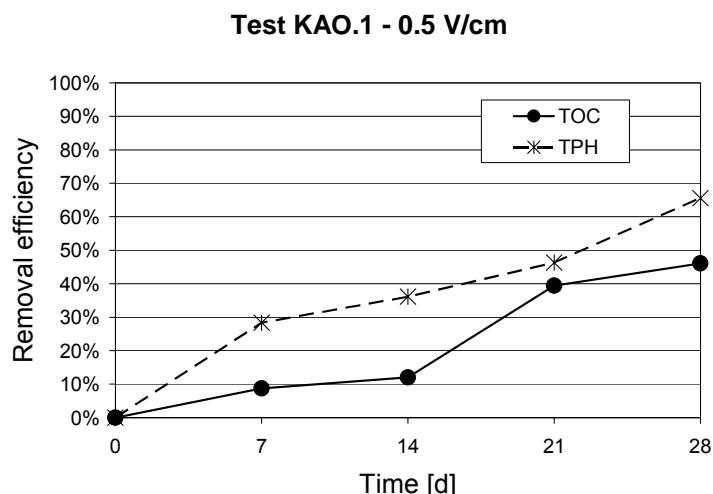


**Figure 4.10 – Contaminant removals achieved during test KAO.1.**

The contaminant distribution was evaluated at the end of the experiment. For this purpose, the TPH concentrations were evaluated at different distances from the electrodes. As can be seen from Table 4.8 and from Figure 4.11, the contaminant profile along the soil sample ranged from 40.8 g/kg<sub>DW</sub> to 67.1 g/kg<sub>DW</sub>. Overall, the residual contaminant content can be considered evenly distributed along the soil specimen, with some variations (e.g. higher concentrations in the sections closer to the anode) that are thought to be due to sample heterogeneity, which commonly characterizes the spatial distribution of the hydrophobic compounds, like diesel fuel, in soils and sediments.

These results suggest that:

- The electrooxidation process occurs in all the treated volume, in agreement with the microconductor principle (Rahner et al., 2002);
- The contribution of the electrokinetic transport (i.e. electroosmotic advection, being the target pollutants apolar compounds, not influenced by electromigration) the contaminant removal was negligible under the tested conditions.

**Table 4.8 – Contaminant and soil humidity distribution along the soil specimen at the end of test KAO.1.**

Normalized distance from cathode	TPH [g/kg <sub>DW</sub> ]	Humidity [%]
0.1	42.3	38.6%
0.3	46.8	36.8%
0.5	40.8	36.9%
0.7	52.4	37.3%
0.9	67.1	36.6%

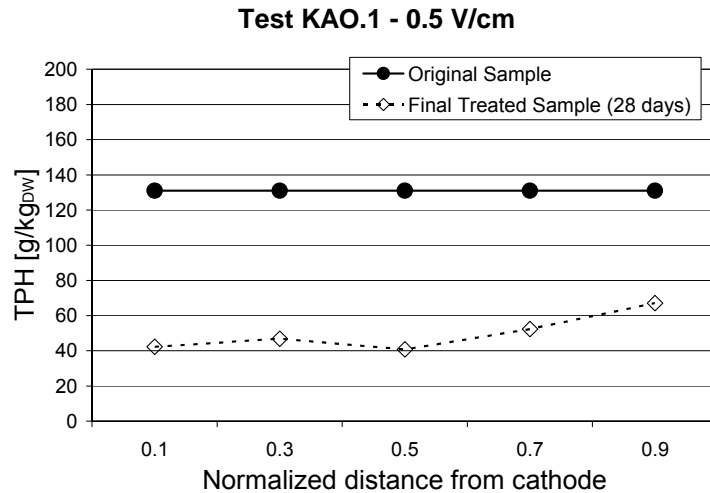


**Figure 4.11 – Contaminant distribution along the soil specimen at the end of test KAO.1.**

Since no solution was dosed to the soil specimen during the test, the water content of the soil sample was monitored at the beginning and at the end of the treatment, to assess any desiccation effect that could have affected the electrochemical processes, which require water to occur.

The initial humidity in the original untreated sample was about 39.5%, while at the end of the treatment the soil humidity ranged from 36.6% near the anode and 38.6% at the cathode side (Table 4.7, Figure 4.12). Therefore, despite the fact that the water content tended to decrease at the anode because of the electroosmotic flow, the humidity slightly changed and soil did not dry out.

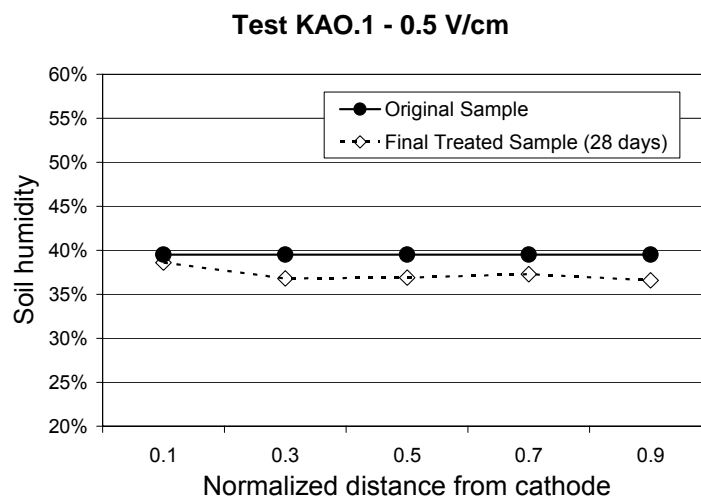


**Figure 4.12 – Soil humidity distribution along the soil specimen at the end of test KAO.1.**

#### 4.3.1.2 Test KAO.2

Test KAO.2 was performed on a 2 kg sample of diesel-contaminated kaolin for 28

days, with an applied constant voltage of 10 V, corresponding to a specific voltage gradient of 1 V/cm (Table 4.9). The soil sample used for this test was prepared at the same time of the sample used for test KAO.1. Hence, it was characterized by an initial TOC concentration of 208.1 g/kg<sub>DW</sub> and a TPH content about 131.0 g/kg<sub>DW</sub>, with a soil humidity about 39.5% and a pH of 6.0.

**Table 4.9 – Main features of test KAO.2.**

Test name	KAO.2	
Matrix	kaolin	
Contaminant	diesel fuel	
Sample weight	2	[kg]
Sample length	10	[cm]
Sample volume	1.0	[L]
Sample density	2.0	[kg/L]
Test duration	28	[d]
Voltage (constant)	10	[V]
Specific voltage	1.0	[V/cm]

As can be seen from Table 4.10 and from Figure 4.13, at the beginning of the test an electric current of 1.4 mA was encountered. The current rapidly increased up to 17 mA (peak value) and then it decreased to reach a steady state value of 2.2 mA. As in test KAO.1, the drop of the current started to be appreciated soon after the beginning of the test.

Despite the rapid current decrease, a significant electroosmotic flux occurred from the anode to the cathode during the treatment, thus at the end of the trial about 44.6 mL of water were found to be accumulated in the tank at the cathode compartment (see Table 4.10 and Figure 4.14). As in the previous test, most of the water that was transported because of the electroosmotic moved towards the cathode while the current was above 5 mA, i.e. during the first day of the trial. In fact, the electroosmotic flow became negligible from the second day of the experiment on.

**Table 4.10 – Results of the electric current and electroosmotic flow monitoring during test KAO.2.**

Time [h]	Time [d]	Current [mA]	Water collected at cathode compartment [mL]
0.0	0.0	1.4	0.0
0.17	0.007	11	0.0
0.33	0.014	12	0.0
0.50	0.021	17	0.0
1	0.042	16	4.3
2	0.083	9	16.1
6	0.3	5	44.0
24	1.0	2.2	46.6
48	2	2.2	46.6
168	7	2.2	46.6
336	14	2.2	46.6
504	21	2.2	44.6
672	28	2.2	44.6

**Test KAO.2 - 1 V/cm**

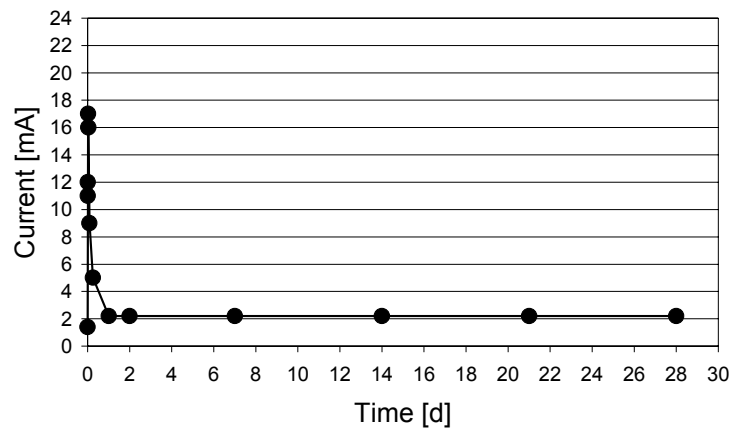


**Figure 4.13 – Electric current recorded during test KAO.2.**

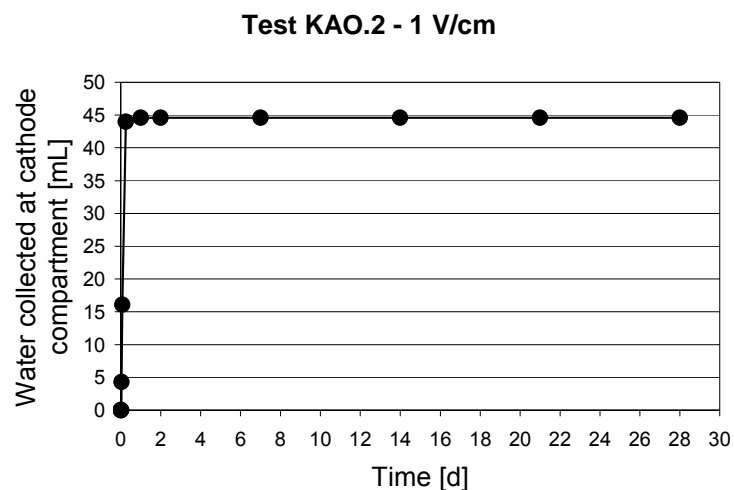


**Figure 4.14 – Electroosmotic flow recorded during test KAO.2.**

The evolution of the soil pH profile (shown in Table 4.11, Figure 4.15 and Figure 4.16) was similar to that encountered during the previous experiment, characterized by the acidification of the soil at the anode side and by the basification of the soil near the cathode, already occurring a few days after the beginning of the run.

As previously reported, the sweeping of the acid front resulted to be predominant than the migration of the base front, therefore at the end of the test the soil resulted to be acidified, except for the sections closer to the cathode, where alkaline conditions were created (Figure 4.16). Once more, during the third and fourth week of the treatment the pH at the cathode side tended to decrease because of the migration of the acid front, thus changing from 8.5 to 7.9.

**Table 4.11 – Soil pH profile during test KAO.2.**

Normalized distance from cathode	Time [d]							
	0	1	2	7	14	21	28	
0.1	6.0	6.0	8.8	8.1	8.5	8.4	7.9	
0.3	6.0	6.0	6.2	6.4	5.8	6.1	6.4	
0.5	6.0	6.1	6.1	5.1	4.5	5.1	5.4	
0.7	6.0	6.1	5.1	5.0	4.3	4.5	4.5	
0.9	6.0	4.0	3.8	3.8	3.8	3.9	4.0	

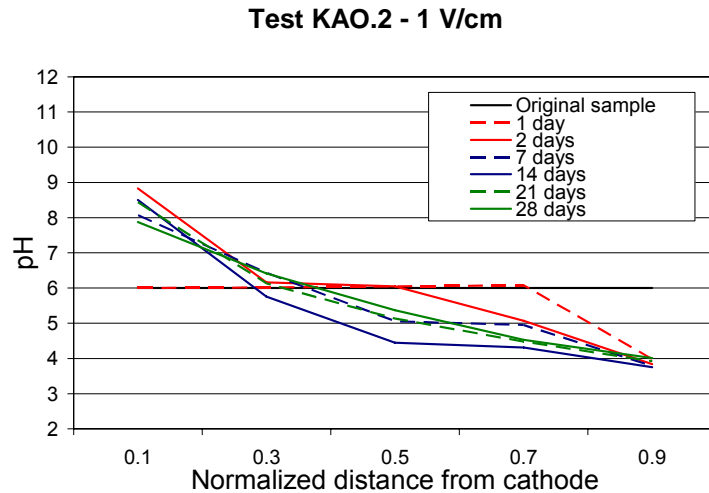


**Figure 4.15 – Soil pH profile recorded during test KAO.2.**

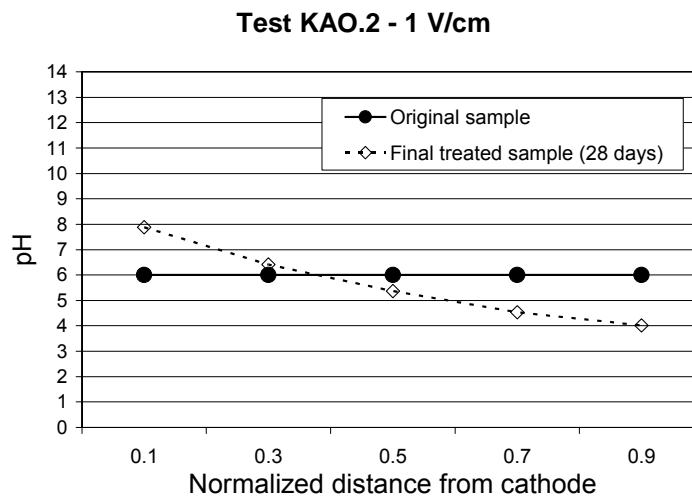


**Figure 4.16 – Soil pH profile recorded at the beginning and end of test KAO.2.**

The contaminant removals achieved during this test were higher than those encountered in test KAO.1 (Table 4.12), with a final TOC removal about 54% and a TPH removal of 80%. As in the previous case, both the TOC and TPH removals improved considerably with treatment duration (Figure 4.18). As expected, the TOC removal was always lower than the the TPH removal.

However, unlike the results achieved in the previous test, in this case also the TOC removal started to improve significantly even during the first week of the treatment (Figure 4.18). It can be supposed that the higher voltage applied during this test (i.e. 1 V/cm than the previous 0.5 V/cm) resulted not only in a higher removal of the organic pollutants, but also in a more rapid mineralization process.



Table 4.12 – Contaminant removals achieved during test KAO.2.

Elapsed time [d]	TOC [g/kg <sub>DW</sub> ]	TPH [g/kg <sub>DW</sub> ]	TOC Removal	TPH Removal
0	208.1	131.0	-	-
7	113.6	65.0	45%	50%
14	109.2	60.3	48%	54%
21	107.8	30.9	48%	76%
28	95.5	26.6	54%	80%

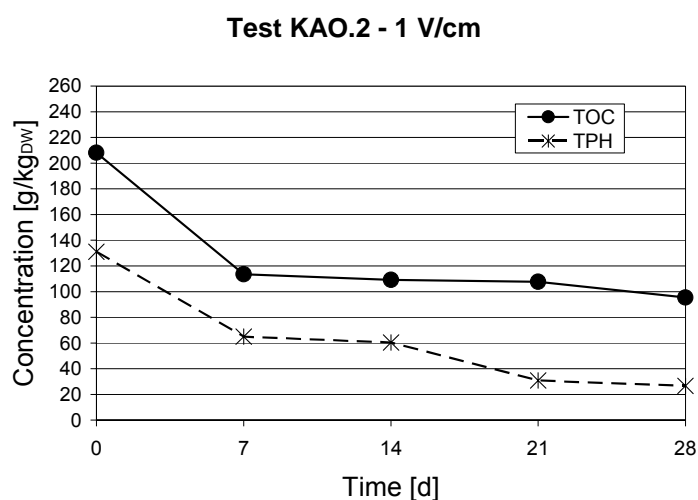


Figure 4.17 – Contaminant concentrations in the soil samples achieved during test KAO.2.

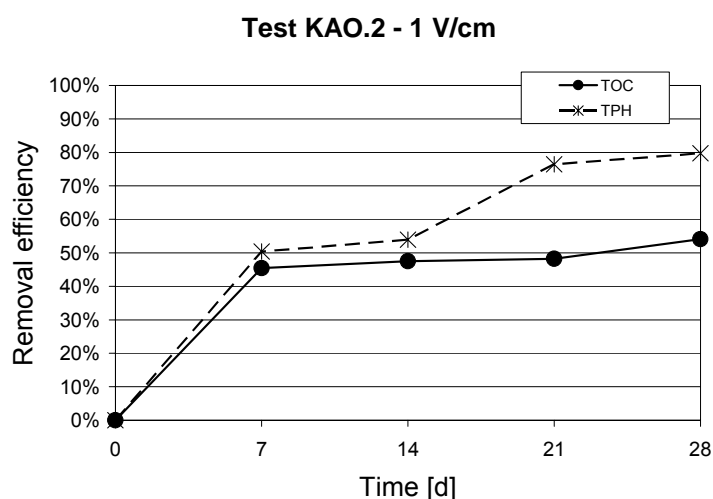


Figure 4.18 – Contaminant removals achieved during test KAO.2.

As for the contaminant distribution at the end of the experiment, the results achieved confirmed that the electrochemical process resulted in an evenly distributed final contaminant distribution (see Table 4.13 and Figure 4.19), with the oxidation processes occurring in all the treated volume.

Moreover, as in the previous test, the soil humidity did not change significantly from the initial value (about 39.5%), the final values ranging from 38.5% in the middle part of the specimen to 40.5% at the anode side (Table 4.13, Figure 4.20).

**Table 4.13 – Contaminant and soil humidity distribution along the soil specimen at the end of test KAO.2.**

Normalized distance from cathode	TPH [g/kg <sub>DW</sub> ]	Humidity [%]
0.1	18.7	39.5%
0.3	28.0	39.2%
0.5	29.5	38.5%
0.7	30.6	39.1%
0.9	30.3	40.5%

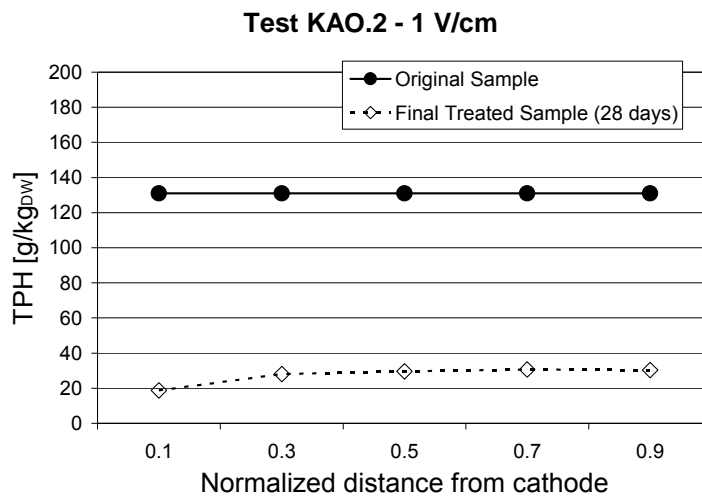


**Figure 4.19 – Contaminant distribution along the soil specimen at the end of test KAO.2.**

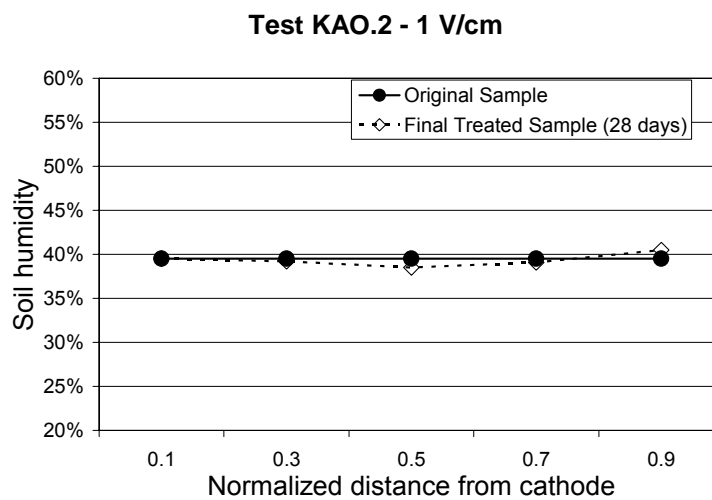


**Figure 4.20 – Soil humidity distribution along the soil specimen at the end of test KAO.2.**

### 4.3.1.3 Test KAO.3

Test KAO.3 was performed on a 2 kg sample of diesel-contaminated kaolin for 28 days, with an applied constant voltage of 30 V, corresponding to a specific voltage gradient of 3 V/cm (Table 4.14). The soil sample showed an initial TOC concentration of 221.1 g/kg<sub>DW</sub>, with a TPH concentration of 185.3 g/kg<sub>DW</sub>, a soil humidity about 36.9% and a pH of 6.0.

**Table 4.14 – Main features of test KAO.3.**

Test name	KAO.3	
Matrix	kaolin	
Contaminant	diesel fuel	
Sample weight	2	[kg]
Sample length	10	[cm]
Sample volume	1.0	[L]
Sample density	2.0	[kg/L]
Test duration	28	[d]
Voltage (constant)	30	[V]
Specific voltage	3.0	[V/cm]

As for the electric current, an initial value of 26 mA was registered, while 4 mA were measured at the steady state (see Table 4.15 and Figure 4.21), with a rapid decrease starting just after the application of the voltage gradient. Differently from the previous test, in this case a initial increase in the current flowing could not be appreciated, even if it may have occurred during the first minutes of the process, and may not have been recorded because of the monitoring timing.

As previously observed, the electroosmotic flow was significant when the current was above 5 mA. As shown in Table 4.15 and Figure 4.22, at the end of the trial about 22.8 mL of water were found to be accumulated in the tank at the cathode compartment, mainly resulting from the electroosmotic flow occurring during the first week of the test.

Table 4.15 – Results of the electric current and electroosmotic flow monitoring during test KAO.3.

Time [h]	Time [d]	Current [mA]	Water collected at cathode compartment [mL]
0.0	0.0	26	0.0
0.17	0.01	22	0.0
0.33	0.01	15	0.0
0.5	0.02	17	0.0
1	0.04	18	0.0
2	0.08	16	0.0
4	0.17	14	1.3
6	0.25	10.5	2.4
25	1.04	7.5	6.5
50	2.08	5.5	14.6
144	6	4.4	22.7
336	14	4.4	22.8
360	15	4.4	22.8
504	21	4.4	22.8
672	28	4.4	22.8

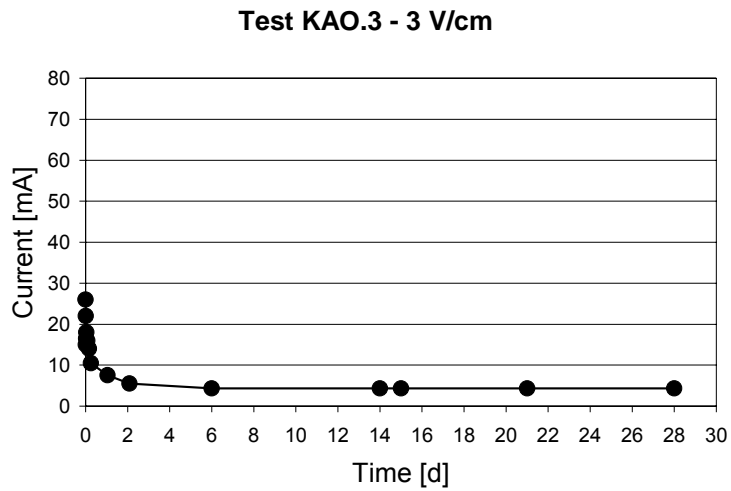
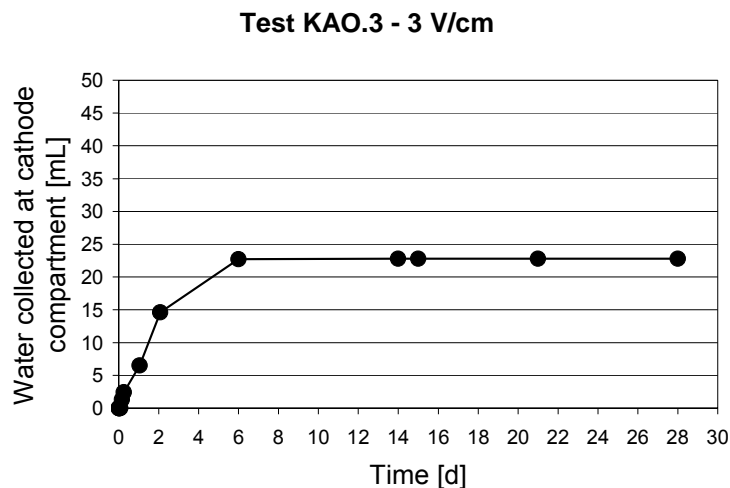


Figure 4.21 – Electric current recorded during test KAO.3.



**Figure 4.22 – Electroosmotic flow recorded during test KAO.3.**

The evolution of the soil pH profile (see Table 4.16, Figure 4.24 and Figure 4.24) showed the expected acidification of the soil at the anode side and the basification of the soil near the cathode, starting already the day after the beginning of the process. By the end of the test, the pH had dropped to 3.9 at the anode side and had increased up to 7.9 near the cathode, even with a decline from the highest values, which were registered at the beginning of the test (pH about 10.0 near the cathode). As can be seen from Table 4.16, during the experiment, and particularly from the 2<sup>nd</sup> to the 21<sup>st</sup> day of the test, decreases in the soil pH near the cathode and increases in the pH near the anode were encountered. This effect was not expected, and it was not possible to explain it as a consequence of the chemical processes involved in the electrochemical treatment. Since no similar behavior was encountered during the previous tests performed (see tests KAO.1, and KAO.2), this can be considered due to errors in the pH measurements or in the soil sampling procedures.

**Table 4.16 – Soil pH profile during test KAO.3.**

Normalized distance from cathode	Time [d]							
	0	1	2	7	14	21	28	
0.1	6.0	10.0	7.8	6.9	6.8	9.3	7.9	
0.3	6.0	6.6	5.8	5.5	7.4	9.1	7.7	
0.5	6.0	6.0	5.6	5.5	6.7	4.6	3.8	
0.7	6.0	4.7	5.6	5.6	3.9	4.4	3.7	
0.9	6.0	3.9	4.5	5.2	3.0	4.0	3.9	

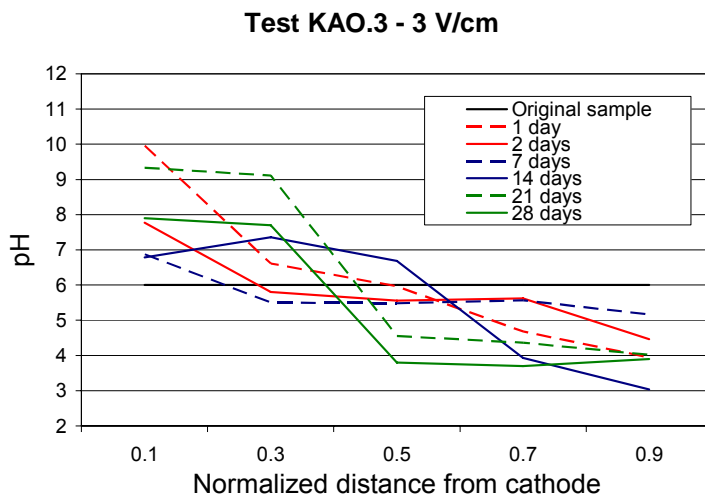


Figure 4.23 – Soil pH profile recorded during test KAO.3.

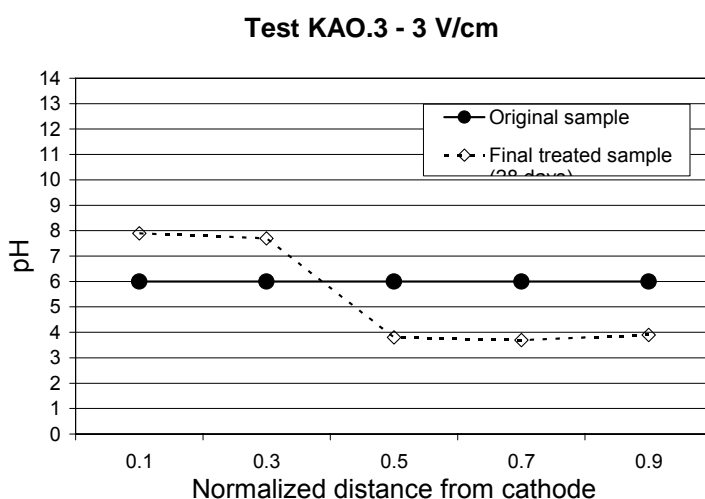


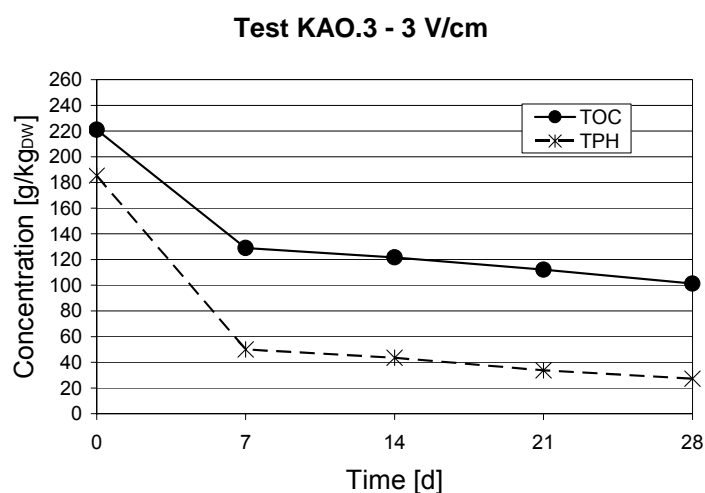
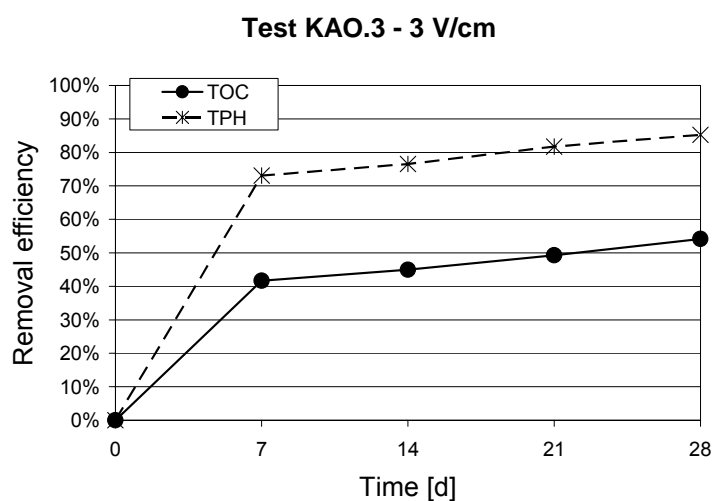
Figure 4.24 – Soil pH profile recorded at the beginning and at the end of test KAO.3.

A significant improvement of the contaminant removal efficiency was not encountered during this test, in comparison to the previous experiment (test KAO.2), when a specific voltage of 1 V/cm was applied. In fact, while test KAO.2 resulted in a 54% TOC removal and in an 80% TPH removal, test KAO.3 did not show any improvement in system efficiency as for TOC removal (which was yet about 54%), while the final TPH removal was about 85% (see Table 4.17, Figure 4.25 and Figure 4.26).

As in test KAO.2, both the TOC and TPH removal efficiencies significantly increased with treatment duration, good results being achieved even at the end of the first week of treatment (Figure 4.26), when about 42% TOC removal and 73% TPH removal were achieved.

**Table 4.17 – Contaminant removals achieved during test KAO.3.**

Elapsed time [d]	TOC [g/kg <sub>DW</sub> ]	TPH [g/kg <sub>DW</sub> ]	TOC Removal	TPH Removal
0	221.1	185.3	-	-
7	128.9	49.9	42%	73%
14	121.7	43.6	45%	76%
21	112.1	33.8	49%	82%
28	101.3	27.4	54%	85%


**Figure 4.25 – Contaminant concentrations recorded during test KAO.3.**

**Figure 4.26 – Contaminant removals achieved during test KAO.3: concentrations (a) and removal efficiencies (b).**

Once more, the final contaminant distribution in the treated sample proved to be evenly distributed along the soil specimen (see Table 4.18 and Figure 4.27).

As in the previous tests, the soil humidity did not change significantly during the

run, the initial water content being about 36.9%, the final values ranging from 34.1% to 40.1% (Table 4.18, Figure 4.28).

**Table 4.18 – Contaminant and soil humidity distribution along the soil specimen at the end of test KAO.3.**

Normalized distance from cathode	TPH [g/kg <sub>DW</sub> ]	Humidity [%]
0.1	35.9	41.0%
0.3	28.8	36.6%
0.5	36.2	34.1%
0.7	28.0	34.3%
0.9	35.6	35.9%

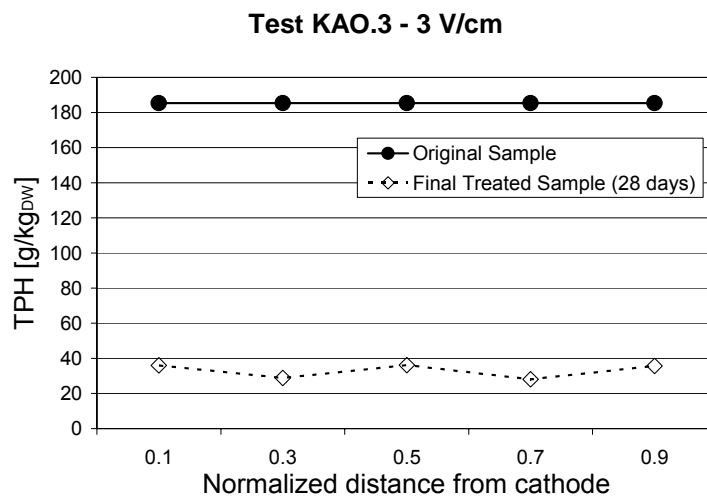


**Figure 4.27 – Contaminant distribution along the soil specimen at the end of test KAO.3.**

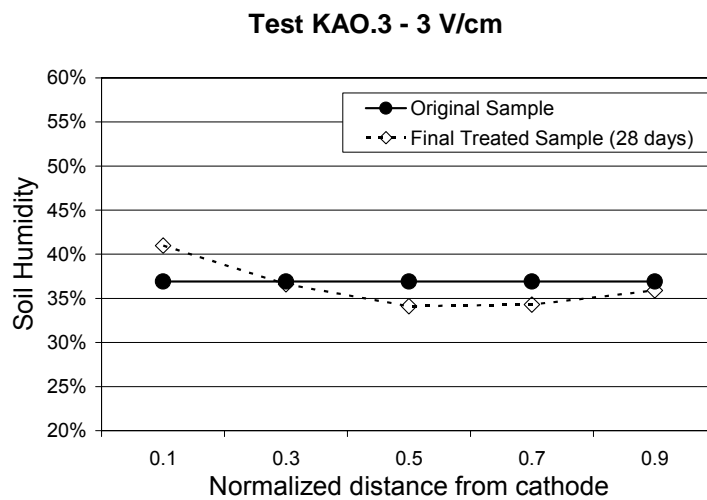


**Figure 4.28 – Soil humidity distribution along the soil specimen at the end of test KAO.3.**



#### 4.3.1.4 Test KAO.4

Test KAO.4 was performed on a 2 kg sample of diesel-contaminated kaolin for 28 days, with an applied constant voltage of 60 V, corresponding to a specific voltage gradient of 6 V/cm (Table 4.19). The soil sample showed an initial TOC concentration of 185.0 g/kg<sub>DW</sub>, with a TPH concentration of 179.8 g/kg<sub>DW</sub>, and a soil humidity about 37.2%. As in the previous tests, the soil pH was 6.0.

An initial current of 150 mA was measured at the beginning of the experiment, while 9 mA were encountered at the steady state, as shown in Table 4.20 and Figure 4.29. Despite the high current values encountered during the test, the current trend was once more characterized by a rapid decrease, and by some fluctuations during the period from the 1<sup>st</sup> to the 9<sup>th</sup> day of the treatment, when some temporal rebounds of the current flowing were encountered (see for example 12 mA measured on the 9<sup>th</sup> day versus 8 mA recorded on the 1<sup>st</sup> day).

A significant electroosmotic flow occurred during the first 13 days of the test, and 11.1 mL of water accumulated in the tank at the cathode compartment during the experiment (see Table 4.20 and Figure 4.30).

As can be seen from Table 4.21, Figure 4.31 and Figure 4.32, the pH changes induced by water electrolysis during the electrochemical treatment were particularly evident, therefore the soil pH rose up to 10.8 near the cathode and dropped down to 3.0 at the anode side a few days after the beginning of the process. Moreover, during this test a decrease in the soil pH near the cathode started to be appreciated from the 14<sup>th</sup> day of the trial, therefore the soil pH at the cathode side decreased to 5.9 by the end of the test. Consequently, the final soil pH profile at the end of the test was characterized by acid conditions along all the soil specimen (Figure 4.32).

**Table 4.19 – Main features of test KAO.4.**

Test name	KAO.4	
Matrix	kaolin	
Contaminant	diesel fuel	
Sample weight	2	[kg]
Sample length	10	[cm]
Sample volume	1.0	[L]
Sample density	2.0	[kg/L]
Test duration	28	[d]
Voltage (constant)	60	[V]
Specific voltage	6.0	[V/cm]

Table 4.20 – Results of the electric current and electroosmotic flow monitoring during test KAO.4.

Time [h]	Time [d]	Current [mA]	Water collected at cathode compartment [mL]
0	0.0	150	0.0
0.17	0.01	60	0.0
0.5	0.02	50	0.2
1	0.04	46	2.6
2	0.08	36	3.6
4	0.17	26	6.3
8	0.33	21	6.9
25	1.04	8	8.2
50	2.08	10	8.7
216	9	12	10.9
312	13	9	11.1
336	14	9	11.1
360	15	9	11.1
504	21	9	11.1
528	22	9	11.1
672	28	9	11.1

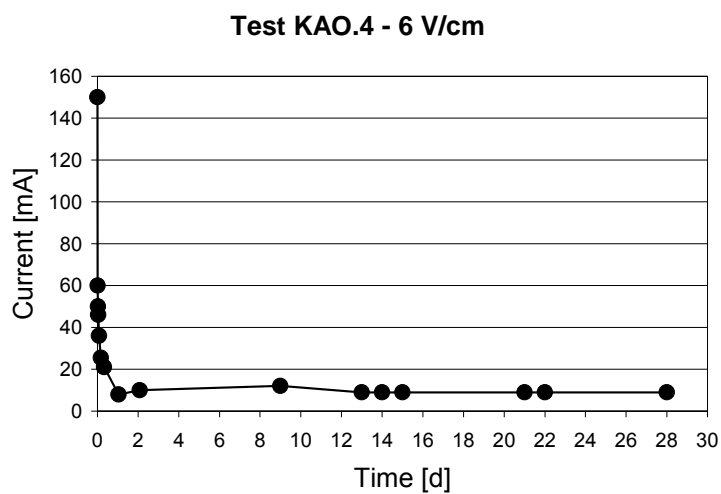


Figure 4.29 – Electric current recorded during test KAO.4.

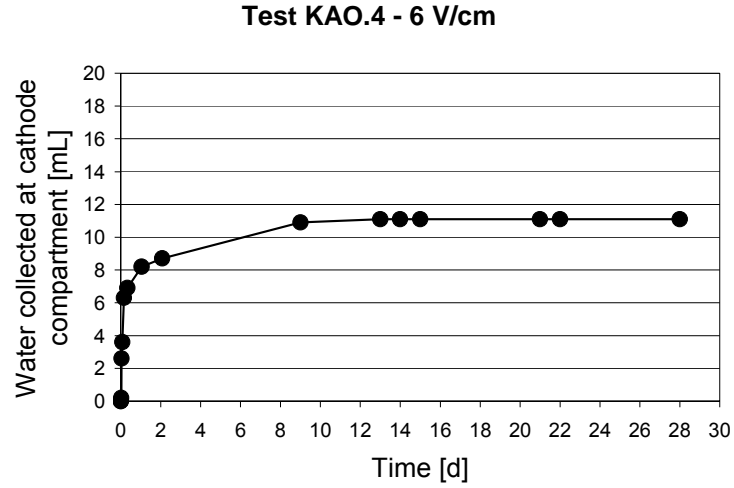


Figure 4.30 – Electroosmotic flow recorded during test KAO.4.

Table 4.21 – Soil pH profile during test KAO.4.

Normalized distance from cathode	Time [d]							
	0	1	2	7	14	21	28	
0.1	6.0	8.0	9.0	10.8	10.4	10.2	5.9	
0.3	6.0	8.0	8.2	8.6	5.2	5.7	5.4	
0.5	6.0	7.4	7.6	7.0	5.2	4.5	4.7	
0.7	6.0	7.1	6.5	4.4	4.2	4.1	3.9	
0.9	6.0	3.4	3.0	4.0	4.0	3.8	3.4	

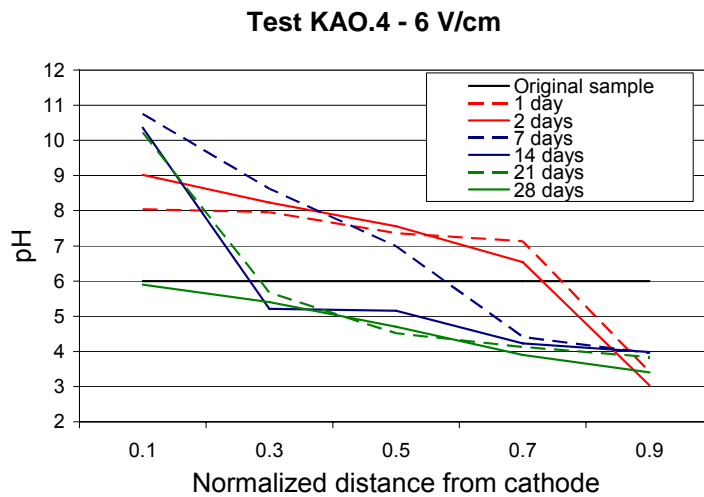
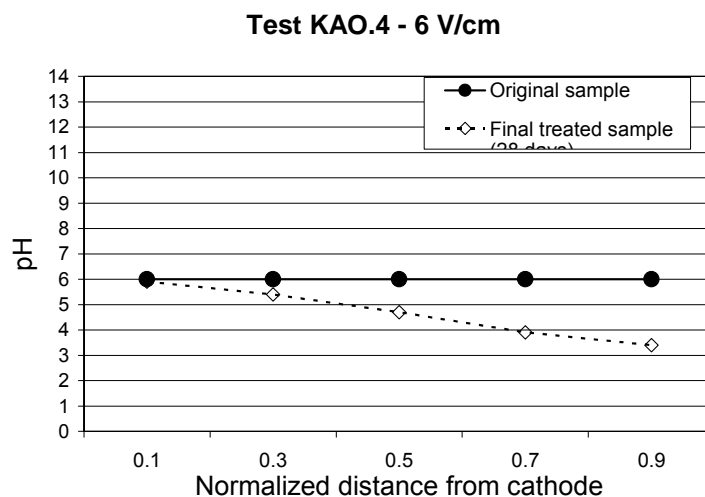


Figure 4.31 – Soil pH profile recorded during test KAO.4.



**Figure 4.32 – Soil pH profile recorded at the beginning and at the end of test KAO.4.**

During this test, the contaminant removal was not monitored while the test was in progress and the TOC and TPH contents were measured only at the beginning and at the end of the trial. The results are presented in Table 4.22, Figure 4.33 and Figure 4.34. As can be seen from the data shown, an increase in the applied voltage from 3 V/cm (applied in test KAO.3) to 6 V/cm (applied in the present test), resulted in a very limited improvement of the TOC removal, which rose from 54% to 55%. At the same time, the TPH removal was about 78%, which was even lower than the TPH removal efficiency achieved in test KAO.3 (85%).

This drop in the TPH removal efficiency from test KAO.3 to KAO.4 can be considered negligible and mainly due to differences in the initial contaminant content of the soil samples. In sum, both the TOC and the TPH removals achieved during test KAO.3 and KAO.4 can be considered of the same order of magnitude, thus suggesting that the increase in the applied voltage from 3 V/cm to 6 V/cm did not result in an improvement of the treatment efficiency.

**Table 4.22 – Contaminant removals achieved during test KAO.4.**

Elapsed time [d]	TOC [g/kg <sub>DW</sub> ]	TPH [g/kg <sub>DW</sub> ]	TOC Removal	TPH Removal
0	185.0	179.8	-	-
28	84.0	40.3	55%	78%

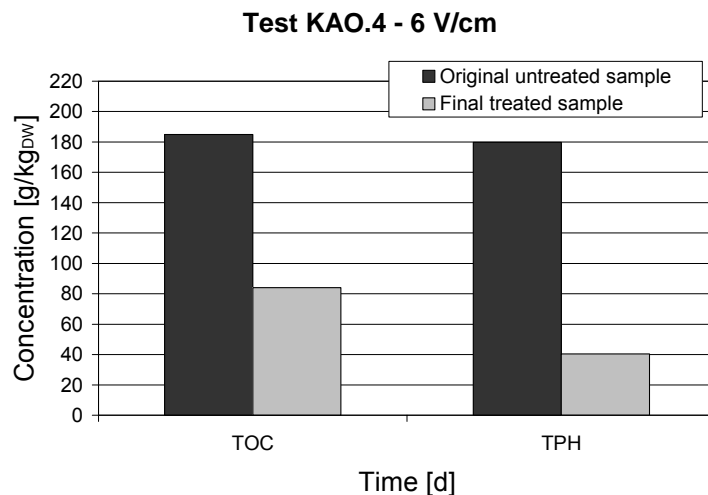


**Figure 4.33 – Contaminant concentrations recorded during test KAO.4.**

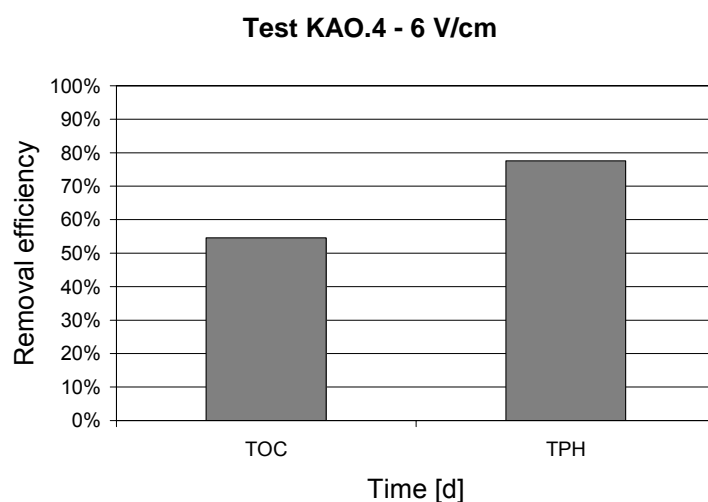


**Figure 4.34 – Contaminant removals achieved during test KAO.4.**

As in the previous tests, the final contaminant contents in the treated soil proved to be evenly distributed along the soil specimen (see Table 4.23 and Figure 4.35), while the soil humidity in the treated sample ranged from 32.9% from the soil near the anode to 37.8% at the cathode side (Figure 4.36).

**Table 4.23 – Contaminant and soil humidity distribution along the soil specimen at the end of test KAO.4.**

Normalized distance from cathode	TPH [g/kg <sub>DW</sub> ]	Humidity [%]
0.1	41.5	37.8%
0.3	38.6	35.9%
0.5	39.0	34.5%
0.7	48.2	33.3%
0.9	50.7	32.9%

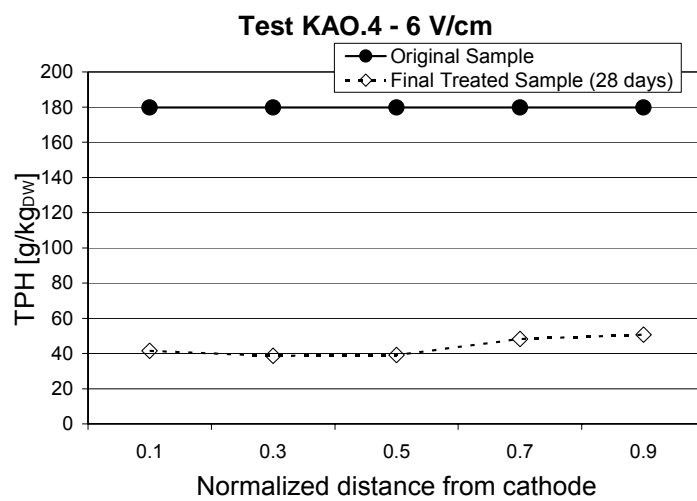


**Figure 4.35 – Contaminant distribution along the soil specimen at the end of test KAO.4.**

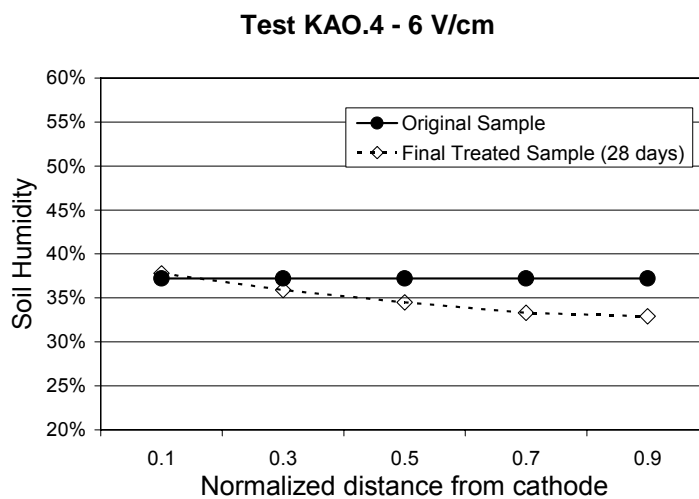


**Figure 4.36 – Soil humidity distribution along the soil specimen at the end of test KAO.4.**

#### 4.3.1.5 Test KAO.5

One additional test (test KAO.5, Table 4.24) was performed on diesel-contaminated kaolin to assess treatment efficiencies in case of larger soil specimen. In this test, which was conducted using Setup 1, the soil specimen had a length of 50 cm, with a cross section of 64 cm<sup>2</sup> (circular section with a diameter of 9 cm). As in test KAO.2, during test KAO.5 a specific voltage gradient of 1 V/cm (corresponding to a total voltage of 50 V) was applied for 4 weeks (28 days).

**Table 4.24 – Main features of test KAO.5.**

Test name	KAO.5	
Matrix	kaolin	
Contaminant	diesel fuel	
Sample weight	6.4	[kg]
Sample length	50	[cm]
Sample volume	3.2	[L]
Sample density	2.0	[kg/L]
Test duration	28	[d]
Voltage (constant)	50	[V]
Specific voltage	1.0	[V/cm]

At the beginning of the test a current of 7 mA was recorded, while at the end of the experiment the current flowing was about 0.3 mA (Table 4.25, Figure 4.37). As can be seen from Table 4.25 and Figure 4.38, the application of the electric field resulted in the occurrence of an electroosmotic flow from the anode towards the cathode, which was important especially in the first two days of the trial. As a result, at the end of the test 11 mL of water were found to be collected in the tank at the cathode compartment.

**Table 4.25 – Results of the electric current and electroosmotic flow monitoring during test KAO.5.**

Time [h]	Time [d]	Current [mA]	Water collected at cathode compartment [mL]
0	0	7	0.0
24	1	3.2	8.0
48	2	3.1	9.0
168	7	1.0	11.0
336	14	0.4	11.0
528	22	0.3	11.0
672	28	0.3	11.0

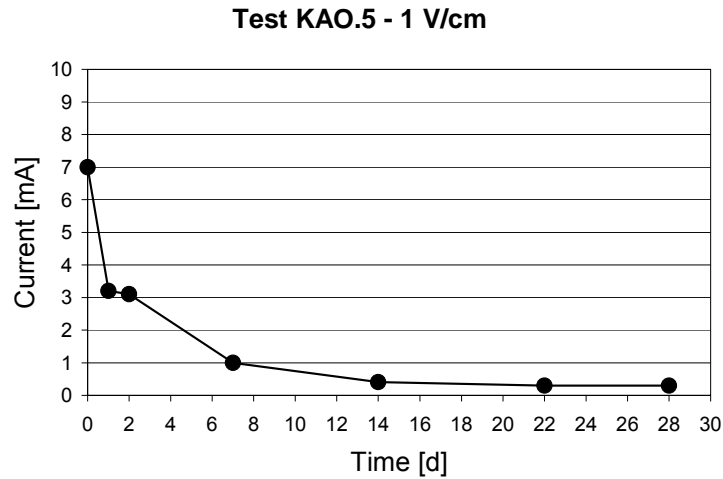


Figure 4.37 – Electric current recorded during test KAO.5.

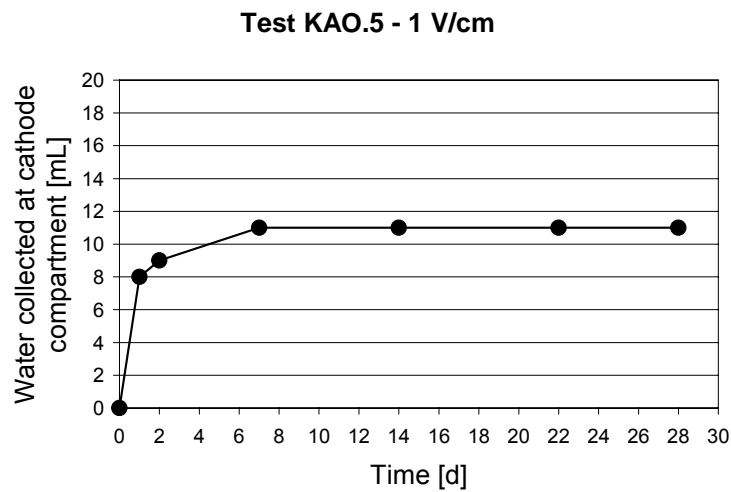


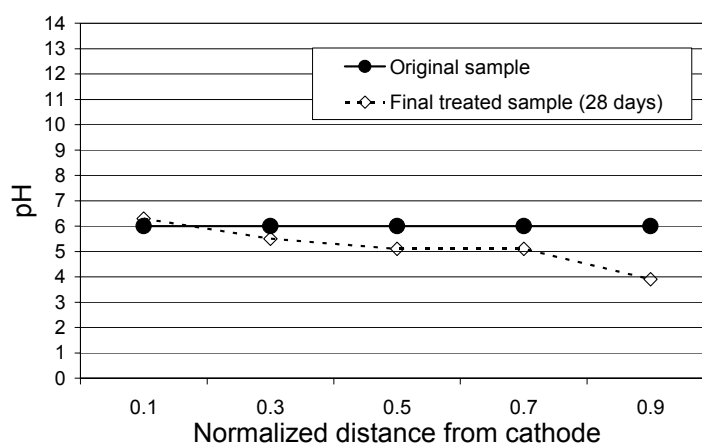
Figure 4.38 – Electroosmotic flow recorded during test KAO.5.

Since the experimental setup used to conduct this test did not allow opening the reaction cell while the test was in progress, the soil pH profile was measured only at the beginning and at the end of the process. The results, reported in Table 4.26 and in Figure 4.39, indicated an acidification of the soil at the anode side and a slight basification near the cathode.



**Table 4.26 – Soil pH at the beginning and at the end of test KAO.5.**

Normalized distance from cathode	Time [d]	
	0	28
0.1	6.0	6.3
0.3	6.0	5.5
0.5	6.0	5.1
0.7	6.0	5.1
0.9	6.0	3.9

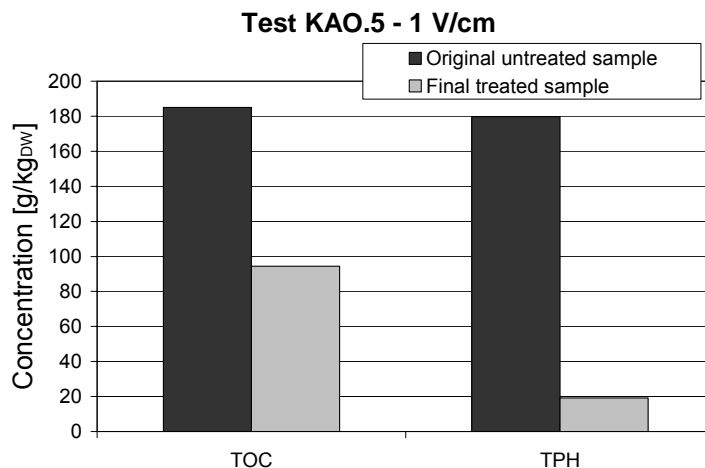
**Test KAO.5 - 1 V/cm**

**Figure 4.39 – Soil pH profile recorded at the beginning and at the end of test KAO.5.**

As for the contaminant removal, the test resulted in 49% TOC removal and 89% TPH removal (the results are shown in Table 4.31, Figure 4.40 and Figure 4.41), thus confirming, despite some variability, probably due to different initial contaminant concentrations, the results achieved with the same specific voltage on a smaller soil specimen during test KAO.2.

These results are quite important as they indicate that no scale effect affects the electrochemical process, provided that a sufficient voltage gradient (e.g. 1 V/cm) is created across the electrodes.

**Table 4.27 – Contaminant concentration and removals achieved during test KAO.5.**

Elapsed time [d]	TOC [g/kg <sub>DW</sub> ]	TPH [g/kg <sub>DW</sub> ]	TOC Removal	TPH Removal
0	185.0	179.8	-	-
28	94.4	19.2	49%	89%



**Figure 4.40 – Contaminant concentrations recorded during test KAO.5.**

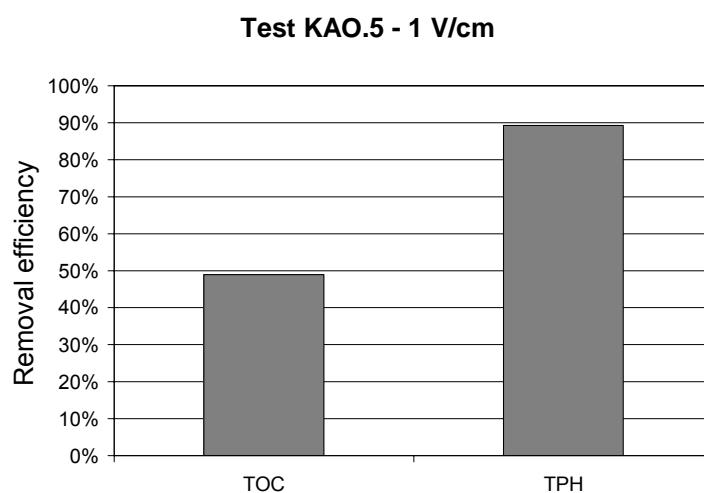


**Figure 4.41 – Contaminant removals achieved during test KAO.5.**

The final TOC and TPH distribution were evaluated at the end of the test (see Table 4.28, Figure 4.42 and Figure 4.43). As expected, the results indicated that no spatial trend could be detected in the treated soil sample.

**Table 4.28 – Contaminant and soil humidity distributions along the soil specimen at the end of test KAO.5.**

Normalized distance from cathode	TOC [g/kg <sub>DW</sub> ]	TPH [g/kg <sub>DW</sub> ]	Humidity [%]
0.1	170.2	17.9	9.9%
0.3	87.1	19.9	11.3%
0.5	81.7	16.7	14.2%
0.7	89.4	24.4	16.6%
0.9	100.1	32.0	18.1%

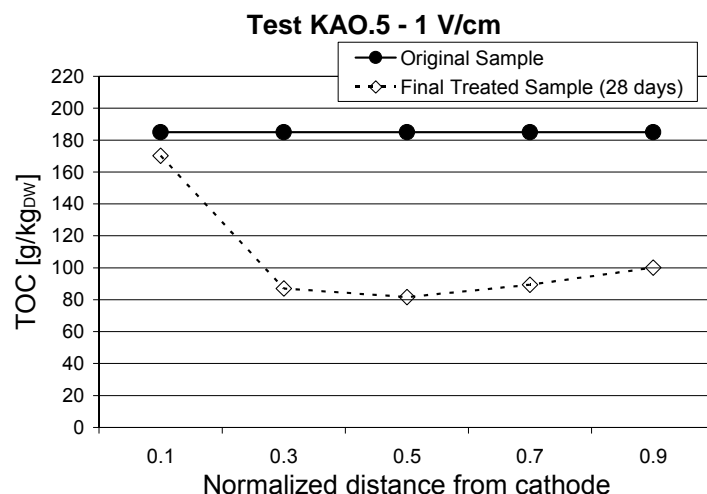


**Figure 4.42 – TOC distribution along the soil specimen at the end of test KAO.5.**

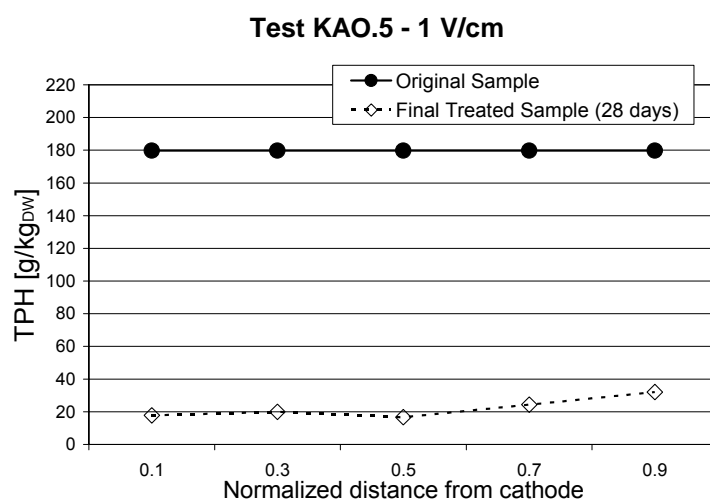


**Figure 4.43 – TPH distribution along the soil specimen at the end of test KAO.5.**

At the end of this run, the contaminant content in the fluid collected in the tank at the cathode compartment was measured, in order to evaluate the contaminant removal due to the electroosmotic transport along the soil specimen. About 11 mL were collected at the cathode side, which were characterized by a TOC concentration of 875.2 g/L and by a TPH content about 726.4 g/L (Table 4.29). Therefore, the total TOC content in the water sample was about 9.6 g, while the TPH content was 8.0 g. The soil specimen used for the experiment had a mass of about 6.4 kg and showed a TOC concentration about 185.0 g/kg<sub>DW</sub> and a TPH concentration of 179.8 g/kg<sub>DW</sub>, which corresponded to a total contaminant content of 1184.0 g of TOC and 1150.7 g of TPH. Hence, the fraction of the pollutant content removed from the soil specimen because of the electroosmotic transport along the soil specimen was about 0.8% for TOC and 0.7% for TPH, which can be considered negligible contributions to the overall contaminant loss.

This confirmed that the main pathway for contaminant removal is based on the

electrooxidation reactions induced by the electric field, while the influence of transport phenomena on the contaminant removal can be considered negligible.

**Table 4.29 – Contaminant and soil humidity distribution along the soil specimen at the end of test KAO.5.**

Volume	11	[mL]
TOC	875.2	[g/L]
TPH	726.4	[g/L]
pH	3.3	[-]

#### 4.3.1.6 Test KAO.6

This test was performed on a sample of diesel-contaminated kaolin without the application of any electric current, as a reference test (i.e. blank experiment) to assess any mass loss of contaminants due to evaporation or other chemical, physical or biological degradation phenomena not linked with the electrochemical processes. Like tests KAO.1, KAO.2, KAO.3 and KAO.4, during this trial was performed with Setup 2 on a 2-kg soil sample and lasted for four weeks (Table 4.30).

The tests was conducted in parallel with test KAO.3; thus, like in test KAO.3, the original soil sample was characterized by a TOC content of 221.1 g/kg<sub>DW</sub>, a TPH content of 185.3 g/kg<sub>DW</sub>, a soil water content of 36.9% and a pH of 6.0.

**Table 4.30 – Main features of test KAO.6.**

Test name	KAO.6	
Matrix	kaolin	
Contaminant	diesel fuel	
Sample weight	2	[kg]
Sample length	10	[cm]
Sample volume	1.0	[L]
Sample density	2.0	[kg/L]
Test duration	28	[d]
Voltage (constant)	0	[V]
Specific voltage	0.0	[V/cm]

At the end of the trial, the soil sample showed a TOC content about 209.7 g/kg<sub>DW</sub> and a TPH content about 144.5 g/kg<sub>DW</sub> (Table 4.31). The final soil humidity was 35.2%, while the soil pH did not change during the experiment.

The loss of contaminants during the trial was about 5% for TOC and 22% for TPH. These results indicate that a certain amount of pollutants can be removed due evaporation and other natural processes, but the contaminant losses encountered during this test are

significantly lower than those achieved by electrochemical methods during the previous experiments, which ranged from 46% to 55% for TOC and from 66% to 85% for TPH. The fact that the decrease in the TPH content was significantly higher than that achieved for TOC suggest that a significant part of the hydrocarbons in the soil sample were partially degraded, thus, they no longer contribute to the TPH content in the soil sample at the end of the test. Nevertheless, only the 5% of the total organic matter was completely mineralized or lost because of evaporation.

**Table 4.31 – Contaminant concentrations and losses during test KAO.6**

Elapsed time [d]	TOC [g/kg <sub>DW</sub> ]	TPH [g/kg <sub>DW</sub> ]	TOC Loss	TPH Loss
0	221.1	185.3	-	-
28	209.7	144.5	5%	22%

#### 4.3.1.7 EK-Fenton test

This test was performed to evaluate the effects of a combined treatment including the electrochemical process and traditional chemical oxidation with hydrogen peroxide. This technique, often named as electrokinetic-Fenton process or EK-Fenton, has been regarded by various Authors (Yang and Liu, 2001; Kim et al., 2005a; Park et al., 2005; Kim et al., 2006) as effective for the removal of different apolar and immobile organic pollutants, including PAHs and chlorinated solvents (see Chapter 2.4.2). Unlike most of the experiments reported in literature, the test performed here was unenhanced, i.e. no acid solution or conditioning fluid was provided to improve soil conductivity and the electroosmotic flow rate.

The test was performed with Setup 2 and lasted for 4 weeks (28 days). During the trial, a 2 kg-kaolin specimen, having a length of 10 cm, was tested under a constant voltage gradient of 10 V, corresponding to a specific voltage of 1 V/cm. At the same time, 1 L of 3% solution of hydrogen peroxide was dosed at the anode compartment, behind the electrode to enhance the pollutant mineralization in the soil sample. Since holed electrodes were used during the test, the oxidant solution was allowed to flow across the anode and into the soil specimen. The solution was dosed at the anode side to allow the electroosmotic flux, flowing from the anode towards the cathode, to enhance the transport of the oxidant agent along the soil specimen, as suggested by previous works (Yang and Liu, 2001; Kim et al., 2005a, Park et al., 2005). The solution collected at the cathode was then recirculated at the anode compartment to use the residual hydrogen peroxide existing in the fluid. The dosage of the hydrogen peroxide solution at the anode compartment also resulted in a hydraulic gradient of 1 cm/cm across the soil specimen, between the anode and the cathode.

Since a fresh hydrogen peroxide solution was only dosed once at the beginning of the experiment, it was expected to influence the mineralization process only during the first days of the test, as it is known to be characterized by a limited stability into soils, and to be rapidly consumed by various chemical reactions with the soil organic matter (ITRC, 2005).

The soil sample used to perform test KAO.HP was characterized by an initial TOC content of 173.5 g/kg<sub>DW</sub>, a TPH concentration of 134.8 g/kg<sub>DW</sub>, a soil humidity of 38.3% and a pH of 6.0.

The main features of test KAO.HP are reported in Table 4.32.

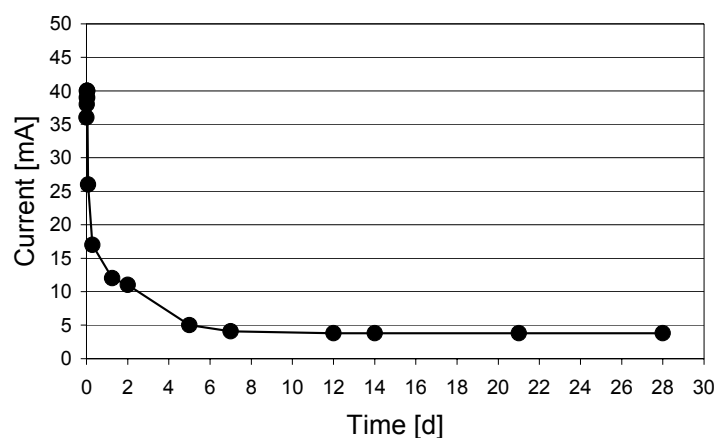
**Table 4.32 – Main features of test KAO.HP.**

Test name	KAO.HP	
Matrix	kaolin	
Contaminant	diesel fuel	
Sample weight	2	[kg]
Sample length	10	[cm]
Sample volume	1.0	[L]
Sample density	2.0	[kg/L]
Test duration	28	[d]
Voltage (constant)	10	[V]
Specific voltage	1.0	[V/cm]
Oxidant dosed at anode compartment	H <sub>2</sub> O <sub>2</sub>	
Oxidant concentration	3%	
Initial current	36	[mA]
Final current	3.8	[mA]

As can be seen from Table 4.33 and Figure 4.44, at the beginning of the trial a current of about 36 mA was encountered; the current gradually increase during the first hour of the experiment up to 40 mA, then started to decrease and reached a steady state value (3.8 mA) 12 days after the beginning of the test. During the experiment, it was not possible to measure the amount of the electroosmotic flow induced by the electric field, as it was superimposed to the flow caused by the hydraulic gradient between anode and cathode.

**Table 4.33 – Results of the electric current monitoring during test KAO.HP.**

Time [h]	Time [d]	Current [mA]
0.0	0.0	36
0.17	0.007	38
0.33	0.014	39
0.50	0.021	40
0.67	0.028	40
0.83	0.035	40
1	0.042	39
2	0.083	26
7	0.292	17
30	1.25	12
48	2	11
120	5	5.0
168	7	4.1
288	12	3.8
336	14	3.8
504	21	3.8
672	28	3.8

**Test KAO.HP - 1 V/cm****Figure 4.44 – Electric current recorded during test KAO.HP.**

The pH profile of the soil specimen was monitored during the test. Unlike the tests performed with the sole use of the voltage gradient (e.g test KAO.2, when a specific voltage of 1 V/cm was applied), in this case the entire soil specimen was significantly acidified since the first days of the test, without a noticeable basification of the soil near the cathode (data are shown in Table 4.34, Figure 4.45 and Figure 4.46). As a result, at the end of the experiment the soil pH ranged from 3.6 at the anode side and 4.4 at the cathode side.

Overall, it is thought that the hydraulic flow due to the dosage of the oxidizing solution at the anode compartment helped the advance of the acid front from the anode towards the cathode, thus resulting in a rapid acidification of all the soil profile.

**Table 4.34 – Soil pH profile during test KAO.HP.**

Normalized distance from cathode	Time [d]								
	0	1	2	5	7	14	21	28	
0.1	6.0	6.1	5.8	4.4	4.2	4.3	4.0	4.4	
0.3	6.0	5.9	4.7	4.4	3.6	3.6	3.8	3.9	
0.5	6.0	5.0	3.7	3.4	3.5	3.6	3.9	3.7	
0.7	6.0	4.3	3.1	3.6	3.8	3.4	3.6	3.7	
0.9	6.0	3.3	2.9	3.5	3.3	3.3	3.5	3.6	

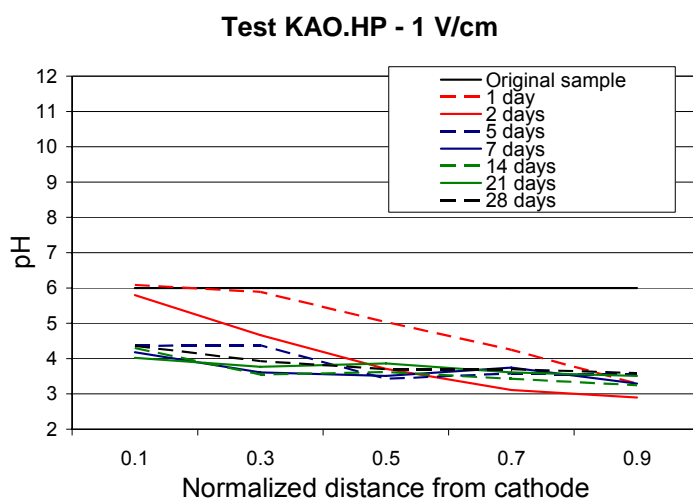


**Figure 4.45 – Soil pH profile recorded during test KAO.HP.**

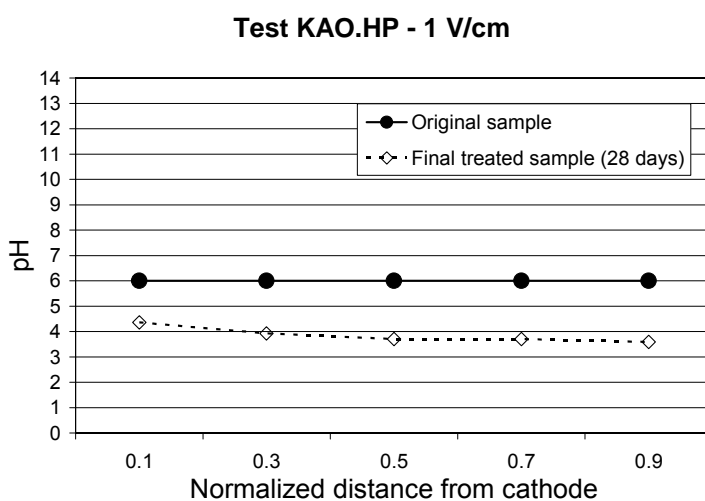


**Figure 4.46 – Soil pH profile recorded at the beginning and at the end of test KAO.HP.**



The contaminant removals achieved during this test are reported in Table 4.35 and shown in Figure 4.47 and Figure 4.48. The EK-Fenton process resulted in a quite rapid contaminant degradation with high removal efficiencies being achieved both for TOC and for TPH even 1 or 2 days after the beginning of the test. However, the overall removal efficiencies achieved during this test (42% TOC removal and 84% TPH removal) were not higher than those recorded at the end of test KAO.2, which was performed with the sole use of the electrochemical process, and which resulted in about 54% TOC removal and 80% TPH removal. The limited differences in the removal efficiencies achieved during the two tests may be due to different initial contaminant concentration in the treated samples. It is believed that the dosage of the hydrogen peroxide solution lead to a certain mineralization of the target organics in the first days of the test. Nevertheless, its effect was negligible in comparison to the electrooxidation process, which worked less rapidly but effectively.

For convenience, the contaminant removal efficiencies achieved during tests KAO.2 and KAO.HP are compared in Figure 4.49.

**Table 4.35 – Contaminant removals achieved during test KAO.HP.**

Elapsed time [d]	TOC [g/kg <sub>DW</sub> ]	TPH [g/kg <sub>DW</sub> ]	TOC Removal	TPH Removal
0	173.5	134.8	-	-
1	116.5	47.7	33%	65%
2	114.0	45.1	34%	67%
7	-	41.1	-	70%
14	102.0	39.7	41%	71%
21	103.1	39.5	41%	71%
28	100.7	21.4	42%	84%

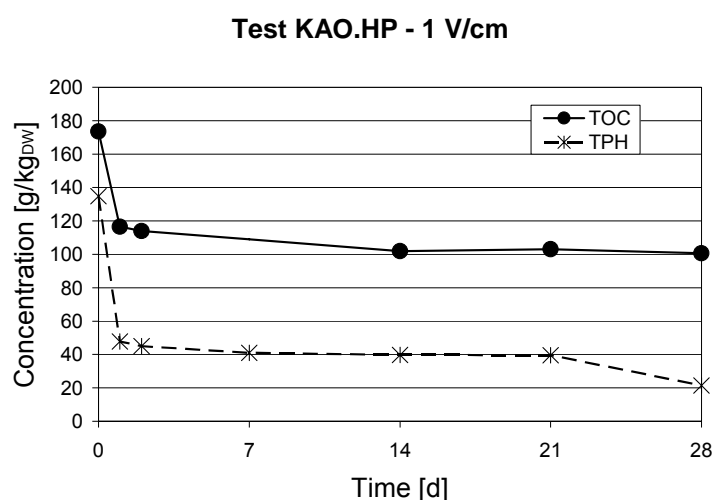


**Figure 4.47 – Contaminant concentrations recorded during test KAO.HP.**

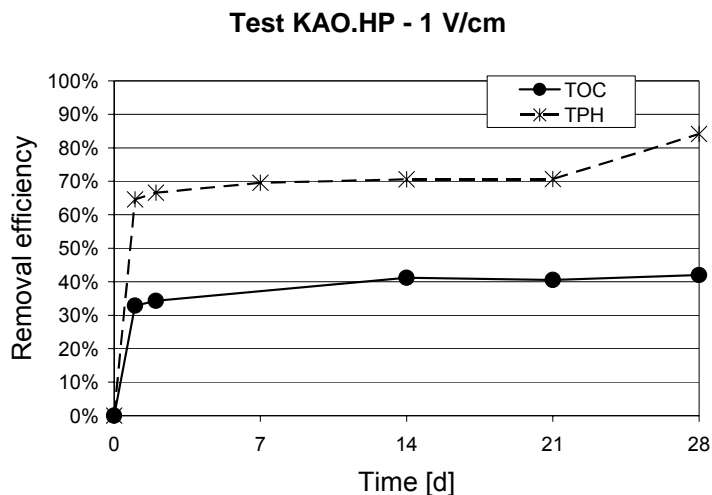


Figure 4.48 – Contaminant removals achieved during test KAO.HP.

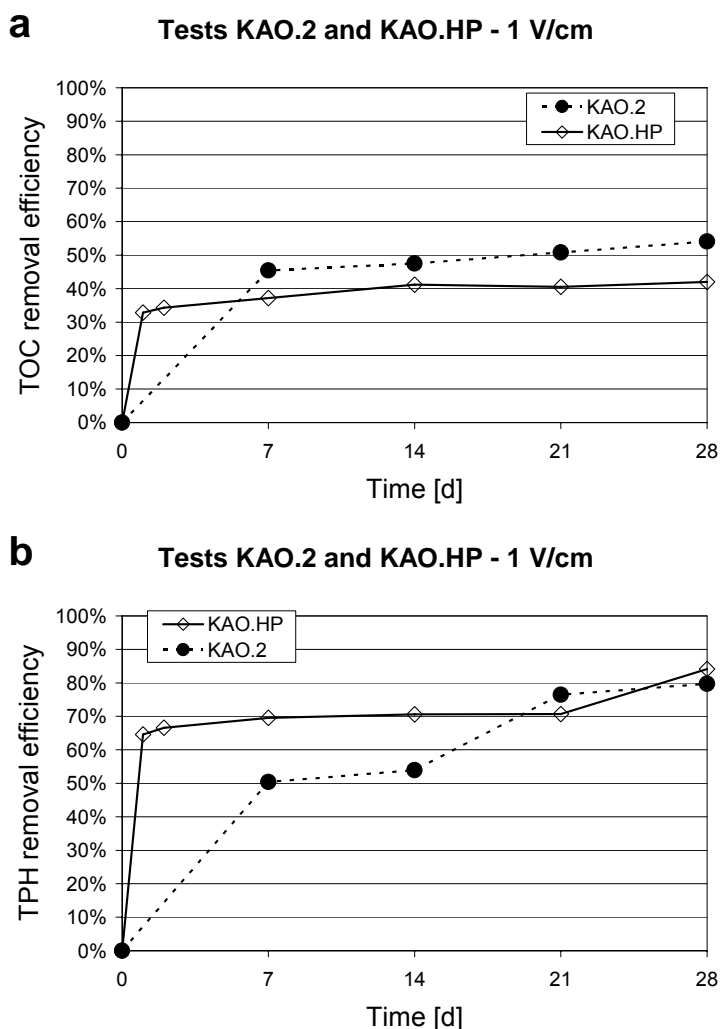


Figure 4.49 – Comparison of the contaminant removal efficiencies achieved during tests KAO.2 (performed with a voltage gradient of 1 V/cm) and KAO.HP (performed with a voltage gradient of 1 V/cm and 3% hydrogen peroxide as anolyte solution).

As can be seen from Table 4.36, Figure 4.50 and Figure 4.51, the contaminant

removal achieved during this combined treatment can be considered uniform in the treated volume, both the TOC and TPH concentration having been found quite evenly distributed along the soil specimen at the end of the test. This evidence was quite peculiar, since the electrooxidation process was already observed to act uniformly in the soil volume, but the chemical oxidation treatment is well-known to be highly space dependent, i.e. its effectiveness decreasing as distance increases from the injection point, even during EK-Fenton processes (Kim et al., 2005; Park et al., 2005). According to these facts, the mineralization efficiency was expected to be highest at the anode side, because of a stronger oxidation due to the addition of the hydrogen peroxide solution. On the opposite, the fact that the contaminant removal was uniform within the treated volume suggested that the mineralization effect due to chemical oxidation with hydrogen peroxide was negligible compared to the effects of the electrooxidation process. This was probably due to the low permeability of the target soil, which probably limited the reactant flow and constrained the contact between the liquid oxidant agents and the pollutants. It is believed that the flux of the oxidant solution along the soil specimen mainly occurred through preferential flow pathways, as commonly occurs in low-permeability soils. This probably limited the contact between the oxidizing solution and the target pollutants.

**Table 4.36 – Contaminant distribution along the soil specimen at the end of test KAO.HP.**

Normalized distance from cathode	TOC [g/kg <sub>DW</sub> ]	TPH [g/kg <sub>DW</sub> ]
0.1	109.1	45.3
0.3	90.5	15.4
0.5	96.4	22.1
0.7	101.7	49.0
0.9	105.7	31.5

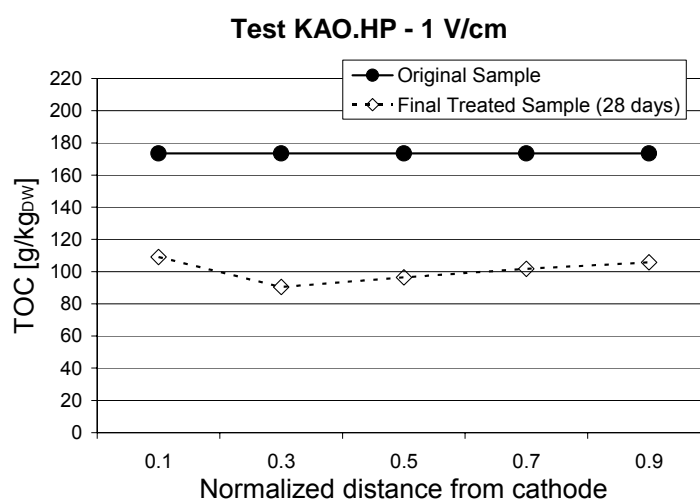


**Figure 4.50 – TOC distribution along the soil specimen at the beginning and at the end of test KAO.HP.**

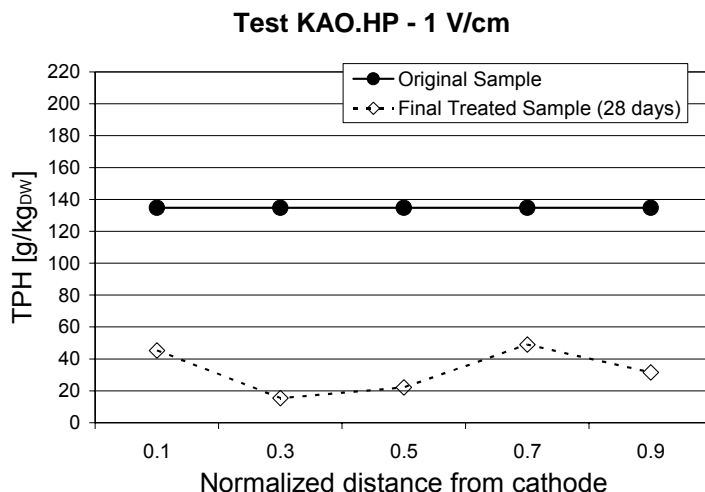


**Figure 4.51 – TPH distribution along the soil specimen at the beginning and at the end of test KAO.HP.**

In sum, the combined application of electrooxidation and of traditional chemical oxidation, with the dosage of oxidant agents at the anode compartment (EK-Fenton process) did not lead to an improvement of the removal efficiencies under to tested conditions in comparison to the sole use of the electric fields

Despite it has been reported (Kim et al., 2005a; Kim et al., 2006) that reactant flows could be enhanced during the soil electrochemical treatment because of the electroosmotic flow induced by the electric field, the results achieved here seem to suggest that this event did not occur under the conditions considered in this study. This is thought to be due to the fact that the electrochemical process was unenhanced, and was therefore characterized by low current intensities and a very limited electroosmotic flow. Under these conditions, hydrogen peroxide could hardly have been introduced into the soil specimen (Kim et al., 2005a). It is believed that if the treatment had been enhanced, with the addition of conditioning fluids (e.g. an electrolyte solution) to improve soil conductivity, the electroosmotic transport could have successfully promoted the migration of the additional oxidant agent along the soil specimen.

## 4.3.2 Tests on diesel-contaminated bentonite

### 4.3.2.1 Test BEN.1

Test BEN.1 was performed on a 2 kg sample of diesel-contaminated bentonite clay for 28 days, with an applied constant voltage of 5 V, corresponding to a specific voltage gradient of 0.5 V/cm (Table 4.37).

The soil sample used for the tests showed an initial TOC concentration of 264.8 g/kg<sub>DW</sub> and a TPH content about 176.0 g/kg<sub>DW</sub>; the soil humidity was about 40.3%. As

observed in Chapter 4.2.1, this soil was strongly alkaline, with a pH about 10.0.

**Table 4.37 – Main features of test BEN.1.**

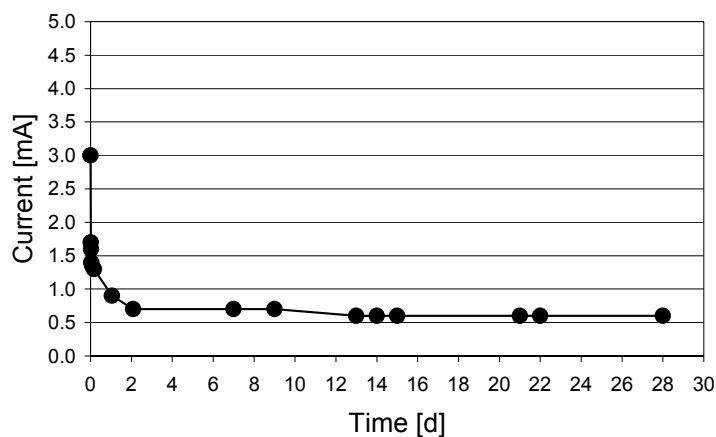
Test name	BEN.1	
Matrix	bentonite	
Contaminant	diesel fuel	
Sample weight	2	[kg]
Sample length	10	[cm]
Sample volume	1.0	[L]
Sample density	2.0	[kg/L]
Test duration	28	[d]
Voltage (constant)	5	[V]
Specific voltage	0.5	[V/cm]

In Table 4.38 and Figure 4.52, the values of the electric current recorded during the test are presented. As can be seen from the data shown, the current values encountered in the tests performed on diesel-contaminated bentonite were much lower than the values recorded for kaolin, when the same voltage gradient was applied (see Section 4.3.1.1 for comparison). In fact, at the beginning of test BEN.1, an electric current of only 3.0 mA was measured, while about 16 mA were encountered in test KAO.1, when the same specific voltage was applied to a kaolin sample. Similarly to kaolin, also during test BEN.1 the current rapidly decreased after the application of the voltage gradient and reached a steady state value (0.6 mA) within two weeks of test.

Being the current values so low, no electroosmotic flow was encountered during the run.

**Table 4.38 – Results of the electric current and electroosmotic flow monitoring during test BEN.1.**

Time [h]	Time [d]	Current [mA]	Water collected at cathode compartment [mL]
0	0.0	3.0	0.0
0.16667	0.01	1.7	0.0
0.5	0.02	1.6	0.0
1	0.04	1.4	0.0
2	0.08	1.4	0.0
4	0.17	1.3	0.0
25	1.04	0.9	0.0
50	2.08	0.7	0.0
168	7	0.7	0.0
216	9	0.7	0.0
312	13	0.6	0.0
336	14	0.6	0.0
360	15	0.6	0.0
504	21	0.6	0.0
528	22	0.6	0.0
672	28	0.6	0.0

**Test BEN.1 - 0.5 V/cm****Figure 4.52 – Electric current recorded during test BEN.1.**

The pH profile monitored during the run was significantly different from the pH profiles measured in the tests performed on diesel-contaminated kaolin (Table 4.39, Figure 4.53 and Figure 4.54). In fact, for the bentonite sample, the pH changes were about 1.1 or less, much more limited than those recorded for kaolin were. The soil target the anode showed a certain basification during the first days of the test, rising from 10.0 up to 10.4, and then it decreased again to 10.0, probably because of the production of the hydrogen ions deriving from water electrolysis. The resulting pH profile at the end of the test ranged

from 10.0 at the anode side to 11.1 near the cathode. In sum, it can be supposed that the strong buffer capacity of the bentonite limited the pH changes, constrained the acidification of the soil at the anode side, and resulted in a slight basification of the soil specimen.

**Table 4.39 – Soil pH profile during test BEN.1.**

Normalized distance from cathode	Time [d]							
	0	1	2	7	14	21	28	
0.1	10.0	10.7	10.5	10.6	10.9	11.0	11.1	
0.3	10.0	10.6	10.4	10.7	10.7	11.0	11.0	
0.5	10.0	10.5	10.6	10.5	10.7	11.0	11.0	
0.7	10.0	10.4	10.4	10.5	10.7	10.7	10.1	
0.9	10.0	10.3	10.4	10.4	10.6	10.6	10.0	

**Test BEN.1 - 0.5 V/cm**

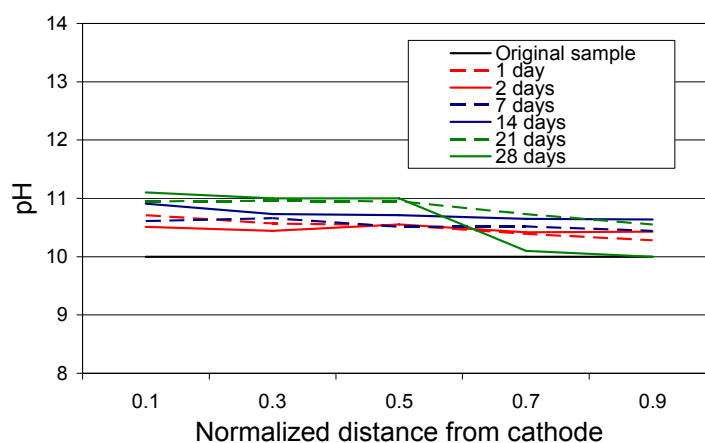


**Figure 4.53 – Soil pH profile recorded during test BEN.1.**

**Test BEN.1 - 0.5 V/cm**

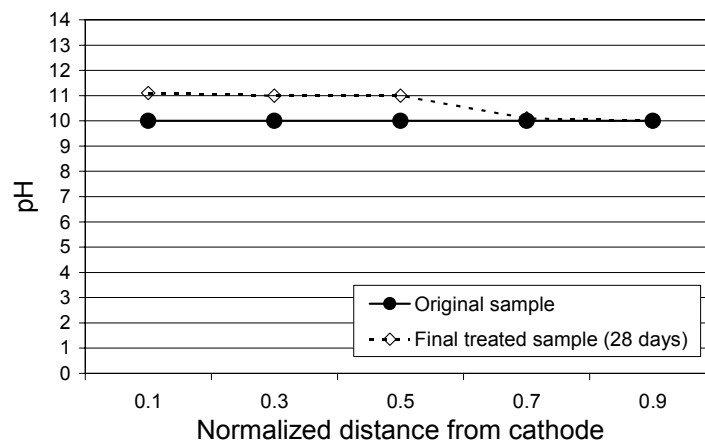


**Figure 4.54 – Soil pH profile at the beginning and at the end of test BEN.1.**

Like in the tests performed on kaolin, the TOC and TPH removals were evaluated during this test. The results achieved, presented in Table 4.40, Figure 4.55 and Figure 4.56, indicated that very high contaminant removal occurred, with a TOC removal of 50% after a two-week treatment. The TOC removal increased up to 57% by the end of the third week of the run, and to 60% by the end of the test. The TPH removals followed a similar trend, with a removal efficiency of 42% on the 14<sup>th</sup> day of treatment, of 59% on the 21<sup>st</sup> day and of 73% at the end of the process (28<sup>th</sup> day).

As can be clearly seen from Figure 4.56, the contaminant removal significantly improved with time, showing the same behavior encountered for kaolin. In this case, however, the overall removal efficiencies were much higher than those achieved for kaolin were. For example, test KAO.1, when an applied voltage of 0.5 V/cm was applied, resulted in 46% TOC removal and 66% TPH removal, much lower than the removal efficiencies achieved here under the same specific voltage gradient.

**Table 4.40 – Contaminant removals achieved during test BEN.1.**

Elapsed time [d]	TOC [g/kg <sub>DW</sub> ]	TPH [g/kg <sub>DW</sub> ]	TOC Removal	TPH Removal
0	264.8	176.0	-	-
7	-	-	-	-
14	131.6	102.2	50%	42%
21	113.4	72.8	57%	59%
28	107.0	47.0	60%	73%

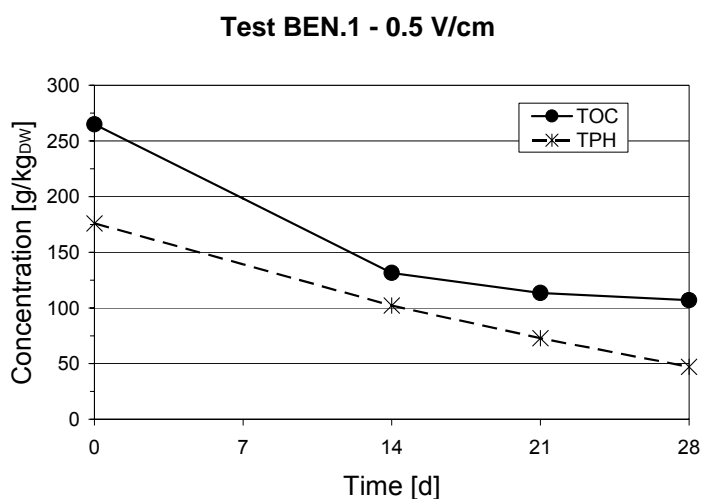


**Figure 4.55 – Contaminant concentrations recorded during test BEN.1.**



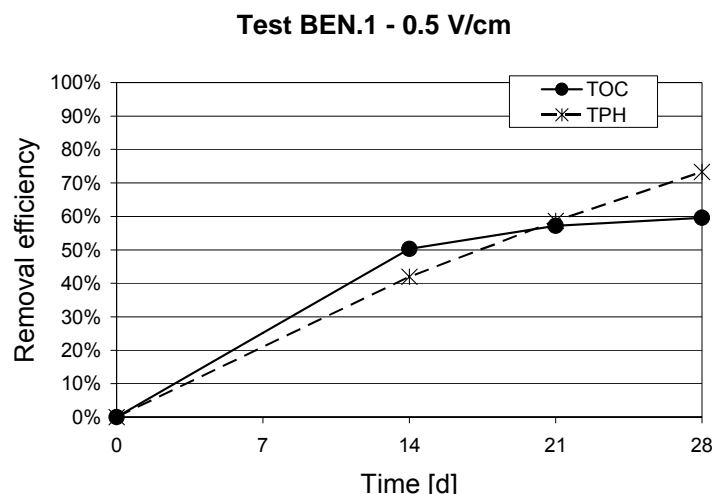


**Figure 4.56 – Contaminant removals achieved during test BEN.1.**

The TPH distribution was evaluated at the end of the experiment (Table 4.41, Figure 4.57) to assess any influence of the electrode distance or of the transport phenomena on the pollutant removal. The TPH concentration in the soil sample ranged from 21.9 g/kg<sub>DW</sub> in the middle of the specimen to 57.1 g/kg<sub>DW</sub> in the section closest to the cathode. Despite this variability, that can be considered due to a quite heterogeneous distribution of the hydrophobic pollutants of concern, as expected, no significant influence of the electrode distance or of the transport phenomena was detected for bentonite.

The final soil water content ranged from 36.7% for the soil near the anode, to 41.3% at the cathode site, with an almost linear distribution in space (Figure 4.58).

**Table 4.41 – Contaminant and soil humidity distribution along the soil specimen at the end of test BEN.1.**

Normalized distance from cathode	TPH [g/kg <sub>DW</sub> ]	Humidity [%]
0.1	57.1	41.3%
0.3	54.2	39.4%
0.5	21.9	37.4%
0.7	22.9	36.7%
0.9	54.3	36.7%

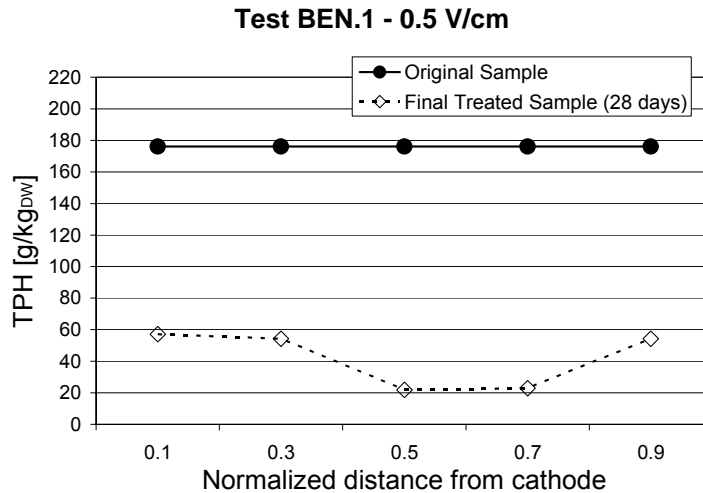


**Figure 4.57 – Contaminant distribution along the soil specimen at the end of test BEN.1.**

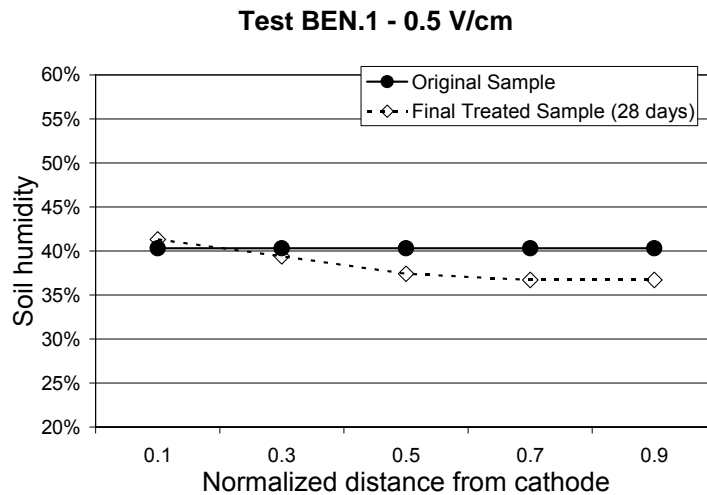


**Figure 4.58 – Soil humidity distribution along the soil specimen at the end of test BEN.1.**

#### 4.3.2.2 Test BEN.2

Similarly to test BEN.1, test BEN.2 was performed on a 2 kg sample of diesel-contaminated clay for 28 days, with an applied constant voltage of 10 V, corresponding to a specific voltage gradient of 1 V/cm (Table 4.42).

The process was conducted in parallel with test BEN.1. Therefore, the contaminant removal efficiencies were calculated in reference to the same original soil sample, which was characterized by a TOC concentration of 264.8 g/kg<sub>DW</sub>, TPH content about 176.0 g/kg<sub>DW</sub>, a soil humidity about 40.3% and a pH of 10.0.

**Table 4.42 – Main features of test BEN.2.**

Test name	BEN.2	
Matrix	bentonite	
Contaminant	diesel fuel	
Sample weight	2	[kg]
Sample length	10	[cm]
Sample volume	1.0	[L]
Sample density	2.0	[kg/L]
Test duration	28	[d]
Voltage (constant)	10	[V]
Specific voltage	1.0	[V/cm]

During the test, the electric current started from about 6.0 mA (e.g. two times the current encountered at the beginning of tests BEN.1) and rapidly decreased, reaching a steady state value of 0.05 mA (Table 4.43 and Figure 4.59).

As in the previous experiment, an electroosmotic flux did not occur, being the electric currents flowing very low.

**Table 4.43 – Results of the electric current and electroosmotic flow monitoring during test BEN.2.**

Time [h]	Time [d]	Current [mA]	Water collected at cathode compartment [mL]
0	0.0	6.0	0.0
0.5	0.0	2.7	0.0
1	0.0	2.6	0.0
2	0.1	2.9	0.0
4	0.2	3.0	0.0
8	0.3	2.8	0.0
25	1.0	1.7	0.0
50	2.1	1.4	0.0
168	7.0	1.3	0.0
216	9.0	1.1	0.0
312	13.0	1.1	0.0
336	14.0	0.6	0.0
504	21.0	0.05	0.0
528	22.0	0.05	0.0
672	28.0	0.05	0.0

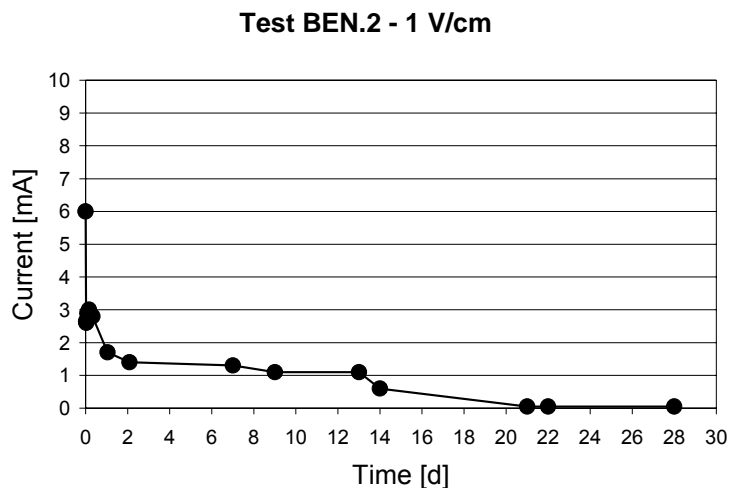


**Figure 4.59 – Electric current recorded during test BEN.2.**

The evolution of the pH profile encountered during this test (see Table 4.44, Figure 4.60 and Figure 4.61) was similar to that recorded during test BEN.1. Indeed, the pH increased during the electrochemical treatment along all the soil specimen, arising to about 11.0 at the cathode side and to 10.6 at the anode side, already a few days after the beginning of the experiment. Besides this basification effect, an acidification process also started to occur near the anode during the third and fourth weeks of the run, resulting in a decrease of the soil pH in this area at the end of the test. The final pH profile ranged from 9.7 at the anode side to 11.0 at the cathode side (Figure 4.61).

**Table 4.44 – Soil pH profile during test BEN.2.**

Normalized distance from cathode	Time [d]							
	0	1	2	7	14	21	28	
0.1	10.0	10.8	11.0	11.0	10.8	10.8	11.0	
0.3	10.0	10.9	11.0	10.9	10.7	10.9	10.9	
0.5	10.0	10.9	10.8	10.9	10.7	10.9	10.9	
0.7	10.0	10.8	11.0	10.9	10.8	10.8	10.8	
0.9	10.0	10.6	10.6	10.6	10.6	10.3	9.7	

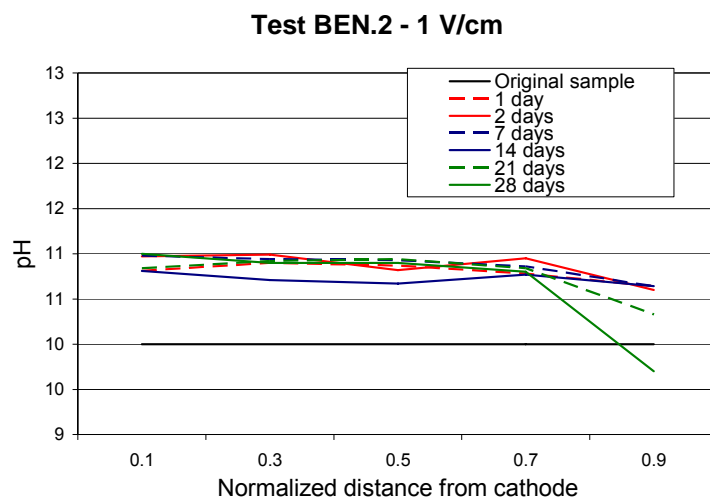


**Figure 4.60** – Soil pH profile recorded during test BEN.2.

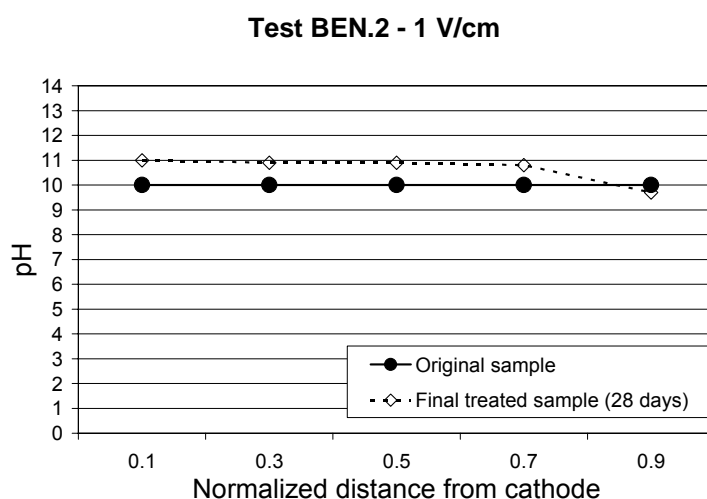


**Figure 4.61** – Soil pH profile at the beginning and at the end of test BEN.2.

The TOC and TPH removal efficiencies attained during this test, which are presented in Table 4.45, Figure 4.62 and Figure 4.63, were even higher than those encountered during test BEN.1. In fact, at the end of the test, a 69% TOC removal and an 87% TPH removal were achieved, with removal efficiencies appreciably improving with time.

**Table 4.45** – Contaminant removals achieved during test BEN.2.

Elapsed time [d]	TOC [g/kg <sub>DW</sub> ]	TPH [g/kg <sub>DW</sub> ]	TOC Removal	TPH Removal
0	264.8	176.0	-	-
7	184.2	77.0	30%	56%
14	127.4	71.4	52%	59%
21	95.5	55.0	64%	69%
28	81.6	23.0	69%	87%

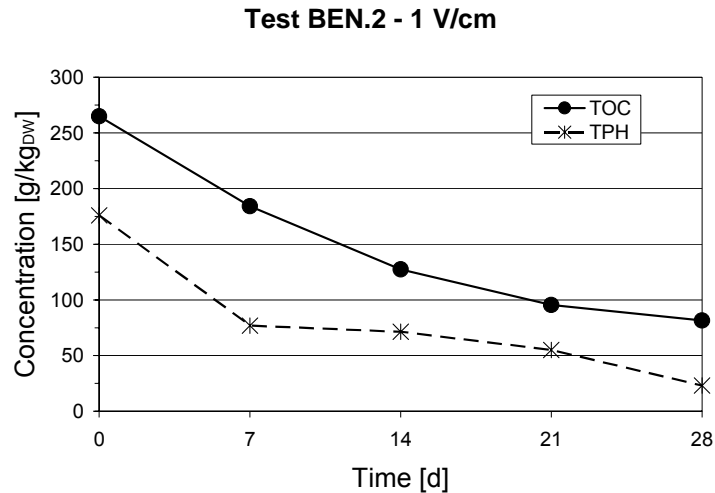


Figure 4.62 – Contaminant removals achieved during test BEN.2: concentrations (a) and removal efficiencies (b).

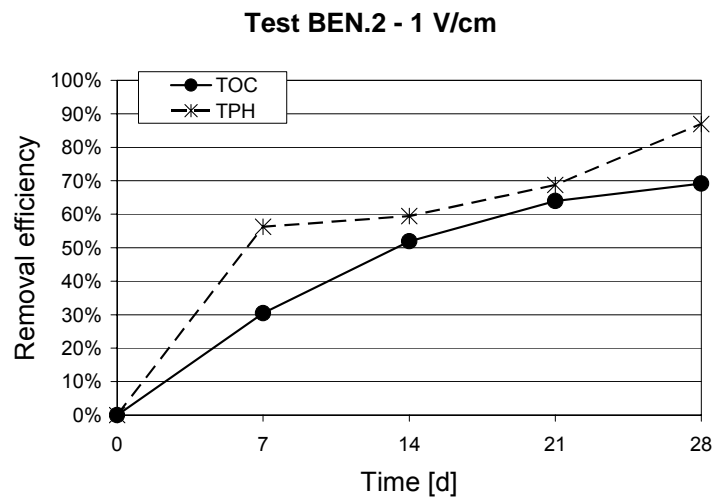


Figure 4.63 – Contaminant removals achieved during test BEN.2: concentrations (a) and removal efficiencies (b).

Once more, apart from a certain sample heterogeneity, an evenly distributed final TPH profile was encountered at the end of the test (Table 4.46 and Figure 4.64).

The final soil water content ranged from 37.7% at the anode side, to 47.7% at the cathode site, with an almost linear trend in space (Figure 4.65).

**Table 4.46 – Contaminant and soil humidity distribution along the soil specimen at the end of test BEN.2.**

Normalized distance from cathode	TPH [g/kg <sub>DW</sub> ]	Humidity [%]
0.1	20.4	47.7%
0.3	19.4	43.6%
0.5	15.6	43.4%
0.7	20.0	41.6%
0.9	39.0	37.7%

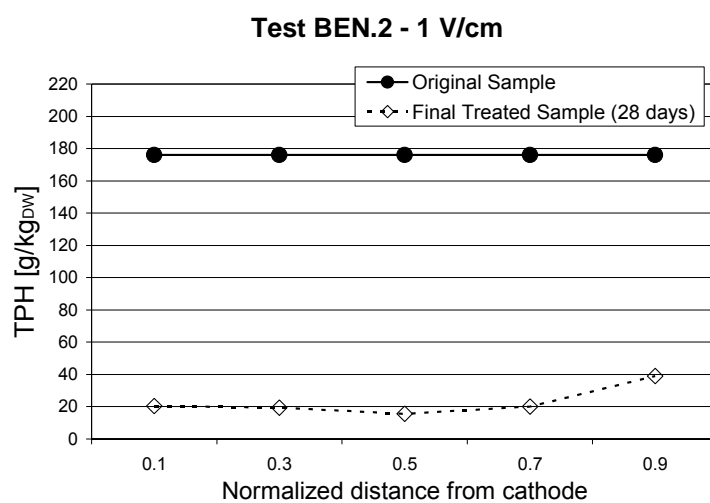


**Figure 4.64 – Contaminant distribution along the soil specimen at the end of test BEN.2.**

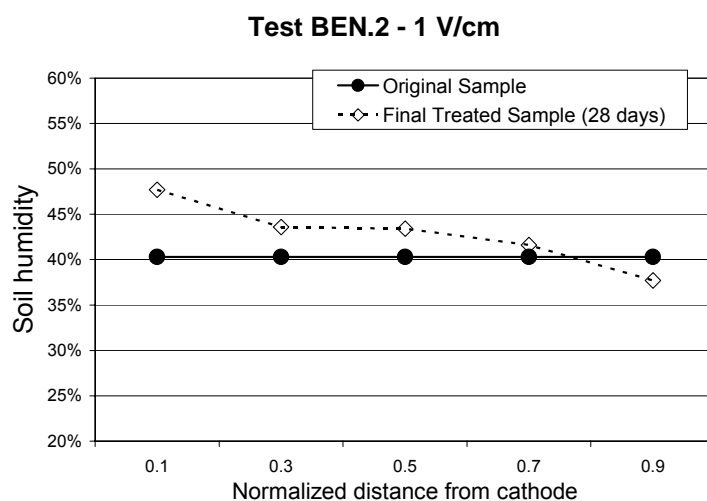


**Figure 4.65 – Soil humidity distribution along the soil specimen at the end of test BEN.2.**

## 4.4 Discussion

The results of the tests performed on the diesel-contaminated soils are compared and discussed as follows. Besides the effectiveness of electrooxidation in the contaminant removal, the influence of external parameters, such as the electric current, the electroosmotic flow, the soil pH and the soil moisture content were also considered.

### 4.4.1 Diesel Fuel Remediation

#### 4.4.1.1 Contaminant removal efficiencies

The contaminant removals attained during the tests performed during this study are summarized in Table 4.47.

Overall, electrochemical oxidation proved to be effective for the remediation of fine-grain soils contaminated by diesel fuel. A significant oxidation of the target pollutants was in fact achieved by the electrochemical methods, which resulted in about 46-55% TOC removal and 66-85% TPH removal for kaolin, and in 60-69% TOC removal and 73-87% TPH removal for bentonite.

One test was performed on diesel contaminated kaolin without the applications of electric current (KAO.6), as a reference test to assess any loss of contaminants due to volatilization or other chemical, physical or biological phenomena not linked with the electrochemical processes. The loss of contaminants during the trial was about 5% for TOC and 22% for TPH, significantly lower than the removal achieved with the application of the electric field in the other tests performed on the diesel-contaminated kaolin.

Test KAO.5 was performed on a 50 cm long kaolin specimen, in order to assess any scale effect that could affect the effectiveness of the electrochemical remediation. The contaminant removals achieved during this test (49% TOC removal and 89% TPH removal) were of the same order of magnitude as the results attained on a 10 cm long soil specimen (test KAO.2) with the same specific voltage (1 V/cm). Therefore, it can be thought that the effectiveness of the electrochemical process does not depend from the distance across the electrodes, provided that a sufficient voltage gradient is applied to the soil.

In all the samples considered in the study, the TOC removal was found to be lower than the TPH removal, except for one sample collected at the 14<sup>th</sup> day of test BEN.1, which showed very similar values for TOC removal (59%) and TPH removal (57%). This evidence is due to the fact that TOC represents all the organic matter in a soil sample. Therefore, it accounts also for the presence of by-products that derive from the degradation



of petroleum hydrocarbons, which on the opposite may not appear in the TPH content.

**Table 4.47 – Results of the tests performed on diesel-contaminated soils: TOC and TPH removals.**

Test	Specific voltage [V/cm]	Elapsed time [d]	TOC concentration [g/kg <sub>DW</sub> ]	TPH concentration [g/kg <sub>DW</sub> ]	TOC Removal	TPH Removal
KAO.1	0.5	0	208.1	131.0	-	-
		7	189.9	93.8	9%	28%
		14	183.1	83.7	12%	36%
		21	126.0	70.3	39%	46%
		28	112.3	45.2	46%	66%
KAO.2	1	0	208.1	131.0	-	-
		7	113.6	65.0	45%	50%
		14	109.2	60.3	48%	54%
		21	107.8	30.9	48%	76%
		28	95.5	26.6	54%	80%
KAO.3	3	0	221.1	185.3	-	-
		7	128.9	49.9	42%	73%
		14	121.7	43.6	45%	76%
		21	112.1	33.8	49%	82%
		28	101.3	27.4	54%	85%
KAO.4	6	0	185.0	179.8	-	-
		28	84.0	40.3	55%	78%
KAO.5	1	0	185.0	179.8	-	-
		28	94.4	19.2	49%	89%
KAO.6	0	0	221.1	185.3	-	-
		28	209.7	144.5	5%	22%
BEN.1	0.5	0	264.8	176.0	-	-
		7	-	-	-	-
		14	131.6	102.2	50%	42%
		21	113.4	72.8	57%	59%
		28	107.0	47.0	60%	73%
BEN.2	1	0	264.8	176.0	-	-
		7	184.2	77.0	30%	56%
		14	127.4	71.4	52%	59%
		21	95.5	55.0	64%	69%
		28	81.6	23.0	69%	87%

The influence of the main design parameters, as the applied voltage, the treatment duration and the soil mineralogy, is discussed as follows.

#### *4.4.1.2 Influence of the applied voltage*

The influence of the voltage gradient applied on the effectiveness the electrochemical processes was investigated during the research.

As can be seen from Figure 4.66, in the tests performed on diesel-contaminated kaolin, the TPH removal after 28 days of treatment improved quite significantly as the applied voltage increased from 0.5 V/cm to 1 V/cm, ranging from 66% in test KAO.1 to 80% in test KAO.2. However, as the voltage increased to 3 V/cm, the TPH removal slightly improved to 85%. During test KAO.4 (6 V/cm) the removal efficiency was even lower than those achieved in tests KAO.2 and KAO.3: this is thought to be due to the differences in the contaminant concentration in the original untreated soil samples, therefore the result achieved in test KAO.4 with 6 V/cm can be considered of the same order of magnitude of those attained in tests KAO.2 and KAO.3. During the same tests, also the TOC removal increased from 46% to 54% as the specific voltage increase from 0.5 V/cm to 1 V/cm, but it remained almost constant afterwards.

A similar behavior was encountered during the tests performed on diesel-contaminated bentonite, when a TPH removal improved from 73% to 87% as the applied voltage increased from 0.5 V/cm to 1 V/cm, and in the meanwhile the TOC removal improved similarly from 60% to 69%.

In sum, a certain influence of the applied voltage was encountered during the tests, with a quite significant improvement of the treatment efficiency as the voltage increased from 0.5 V/cm to 1 V/cm, but the system effectiveness proved to remain almost constant afterwards. This suggests that there is no need to increase the applied voltage above 1 V/cm to achieve a good hydrocarbon mineralization.

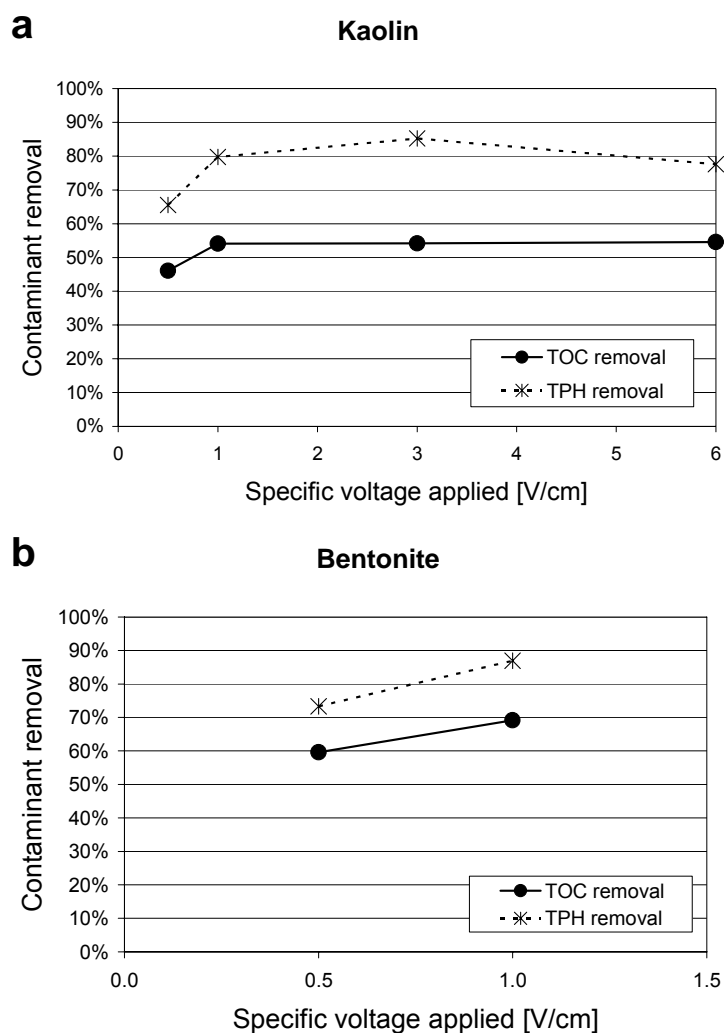


Figure 4.66 – Comparison of the TOC and TPH removal efficiencies achieved during the tests performed on diesel contaminated kaolin (a) and bentonite (b): influence of the applied voltage.

#### 4.4.1.3 Influence of the treatment duration

During tests KAO.1, KAO.2, KAO.3, BEN.1 and BEN.2, the increase of the contaminant removal efficiency with time was monitored.

As can be seen from Figure 4.67, both the TOC and the TPH removals significantly improved with time during the experiments. However, the time dependency was different for different voltages. In fact, for the diesel-contaminated kaolin samples (the results are compared in Figure 4.67), when the lowest voltage was applied (i.e. 0.5 V/cm), the contaminant removal gradually increased, and more than 20 days were required to achieve a good contaminant removal efficiency (e.g. more than 40% TOC removal and 60% TPH removal). Differently, when higher voltages were applied, these remediation performances could be achieved in shorter times, i.e. about 15 days for 1 V/cm and less than 10 days for 3 V/cm. An increase in the applied voltage therefore allowed to achieve a good contaminant

removal in shorter times than lower voltages, but this advantage is counterbalanced by the fact that higher specific voltages (e.g. 3 V/cm or more) result in higher energy expenditures (see Chapter 4.4.7 for energy consumption estimation) and may require more complicated setups for real-scale applications.

Like for kaolin, also the contaminant removals achieved for bentonite proved to increase significantly with time (Figure 4.68), therefore more than two weeks were required to achieve a TOC and TPH removal higher than 50%.

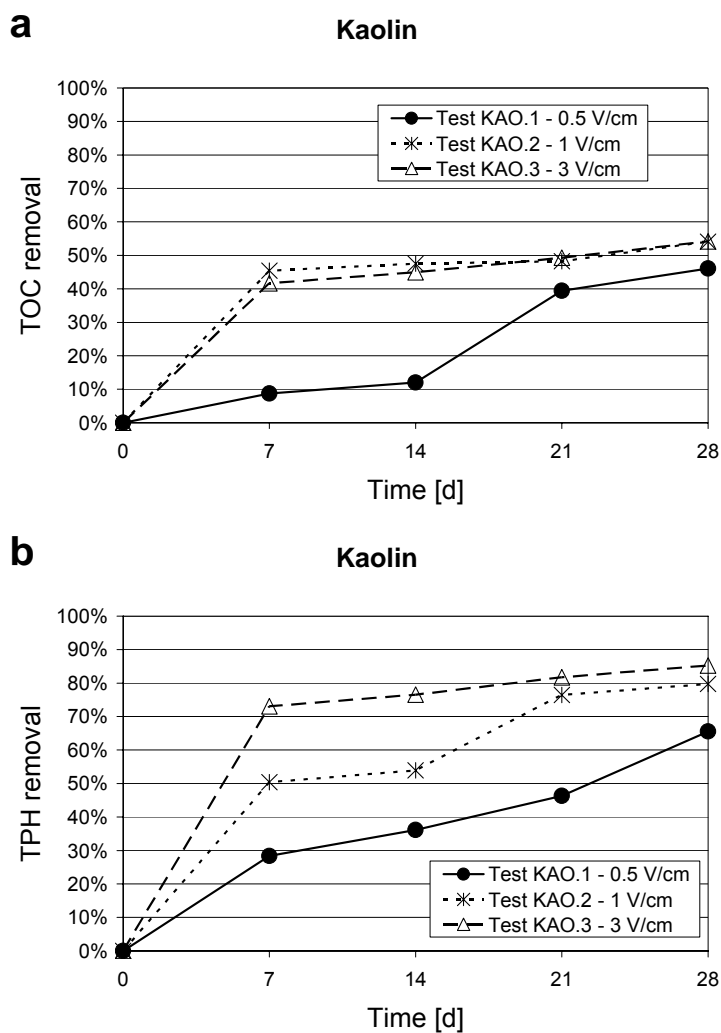


Figure 4.67 – Comparison of the TOC (a) and TPH (b) removal efficiencies achieved during tests KAO.1, KAO.2 and KAO.3, performed on diesel contaminated kaolin: influence of the treatment duration.

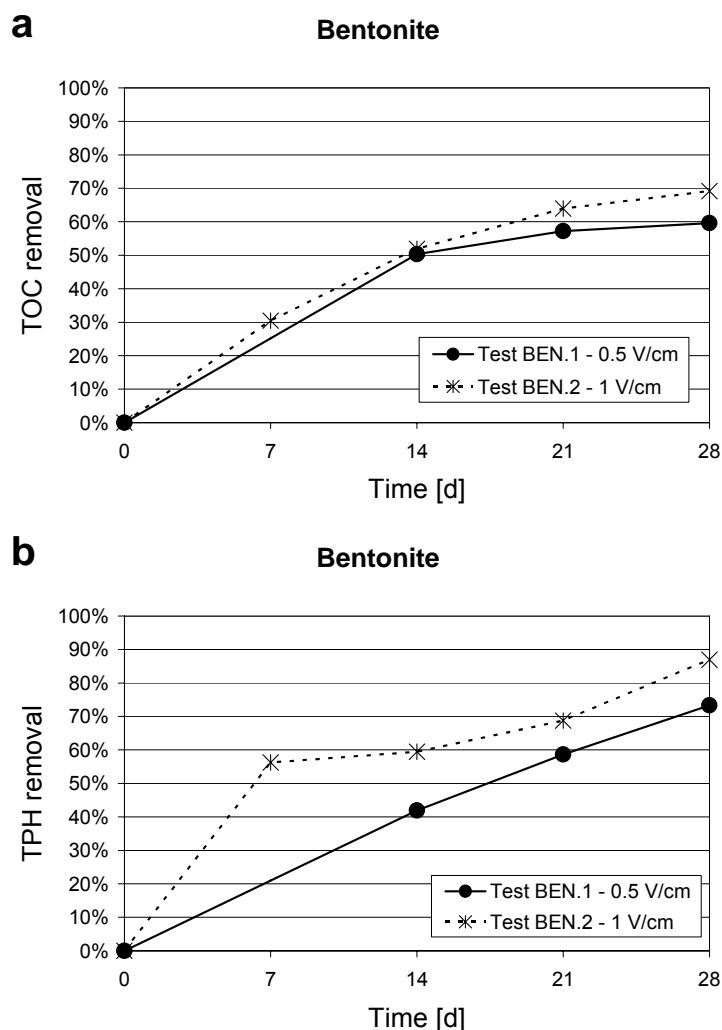


Figure 4.68 – Comparison of the TOC (a) and TPH (b) removal efficiencies achieved during tests BEN.1 and BEN.2, performed on diesel contaminated bentonite: influence of the treatment duration.

#### 4.4.1.4 Influence of the soil mineralogy

As can be seen from the data presented in Table 4.47, the removal efficiencies achieved for bentonite were much higher than those registered for kaolin. To underline this effect, the results attained during the tests performed on diesel contaminated kaolin and bentonite with specific voltages of 0.5 V/cm and 1 V/cm (tests KAO.1, BEN.1, KAO.2 and BEN.2 respectively) are compared in Figure 4.69.

These differences in the treatment performances were not due to a higher conductivity of bentonite, which on the opposite showed lower current intensities (i.e. a higher electric resistivity) than kaolin (see Chapter 4.4.6). Therefore, these results are thought to be due to the different mineralogical composition of the two soils considered in this study, and in particular by different iron contents.

In fact, the removal efficiency achieved for bentonite (iron content about 10180 mg/kg<sub>DW</sub>, manganese content about 44 mg/kg<sub>DW</sub>) were much higher than for kaolin, which

was characterized by a lower metal content (iron content about 2794 mg/kg<sub>DW</sub> and manganese content about 34 mg/kg<sub>DW</sub>). The XRD analysis of the two target soils (see Chapter 4.2.2.1) also showed that a certain amount of the iron content could be attributed to the magnetite, which is known to be a microconductor, although it was not possible to quantify the amount of the different iron minerals in the soil samples.

The large reservoir of iron that is present in naturally occurring iron-containing minerals is supposed to act as a microconductor source, promoting redox reactions and the formation of H<sub>2</sub>O<sub>2</sub> and to enhance the Fenton-like reactions that lead to the production of hydroxyl radicals ( $\bullet$ OH), mainly responsible for the oxidation processes (Rahner et al., 2002; Isosaari et al., 2007).

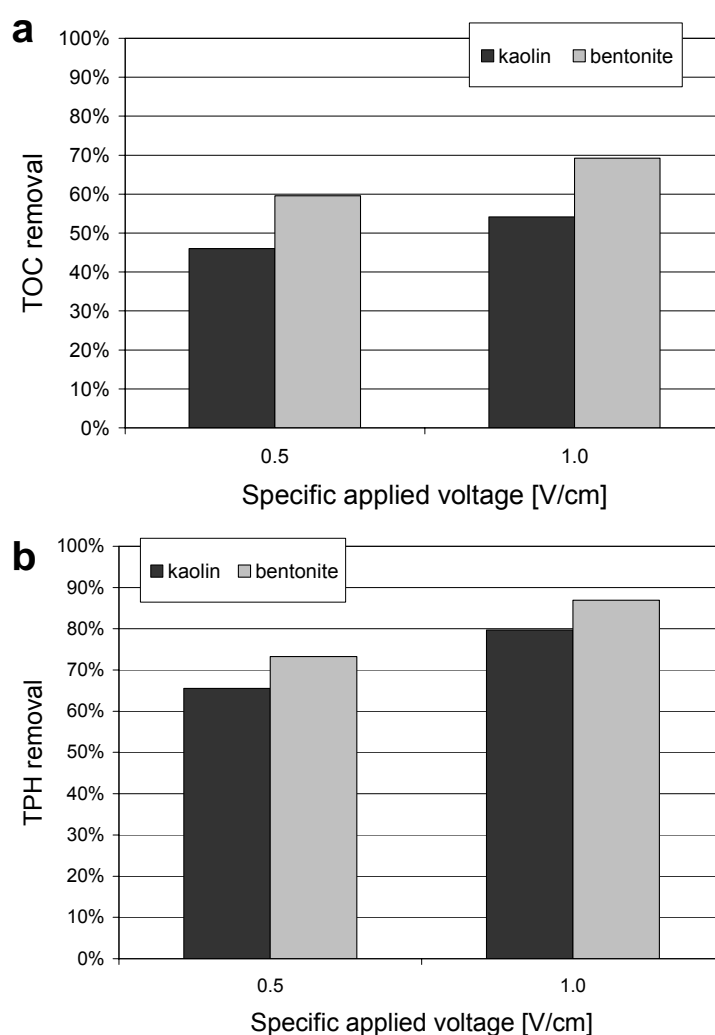


**Figure 4.69 – Comparison of the TOC (a) and TPH (b) removals during the performed on diesel-contaminated soils: influence of the soil type.**

#### 4.4.2 Electroosmotic flow

During the experiments performed on diesel contaminated kaolin, an electroosmotic flow occurred when the intensity of the electric current was appreciable (e.g. for current of

the order of magnitude of 5 mA or above). The electroosmotic flow rates were already known to be dependent on many factors, including voltage, current and characteristics of the electrolyte solution (see Chapter 2.3.1.1). In particular, the electroosmotic flow was reported to increase appreciably as the electric current flowing increases (Hamed and Bhadra, 1997; Kim et al., 2005a).

During the tests performed here, the electric current showed to start to decrease a few hours after the beginning of the tests. Therefore, the electroosmotic flow, when occurring, was appreciable only in the first days of treatment, and became negligible afterwards. The electroosmotic flow had already been reported to decrease rapidly with time during the electrochemical treatment of soils, especially when no ionic solution was added to the soil and the resulting current was weak (Reddy et al., 2006; Isosaari et al., 2007).

In this study, the volume of the pore fluid collected at cathode compartment during the tests, was limited, about 7 mL, 42 mL, 22 mL, 13 mL and 11 mL for tests KAO.1, KAO.2, KAO.3, KAO.4 and KAO.5 respectively, with no clear dependence on the applied voltage. This may suggest that even slight differences in the original soil samples (and therefore in the pore fluid compositions) could have notably affected the electroosmotic flow.

In both the tests performed on bentonite, the electroosmotic flux was negligible, as the current densities were much lower than for kaolin, being about 3-6 mA at the beginning of the trials and lower than 2 mA after a one-day treatment. However, since a very good contaminant removal was achieved during these tests (see Chapter 4.3.2), the occurrence of the electroosmotic flux does not seem to be necessary to attain the mineralization of the organic pollutants, although a significant electroosmotic flow was previously considered necessary to provide fresh water for electrolysis and for further redox reactions (Röhrs et al., 2002).

### **4.4.3 Contaminant transport**

The final contaminant concentrations were found to be almost evenly distributed along the treated sample (Figure 4.70), besides a certain sample variability, which can be considered characteristic of the soil pollution due to hydrophobic compounds. In fact, fluctuations in the contaminant concentrations of  $\pm 10\%$  or even more can be considered usual of the typical inhomogeneous distribution of HOCs in environmental matrices (Kim et al., 2005a).

The results suggest that the oxidation reactions occurred within all the treated volume and not only close to the electrodes. This is in agreement with the microconductor principle (Rahner et al., 2002), according to which the oxidant radicals can be created at all

the interfaces between the microconductor particles and the pore water.

Moreover, the results indicated that the electrokinetic transport of the target pollutants during the test performed, which were electrokinetically unenhanced, can be considered negligible. This result was however expected, as the organic pollutant of concern are apolar molecules, not affected by the electromigration process, while the electroosmotic advection was constrained by the low electroosmotic flows encountered during the tests, as already discussed in Chapter 4.4.2. Previously, it had been already observed that the electrochemically generated dechlorination reactions could be achieved without the transport of the target pollutants (Röhrs et al., 2002).

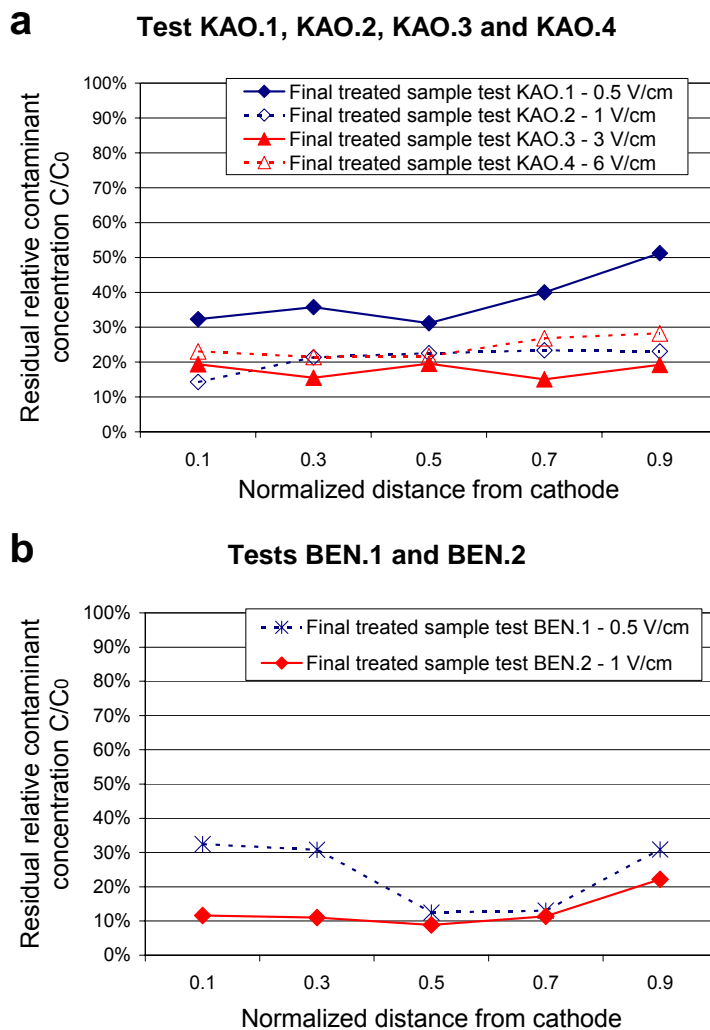


Figure 4.70 – Distribution of the residual contaminant content (ratio of the final contaminant concentration  $C$  and the initial contaminant concentration  $C_0$ ) along the soil specimen for the tests performed on 10 cm long specimen of kaolin (a) and bentonite (b).

#### 4.4.4 Soil pH profiles

During the runs, the soil pH tended to increase at the cathode and to decrease at the anode (Figure 4.71) as a result of water hydrolysis, which, during the electrochemical



treatment, leads to the production of an acid front moving from the anode toward the cathode and a base front moving from the cathode toward the anode.

This effect was particularly evident in the tests performed with kaolin, for which the initial pH (about 6) gradually changed to about 3-4 close to the anode and to about 8-10 near the cathode, important pH changes being encountered even a few days after the beginning of the test.

As the runs continued (e.g. during the last two weeks of the tests), all the soil volume tended to be acidified, as a result of the acid front moving along the soil from the anode towards the cathode. This effect was more evident for the highest specific voltages (i.e. 3-6 V/cm) rather than lowest voltages (0.5-1 V/cm).

Overall, the pH profiles achieved here for kaolin were similar to those previously encountered for the same soil type (Hamed and Bhadra, 1997; Kim et al., 2005a).

When the electroosmotic flow was encountered during the tests performed on the contaminated kaolin samples, the fluid collected at cathode compartment was found to be slightly acidic, with pH ranging from 3.3 to 6.7.

As for bentonite, which was characterized by an initial pH about 10, the pH variations were very limited, because of the high buffer capacity of this soil. Moreover, for this soil, the electrochemical treatment resulted in an increase in the soil pH nearly all along the soil specimen (Figure 4.71b). In fact, the soil pH increased from 10 to about 11 in most of the sample, with the exception of the sections closest to the anode, where the basification effect was neutralized from the production of hydrogen ions ( $H^+$ ), and the pH remained almost unchanged or slightly decreased from the initial values. Some soils had already been reported to tend to alkalinize during the electrochemical treatment, due to their buffer capacity, which may constrain the acidification process (Szpyrkowicz et al., 2007).

At first, the pH changes were expected to influence the system efficiency, since a low pH can enhance the Fenton-like reactions, which lead to the production of hydroxyl radicals. However, the results achieved indicated that there was no correlation between the soil pH profile and the final contaminant distributions, which seemed to be independent from the acid or basic conditions that were created in the soil during the electrochemical processes. In order to support this conclusion, comparisons of the soil pH profiles and of the final contaminant distribution achieved at the end of the tests performed on the 10 cm long soil specimen are shown in Figure 4.72 and Figure 4.73.

In sum, the mineralization process did not seem to be influenced by pH changes, the contaminant removal being of the same order of magnitude both in areas with low and high pH. It is thought that the soil natural iron content was sufficient to enhance the Fenton-like reactions, with no need for a strongly acid pH to be created to promote the radical production.

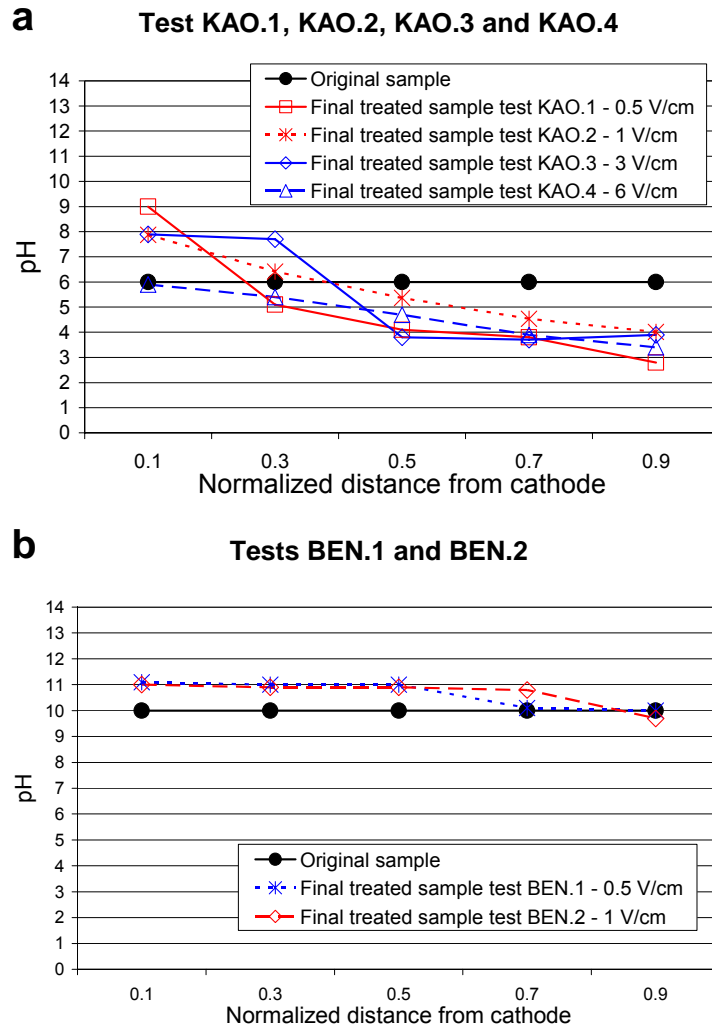


Figure 4.71 – pH profiles achieved at the beginning and at the end (28 days) of the tests performed on 10 cm long soil specimen of kaolin (a) and bentonite (b).

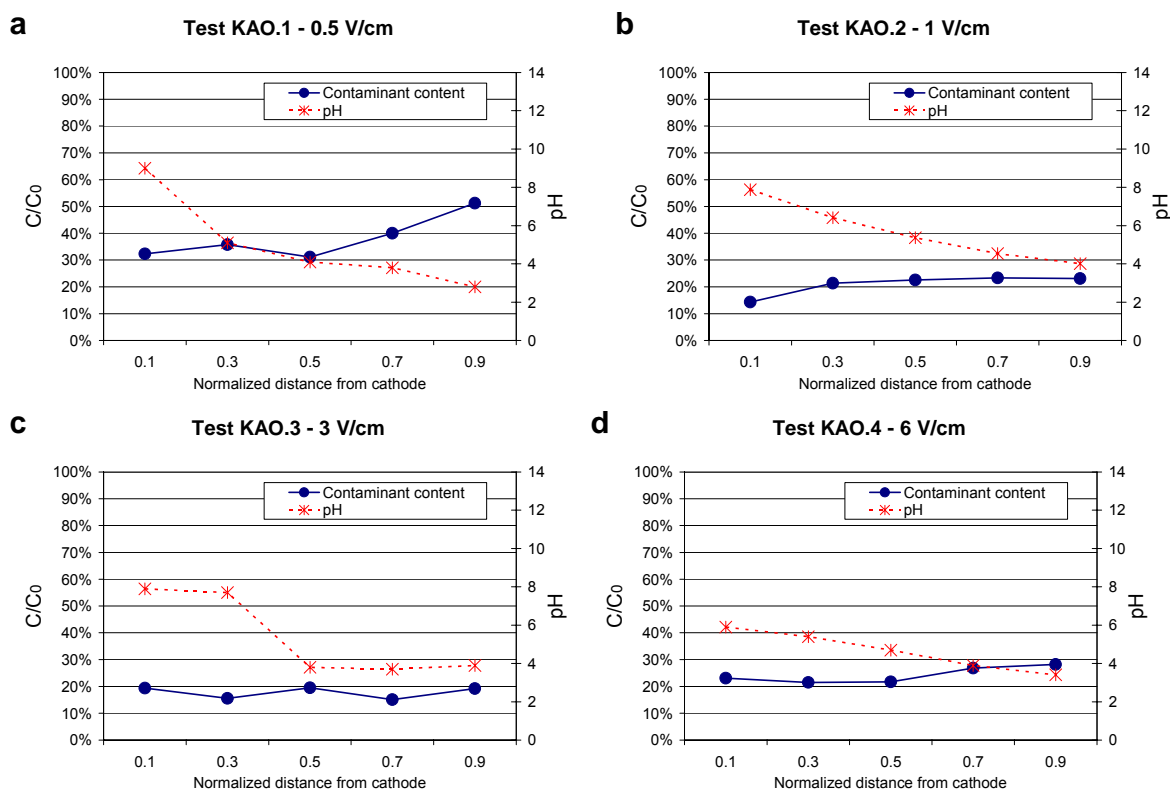


Figure 4.72 – Comparison of the residual contaminant distribution ( $C_0$  initial TPH concentration,  $C$  final TPH concentration) and the final soil pH profiles measured at the end (28<sup>th</sup> days) of tests KAO.1 (a), KAO.2 (b), KAO.3 (c) and KAO.4 (d) performed on diesel-contaminated kaolin.

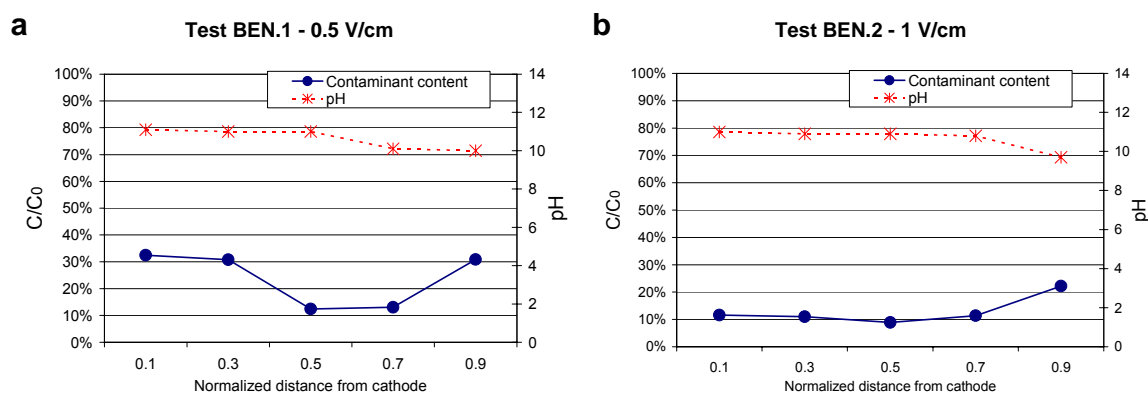


Figure 4.73 – Comparison of the residual contaminant distribution ( $C_0$  initial TPH concentration,  $C$  final TPH concentration) and the final soil pH profiles measured at the end (28<sup>th</sup> days) of tests BEN.1 (a) and BEN.2 (b) performed on diesel-contaminated bentonite.

#### 4.4.5 Soil humidity and temperature

Different physical parameters, like the soil water content and the soil temperature, were monitored during the study.

In the tests performed on the 10 cm long soil specimens, the initial soil moistures were about 36.9-39.5% for kaolin and about 40.3% for bentonite. Despite the fact that no

fluid was provided at the electrodes during the runs, the soil did not dry out, the final soil moisture ranging from 34.1% to 44.0% for kaolin, from 36.7% to 47.7%, and for bentonite. In most the tests performed, the final water content of the treated soil was found to be the highest at the cathode side and the lowest at the anode side, as a result of the electroosmotic flux flowing from the anode towards the cathode. However, the changes in the soil water content were limited, therefore the soil moisture content remained fairly constant and comparable to the initial humidity.

The soil appeared to be compacted near the anode at the end of the tests. This effect had already been observed in previous studies (Isosaari et al., 2007). Moreover, a change in the oxidation state of iron and probably other metals was observed near the anode. In fact, a few weeks after the beginning of the test, some clogging occurred near this electrode, the soil also changing to a yellow-orange color (Figure 4.74), probably because of the formation of iron hydroxides from the soil natural iron content. A further iron supply deriving from the anode corrosion is also known to be possible when iron anodes are used (Haran et al., 1997; Röhrs et al., 2002). In fact, during the electrochemical treatment, the anode may undergo important corrosion phenomena. Dissolved iron(II)-species from the corroded steel anode can act as an electron donor for the electrochemical reactions (Röhrs et al., 2002). If undesired, the corrosion of the anode can be overcome by using inert materials, like platinum or titanium.

In this study, a stainless steel anode was used. Despite the fact that an inert steel electrode was used, it appeared to undergo certain corrosion during the tests performed. Hence, it can be supposed that the anode could have supplied iron to the soil, thus improving the formation of iron hydroxides near the anode.



**Figure 4.74 – Kaolin sample being treated with Setup 2: at the anode (on the right side of the sample), the soil was compacted and changed to a yellow-orange color because of the formation of iron hydroxides from the soil natural iron content and from the electrode corrosion.**

The formation of iron oxides or oxohydrates has already been reported to occur and to be able to block the electrode surface, resulting in a decrease of the flowing current (Rahner et al., 2002). For this reason, sometimes complexing or conditioning agents are used to retard the electrode fouling and to increase the current flowing.

Occasional monitoring of soil temperature did not show any changes, which were however not expected, since an increase in soil temperature is known to occur as a consequence of electric processes only when high currents are flowing (Isosaari et al., 2007).

#### **4.4.6 Electric current intensities**

The electric current was monitored at regular time intervals during each test performed. As shown in Figure 4.75, in all tests the current started to decrease rapidly after the application of the voltage gradient, and reached a steady state value a few days after the beginning of the tests.

In the experiments performed with kaolin (tests KAO.1-KAO.4), the peak values of the electric current ranged from 16 mA to 150 mA, while at the steady state the current was about 1-9 mA. During test KAO.5, which was performed on a 50 cm long kaolin specimen, the maximum current value, about 17 mA, was achieved 1 day after the beginning of the test, then the current gradually decreased and at the steady state it was lower than 0.01 mA.

When the bentonite clay was tested (trials BEN.1 and BEN.2), the values of the electric current were much lower than those registered with kaolin, the initial values ranging from 3 mA to 6 mA, with steady state values of 0.05-0.6 mA.

Commonly, in electrochemical and electrokinetic tests, the currents flowing across the soil are found to be decreasing with time after an initial period of increase, which may last for several hours (Kim et al., 2005a). In fact, the capacitive current due to the application of the voltage gradient decreases and is zero at the steady state. Moreover, the metal oxide and hydroxide precipitation reduces the number of ions and of microconductors available to carry the charge and increases the soil electric resistance (Rahner et al., 2002; Röhrs et al., 2002; Lynch et al., 2007). Current densities can also be affected by changes in soil pH, which influence chemical precipitations and dissolutions. Therefore, unless conditioning agents are used to adjust the soil pH to low values and to provide new ions as charge carriers, the soil resistivity increases, and the current decreases with time (Reddy et al., 2006).

Here, the initial increases in the flowing electric current were not recorded in all the tests performed. This is attributed to the timing in the current monitoring procedures, in case the decrease started soon after the application of the voltage gradient (e.g. less than 1 h after the beginning of the experiments). The electric currents measured in the tests

performed here are thought to be so low because the tests were unenhanced, i.e. no buffer solution was added to increase the ion concentration. Similar values were in fact achieved during the unenhanced electrochemical treatment of contaminated soils (Sanromán et al., 2005). It is expected that if an ionic solution had been added to the system, higher current intensities would have been recorded.

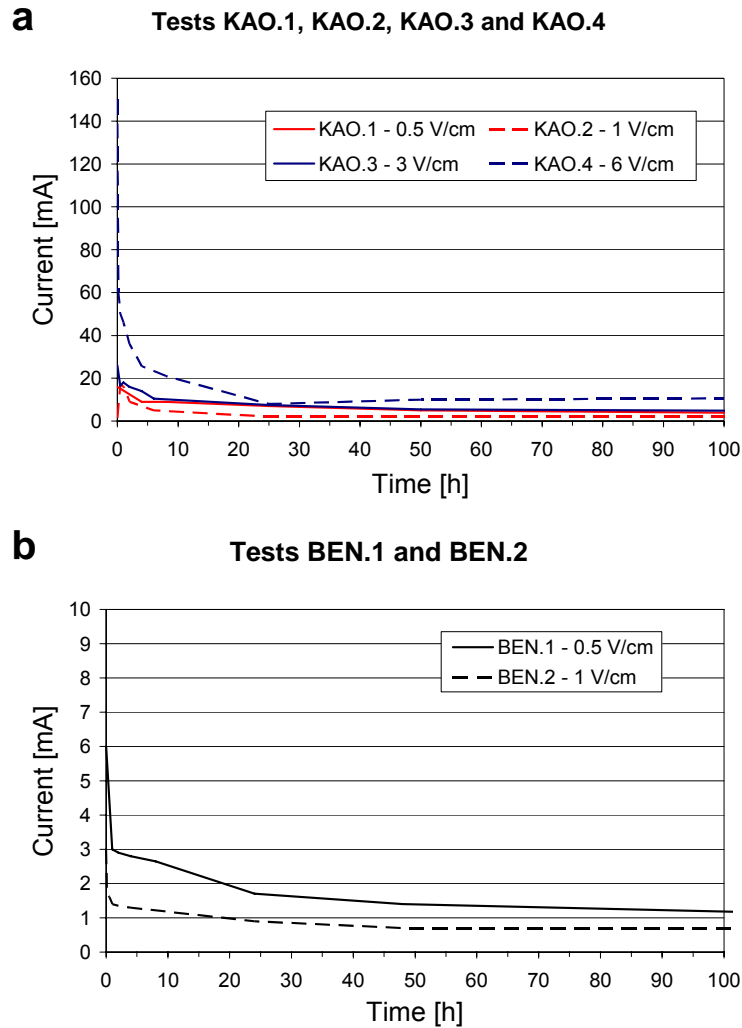


Figure 4.75 – Current intensities measured during the first hours in the tests performed on 10 cm long specimen of diesel-contaminated kaolin (a) (i.e. tests KAO.1, KAO.2, KAO.3, KAO.4) and bentonite (b) (i.e. tests BEN.1 and BEN.2).

#### 4.4.7 Energy consumption

From the values of voltage and current, it was possible to make an approximate estimation of the energy consumption required for a remediation action. In order to calculate the energy expenditure, the current was modeled as an exponential function of time, starting from the peak value, and with a constant component at the steady state, thus neglecting the initial current increase, which was however very limited in most of the tests performed. The following function was used to model the current:

$$i = (i_p - i_{ss}) \cdot \exp(-t/\tau) + i_{ss} \tag{38}$$

Where:

$i_p$  is the peak current value;

$i_{ss}$  is the current value at the steady state;

$t$  is time;

$\tau$  is a time constant.

An approximate estimation of the energy consumption was performed of the tests carried out on 10 cm long soil specimen (i.e. tests KAO.1, KAO.2, KAO.3, KAO.4, BEN.1 and BEN.2). The following functions were determined to model the current intensities for these tests:

- Test KAO.1 (0.5 V/cm):  $i = 15mA \cdot \exp(-t/19h) + 1mA$
- Test KAO.2 (1 V/cm):  $i = 14.8mA \cdot \exp(-t/3h) + 2.2mA$
- Test KAO.3 (3 V/cm):  $i = 21.6mA \cdot \exp(-t/10h) + 4.4mA$
- Test KAO.4 (6 V/cm):  $i = 141mA \cdot \exp(-t/20h) + 9mA$
- Test BEN.1 (0.5 V/cm):  $i = 2.4mA \cdot \exp(-t/8h) + 0.6mA$
- Test BEN.2 (1 V/cm):  $i = 5.95mA \cdot \exp(-t/10h) + 0.05mA$

The parameters calculated for the current modeling are reported in Table 4.48. As can be seen from the data shown, the initial current values increased with the voltage gradient, both for kaolin and for bentonite. Moreover, besides for test KAO.2, when the current was found to be very rapidly decreasing, for kaolin the time constant ( $\tau$ ) was of the order of 10-20 h. The steady state of the capacitative current is commonly considered achieved  $5\tau$  after the application of the voltage. The measured current functions are approximately consistent with this, since the current achieved in the tests performed on kaolin appeared to reach a steady state in about 5-10 days (Figure 4.75).

**Table 4.48 – Estimated parameters for current function modelling during the tests performed. The current was modelled as an exponential function with a steady state component. In the table,  $i_0$  is the initial current,  $i_{ss}$  is the current at the steady state,  $t$  is time and  $\tau$  is a time constant.**

Test	$i_p$ [mA]	$i_{ss}$ [mA]	$\tau$ [h]
KAO.1	16	1	19
KAO.2	17	2.2	3
KAO.3	26	4.4	10
KAO.4	150	9	20
BEN.1	3	0.6	8
BEN.2	6	0.05	10

Once the current function has been modeled, the energy expenditure per unit volume

(E) was calculated according as follows:

$$E = \frac{1}{V_s} \int V \cdot i(t) \cdot dt \quad (39)$$

Where:

$V_s$  is the volume of treated soil;

$i$  is the electric current flowing;

$V$  is the applied voltage;

$t$  is time.

The maximum power required for the test ( $W_{\max}$ ) was calculated as the product of the maximum current recorded ( $i_{\max}$ ) and of the applied voltage (V):

$$W_{\max} = i_{\max} \cdot V \quad (40)$$

For the tests performed on kaolin (the soil samples having a volume of about 1 L and a mass about 2 kg) the estimated energy expenditure increased with the applied voltage, ranging from 17 kJ/L, corresponding to 4.7 kWh/m<sup>3</sup> (test KAO.1, 0.5 V/cm) to 1933 kJ/L, corresponding to 537 kWh/m<sup>3</sup> (test KAO.4, 6 V/cm). The maximum applied power (corresponding to the maximum current) was about 0.08-9.0 W.

For bentonite, the energy expenses were lower than for kaolin, since the applied currents were lower than those recorded with kaolin were. In this case, the energy expenditures were about 3.5-7.6 kJ/L (0.98-2.1 kWh/m<sup>3</sup>), with maximum required powers of 0.015-0.6 W.

Thus, according to the results achieved, the process seems to require low energy expenditures, being the current densities applied very low (about 0.01-1 mA/cm<sup>2</sup>).

## 4.5 Conclusions

During this research, several experiments were performed at laboratory scale to assess the feasibility of using electrochemical oxidation for the remediation of petroleum hydrocarbons from different types of fine grain soils. Two types of soils were considered: a silty soil, mainly composed of kaolin, and a bentonite clayey soil, mainly composed of montmorillonite, while diesel fuel was used as a model contaminant.

According to the results achieved, electrooxidation proved to be effective for the removal of the target pollutants from fine-grain soils. About 46-55% TOC removals and 66-85% TPH removals were attained after four-week processes on kaolin samples, while about 60-69% TOC removals and 73-87% TPH removals were achieved for bentonite.

The combined application of electrooxidation and of traditional chemical oxidation, with the dosage of oxidant agents at the anode compartment (EK-Fenton process) did not



lead to an improvement of the removal efficiencies under the tested conditions, in comparison to the sole use of the electric fields.

As for the most important design parameters, the applied voltage seems to have a limited influence on the efficiency of the remediation action, good results being achieved with specific voltages as low as 1 V/cm. Conversely, the remediation efficiency proved to increase significantly with process duration. For example, the application of a constant voltage of 1 V/cm to a bentonite sample led to 30% TOC removal after 7 days, but the TOC removal increased to 69% after a 28-day treatment. Hence, for real scale applications of electrooxidation, a treatment of a few weeks can be recommended rather than a process of a few days. The process effectiveness seems also to be affected by soil mineralogy, and primarily by the soil iron content, hence, a significant iron content in the treated soil is thought to be able to improve the effectiveness of this remediation method.

The electric currents flowing across the electrodes during the tests were found to be rapidly decreasing after the application of the voltage gradient, and to reach a steady state within a few days of treatment. The current values at the steady state were about 1-9 mA for kaolin and below 1 mA for bentonite. The recorded current densities were about 0.1-1 mA/cm<sup>2</sup> at the beginning of the tests and they significantly decreased with time. These low values of applied voltages and of electric currents allowed to conduct the electrochemical process with very low energy expenditures, below 2 MJ/L (550 kWh/m<sup>3</sup>).

The final contaminant concentrations were found to be evenly distributed across the treated samples. This suggests that the oxidation reactions occur within all the treated volume and not only close to the electrodes, in agreement with the microconductor principle. Moreover, the results indicate that the pollutants electrokinetic transport during the test performed, which were unenhanced, can be considered negligible. An investigation on the contaminant content in the water collected at cathode compartment confirmed that the pollutant removal from the soil specimen due to the electroosmotic advection was negligible.

The buffer capacity of the soil can affect soil pH changes, by determining the tendency of the treated medium towards acidification or basification. However, the remediation efficiency does not seem to be influenced by changes in soil pH, nor by the occurrence of the electroosmotic flux, which does not seem to be necessary to achieve a significant mineralization of the organic pollutants.

The results achieved are very encouraging, since the recovery of fine-grain soils is often very difficult to be achieved with conventional remediation methods, since their low permeability can constrain the applicability of many techniques for soil recovery. On the whole, electrochemical oxidation seems to be effectively and amenably applicable for the mineralization of many organics with low energy expenditure, especially in finest soils, like clays, with significant iron contents.



# Chapter 5

## Feasibility studies

This chapter presents the results of various feasibility studies that were conducted to assess the applicability of electrooxidation for the remediation of different contaminated soils and sediments.

The research included three experimental investigations, about river sediments contaminated by PAHs (see Section 5.1), silty soils contaminated by organolead compounds (Section 5.2) and clayey soils contaminated by landfill leachate (Section 5.3). The first two cases regarded the “Trento Nord” contaminated site, one of the major contaminated sites in Italy, which in the last century was heavily contaminated by improper management of industrial activities and which still poses important environmental concerns. The third investigation focused on the application of electrooxidation for the recovery of a landfill clay barrier contaminated by leachate; this technique could be of interest either for the recovery of old landfills, in case of a failure of the liner systems, or as a new engineering solution for new landfill plants.

This part of the thesis regards a more practical context than the previous chapters, mainly devoted to evaluate the applicability of the remediation technique of concern on really or potential contamination cases. Thus, these studies dealt with more complex contaminated environmental matrices and were characterized by a more pragmatic approach than the research presented in Chapter 4.

### 5.1 PAH-contaminated sediments

This study was undergone to investigate the feasibility of using electrochemical oxidation to degrade sorbed PAHs in freshwater sediments, in case of old date contamination. Three laboratory tests were performed to assess the contaminant removal

due to the electrooxidation processes, with specific voltages ranging from 1 V/cm to 2 V/cm and test durations up to 4 weeks.

### **5.1.1 Contaminants**

#### *5.1.1.1 Polycyclic aromatic hydrocarbons*

PAHs are a group of organic molecules composed of fused benzene rings (Figure 5.1), classified among hydrophobic organic compounds (HOCs).

PAHs are released during the incomplete combustion of coal, petroleum products and wood. Natural sources include volcanic eruptions as well as forest and prairie fires. Anthropogenic sources, which can be considered the major route of entry of PAHs into the environment, include combustion, gasification and liquefaction of fossil fuels, coke production, asphalt and coal tar production, fuel processing, oil and diesel spills, waste incineration and motor vehicle emissions (Wild and Jones, 1995; Harvey, 1997; Henner et al., 1997; O'Mahony et al., 2006; Searle and Mitchell, 2006).

The main sources of PAHs in Western Europe are electrical and thermal energy production plants, waste incineration, road traffic and many industrial activities, e.g. coal carbonation, catalytic cracking of crude oil and aluminum production (Harrad, 2000). Limited quantities of non-carcinogenic PAHs (e.g. naphthalene, anthracene, phenanthrene and pyrene) are also industrially produced in pure forms, to be used as standard materials, as for the synthesis of dye, pesticides and pharmaceuticals (Harrad, 2000).

Once released, PAHs tend to persist in the environment and to occur in natural media such as soil, sediments, water and air, resulting in a widespread environmental distribution. In particular, due to their hydrophobic nature and low water solubility, they can become rapidly associated with sediments (Harvey, 1997; Henner et al., 1997; Cuypers et al., 1998). Apolar organic pollutants, like PAHs, can also attach to dissolved organic material in soils and sediments, and may consequently be transported in water (De Serres and Bloom, 1995).

Their presence in environmental matrices is of great concern due to their high toxicity, carcinogenic effects and environmental persistence (Wild and Jones, 1995; Henner et al., 1997; IARC, 1983a,b). For this reason, they have been listed by the United States Environmental Protection Agency and by the European Community as priority environmental pollutants and they have been subject of detailed research for more than 30 years (Wild and Jones, 1995; Henner et al., 1997; O'Mahony et al., 2006; Haapea and Tuhkanen, 2006).

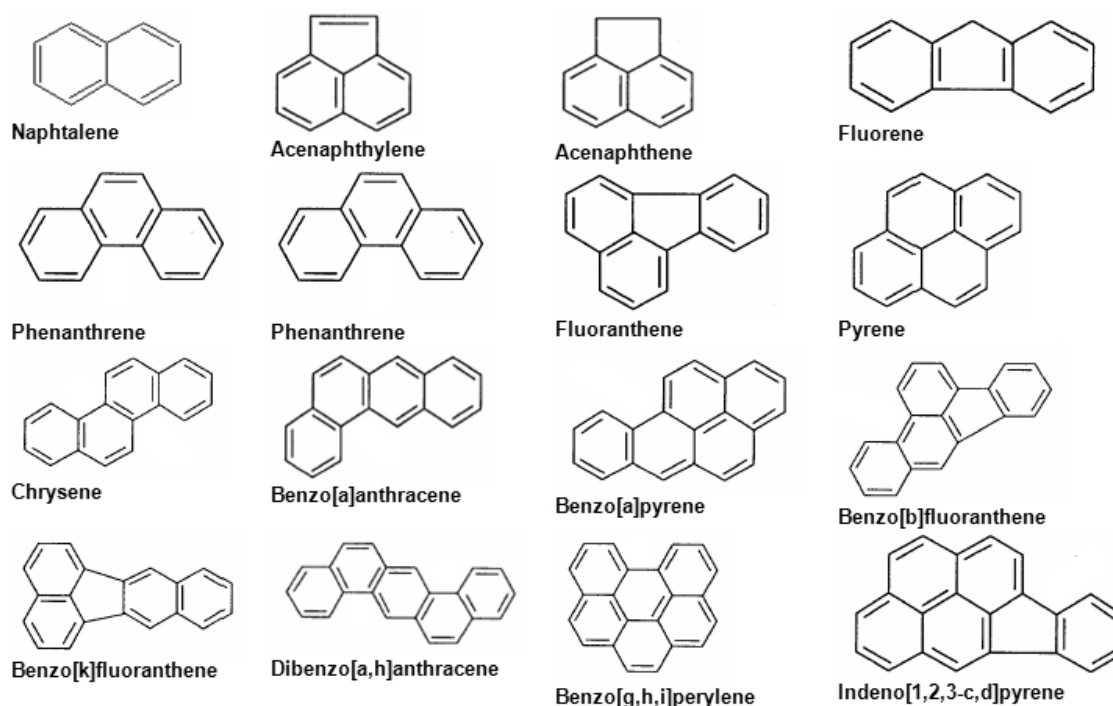


**Figure 5.1 – Polycyclic aromatic hydrocarbons.**

Individual PAHs differ substantially in their physical and chemical properties. Overall, PAHs have low solubilities and low volatilities, while their lipophilicity is high, as measured by the octanol-water partition coefficient ( $K_{ow}$ ). This parameter is the ratio of the concentration of a chemical in octanol ( $C_o$ ) and in water ( $C_w$ ) at equilibrium and at a specified temperature (De Serres and Bloom, 1995; Harrad, 2000; Suthersan, 2001):

$$K_{ow} = \frac{C_o}{C_w} \quad (41)$$

$K_{ow}$  quantitatively describes the extent to which an organic chemical compounds distributes itself between the aqueous phase and the environmental solids (e.g. soil, sediment, suspended sediment, wastewater solids, etc.) (Suthersan, 2001). Hence, it is often used to indicate the fate of pollutants in the environment, as it represents the tendency of a chemical to remain sorbed onto organic matter (high  $K_{ow}$  values) or to dissolve in water (low  $K_{ow}$  values).

Since octanol is a good surrogate phase for lipids in living organisms, the  $K_{ow}$  coefficient can also represent how a chemical would thermodynamically distribute between the organism lipids and water (Harrad, 2000). Usually, compounds with a  $K_{ow}$  of  $10^5$ - $10^6$  or more are considered lipophilic (De Serres and Bloom, 1995).

Moreover, besides the chemical equilibrium between solid and liquid phase, the  $K_{ow}$  coefficient can also represent the environmental- and health-concerns of an organic pollutant, as it is correlated with the bioconcentration factor (BCF), which measures the concentration of that chemical in organisms, and to the adsorption coefficient  $K_{oc}$ , which

measures the ability of that chemical to attach to particulate organic matter rather than to remain dissolved in water (De Serres and Bloom, 1995).

$K_{oc}$  is commonly used to model the contaminant mobility and transport, but it also affects the availability towards chemical and biological degradation (De Serres and Bloom, 1995).

In sum,  $K_{ow}$ ,  $K_{oc}$  and BCF characterize the overall environmental concerns of organic pollutants, as they represent both the environmental fate and behavior (through the adsorption/desorption mechanisms) of these chemicals, and the bioaccumulation, i.e. their tendency to accumulate in the tissues of living organisms (De Serres and Bloom, 1995; Suthersan, 2001).

As for PAH species, the lower molecular weight PAHs (light PAHs, which are characterized by the presence of 2 or 3 aromatic rings) are more volatile, water soluble and less lipophilic than the high molecular weight PAHs (heavy PAHs, with 4, 5 or 6 aromatic rings) (Henner et al., 1997). These physico-chemical properties also determine the environmental behavior of different PAH species, as the transfer and turnover of low molecular weight PAHs are more rapid than that of the heavy PAHs (Wild and Jones, 1995).

PAHs are commonly classified as nonhalogenated semivolatile organic compounds (SVOCs) (FRTR, 2002) and they are regarded as persistent organic pollutants (POPs), their persistence increasing with ring number. It is also reported that the greater the number of benzene rings in the PAH molecule, the greater the resistance to degradation (Bossert and Bartha, 1986; Henner et al., 1997), thus the recovery of heavy PAHs is commonly more difficult to achieve than the removal of light PAHs.

Summarized and detailed lists of the PAH species considered in this study are provided in Table 5.1 and Table 5.2 respectively.

**Table 5.1 – Summary of the main physical and chemical properties of the PAHs considered in this study (Wild and Jones, 1995; Muller, 2002).**

PAH specie	Chemical formula	Molecular weight	Partition coefficient Log(K <sub>ow</sub> )	Number of aromatic rings
naphthalene	C <sub>10</sub> H <sub>8</sub>	128.2	3.28	2
acenaphtene	C <sub>12</sub> H <sub>8</sub>	152.2	3.98	2
acenaphtylene	C <sub>12</sub> H <sub>10</sub>	154.2	4.07	2
fluorene	C <sub>13</sub> H <sub>10</sub>	166.2	4.18	2
phenantrene	C <sub>14</sub> H <sub>10</sub>	178.2	4.45	3
anthracene	C <sub>14</sub> H <sub>10</sub>	178.2	4.45	3
fluoranthene	C <sub>16</sub> H <sub>10</sub>	202.3	4.90	3
pyrene	C <sub>16</sub> H <sub>10</sub>	202.3	4.88	4
chrysene	C <sub>18</sub> H <sub>12</sub>	228.2	5.16	4
benzo(a)anthracene	C <sub>18</sub> H <sub>12</sub>	228.2	5.61	4
benzo(b)fluoranthene	C <sub>20</sub> H <sub>12</sub>	252.3	6.04	4
benzo(k)fluoranthene	C <sub>20</sub> H <sub>12</sub>	252.3	6.06	4
benzo(a)pyrene	C <sub>20</sub> H <sub>12</sub>	252.3	6.06	5
benzo(g,h,i)perylene	C <sub>22</sub> H <sub>12</sub>	276.3	6.50	6
indeno(1,2,3-cd)pyrene	C <sub>22</sub> H <sub>12</sub>	276.3	6.58	6
dibenzo(a,h)anthracene	C <sub>22</sub> H <sub>14</sub>	278.4	6.84	6

Table 5.2 – Physico-chemical properties of different PAH species (Wild and Jones, 1995; Muller, 2002).

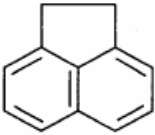
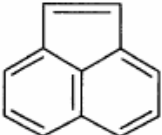
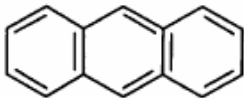
PAH species	Acenaphthene	Acenaphthylene	Anthracene
<b>Chemical formula</b>	C <sub>12</sub> H <sub>10</sub>	C <sub>12</sub> H <sub>8</sub>	C <sub>14</sub> H <sub>10</sub>
<b>Chemical structure</b>			
<b>Molecular weight</b>	154.21 g/mol	152.20 g/mol	178.2 g/mol
<b>Color</b>	white	no data	colorless with violet fluorescence when pure; yellow with green fluorescence when impure
<b>Physical state</b>	solid (needles)	solid (prisms/plates)	solid (tablet or prism)
<b>Melting point</b>	95°C	92-93°C	218°C
<b>Boiling point</b>	96°C	265-275°C	340-342°C
<b>Solubility in water</b>	1.93 mg/L	3.93 mg/L	0.076 mg/L
<b>Organic solvents</b>	alcohol, methanol, propanol, chloroform, benzene, toluene, acetic acid	alcohol, ether, benzene	acetone, benzene, carbon disulphide, carbon tetrachloride, chloroform, ether, ethanol, methanol, toluene
<b>Partition coefficients:</b>			
<b>log K<sub>ow</sub></b>	3.98	4.07	4.45
<b>log K<sub>oc</sub></b>	3.66	1.40	4.15
<b>Vapor pressure</b>	4.47 · 10 <sup>-3</sup> mmHg at 20°C	0.029 mmHg at 20°C	1.7 · 10 <sup>-5</sup> mmHg at 25°C
<b>Henry's law constant</b>	7.91x10 <sup>-5</sup> atm·m <sup>3</sup> /mol	1.45x10 <sup>-3</sup> atm·m <sup>3</sup> /mol	1.77x10 <sup>-5</sup> atm·m <sup>3</sup> /mol



Table 5.2 (continues) - Physico-chemical properties of different PAH species (Wild and Jones, 1995; Muller, 2002).

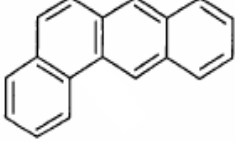
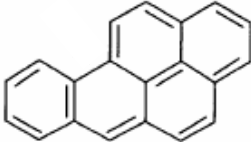
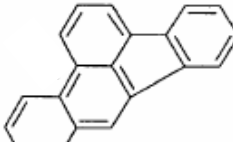
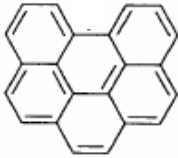
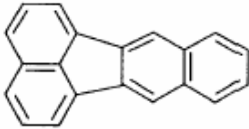
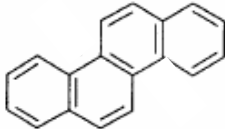
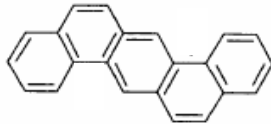
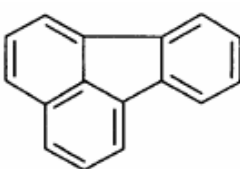
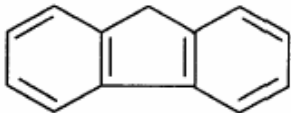
PAH species	Benzo[a]anthracene	Benzo[a]pyrene	Benzo[b]fluoranthene
<b>Chemical formula</b>	C <sub>18</sub> H <sub>12</sub>	C <sub>20</sub> H <sub>12</sub>	C <sub>20</sub> H <sub>12</sub>
<b>Chemical structure</b>			
<b>Molecular weight</b>	228.29 g/mol	252.3 g/mol	252.3 g/mol
<b>Color</b>	yellow-blue fluorescence	pale yellow	Colorless
<b>Physical state</b>	solid (plates or needles)	solid (plates or recrystall. from benzene/ligroin)	solid (needles)
<b>Melting point</b>	158-159°C	179°C	168°C
<b>Boiling point</b>	400°C; 435°C sublimes	310-312°C at 10 mmHg; 495°C	no data
<b>Solubility in water</b>	0.010 mg/L	2.3x10 <sup>-3</sup> mg/L	0.0012 mg/L
<b>Organic solvents</b>	slightly soluble in acetic acid and hot ethanol; soluble in acetone and diethyl ether; very soluble in benzene	sparingly soluble in ethanol and methanol; soluble in benzene, toluene, xylene, and ether	slightly soluble in benzene, acetone
<b>Partition coefficients:</b>			
<b>log K<sub>ow</sub></b>	5.61	6.06	6.04
<b>log K<sub>oc</sub></b>	5.30	6.74	5.74
<b>Vapor pressure</b>	2.2 · 10 <sup>-3</sup> mmHg at 20°C	5.6 · 10 <sup>-9</sup> mmHg at 20°C	5.0 · 10 <sup>-7</sup> mmHg at 20-25°C
<b>Henry's law constant</b>	1x10 <sup>-6</sup> atm·m <sup>3</sup> /mol	4.9x10 <sup>-7</sup> atm·m <sup>3</sup> /mol	1.22x10 <sup>-5</sup> atm·m <sup>3</sup> /mol

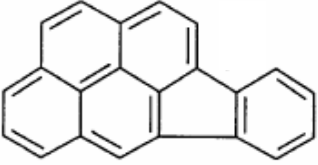
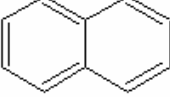
Table 5.2 (continues) - Physico-chemical properties of different PAH species (Wild and Jones, 1995; Muller, 2002).

PAH species	Benzo[g,h,i]perylene	Benzo[k]fluoranthene	Chrysene
Chemical formula	C <sub>22</sub> H <sub>12</sub>	C <sub>20</sub> H <sub>12</sub>	C <sub>18</sub> H <sub>12</sub>
Chemical structure			
Molecular weight	276.34 g/mol	252.30 g/mol	228.3 g/mol
Color	pale yellow-green	pale yellow	colorless with blue or red-blue fluorescence
Physical state	solid (plate)	solid (needles)	solid (plates)
Melting point	273°C	215.7°C	255-2560°C
Boiling point	550°C	480°C	4480°C
Solubility in water	0.0012 mg/L	2.3x10 <sup>-3</sup> mg/L	2.8x10 <sup>-3</sup> mg/L
Organic solvents	slightly soluble in benzene, acetone	sparingly soluble in ethanol and methanol; soluble in benzene, toluene, xylene, and ether	slightly soluble in acetone; carbon disulphide, diethyl ether, ethanol, acetic acid, toluene, xylene; soluble in benzene
Partition coefficients:			
log K <sub>ow</sub>	6.04	6.06	5.16
log K <sub>oc</sub>	5.74	6.74	5.30
Vapor pressure	5.0 · 10 <sup>-7</sup> mmHg at 20-25°C	5.6 · 10 <sup>-9</sup> mmHg at 20°C	6.30 · 10 <sup>-7</sup> mmHg at 25°C
Henry's law constant	1.22x10 <sup>-5</sup> atm·m <sup>3</sup> /mol	4.9x10 <sup>-7</sup> atm·m <sup>3</sup> /mol	1.05x10 <sup>-5</sup> atm·m <sup>3</sup> /mol

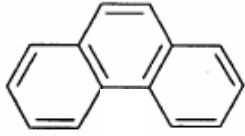
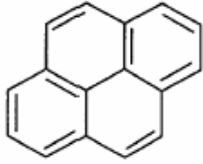
**Table 5.2 (continues) - Physico-chemical properties of different PAH species (Wild and Jones, 1995; Muller, 2002).**

PAH species	Dibenzo[a,h]anthracene	Fluoranthene	Fluorene
<b>Chemical formula</b>	C <sub>22</sub> H <sub>14</sub>	C <sub>16</sub> H <sub>10</sub>	C <sub>13</sub> H <sub>10</sub>
<b>Chemical structure</b>			
<b>Molecular weight</b>	278.35 g/mol	202.26 g/mol	166.2 g/mol
<b>Color</b>	colorless	pale yellow	white
<b>Physical state</b>	solid (plates or leaflets)	solid (needles or plates)	solid (leaflets or flakes; crystalline plates)
<b>Melting point</b>	262 °C	11 °C	116-117 °C
<b>Boiling point</b>	no data	~ 375 °C	295 °C
<b>Solubility in water</b>	5x10 <sup>-4</sup> mg/L	0.20-0.26 mg/L	1.68-1.98 mg/L
<b>Organic solvents</b>	slightly soluble in ethyl alcohol soluble in acetone, acetic acid, benzene, toluene and xylene	soluble in alcohol, ether, benzene, acetic acid	soluble in acetic acid, acetone, benzene, carbon disulphide, carbon tetrachloride, diethyl ether, ethanol, pyrimidine, toluene
<b>Partition coefficients:</b>			
<b>log K<sub>ow</sub></b>	6.84	4.90	4.18
<b>log K<sub>oc</sub></b>	6.52	4.58	3.86
<b>Vapor pressure</b>	1 · 10 <sup>-10</sup> mmHg at 20 °C	5.0 · 10 <sup>-6</sup> mmHg at 25 °C	3.2 · 10 <sup>-4</sup> mmHg at 20 °C
<b>Henry's law constant</b>	7.3x10 <sup>-8</sup> atm·m <sup>3</sup> /mol	6.5x10 <sup>-6</sup> atm·m <sup>3</sup> /mol	1.0x10 <sup>-4</sup> atm·m <sup>3</sup> /mol

**Table 5.2 (continues) - Physico-chemical properties of different PAH species (Wild and Jones, 1995; Muller, 2002).**

PAH species	Indeno[1,2,3-c,d]pyrene	Naphthalene
Chemical formula	C <sub>22</sub> H <sub>12</sub>	C <sub>10</sub> H <sub>8</sub>
Chemical structure		
Molecular weight	276.3 g/mol	128.2 g/mol
Color	yellow plates or needles showing a greenish-yellow fluorescence	white
Physical state	solid (plates or needles)	Solid (flakes)
Melting point	163.6°C	80.2°C
Boiling point	530°C	218°C
Solubility in water	0.062 mg/L	32mg/L
Organic solvents	soluble in organic solvents	soluble in organic solvents
Partition coefficients: log K <sub>ow</sub> log K <sub>oc</sub>	6.58 6.20	3.5 -
Vapor pressure	~10 <sup>-11</sup> -10 <sup>-5</sup> mmHg at 20 <sup>o</sup> C	1.8 · 10 <sup>-11</sup> mmHg at 25°C
Henry's law constant	6.95x10 <sup>-8</sup> atm·m <sup>3</sup> /mol	5.0x10 <sup>-2</sup> atm·m <sup>3</sup> /mol

**Table 5.2 (continues) - Physico-chemical properties of different PAH species (Wild and Jones, 1995; Muller, 2002).**

PAH species	Phenanthrene	Pyrene
Chemical formula	C <sub>14</sub> H <sub>10</sub>	C <sub>16</sub> H <sub>10</sub>
Chemical structure		
Molecular weight	178.2	202.3
Color	Colorless	Colorless, pale yellow plates (recrystallized from toluene) or slight blue fluorescence (recrystallized from ethanol or sublimation)
Physical state	Solid (plates, crystals or leaflets)	Solid (plates or tablets)
Melting point	100°C	156°C
Boiling point	340°C	393-404°C
Solubility in water	1.20 mg/L	0.077 mg/L
Organic solvents	soluble in acetic acid, benzene, carbon tetrachloride, carbon disulphide, anhydrous diethyl ether, toluene, ethanol	soluble in benzene, carbon disulphide, diethyl ether, alcohol, petroleum ether, toluene
Partition coefficients: log K <sub>ow</sub> log K <sub>oc</sub>	4.45 4.15	4.88 4.58
Vapor pressure	6.8x10 <sup>-4</sup> mmHg 25 <sup>0</sup> C	2.5x10 <sup>-5</sup> mmHg at 25 <sup>0</sup> C
Henry's law constant	2.56x10 <sup>-5</sup> atm-m <sup>3</sup> /mol	1.14x10 <sup>-5</sup> atm-m <sup>3</sup> /mol

### 5.1.1.2 PAH remediation

Despite the fact that several remediation techniques have been applied for PAH removal from contaminated soils and sediments, to reach their complete removal is as far as today a challenging task. In particular, the treatment of contaminated sediments is a very complex technical issue, as the sediment low permeability constrains the mass transfer and the application of many remediation methods.

Biodegradation of low-molecular weight PAHs by bacteria and microorganisms has been documented by various Authors, but high-molecular weight PAHs (with 5 or 6

aromatic rings) proved to be more recalcitrant to biological degradation (Cerniglia, 1992; Luthy et al., 1994; Henner et al., 1997; Masten and Davies, 1997; Muller, 2002; Antizar-Ladislao et al., 2005; O'Mahony et al., 2006; Haapea and Tuhkanen, 2006). It is believed that the limited mass transfer and bioavailability of PAHs can constrain their bioremediation in soils (Luthy et al., 1994; Taylor Jones, 2001), because PAHs tend to be tightly sorbed onto soil particles and organic matter.

For the same reasons, even though contaminants may desorb or be converted into more mobile forms through natural (chemical and biological) processes, the natural attenuation of PAHs is commonly very limited, and these compounds are regarded as persistent pollutants (De Serres and Bloom, 1995).

The fact that in natural soils PAHs are commonly strongly sorbed and incorporated into organic matter is also thought to act as a sort of detoxification process, which, by reducing their bioavailability and their mass transfer, may reduce their toxic effect towards natural microbial community (Richnow et al., 1995; Huling and Pivetz, 2006).

Sometimes environment-friendly solvents are used to solubilize PAHs and to enhance their contact with degrading bacteria (Taylor Jones, 2001; Gong et al., 2005; Gong et al., 2006). Even so, a complete remediation of heavily contaminated soils is still difficult to achieve by biological methods. For this reason, the use of chemical techniques has gained much interest for PAH remediation, since these methods can offer a rapid and aggressive alternative that is not so sensitive to the type and concentration of these contaminants as biological processes are (O'Mahony et al., 2006).

Among physical and chemical remediation techniques, soil venting is usually ineffective in the remediation of PAH-contaminated soils, because of PAH low volatility. In addition, the use of solvents or surfactants is usually discouraged because of the high solvent concentrations that are generally required to achieve good results (Luthy et al., 1994; Masten and Davies, 1997; Silva et al., 2005).

Chemical oxidation (main features are outlined in detail in Chapter 2.4.2.1) seems to be able to overcome these limitations and to be a promising technique for the remediation of environmental matrices contaminated by recalcitrant PAHs. The oxidants that are most commonly used for environmental purposes are ozone, hydrogen peroxide, permanganate and persulfate (ITRC, 2005). Also certain AOPs, like Fenton's reagent, activated persulfate and perozone, have been applied for PAH remediation.

Among the different available oxidants, gaseous ozone is considered as a very effective agent for the treatment of soils and sediments contaminated by PAHs, and it has been extensively applied for this purpose (Masten and Davies, 1997; U.S.EPA, 1998; Choi et al., 2002; Kim and Choi, 2002; ITRC, 2005; O'Mahony et al., 2006; Haapea and Tuhkanen, 2006; Rivas, 2006). Among the liquid oxidants, the experience is quite extended only as for the use of Fenton's reagent (Watts et al., 1996; Kong et al., 1998; Nam et al.,

2001; Watts et al., 2002; Kakarla et al., 2002; Bogan and Trbovic, 2003; Quan et al., 2003; ITRC, 2005; Watts et al., 2005; Flotron et al., 2005; Bissey et al., 2006; Rivas, 2006; Sun et al., 2007), while it is limited for other reactants, as permanganate and persulfate, as well as for other AOPs, even if they are theoretically considered amenable techniques for PAH degradation (Brown et al., 2003; Liang et al., 2004a,b; ITRC, 2005).

Chemical oxidation can also be applied in combination with bioremediation. Several Authors have in fact reported that the oxidation can enhance the biodegradability of PAHs, the application of chemical pre-oxidation having found to overcome the PAH recalcitrance to biodegradation (Nam et al., 2001; Haapea and Tuhkanen, 2006; Kulik et al., 2006; Rivas, 2006; Sun et al., 2007).

Under certain conditions, the mineralization effect can be achieved by using a pressurized hot water flux (about 250-300°C) as extracting or oxidant agent (Dadkhah and Akgerman, 2002; Kronholm et al., 2003). This technique, named supercritical water oxidation, has recently proved to be capable of degrading PAHs in polluted environmental matrices.

So far, a few Authors have studied the removal of PAHs from soils and sludges by electrochemical methods, mainly devoting their attention to EK-Fenton processes or surfactant-enhanced electrokinetic remediation (Chung and Kamon, 2005; Lee et al., 2005a; Kim et al., 2005a; Kim et al., 2005ab; Park et al., 2005a; Kim et al., 2006; Reddy et al., 2006). A few studies focused on the electrochemical contaminant degradation (Doering et al., 2001a,b; ; Isosaari et al., 2007; Zheng et al., 2007). The results of these studies were encouraging, and suggested that PAHs can be effectively removed from clayey soils (Doering et al., 2001a,b; Isosaari et al., 2007), though with removal efficiencies dependent on the soil type (Isosaari et al., 2007).

Most of these studies investigated the combined effect of electrooxidation and electrokinetic removal, i.e. aimed at removing PAHs either by flushing them or by decomposing them by electrochemical oxidation. Despite the fact that PAHs are apolar molecules and do not carry any electric charge, they can in fact be transported with the electroosmotic flux (Reddy et al., 2006; Isosaari et al., 2007). However, the low recovery of organic compounds in the catholyte solutions during combined electrokinetic-electrochemical tests suggested that the main part of the pollutant removal was achieved via electrooxidation, rather than via electromigration (Röhrs et al., 2002; Reddy et al., 2006; Isosaari et al., 2007).

### *5.1.1.3 Contaminated site*

The contaminated sediments of concern were collected in a canal in Trento (Italy), named “Roggia Campotrentino” or “Fossa Campotrentino” (see Figure 5.2 and Figure 5.3),

which for several decades had received industrial wastewater polluted by organic and inorganic compounds, deriving from a coal tar production site.

The sediment pollution of this ditch was linked to a former industrial pole (Carbochimica s.r.l.), located in the northern periphery of Trento, which was mainly devoted to the production of pitch and tar, with industrial processes involving the use of PAHs. The factory started its activity at the beginning of XIX century and occupied an area of about 42700 m<sup>2</sup>. Besides the production of pitches and tars, other industrial processes were established in the factory during its activity, including the production of naphthalene and wood preservatives. The factory closed down in the 1970s and the site is at present abandoned.

In the 1990s, several monitoring campaigns were conducted to investigate the environmental pollution conditions in this area. During the investigations, the soil in the former industrial plant was found to be heavily contaminated by PAHs, BTEX and phenols, mainly deriving from a bad management of the industrial activity, improper waste disposal procedures in the plant areas and leaking from the storage facilities.

The soil contamination in the former industrial area mainly involves the superficial layer of filling material and the underlying silty and sandy soils up to a depth of about 10-15 m below the ground level; the total volume of contaminated soil is about 151000 m<sup>3</sup> (Andreottola and Simonini, 2004). The soil pollution also resulted in the formation of a groundwater plume with significant amounts of BTEX and PAHs being detected in the groundwater.

Since in the first half of the last century the discharge of untreated industrial wastewater into the nearby rivers and channel was a common practice in Italy, the production process carried out at the Carbochimica plant also resulted in a major contamination of the surrounding channels and rivers, where high contamination concentrations were found in the sediments. In particular, the industrial activities resulted in the contamination of the sediments of the “Fossa Campotrentino” and of “Rio Lavisotto”, where high PAH concentrations are currently detected.

At present, a hydraulic barrier is working at the south border of the former industrial area, to avoid the downstream spreading of these contaminants. The polluted groundwater is pumped out by a group of wells, treated by ozonation and adsorption on granular activated carbons and subsequently discharged into a ditch (Rio Lavisotto). A remediation action for the recovery of the contaminated soil has been planned by the local authorities.



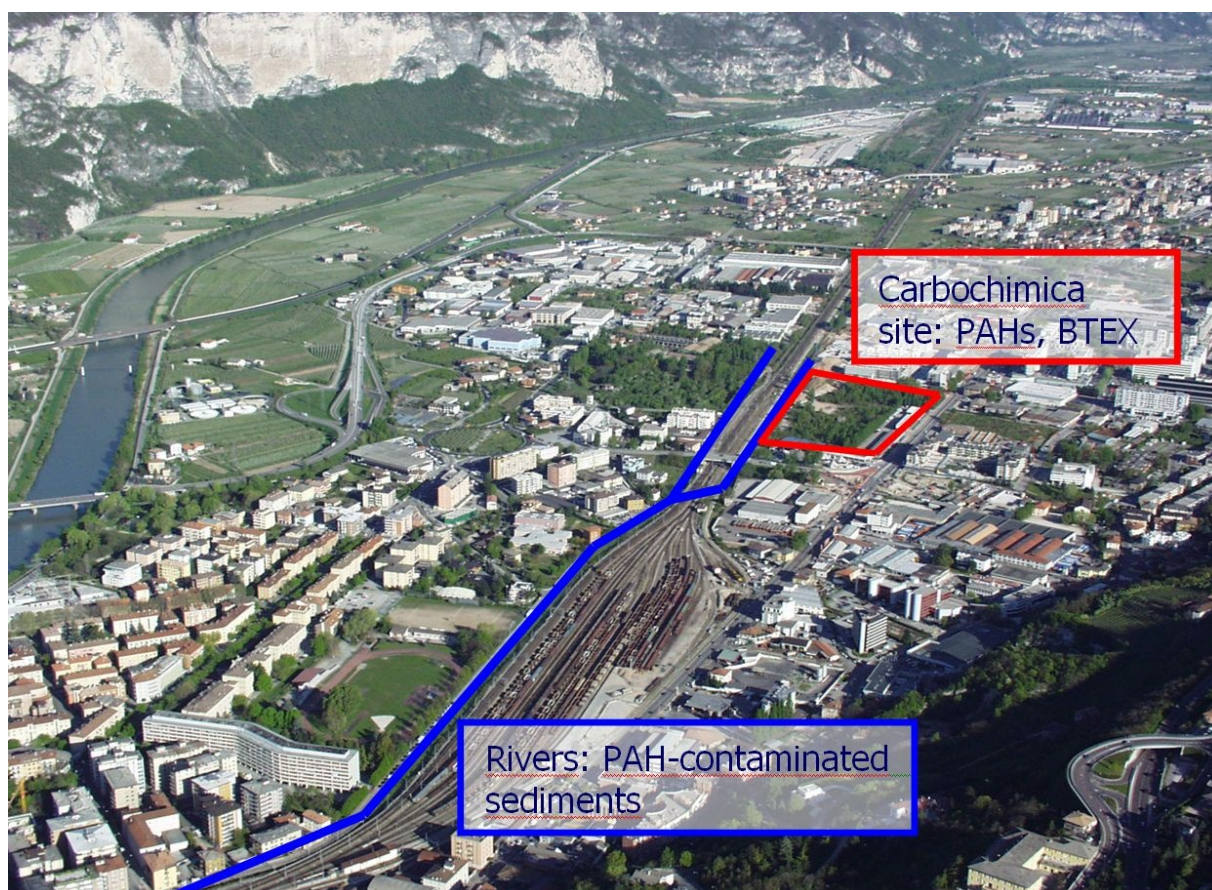


**Figure 5.2 – Contaminated sites in the northern suburbs of Trento (Italy): the picture indicates the Carbochimica site, location of a former coal tar production, now contaminated by PAHs and BTEX, and the rivers contaminated by PAHs.**



**Figure 5.3 – Picture of the “Roggia Campotrentino” or “Fossa Campotrentino” canal, in the northern suburbs of Trento (Italy), heavily contaminated by PAHs.**

From a hydrologic point of view, in this area the hydrographic system is dominated by the Adige River, which flows from North to South along the Brenner valley. In the last part of the XVIII century, the course of the river Adige was subject to a major realignment towards the western part of the valley, in order to protect Trento town centre from flooding events. At the same time, a complex network of ditches and streams was created, to be used

to drain the surrounding fields or for irrigation purposes. These include Rio Lavisotto, Fossa Armanelli, Fossa SLOI, Fossa delle Bettine, Roggia Campotrentino (Figure 5.4). Due to the urbanization of the last century, the ditches were incorporated in the urban area and some of them were covered, while other still exist as open water bodies. All these channels flow from north to south and are direct or indirect tributaries of the Adige River. Being nowadays only used to collect rainfall, their flow is highly dependent on seasonal and meteorological variations (Collins et al., 2005).

All the ditches and streams are property of the local authority (Provincia Autonoma di Trento) and, together with the former industrial areas, they are going to be recovered within the project of redeveloped and regeneration of the “Trento Nord” contaminated site.

The Roggia Campotrentino canal (Figure 5.3), where the samples used for this study were collected, was used to discharge industrial wastewater by the Carbochimica industrial plant during the factory activity. Consequently, the fluvial sediments are nowadays characterized by a high content of organic pollutants. The canal has a length of about 6.5 km and flows from north to south in Trento town, i.e. from the industrial area towards the city centre (Figure 5.2), where it enters the Rio Lavisotto.

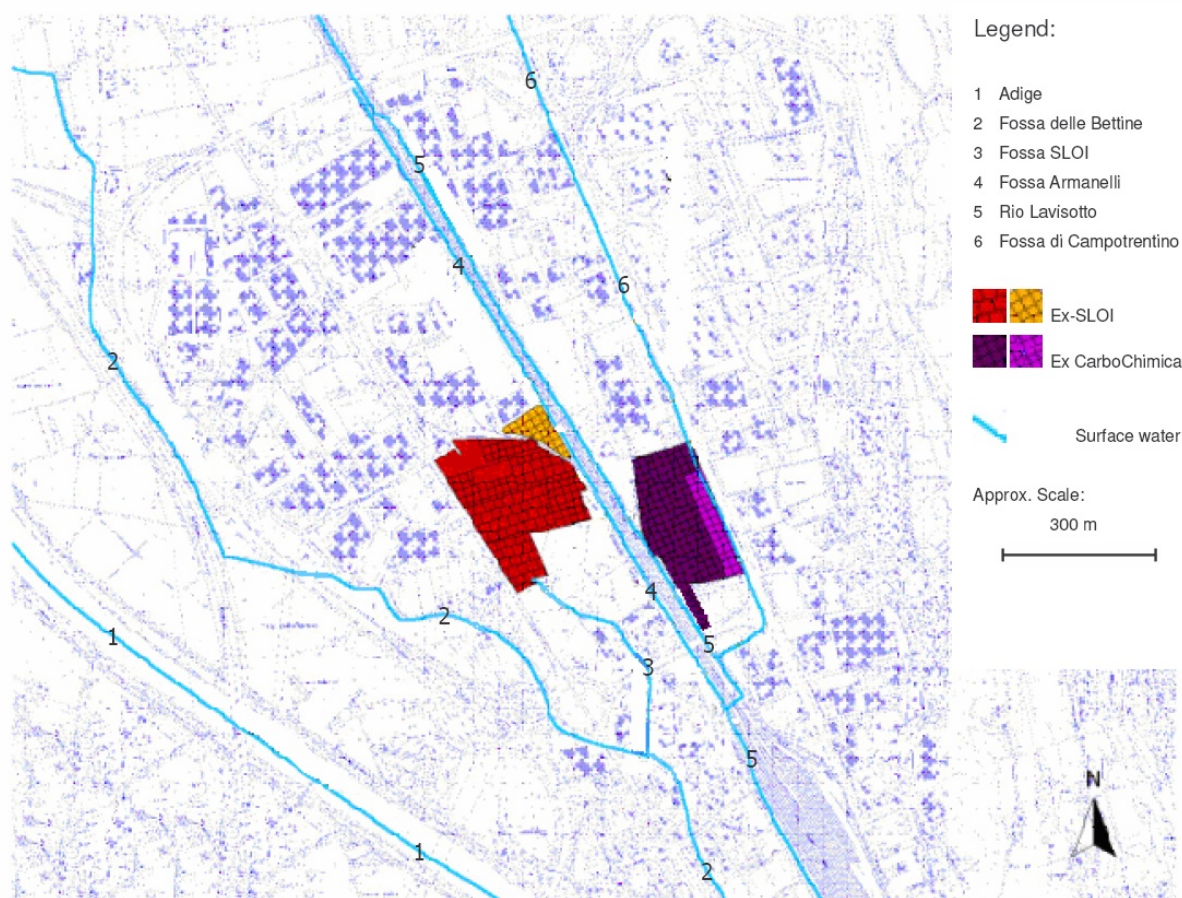


**Figure 5.4 – Map of the former industrial poles and of ditches, streams and rivers in the northern suburbs of Trento (Collins et al., 2005).**

## 5.1.2 Experimental investigation

### 5.1.2.1 Materials

Several samples (total weight about 10 kg) of fine-grain sediments were collected from the first 30-40 cm layer at the bottom of the above-mentioned canal; these samples were then mixed together and mechanically stirred to produce a homogeneous sample.

At first, the collected sediments were characterized and analyzed for BTEX (i.e. aromatic hydrocarbons: benzene, toluene, ethylbenzene, xylene), PAHs, pH and total organic matter, represented by the value of TOC. Both organic pollutants and natural organic matter occurred in the sediment samples, which proved to be contaminated by PAHs, but not by BTEX, whose presence was detected just in traces. The initial total PAH concentration in sediment samples ranged from about 1090 mg/kg<sub>DW</sub> to 1522 mg/kg<sub>DW</sub> (light PAHs about 731-1366 mg/kg<sub>DW</sub>, heavy PAHs about 139-359 mg/kg<sub>DW</sub>) and a 90% degradation was required to meet the remediation goals. The initial PAH concentrations in the samples proved to be highly variable, because the pollutant distribution in the sediments was not homogeneous. The TOC content was about 88-99 g/kg<sub>DW</sub>.

The sediments also showed a significant metal content, with a total iron concentration about 30621 mg/kg<sub>DW</sub> and a manganese content about 614 mg/kg<sub>DW</sub>.

The grain size of the target sediments is reported in Table 5.3. As can be seen from the data shown, most of the sediments is composed of silt (BSI, 1999), having a dimensions mainly ranging from 5  $\mu\text{m}$  and 100  $\mu\text{m}$ .

The sediment pH was about 7.8. In order to evaluate the buffer capacity of the sediments of concern, the pH variations due to acid or base additions were measured. For this purpose, two tests were conducted on two 20 g sediment samples added with demineralized water to achieve conditions of soil slurries (total volume of 50 mL). The samples were gradually added 1 M HCl and 1 M NaOH solutions and the resulting pH changes were recorded. The results are shown in Figure 5.5. As indicated, the sediment pH could be quite easily increased above 12, which required the dosage of 0.03 mol of NaOH, while 0.03 mol of HCl were necessary to decrease the pH below 2.

**Table 5.3 – Main features of the sediments of concern.**

Grain size	Amount
> 100 $\mu\text{m}$	3%
20 ÷ 100 $\mu\text{m}$	32%
10 ÷ 20 $\mu\text{m}$	11%
5 ÷ 10 $\mu\text{m}$	24%
< 5 $\mu\text{m}$	30%

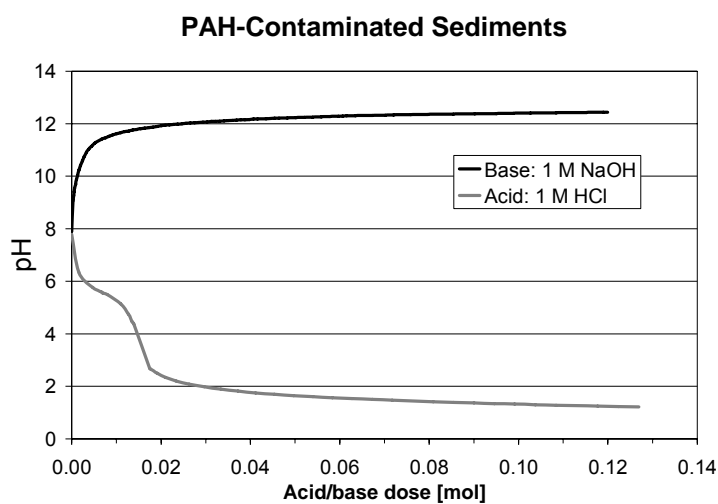


**Figure 5.5 – pH variations in the PAH-contaminated sediment samples after acid or base additions. The pH increase was obtained by adding 1 M NaOH to a sediment sample of 20 g having a volume of 50 mL; the pH decrease was obtained in the same way by adding 1 M HCl.**

### 5.1.2.2 Research scheme

The aim of this study aimed was to investigate the effectiveness of electrochemical oxidation for the remediation of river sediments contaminated by PAHs.

Three laboratory tests were performed during this study (Table 5.4). The first test (test PAH.1) was a preliminary experiment, which lasted for two weeks (14 days) with an applied voltage of 15 V (specific voltage of 1.5 V/cm). The second and the third tests (test PAH.2 and test PAH.3) lasted for four weeks and the applied voltages were 10 V and 20 V respectively (specific voltages of 1 V/cm and 2 V/cm). During these latter tests, the contaminant removal was also evaluated at different times while the treatments were in progress (7, 14 and 21 days after the beginning of the experiment).

Test PAH.1 was performed with Setup 1 (see Chapter 3.1 for a detailed description of the experimental device), on a cylindrical specimen having a length of 10 cm and a diameter of 9 cm, i.e. a volume of about 0.64 L; the specimen mass was about 1 kg. Both test PAH.2 and test PAH.3 were performed with Setup 2 (Chapter 3.1) on specimens

having dimensions of 10 cm in length, 10 cm in height and 10 cm in width, with a mass about 2 kg. The sediment samples were saturated with demineralized water and carefully stirred before being inserted in the electrochemical cell.

**Table 5.4 – List of the laboratory tests performed on PAH-contaminated sediments.**

<b>Test</b>	<b>Sample length [cm]</b>	<b>Applied voltage [V]</b>	<b>Specific voltage [V/cm]</b>	<b>Duration [d]</b>
PAH.1	10	15	1.5	14
PAH.2	10	10	1	28
PAH.3	10	20	2	28

To assess the efficiency of the tested treatments, the removal percentages were calculated for single PAH species and for PAH summation, as well as for TOC, which represents the total amount of the organic matter in the sample, both from natural and anthropogenic origins. The results were also correlated with PAH species, with the partition coefficient  $K_{ow}$  and with the pH profile in tested specimen. The PAH distribution along the sediment specimen, the contaminant transport and the time-dependency of the process were also investigated. The PAH volatilization was evaluated during test PAH.1, while ecotoxicity tests were carried out on the sediment samples before and after tests PAH.2 and PAH.3.

### 5.1.3 Results and Discussion

The results achieved during the study about the PAH-contaminated river sediments are presented and discussed as follows.

#### 5.1.3.1 Contaminant removal

##### 5.1.3.1.1 Test PAH.1

The first laboratory test carried out on PAH-contaminated sediments (test PAH.1) was performed with Setup 1 to assess the effectiveness of electrooxidation in removing the target contaminants. During the trial, was tested under a constant voltage of 15 V (specific voltage 1.5 V/cm) for 14 days. The main features of test PAH.1 are listed in Table 5.5.

At the beginning of the test a current of about 50 mA was encountered, then the current gradually decreased and the steady-state current was about 4 mA at the end of the trial. As a result of the electric current flowing across the specimen, a significant

electroosmotic flow was induced towards the cathode during the first days of the test, therefore at the end of the experiment 103 mL of water were found to be accumulated in the tank for water collection at the cathode compartment.

**Table 5.5 – Main features of test PAH.1.**

test name	PAH.1	
sample matrix	freshwater sediments	
contaminants	PAHs	
sample weight	1	[kg]
sample volume	0.64	[L]
sample density	1.6	[kg/L]
test duration	14	[d]
voltage (constant)	15	[V]
specific voltage (constant)	1.5	[V/cm]
initial current	50	[mA]
final current	4	[mA]
pore fluid collected at cathode compartment	103	[mL]

The main results achieved are reported in Table 5.6 and in Figure 5.6. As can be seen from the data shown, at the end of the trial an 85% total PAH removal was encountered, with a light PAH removal of 90% and a heavy PAH removal about 75%. The final total PAH concentration in the treated sample about 162.8 mg/kg<sub>DW</sub>.

The overall removal efficiencies attained during this preliminary test were very satisfying, as the target sediments were characterized by a very high contaminant content and, because of their low permeability and high sorption capacity, they had proven to be very recalcitrant to chemical degradation and to require high reactant dosages to achieve a good contaminant removal (Ferrarese et al., 2008). Hence, these results suggested that electrochemical oxidation could be applied effectively and easily for the remediation of these sediments.

The TOC removal was about 14%: this low value of TOC removal can be considered due to the very high natural organic matter content in the sediment samples.

Table 5.6 – Results of test PAH.1: contaminant concentrations and removal efficiencies.

Parameter		Original untreated sample	Final treated sample	Removal efficiency
1 naphthalene	[mg/kg <sub>DW</sub> ]	54.1	1.6	97%
2 acenaphthylene	[mg/kg <sub>DW</sub> ]	1.5	0.2	88%
3 acenaftene	[mg/kg <sub>DW</sub> ]	101.7	7.2	93%
4 fluorene	[mg/kg <sub>DW</sub> ]	65.4	3.9	94%
5 phenantrene	[mg/kg <sub>DW</sub> ]	278.9	21.5	92%
6 anthracene	[mg/kg <sub>DW</sub> ]	55.7	3.6	94%
7 fluoranthene	[mg/kg <sub>DW</sub> ]	173.4	34.9	80%
8 pyrene	[mg/kg <sub>DW</sub> ]	116.2	21.3	82%
9 chrysene	[mg/kg <sub>DW</sub> ]	45.9	9.9	78%
10 benzo(a)anthracene	[mg/kg <sub>DW</sub> ]	30.0	7.6	75%
11 benzo(b)fluoranthene	[mg/kg <sub>DW</sub> ]	56.8	16.0	72%
12 benzo(k)fluoranthene	[mg/kg <sub>DW</sub> ]	21.2	5.5	74%
13 benzo(a)pyrene	[mg/kg <sub>DW</sub> ]	41.5	11.3	73%
14 dibenzo(a,h)anthracene	[mg/kg <sub>DW</sub> ]	3.4	1.0	70%
15 benzo(g,h,i)perylene	[mg/kg <sub>DW</sub> ]	20.7	7.7	63%
16 indeno(1,2,3-cd)pyrene	[mg/kg <sub>DW</sub> ]	22.9	9.6	58%
Total light PAHs (1-7)	[mg/kg <sub>DW</sub> ]	730.7	72.8	90%
Total heavy PAHs (8-16)	[mg/kg <sub>DW</sub> ]	358.6	89.9	75%
Total PAHs	[mg/kg <sub>DW</sub> ]	1089.3	162.8	85%
TOC	[g/kg <sub>DW</sub> ]	99.0	85.6	14%
pH	[-]	7.8	7.7	-

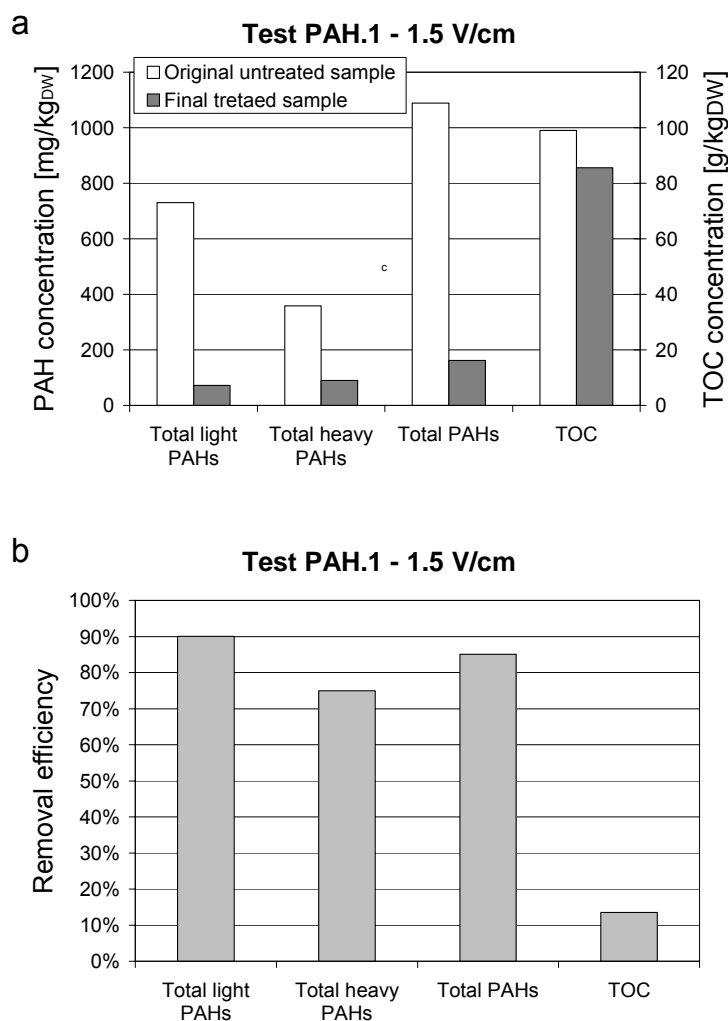


**Figure 5.6 – Results of test PAH.1: contaminant concentrations (a) and removal efficiencies (b).**

#### 5.1.3.1.2 Tests PAH.2 and PAH.3

Based on the result of the preliminary test PAH.1, other two laboratory tests, named test PAH.2 and PAH.3, were performed with Setup 2 to assess the influence of the applied voltage and of the treatment duration on PAH removal efficiency, in order to optimize the remediation conditions. For this purposes, during the experiments two voltages (1-2 V/cm) were tested and samples were collected from the specimen being treated at regular time intervals (i.e. on the 7<sup>th</sup>, 14<sup>th</sup>, 21<sup>st</sup> day after the beginning of the trial) to evaluate the extent of the oxidation process.

The main features of these experiments are listed in Table 5.7 and Table 5.8.

During these tests, the initial current values were about 6.5 mA (test PAH.2) and 50 mA (test PAH.3), while at the end of both trials the electric current was below 1 mA.

The results achieved are presented in Table 5.9 and Table 5.10 for test PAH.2 and in Table 5.11 and Table 5.12 for test PAH.3.



**Table 5.7 – Main features of test PAH.2.**

test name	PAH.2	
sample matrix	freshwater sediments	
contaminants	PAHs	
sample weight	2	[kg]
sample volume	1.0	[L]
sample density	2.0	[kg/L]
test duration	28	[d]
voltage (constant)	10	[V]
specific voltage (constant)	1.0	[V/cm]
initial current	6.5	[mA]
final current	0.009	[mA]

**Table 5.8 – Main features of test PAH.3.**

test name	PAH.3	
sample matrix	freshwater sediments	
contaminants	PAHs	
sample weight	2	[kg]
sample volume	1.00	[L]
sample density	2.0	[kg/L]
test duration	28	[d]
voltage (constant)	20	[V]
specific voltage (constant)	2.0	[V/cm]
initial current	50	[mA]
final current	0.001	[mA]

During test PAH.2 (applied voltage 1 V/cm), a 72% total PAH removal was encountered 7 days after the beginning of the run. As the trial proceeded, the total PAH removal gradually increased to 74% (14<sup>th</sup> day), 81% (21<sup>st</sup> day) and 91% by the end of the test (28<sup>th</sup> day). In the meanwhile, the TOC removal increased from about 2% (7<sup>th</sup> day) to 8% (14<sup>th</sup> day), 17% (21<sup>st</sup> day) and 25% (28<sup>th</sup> day, end of the test).

Higher removal efficiencies were encountered during test PAH.3, when a higher specific voltage (2 V/cm) was applied. In this case the total PAH removal efficiency was about 33% 7 days after the beginning of the treatment, but it rapidly increased to 85% on the 14<sup>th</sup> day, to 93% on the 21<sup>st</sup> day and 96% at the end of the test (28<sup>th</sup> day).

A certain variability was encountered in the PAH content of the samples. For example, during test PAH.2 the heavy PAH content in the second week was higher than that recorded in the first week of the process. Similarly, during test PAH.3, the heavy PAH content in the third week was higher than that in the previous week. This can be considered due to the natural sample heterogeneity, which is a typical feature of PAH contaminations, and which may have affected the results.

The results achieved in tests PAH.2 and PAH.3 are consistent with the removal efficiencies measured at the end of test PAH.1, which resulted in a total PAH removal efficiency about 85% after a two-week treatment.

It must be point out that a significant dependency of the system efficiency on the treatment duration was encountered, therefore a treatment of a few weeks can be significantly more effective than a treatment of a few days. These results confirmed the conclusions that were drawn for the diesel fuel contaminated soils in Chapter 4.

Also in tests PAH.2 and PAH.3, the removal efficiencies for heavy PAH species were lower than for light PAH species and the TOC removal was very limited. This effect is discussed in detail in Section 5.1.3.2.

**Table 5.9 – Results of test PAH.2: contaminant concentrations in the original sample and 7, 14, 21 and 28 days after the beginning of the test.**

Elapsed time	[d]	0	7	14	21	28
1 naphthalene	[mg/kg <sub>DW</sub> ]	55.2	6.2	6.8	4.9	1.3
2 acenaphtylene	[mg/kg <sub>DW</sub> ]	0.7	0.3	0.1	0.3	0.2
3 acenaftene	[mg/kg <sub>DW</sub> ]	162.6	29.1	24.8	18.2	6.3
4 fluorene	[mg/kg <sub>DW</sub> ]	78.2	16.6	14.6	10.6	3.9
5 phenantrene	[mg/kg <sub>DW</sub> ]	273.7	72.3	61.7	43.8	19.5
6 anthracene	[mg/kg <sub>DW</sub> ]	47.7	15.1	12.8	8.6	3.8
7 fluoranthene	[mg/kg <sub>DW</sub> ]	275.3	90.9	82.4	63.7	30.2
8 pyrene	[mg/kg <sub>DW</sub> ]	46.4	16.3	17.3	13.5	8.5
9 chrysene	[mg/kg <sub>DW</sub> ]	19.5	7.4	8.0	6.2	3.9
10 benzo(a)anthracene	[mg/kg <sub>DW</sub> ]	16.2	6.0	7.6	4.9	3.0
11 benzo(b)fluoranthene	[mg/kg <sub>DW</sub> ]	19.7	9.3	9.6	8.7	5.4
12 benzo(k)fluoranthene	[mg/kg <sub>DW</sub> ]	7.5	3.3	3.6	2.9	1.8
13 benzo(a)pyrene	[mg/kg <sub>DW</sub> ]	13.4	6.2	7.0	5.7	3.9
14 dibenzo(a,h)anthracene	[mg/kg <sub>DW</sub> ]	1.6	0.9	0.8	0.9	0.4
15 benzo(g,h,i)perylene	[mg/kg <sub>DW</sub> ]	7.2	3.9	4.3	4.0	2.6
16 indeno(1,2,3-cd)pyrene	[mg/kg <sub>DW</sub> ]	7.9	4.3	4.2	4.1	2.3
Total light PAHs (1-7)	[mg/kg <sub>DW</sub> ]	893.4	230.6	203.2	150.1	65.1
Total heavy PAHs (8-16)	[mg/kg <sub>DW</sub> ]	139.4	57.6	62.4	50.8	31.8
Total PAHs	[mg/kg <sub>DW</sub> ]	1032.8	288.2	265.5	200.9	96.9
TOC	[g/kg <sub>DW</sub> ]	88.5	87.1	81.2	73.3	66.2

**Table 5.10 – Results of test PAH.2: contaminant removal efficiencies achieved 7, 14, 21 and 28 days after the beginning of the test.**

<b>Elapsed time [d]</b>	<b>7</b>	<b>14</b>	<b>21</b>	<b>28</b>
1 naphthalene	89%	88%	91%	98%
2 acenaphthylene	57%	91%	58%	77%
3 acenaftene	82%	85%	89%	96%
4 fluorene	79%	81%	86%	95%
5 phenantrene	74%	77%	84%	93%
6 anthracene	68%	73%	82%	92%
7 fluoranthene	67%	70%	77%	89%
8 pyrene	65%	63%	71%	82%
9 chrysene	62%	59%	68%	80%
10 benzo(a)anthracene	63%	53%	70%	81%
11 benzo(b)fluoranthene	53%	51%	56%	73%
12 benzo(k)fluoranthene	56%	52%	61%	76%
13 benzo(a)pyrene	54%	48%	58%	71%
14 dibenzo(a,h)anthracene	44%	52%	47%	75%
15 benzo(g,h,i)perylene	46%	40%	44%	64%
16 indeno(1,2,3-cd)pyrene	46%	47%	48%	71%
Total light PAHs (1-7)	74%	77%	83%	93%
Total heavy PAHs (8-16)	59%	55%	64%	77%
Total PAHs	72%	74%	81%	91%
TOC	2%	8%	17%	25%

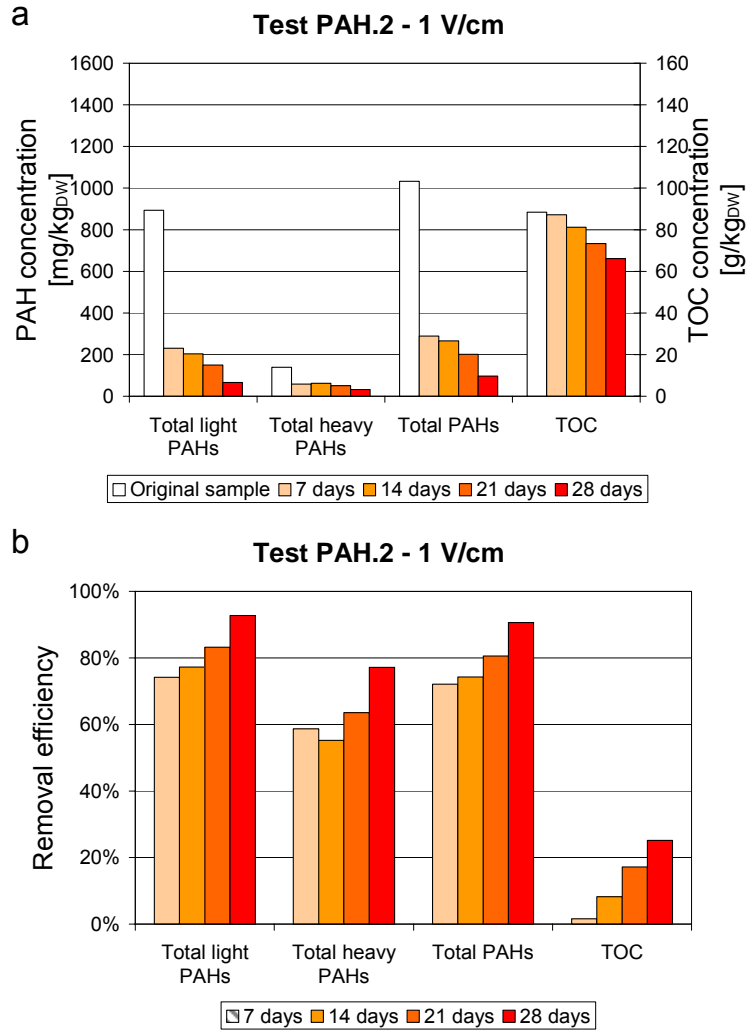


Figure 5.7 – Results of tests PAH.2: contaminant concentrations (a) and removal efficiencies (b).

**Table 5.11 – Results of test PAH.3: contaminant concentrations in the original sample and 7, 14, 21 and 28 days after the beginning of the test.**

Elapsed time	[d]	0	7	14	21	28
1 naphthalene	[mg/kg <sub>DW</sub> ]	99.5	36.0	3.9	0.7	<0.1
2 acenaphtylene	[mg/kg <sub>DW</sub> ]	0.6	<0.1	<0.1	<0.1	<0.1
3 acenaftene	[mg/kg <sub>DW</sub> ]	242.2	154.7	22.8	6.3	0.4
4 fluorene	[mg/kg <sub>DW</sub> ]	123.5	92.5	13.8	5.1	3.5
5 phenantrene	[mg/kg <sub>DW</sub> ]	415.8	288.1	56.6	18.0	7.7
6 anthracene	[mg/kg <sub>DW</sub> ]	77.2	49.4	9.8	3.3	0.4
7 fluoranthene	[mg/kg <sub>DW</sub> ]	407.8	303.8	69.6	29.8	7.6
8 pyrene	[mg/kg <sub>DW</sub> ]	52.1	29.2	12.4	9.7	11.8
9 chrysene	[mg/kg <sub>DW</sub> ]	21.8	13.8	5.2	4.5	5.2
10 benzo(a)anthracene	[mg/kg <sub>DW</sub> ]	18.4	13.8	4.4	3.7	4.5
11 benzo(b)fluoranthene	[mg/kg <sub>DW</sub> ]	23.1	14.9	7.4	7.4	7.9
12 benzo(k)fluoranthene	[mg/kg <sub>DW</sub> ]	8.5	5.8	2.5	2.4	2.7
13 benzo(a)pyrene	[mg/kg <sub>DW</sub> ]	16.1	12.3	6.2	5.6	6.0
14 dibenzo(a,h)anthracene	[mg/kg <sub>DW</sub> ]	1.7	1.0	0.6	0.5	0.6
15 benzo(g,h,i)perylene	[mg/kg <sub>DW</sub> ]	7.4	4.3	3.4	3.7	3.6
16 indeno(1,2,3-cd)pyrene	[mg/kg <sub>DW</sub> ]	7.3	3.5	3.0	2.9	2.7
Total light PAHs (1-7)	[mg/kg <sub>DW</sub> ]	1366.5	924.5	176.5	63.1	19.5
Total heavy PAHs (8-16)	[mg/kg <sub>DW</sub> ]	156.4	98.6	45.1	40.4	45.0
Total PAHs	[mg/kg <sub>DW</sub> ]	1522.9	1023.1	221.5	103.5	64.5
TOC	[g/kg <sub>DW</sub> ]	90.6	78.8	75.1	74.8	70.5

**Table 5.12 – Results of test PAH.3: contaminant removal efficiencies achieved 7, 14, 21 and 28 days after the beginning of the test.**

<b>Elapsed time [d]</b>	<b>7</b>	<b>14</b>	<b>21</b>	<b>28</b>
1 naphthalene	64%	96%	99%	>99%
2 acenaphthylene	>99%	>99%	>99%	>99%
3 acenaftene	36%	91%	97%	>99%
4 fluorene	25%	89%	96%	97%
5 phenantrene	31%	86%	96%	98%
6 anthracene	36%	87%	96%	99%
7 fluoranthene	26%	83%	93%	98%
8 pyrene	44%	76%	81%	77%
9 chrysene	37%	76%	79%	76%
10 benzo(a)anthracene	25%	76%	80%	76%
11 benzo(b)fluoranthene	35%	68%	68%	66%
12 benzo(k)fluoranthene	32%	71%	72%	68%
13 benzo(a)pyrene	24%	61%	65%	63%
14 dibenzo(a,h)anthracene	41%	68%	71%	65%
15 benzo(g,h,i)perylene	42%	54%	50%	51%
16 indeno(1,2,3-cd)pyrene	52%	59%	60%	63%
Total light PAHs (1-7)	32%	87%	95%	99%
Total heavy PAHs (8-16)	37%	71%	74%	71%
Total PAHs	33%	85%	93%	96%
TOC	13%	17%	17%	22%

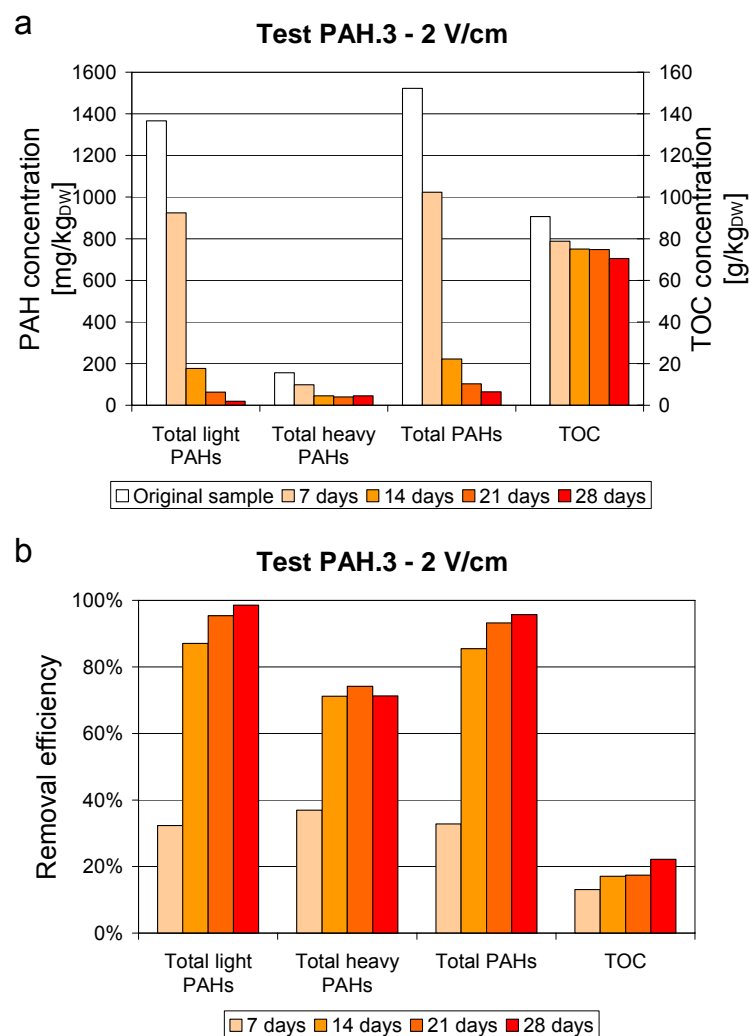


**Figure 5.8 – Results of tests PAH.3: contaminant concentrations (a) and removal efficiencies (b).**

### 5.1.3.2 Contaminant hydrophobicity and removal efficiency

In all the tests performed with the PAH-contaminated sediments, the removal efficiencies for light PAHs were found to be higher than for the heavy PAHs. This can be considered as a typical behavior of PAHs, whose lighter species are generally more available to reactants than heavy species, which are more hydrophobic and more sorbed onto sediments (Zheng et al., 2007; Ferrarese et al., 2008).

For traditional chemical oxidation with hydroxyl radicals  $\cdot\text{OH}$ , the PAH contaminant availability has been well reported to highly influence the treatment efficiency (Kakarka et al., 2002; Watts et al., 2002; Bogan and Trbovic, 2003; ITRC, 2005; Watts et al., 2005; Ferrarese et al., 2008), the least sorbed pollutants (i.e. the species that are less hydrophobic) being the most available for the mineralization processes, while the most hydrophobic and most sorbed molecules proved to be the most resistant to oxidation. This difference in the removal efficiency can be commonly overcome by using vigorous oxidation conditions, i.e.

high oxidant concentrations. In fact, in traditional chemical oxidation, under weak oxidation conditions, the contaminant removal is found to be highly dependent on  $K_{ow}$ , being significantly lower for heavy PAH species than for light compounds. On the opposite, when vigorous oxidation conditions are created, a good removal can be achieved also for heavy PAHs (Ferrarese et al., 2008).

To highlight this effect, the removal efficiency achieved with different PAH species has been compared to the octanol-water partition coefficient ( $K_{ow}$ ). As the  $K_{ow}$  coefficient represents the lipophilicity of a certain chemical, it indicates the tendency of that compound to be sorbed onto organic matter or to dissolve in water. The higher the  $K_{ow}$  coefficient is, the more the PAHs tend to be sorbed onto organic matter. As shown in Figure 5.9, the PAH removal efficiency achieved for test PAH.1 tended to decrease as the value of  $\text{Log}(K_{ow})$  increased, thus indicating that the removal efficiencies were always higher for light PAH species than for heavy PAHs. This effect had already been observed in previous studies for the electrochemical treatment of PAH-contaminated soils (Isosaari et al., 2007; Zheng et al., 2007), the heavier PAH species being more sorbed onto sediments and also more recalcitrant to degradation.

Figure 5.10 and Figure 5.11 show the removal efficiencies achieved during tests PAH.2 and PAH.3 as a function of PAH species and of the partition coefficient  $K_{ow}$ . The results of these tests confirmed that higher removal efficiencies tended to be achieved for light PAH species than for heavy PAHs. However, Figure 5.10 and Figure 5.11 also indicate that as the treatment duration increased, the pollutant removal increased, both for light and heavy PAH species, rising up to 90-99% for light PAHs and about 70-80% for heavy PAHs after a four-week treatment. Thus, it can be concluded that the difference in the removal efficiencies between light and heavy PAHs tends to decrease as the treatment duration increases. It can be assumed that during the first days of treatment, the light PAH species were mainly oxidized, but as the treatment continued, also heavy PAH species were gradually attacked. This suggests that longer treatments would not only lead to better overall removal efficiencies than shorter ones (i.e. higher total PAH removal and higher TOC removal), but would also result in a better mineralization of the more recalcitrant PAH species (e.g. heavy PAHs), which also pose the most important environmental concerns.



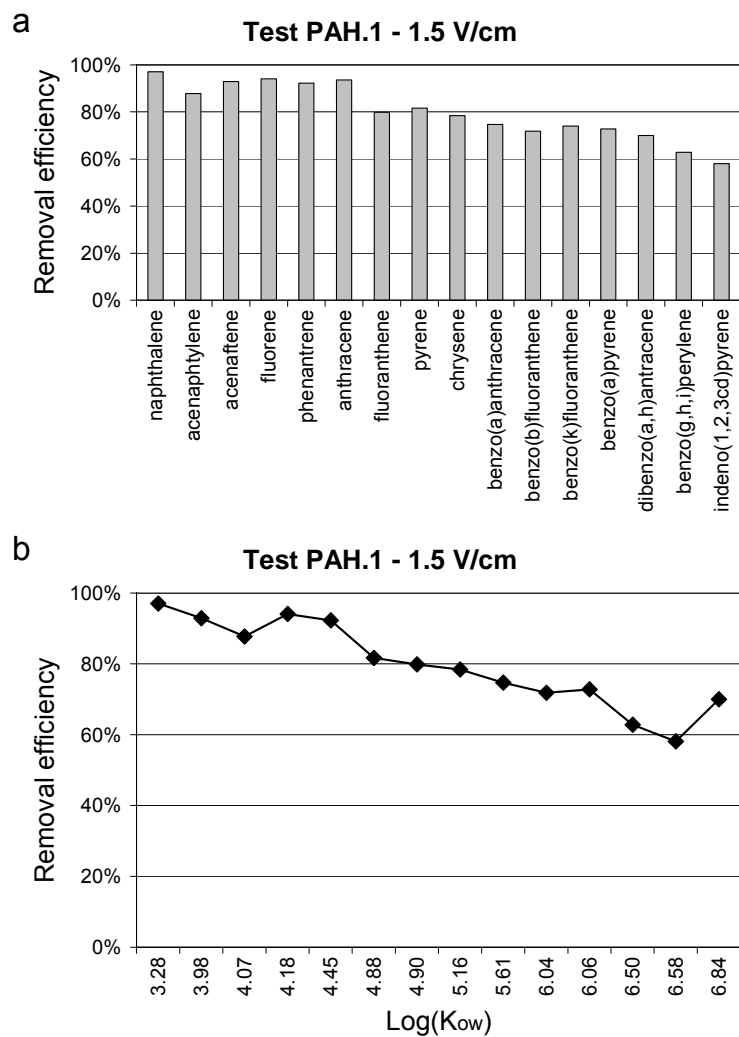


**Figure 5.9 – Results of test PAH.1: removal efficiencies achieved as a function of PAH species (a) and of PAH octanol-water partition coefficient ( $K_{ow}$ ) (b). Since benzo(a)pyrene and benzo(k)fluoranthene are characterized by the same value of  $K_{ow}$ , as well as phenanthrene and anthracene, in the plots only the results for benzo(a)pyrene and for phenanthrene are presented.**

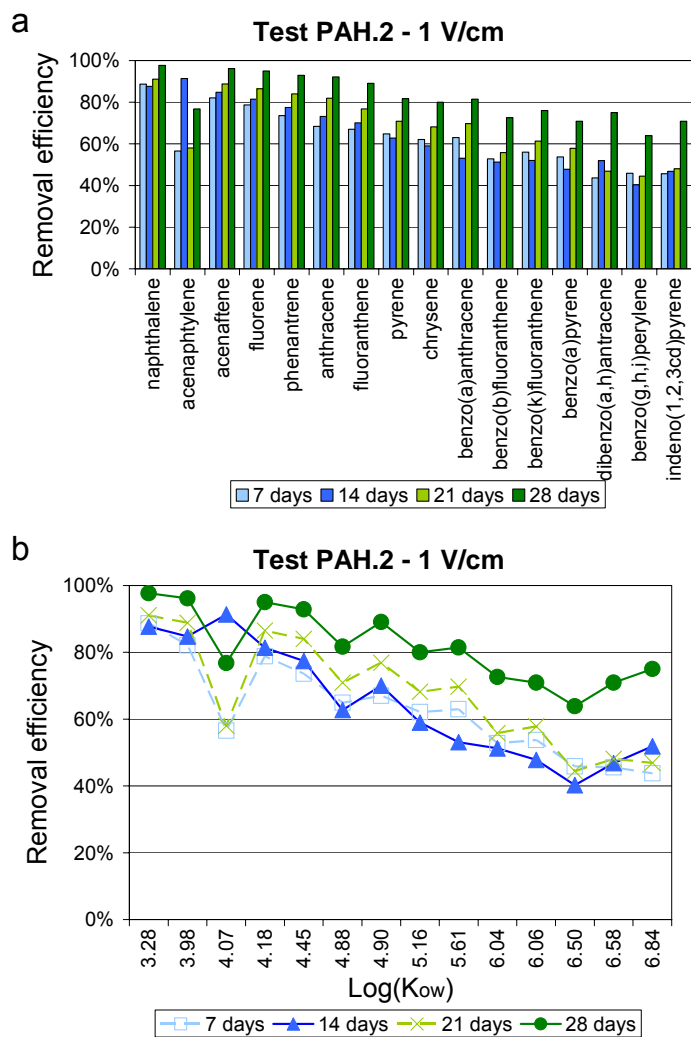


Figure 5.10 – Results of tests PAH.2: removal efficiencies achieved as a function of PAH species (a) and of PAH octanol-water partition coefficient ( $K_{ow}$ ) (b). Since benzo(a)pyrene and benzo(k)fluoranthene are characterized by the same value of  $K_{ow}$ , as well as phenanthrene and anthracene, in the plots only the results for benzo(a)pyrene and for phenanthrene are presented.

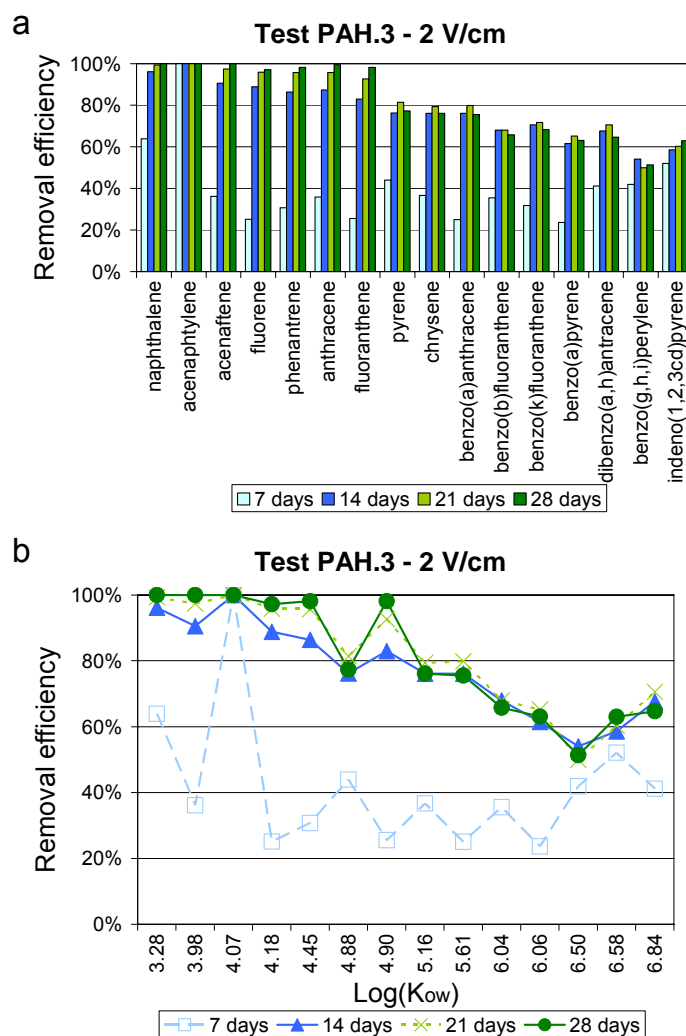


Figure 5.11 – Results of tests PAH.3: removal efficiencies achieved as a function of PAH species (a) and of PAH octanol-water partition coefficient ( $K_{ow}$ ) (b). Since benzo(a)pyrene and benzo(k)fluoranthene are characterized by the same value of  $K_{ow}$ , as well as phenanthrene and anthracene, in the plots only the results for benzo(a)pyrene and for phenanthrene are presented.

### 5.1.3.3 Contaminant distribution and transport

At the end of each trial, a part of the soil specimen was transversally sliced into five segments and each segment was analyzed for pH and contaminant concentrations, in order to assess the extent of electrochemical reactions at different distances from the electrodes and the possible contribution of electrokinetic transport. Contaminant concentrations and pH values in the different segments are presented in Table 5.13 and Figure 5.12 for test PAH.1; Table 5.14 and Figure 5.13 for test PAH.2; Table 5.15 and Figure 5.14 for test PAH.3.

Despite some variability due to natural sample heterogeneity, the final pollutant concentrations were found to be evenly distributed across the treated sample, both for PAHs and for TOC. The same result had been found for diesel fuel-contamination (see

Chapter 4). Once more, because of the heterogeneous distribution of PAHs in the sediments, even quite significant differences can be considered acceptable between the mean values determined in the overall sample representing the whole specimen and in the five samples used to determine the contaminant distribution.

**Table 5.13 – Results of test PAH.1: contaminant concentrations and pH profile along the treated sample at different distances from the electrodes.**

Section		Section 1	Section 2	Section 3	Section 4	Section 5
Normalized distance form cathode		0.1	0.3	0.5	0.7	0.9
1 naphthalene	[mg/kg <sub>DW</sub> ]	1.5	0.0	3.3	2.4	2.6
2 acenaphthylene	[mg/kg <sub>DW</sub> ]	0.2	0.6	0.3	0.1	0.3
3 acenaftene	[mg/kg <sub>DW</sub> ]	7.1	18.6	14.7	8.4	9.4
4 fluorene	[mg/kg <sub>DW</sub> ]	3.5	11.3	9.2	4.1	4.6
5 phenantrene	[mg/kg <sub>DW</sub> ]	21.0	58.8	50.1	23.6	28.8
6 anthracene	[mg/kg <sub>DW</sub> ]	3.5	10.1	8.8	4.2	4.6
7 fluoranthene	[mg/kg <sub>DW</sub> ]	32.8	48.9	38.9	38.9	48.3
8 pyrene	[mg/kg <sub>DW</sub> ]	18.2	69.6	57.4	23.1	18.3
9 chrysene	[mg/kg <sub>DW</sub> ]	8.4	27.3	23.3	10.9	8.7
10 benzo(a)anthracene	[mg/kg <sub>DW</sub> ]	6.1	18.7	15.8	8.3	7.3
11 benzo(b)fluoranthene	[mg/kg <sub>DW</sub> ]	13.5	38.0	30.3	17.8	13.9
12 benzo(k)fluoranthene	[mg/kg <sub>DW</sub> ]	4.6	13.4	11.1	6.1	5.0
13 benzo(a)pyrene	[mg/kg <sub>DW</sub> ]	11.1	27.4	22.1	13.2	8.3
14 dibenzo(a,h)anthracene	[mg/kg <sub>DW</sub> ]	1.3	2.5	1.9	1.4	1.0
15 benzo(g,h,i)perylene	[mg/kg <sub>DW</sub> ]	6.5	15.5	12.1	8.3	7.2
16 indeno(1,2,3-cd)pyrene	[mg/kg <sub>DW</sub> ]	7.8	20.0	15.8	10.9	8.3
Total light PAHs (1-7)	[mg/kg <sub>DW</sub> ]	69.6	148.3	125.3	81.7	98.6
Total heavy PAHs (8-16)	[mg/kg <sub>DW</sub> ]	77.5	232.4	189.8	100.0	78.0
Total PAHs	[mg/kg <sub>DW</sub> ]	147.1	380.7	315.1	181.7	176.5
pH	[-]	10.5	9.72	7.39	7.25	7.02

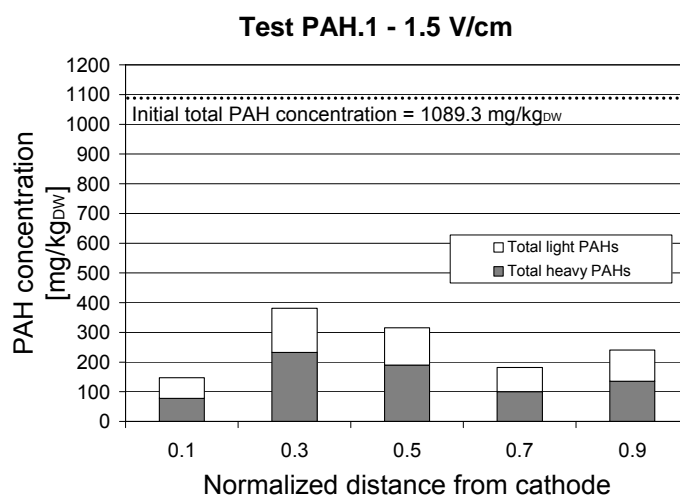


**Figure 5.12 – Concentrations of PAHs along the treated sample at different distances from the electrodes at the end of test PAH.1.**

**Table 5.14 – Results of test PAH.2: contaminant concentrations along the treated sample at different distances from the electrodes.**

Section			Section 1	Section 2	Section 3	Section 4	Section 5
Normalized distance form cathode			0.1	0.3	0.5	0.7	0.9
1	naphthalene	[mg/kg <sub>DW</sub> ]	2.5	10.7	1.0	9.5	0.7
2	acenaphtylene	[mg/kg <sub>DW</sub> ]	0.2	0.4	0.1	0.2	0.0
3	acenaftene	[mg/kg <sub>DW</sub> ]	8.6	54.9	5.9	34.8	7.8
4	fluorene	[mg/kg <sub>DW</sub> ]	5.5	28.7	4.1	18.2	5.5
5	phenantrene	[mg/kg <sub>DW</sub> ]	27.2	123.6	18.2	71.1	23.6
6	anthracene	[mg/kg <sub>DW</sub> ]	5.7	23.3	3.5	12.4	3.7
7	fluoranthene	[mg/kg <sub>DW</sub> ]	43.6	133.3	30.7	74.7	36.5
8	pyrene	[mg/kg <sub>DW</sub> ]	10.7	21.6	8.0	10.9	8.6
9	chrysene	[mg/kg <sub>DW</sub> ]	4.7	9.1	3.7	4.6	3.9
10	benzo(a)anthracene	[mg/kg <sub>DW</sub> ]	3.8	7.2	3.0	4.3	3.2
11	benzo(b)fluoranthene	[mg/kg <sub>DW</sub> ]	6.4	10.4	6.1	4.9	5.9
12	benzo(k)fluoranthene	[mg/kg <sub>DW</sub> ]	2.1	3.7	2.0	2.1	1.9
13	benzo(a)pyrene	[mg/kg <sub>DW</sub> ]	4.8	9.5	5.3	4.1	4.9
14	dibenzo(a,h)anthracene	[mg/kg <sub>DW</sub> ]	0.5	0.8	0.5	0.3	0.4
15	benzo(g,h,i)perylene	[mg/kg <sub>DW</sub> ]	3.0	4.1	3.3	1.8	3.0
16	indeno(1,2,3-cd)pyrene	[mg/kg <sub>DW</sub> ]	3.0	4.4	3.5	1.8	2.5
Total light PAHs (1-7)		[mg/kg <sub>DW</sub> ]	93.3	374.9	63.4	220.9	77.7
Total heavy PAHs (8-16)		[mg/kg <sub>DW</sub> ]	39.0	70.8	35.4	34.7	34.3
Total PAHs		[mg/kg <sub>DW</sub> ]	132.3	445.7	98.8	255.6	112.0
TOC		[g/kg <sub>DW</sub> ]	81.5	79.3	77.4	24.7	72.3

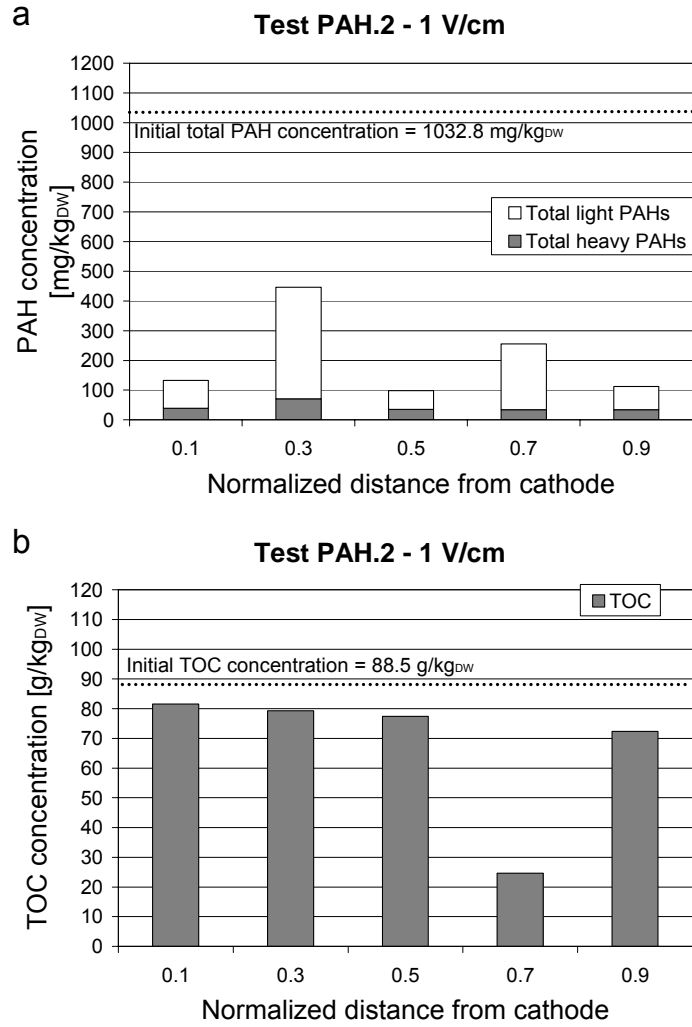


**Figure 5.13 – Concentrations of PAHs (a) and TOC (b) along the treated sample at different distances from the electrodes at the end of test PAH.2.**

**Table 5.15 – Results of test PAH.3: contaminant concentrations along the treated sample at different distances from the electrodes.**

Section		Section 1	Section 2	Section 3	Section 4	Section 5
Normalized distance form cathode		0.1	0.3	0.5	0.7	0.9
1	naphthalene [mg/kg <sub>DW</sub> ]	0.3	0.6	0.3	0.2	1.4
2	acenaphtylene [mg/kg <sub>DW</sub> ]	0.0	0.1	0.0	0.0	0.1
3	acenaftene [mg/kg <sub>DW</sub> ]	1.3	1.5	1.3	0.9	7.9
4	fluorene [mg/kg <sub>DW</sub> ]	0.8	0.7	0.7	0.5	4.6
5	phenantrene [mg/kg <sub>DW</sub> ]	3.4	5.0	3.8	2.9	17.6
6	anthracene [mg/kg <sub>DW</sub> ]	0.6	1.4	0.6	0.4	3.2
7	fluoranthene [mg/kg <sub>DW</sub> ]	5.0	16.0	5.6	4.5	19.8
8	pyrene [mg/kg <sub>DW</sub> ]	12.8	9.2	8.2	10.4	24.4
9	chrysene [mg/kg <sub>DW</sub> ]	5.8	4.2	4.2	4.7	10.5
10	benzo(a)anthracene [mg/kg <sub>DW</sub> ]	5.2	3.2	3.5	3.8	9.6
11	benzo(b)fluoranthene [mg/kg <sub>DW</sub> ]	7.9	7.3	6.5	7.9	12.7
12	benzo(k)fluoranthene [mg/kg <sub>DW</sub> ]	2.7	2.4	2.1	2.6	4.5
13	benzo(a)pyrene [mg/kg <sub>DW</sub> ]	6.7	6.1	5.5	6.1	9.6
14	dibenzo(a,h)anthracene [mg/kg <sub>DW</sub> ]	0.6	0.6	0.5	0.7	0.9
15	benzo(g,h,i)perylene [mg/kg <sub>DW</sub> ]	2.8	3.5	3.1	3.4	4.9
16	indeno(1,2,3-cd)pyrene [mg/kg <sub>DW</sub> ]	2.7	3.2	2.8	3.2	4.4
Total light PAHs (1-7) [mg/kg <sub>DW</sub> ]		11.5	25.3	12.3	9.6	54.6
Total heavy PAHs (8-16) [mg/kg <sub>DW</sub> ]		47.2	39.7	36.4	42.8	81.5
Total PAHs [mg/kg <sub>DW</sub> ]		58.7	65.0	48.7	52.4	136.1
TOC [g/kg <sub>DW</sub> ]		82.0	79.8	77.1	76.6	77.4

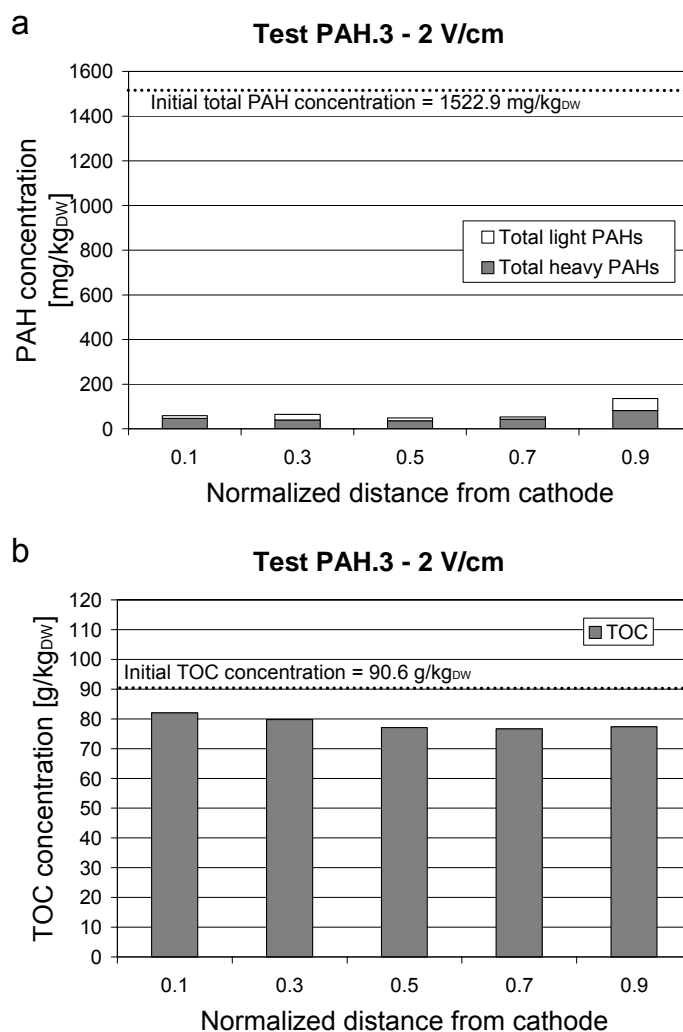


**Figure 5.14 – Concentrations of PAHs (a) and TOC (b) along the treated sample at different distances from the electrodes at the end of test PAH.3.**

#### 5.1.3.4 pH profiles

At the beginning and at the end of test PAH.1, the sediment pH was measured at different distances from the electrodes. As can be seen from Figure 5.15, during the tests, the soil pH tended to increase at the cathode and to decrease at the anode, as a result of water hydrolysis, which leads to the production of an acid front moving from the anode toward the cathode and a base front moving from the cathode toward the anode.

As already observed for diesel fuel-contaminated soils in Chapter 4, these pH changes were expected to influence the system efficiency, since low pH were expected to enhance the Fenton-like reactions, which cause the production of hydroxyl radicals. However, the mineralization process did not seem to be influenced by pH changes, the contaminant removal being evenly distributed both in areas with low and high pH, as shown in Table 5.13 and Figure 5.12.

The differences in soil pH at cathode and anode also influenced metal chemical



equilibrium and they resulted in a different aspect of the sediments near the two electrodes at the end of the trial. As can be seen from Figure 5.16, at the end of test PAH.1, the specimen only showed a brown color near the cathode, due to the contact with the sediments, while the specimen at the anode side showed a yellow-orange color, probably because of the formation of iron hydroxides from the sediment natural iron content and possibly from the iron supply deriving from the anode corrosion.

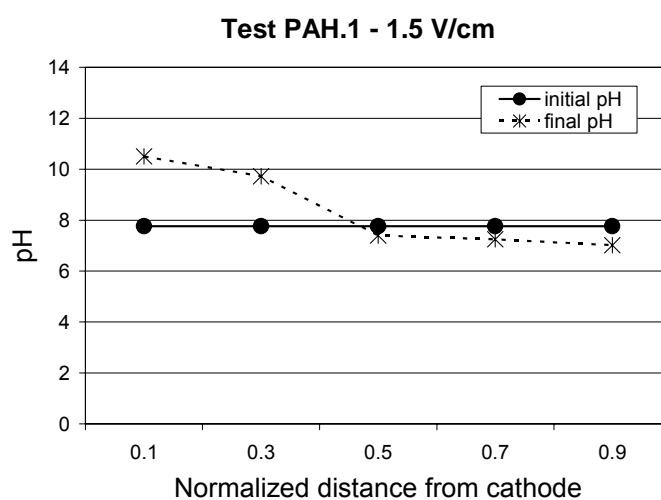


**Figure 5.15 – pH profile across the sediment specimen at the beginning and at the end of test PAH.1.**

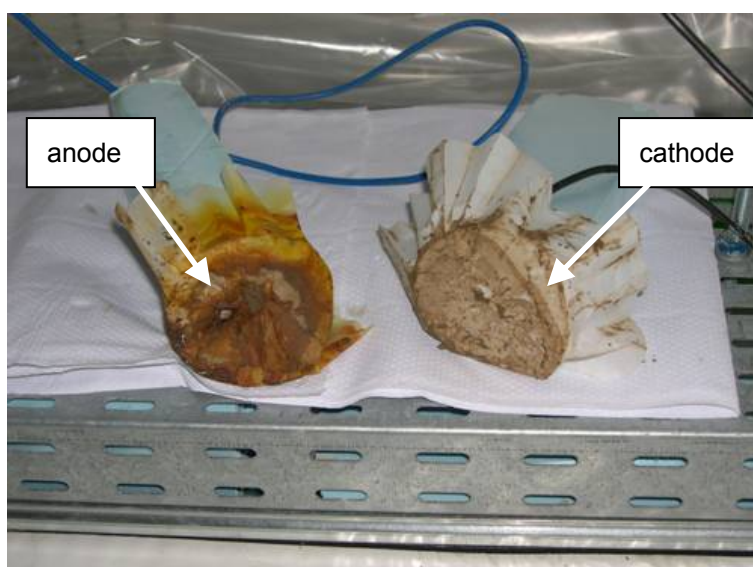


**Figure 5.16 – Electrodes (covered with filter papers) at the end of test PAH.1, lasting for 14 days. The cathode (on the right) showed a brown color due to the contact with the sediments, while the anode (on the left) showed an orange color because of the formation of iron hydroxides from the sediment natural iron content and from the anode corrosion.**

### *5.1.3.5 Electroosmotic flow*

At the end of test PAH.1, 103 mL of pore fluid were found to be accumulated in the

tank at the cathode compartment as a result of the electroosmotic flow. The water collected showed a strongly basic pH (about 9.3), while the TOC content was 525 mg/L. All PAH species were below the detection limit (<0.1 mg/L). Therefore it can be concluded that no significant transport effect occurred as a result of the electroosmotic flow for the target contaminants, which are, indeed, very hydrophobic organic species, with very little water solubilities (Table 5.1). A significant PAH electroosmotic transport was however not expected, since the electroosmotic flow was significant only when the current was sufficiently high (e.g. above 5 mA), i.e. during the first days of the treatments.

#### *5.1.3.6 Contaminant volatilization*

During tests PAH.1, the PAH volatilization was also estimated. The reactor was kept closed while the test was in progress to avoid vapours to diffuse in external air. At the end of the trial, before opening the reactor, the air was sampled onto a ORBO Tube for collecting airborne PAHs. A ORBO-43 (Supelco, Bellefonte, PA) was used for the air sampling and a vacuum pump was used to induce the air flow across the tube (200 mL/min). The ORBO tube was then analyzed by GC to determine the PAH content. The analysis showed that the total PAH content in the tube was less than 0.1 mg, so it can be concluded that no significant contaminant loss due to volatilization occurred during the tests performed.

#### *5.1.3.7 By product formation*

A problem that may arise during the oxidation of PAH contaminated soils is the risk of incomplete mineralization and the consequent production of degradation by-products, which may be of concern because of the high toxicity of certain species. PAHs are known to create a certain number of degradation intermediates, which commonly include aldehydes, ketones, and quinones as main oxidation by-products (oxy-PAHs) (Watts et al., 2002; Brown et al., 2003; Flotron et al., 2005; Lundstedt et al., 2006; Perraudin et al., 2007). Despite the fact that many compounds are known as single PAH derivatives, a complete identification of all PAH by products has not been achieved yet.

Most of PAH derivatives are known to have polar functional groups, which are likely to enhance not only higher aqueous solubility, but also more availability for natural biodegradation than the parental compounds (Brown et al., 2003; Kulik et al., 2006). On the other hand, the fact that in natural soils PAHs are commonly strongly sorbed and incorporated into organic matter is also thought to act as a sort of detoxification process, by reducing the bioavailability and the mass transfer of these contaminants, thus decreasing

their toxic effect towards natural microbial community (Richnow et al., 1995; Sun and Yan, 2007). This effect is absent in desorbed PAH and PAH derivatives, which may therefore be characterized by a stronger toxic effect than the parental compounds. Consequently, a remediation action that resulted in the desorption of PAH molecules without achieving a complete mineralization would even lead to an increase in the toxic effect towards the natural biota, rather than reducing it.

In this study, the identity of the oxidation reaction by-products has not been determined, but the ecotoxicity of the original and final samples has been evaluated in the last experiments (tests PAH.2 and PAH.3), to assess any change in the toxic effect of the sediments toward the local biota. The original untreated sample showed a toxic effect of 0.23 TU50, while the toxic effect in both the treated samples was below the detection limit. These results indicated that the toxic effect of the original sediments was not very high. This was attributed to the fact that PAHs were strongly sorbed onto sediments and did not tend to solubilize in water (Ferrarese et al., 2008). This probably limited their mass transfer and their bioavailability, also preventing them to have a strong toxic effect (Luthy et al., 1994; Taylor and Jones, 2001).

Since the toxic effect became negligible after the tests, the electrochemical treatment did not seem to enhance the sole desorption of the target pollutants, promoting their mineralization in the sorbed form or oxidizing them as soon as they were desorbed. This is in agreement with the findings of Kim et al. (2005) for phenanthrene-contaminated kaolinite.

Moreover, this conclusion was confirmed by the fact that the PAH concentration in the pore fluid collected at cathode compartment during tests PAH.1 was below the detection limit (<0.1 mg/L). This evidence suggests that the electrooxidation could be amenable applied for in situ remediation of soils and sediments, without environmental risks due to uncontrolled pollutant mobilization.

### **5.1.4 Conclusions**

The tests performed allowed to evaluate the feasibility of using electrochemical oxidation for the remediation of PAHs from freshwater sediments, in case of old date contamination.

The target contaminated sediments were collected in a canal in Trento, which for several decades had received industrial wastewater polluted by organic and inorganic compounds, deriving from a coal tar production site. The initial total PAH concentration in sediment samples ranged from about 1090 mg/kg<sub>DW</sub> to 1522 mg/kg<sub>DW</sub> (light PAHs about 731-1366 mg/kg<sub>DW</sub>, heavy PAHs about 139-359 mg/kg<sub>DW</sub>) and a 90% degradation was required to meet the remediation goals. The TOC content was about 88-99 g/kg<sub>DW</sub> and the

sediment pH was about 7.8. The sediments also showed a significant metal content, with a total iron concentration about 30621 mg/kg<sub>DW</sub> and a manganese content about 614 mg/kg<sub>DW</sub>.

Three laboratory tests were performed to assess the effectiveness of electrooxidation in removing the target contaminants. During each trial a sediment sample was tested under a constant voltage gradient (ranging from 1 V/cm to 2 V/cm) for a fixed period of time (up to 28 days).

A total PAH removal of 90% or more was achieved by this method after a four-week treatment, with a light PAH removal about 93% and a heavy PAH removal about 77%. Such removal efficiencies were achieved for specific voltages as low as 1 V/cm. As expected, the removal efficiency for light PAHs was found to be higher than for the heavy PAHs, which are more sorbed compounds and often proved to be more recalcitrant to both biological and chemical degradation than light PAH species. Besides some variability due to sample heterogeneity, the final PAH concentrations were found to be evenly distributed across the treated sample.

The results also indicated that the removal efficiency could be significantly improved by increasing the treatment duration up to a few weeks. Moreover, despite the fact that the removal efficiencies achieved for heavier PAH species were always found to be lower than those attained for light PAHs, longer electrochemical treatments proved also to be able to improve the heavy PAH removal significantly.

The ecotoxic effect of the treated sediment samples was negligible.

In sum, based on the results of this study, electrochemical oxidation showed to be an effective remediation technology, amenable either for the in situ or for the ex situ remediation of the target sediments. The results achieved were very satisfactory, since a good recovery of the sediments of concern proved to be very difficult to be attained, because of their high contaminant concentrations, low permeability, high organic matter and content high sorption capacity.

## 5.2 Silty soils contaminated by organolead compounds

The aim of this research was to assess the effectiveness of electrooxidation for the remediation of a silty soil contaminated by organolead compounds, including tetraethyl lead (TEL), triethyl lead (TREL) and diethyl lead (DEL). The soil samples were collected from different wells at the site of a former tetraalkyllead producing company in Trento. (Italy).

During the study, two laboratory tests were performed on two different soil samples characterized by different contaminant concentrations. In both trials, the samples were tested under a constant specific voltage of 1.5 V/cm for 14 days. The results achieved are presented and discussed as follows.

### 5.2.1 Contaminants

#### 5.2.1.1 Tetraethyl lead and organolead compounds

Tetraethyl lead, also indicated as TEL,  $(\text{CH}_3\text{CH}_2)_4\text{Pb}$  (Figure 5.17), is an organometallic compound which was once commonly used as antiknock agent in gasoline. TEL was first prepared as a pure compound in 1859, but it started to be added to petrol in 1922, to improve the gasoline octane rating. Thanks to its capacity of improve engine performances, by the 1970s, almost all petrol produced around the world contained lead (Landrigan, 2000; Seyferth, 2003a; Seyferth, 2003b; Cook and Gale, 2005). However, soon after the beginning of TEL production, its high toxicity emerged. Several very serious cases of lead poisoning occurred in all operating plants, and a number of workers died in an acute psychosis with hallucinations due to exposure to TEL gas or to contact with TEL oil (Needleman, 1997).

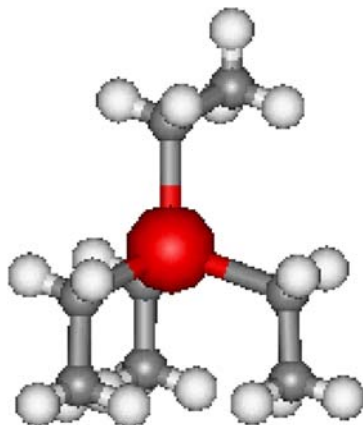


**Figure 5.17 – Molecular structure of tetraethyl lead (Collins et al., 2005).**

Although organic lead compounds are not classifiable as to their carcinogenicity to humans (IARC, 2006), they are known to be highly toxic and to have serious negative effects on human health, in particular badly damaging the nervous system, adversely affecting the mental and neurological development in children and causing hallucinations, psychosis and cardiovascular problems in adults, being toxic even at low levels in blood, as 50 µg/L (Needleman, 1997; Lovei, 1998; Wadge, 1999; Cairney et al., 2002; Landrigan, 2002; Smargiassi et al., 2002; MECA, 2003; Cairney et al., 2004).

Inhalation and ingestion represent the major routes of human exposure to TEL due to the dispersion in the atmosphere and deposition of lead-contaminated particulate (Lovei, 1998; Wadge, 1999; IARC, 2006), while for workers of industrial TEL production plants, the occupational poisoning can occur as a result both of inhalation and of dermal contact, since organolead compounds can be easily absorbed through the skin (Landrigan, 2002; IARC, 2006). The toxicity of TEL is so high that no threshold has been identified under which adverse health effects cannot be detected (Lovei, 1998).

Because of the important adverse effect of the organolead compounds on the environment and on human health, many efforts have been made since the 1970s by most of countries to reduce the organic lead emissions, the most important being the banning of leaded gasoline, with the introduction of the catalytic converter. Thanks to these efforts, most of lead sources have nowadays decreased, and, in spite of the persistence of lead in the environment, this has resulted in a substantial decrease in human exposure, within few years from the banning of leaded gasoline, with a significant decline in blood lead levels (Wadge, 1999; CARB, 2001; Landrigan, 2002; MECA, 2003; IARC, 2006). Unfortunately, in the meanwhile, the widespread use of leaded gasoline had caused the dispersion of lead throughout the environment, causing serious exposure to human communities and to ecosystems (IARC, 2006), while spillages of large quantities of TEL during the production, transportation or blending at oil refineries and petrol stations caused several cases of severe soil and groundwater contamination (Gallert and Winter, 2002).

Under environmental conditions, TEL is a viscous colourless liquid. It is an apolar molecule, highly lipophilic and soluble in petrol and solvents, with very low solubilities in water. When TEL is released into the environment, it undergoes a series of dealkylation reactions (Ouyang et al., 1996; Gallert and Winter, 2002): at first, it is degraded to triethyl lead (TREL,  $(\text{CH}_3\text{CH}_2)_3\text{Pb}^+$ ), which is decomposed to diethyl lead (DEL,  $(\text{CH}_3\text{CH}_2)_2\text{Pb}^{2+}$ ), which can finally be turned, through the very unstable form of monoethyl lead ( $(\text{CH}_3\text{CH}_2)_1\text{Pb}^{3+}$ ), to inorganic lead ( $\text{Pb}^{2+}$ ).

Organolead compounds are more toxic than inorganic lead and their toxicity generally increases with the degree of alkylation, according to the following sequence (Bergmann and Neidhart, 1996; Gallert and Winter, 2002; Unob et al., 2003):



In the atmosphere TEL can be rapidly photocatalytically decomposed by sunlight, by ozone or by hydroxyl radicals to TREL and DEL, which can be further decomposed in the same way, even if they proved to be more stable species (Gallert and Winter, 2002; Unob et al., 2003). In soils, organolead compounds may be persistent over decades, being the natural chemical and biological degradation very limited (Ou et al., 1995; Teeling and Cypionka, 1997).

While TEL is a non-ionic organic molecule, with a low water solubility and a low potential for transport through soils, its degradation products, TREL and DEL, are cations, highly soluble in water, which can be easily be transported in groundwater (Ouyang et al., 1996; Gallert and Winter, 2002). On the whole, the mobility of organolead compounds in the subsurface is dominated both by sorption and by degradation reactions. In fact, while TEL is a typical DNAPL compound, and tends to be immobile and adsorbed onto soil particles, TREL and DEL are quite mobile and tend to form large groundwater plumes. The main features of the target organolead compounds are reported in Table 5.16.

**Table 5.16 – Main chemical and physical data of the organolead compounds considered in this study (Collins et al., 2005).**

Compound		Tetratyl lead	Triethyl lead	Diethyl lead
Abbreviation		TEL	TREL	DEL
Chemical formula		$(\text{CH}_3\text{CH}_2)_4\text{Pb}$	$(\text{CH}_3\text{CH}_2)_3\text{Pb}^+$	$(\text{CH}_3\text{CH}_2)_2\text{Pb}^{2+}$
Molecular weight	[g/mol]	323.4	326.0	297.0
Henry's Law Constant	[-]	30	1.0 E-07	1.0 E-07
$K_{oc}$	[-]	10.58	1.0 E+02	1.0 E+02
$\text{Log}(K_{ow})$	[-]	5.27	-1	-1
Solubility in water	[mg/L]	0.2	2.0 E+04	2.0 E+04
Vapour pressure	[mmHg]	2.25 E-01	1.0 E-08	1.0 E-08
Diffusion coefficient in air	[cm <sup>2</sup> /s]	9.92 E-02	0.0	0.0
Diffusion coefficient in water	[cm <sup>2</sup> /s]	1.56 E-05	1.0 E-05	1.0 E-05

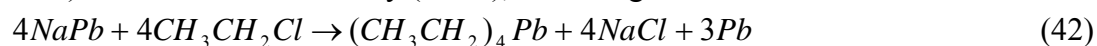
Only a few remediation techniques for soil and groundwater contamination due to organolead compounds have been investigated up to now. Since organic lead species can be extracted from water with the use of organic solvents (Bergmann and Neidhart, 1996), a possible way to remediate environmental media contaminated with TEL is the flushing with solvents and surfactants (Ouyang et al., 1996; Huang et al., 2003). Some studies proved that enhanced bioremediation, with oxygen and nutrient addition, could effectively transform TEL into ionic alkyllead species, but a complete TREL removal is difficult to achieve (Gallert and Winter, 2002; Teeling and Cypionka, 1997). Moreover, water soluble alkyllead compounds showed to be toxic for non-adapted microorganisms (Gallert and Winter, 2002). Also the application of electrokinetic remediation lead to poor results (Alshawabkeh et al., 1998), while the thermal treatment proved to cause serious air pollution problems (Ioannidis and Zouboulis, 2003). Recent studies (Unob et al. 2003) showed organolead compounds to be degraded by hydroxyl radicals  $\cdot\text{OH}$ , but the knowledge about the feasibility of using chemical oxidation for the remediation of organolead compounds is still very limited.

### 5.2.1.2 Contaminated site

The soil samples used in this study were collected from two different wells at the site of a former tetraalkyllead producing company in Trento (Italy), named SLOI srl (Società Lavorazioni Organiche Inorganiche s.r.l.).

The factory, located in the northern suburbs of Trento town (Figure 5.18), started its activities in 1940 and was closed down nearly forty years later, in 1978, after a major accident. At present, the site is abandoned and mainly covered by vegetation. The end product of SLOI s.r.l. was predominantly an antiknock mixture for petrol, called ETILMIX and mainly composed of TEL, dibromoethane and dichloroethane. Apart from these compounds, other chemicals were used in the manufacturing production process, including chlorine, sodium hydroxide, synthetic hydrochloric acid, hydrofluoric acid dimethyl chloride, glycol ethylene, ethylene, lead-sodium alloys, dimethyl bromide, dibromoethane and dichloroethane (Collins et al., 2005).

In this plant, TEL was commercially produced by reacting ethyl chloride ( $\text{CH}_3\text{CH}_2\text{Cl}$ ) with a sodium lead alloy (NaPb), according to the reaction:



In order to extract TEL from the mixture so produced, a process of distillation was employed (Figure 5.19). The by-product was successively recycled into the primary process. Ethyl chloride was produced on site as a result of chlorination of ethyl alcohol using hydrochloric acid from a sodium-chlorine plant (Collins et al., 2005).

The factory occupied an area of about 61000 m<sup>2</sup>, with the portion of the plant



dedicated to the production processes of about 4800 m<sup>2</sup>. The plant included storage areas, offices, staff rooms, laboratories, parking, a railroad yard, and buildings devoted to the production process (Figure 5.20).

According to the local geological service investigations (Collins et al., 2005), the soil profile in this site can be described from the ground level as a thin layer of filling material (about 1 m), a horizon of silty sand (about 5 m), an aquifer characterized by gravel and sand (about 7 m), a layer of clayey and sandy lime with organic matter (about 2 m), another stratum of sands and gravel (about 5 m), and finally some alternations of fine sand and silt (about 15 m) to the total depth of about 35 m below the ground level. In the area the aquifer can be classified as semi-confined. The groundwater table starts at a depth of about 1.5 m and the groundwater flows from north to south with a velocity of about 1 m per day.

During the factory activity, significant amounts of oil and organolead compounds were spilled and drained underground. In the 1990s, after some preliminary investigations, the degree of environmental contamination by organolead compounds was found to be very high, especially in the areas where tetraethyl lead was processed and stored. The high soil contamination also resulted in the contamination of groundwater.

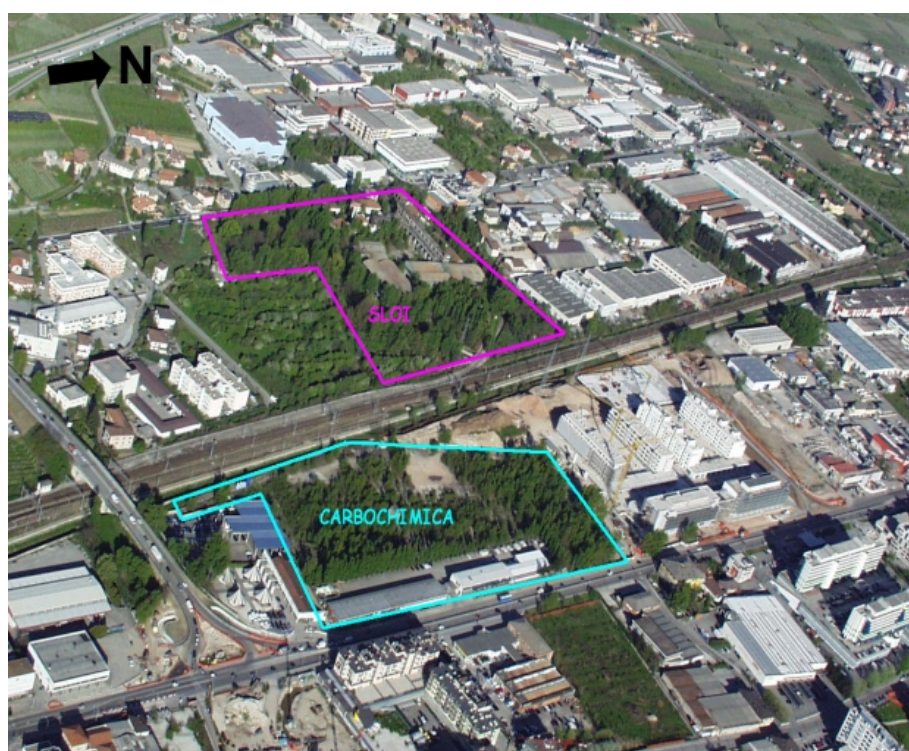


**Figure 5.18 – Overview of the northern suburbs of Trento and locations of the local contaminated sites: the SLOI site (61000 m<sup>2</sup>), contaminated by organolead compounds, and the Carbochimica site (43000 m<sup>2</sup>), contaminated by PAHs.**

Currently, the Italian law does not have a limit for the organolead content in soils and water. For this reason, toxicology studies were carried out by the national and local sanitary services to establish limits to be used as target level in the remediation process for

this contaminated site. As for the contaminant content in groundwater, in 1997 the local sanitary service indicated 0.9  $\mu\text{g/L}$  as the maximum tolerable concentration for total organic lead (TOL, calculated as summation of the TEL, TREL and DEL contributions), while in 2002 the National Sanitary Service stated the limit of 0.1  $\mu\text{g/L}$  for the TEL content. As for the contaminant limits in soils, the local sanitary service indicated a maximum tolerable concentration of 300  $\text{mg/kg}_{\text{DW}}$  for total lead (including both the organic and the inorganic lead compounds) and a limit of 7  $\text{mg/kg}_{\text{DW}}$  for TOL, while the National Sanitary Service indicated a maximum TEL concentration of 0.0068  $\text{mg/kg}_{\text{DW}}$  for industrial-use land and of 0.001  $\text{mg/kg}_{\text{DW}}$  for residential-use land.

The organic lead contamination in the SLOI site involves large soil volumes, with pollutant concentration in the soil that may arrive up to about 1700  $\text{mg/kg}_{\text{DW}}$  for TEL and up to about 2800  $\text{mg/kg}_{\text{DW}}$  for TOL. Being TEL barely mobile in soils, because of its highly hydrophobic nature, the soil pollution mainly involves the most surface layer of filling material and the silty soil up to a depth of 15 m below the ground level.

The soil contamination also resulted in the formation of a groundwater plume having a TEL content up to 2  $\mu\text{g/L}$  and a TOL content up to 130  $\mu\text{g/L}$ , the latter mainly due to the presence of TREL and DEL, which are soluble compounds that tend to migrate with groundwater, thus forming important pollution plumes.

The above-mentioned contaminated site is locally well known for its high pollution levels. However, a present a suitable solution for the recovery of the polluted soils has not yet been identified.

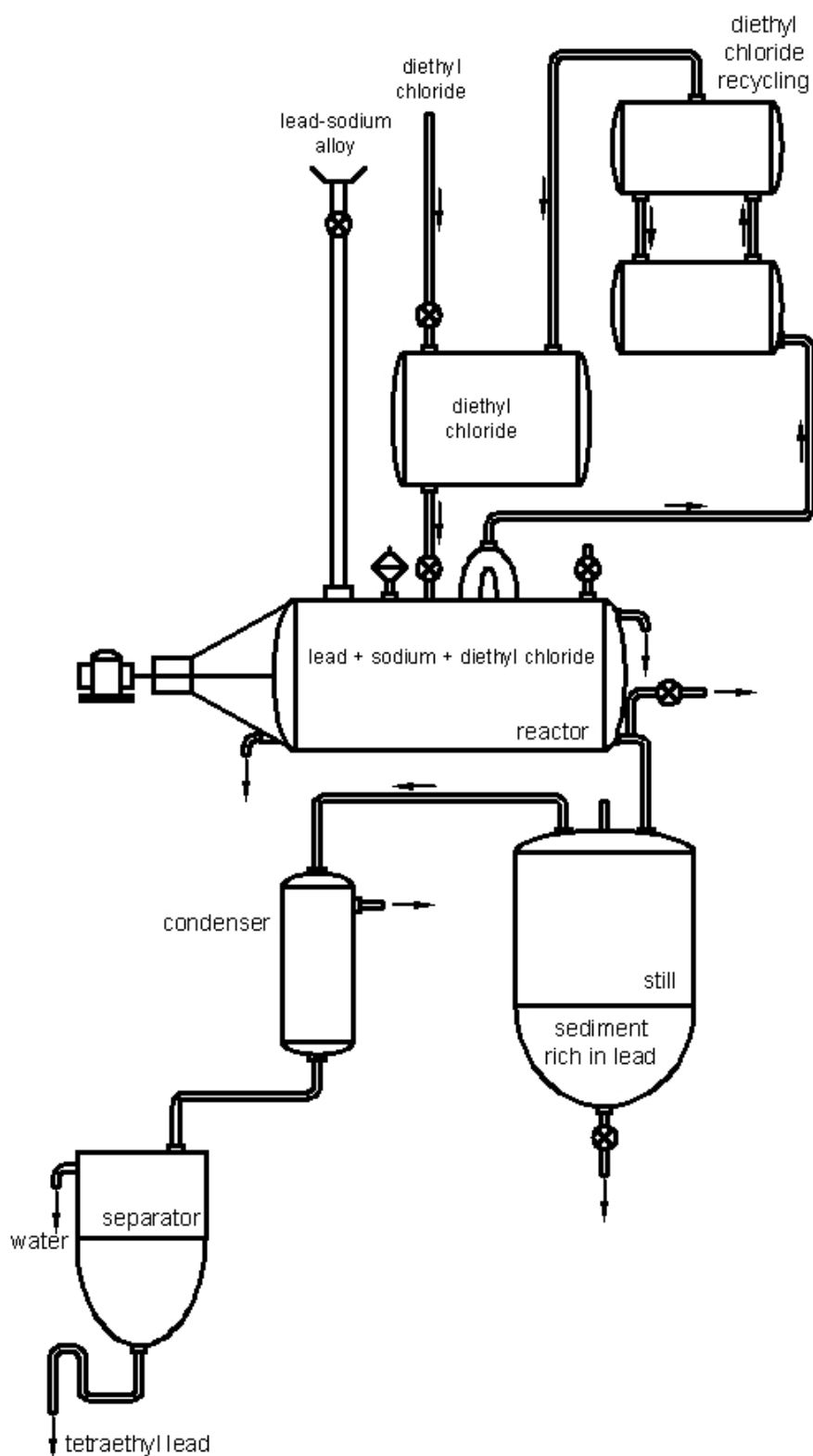


Figure 5.19 – Production process of TEL implemented at the SLOI factory (Collins et al., 2005).

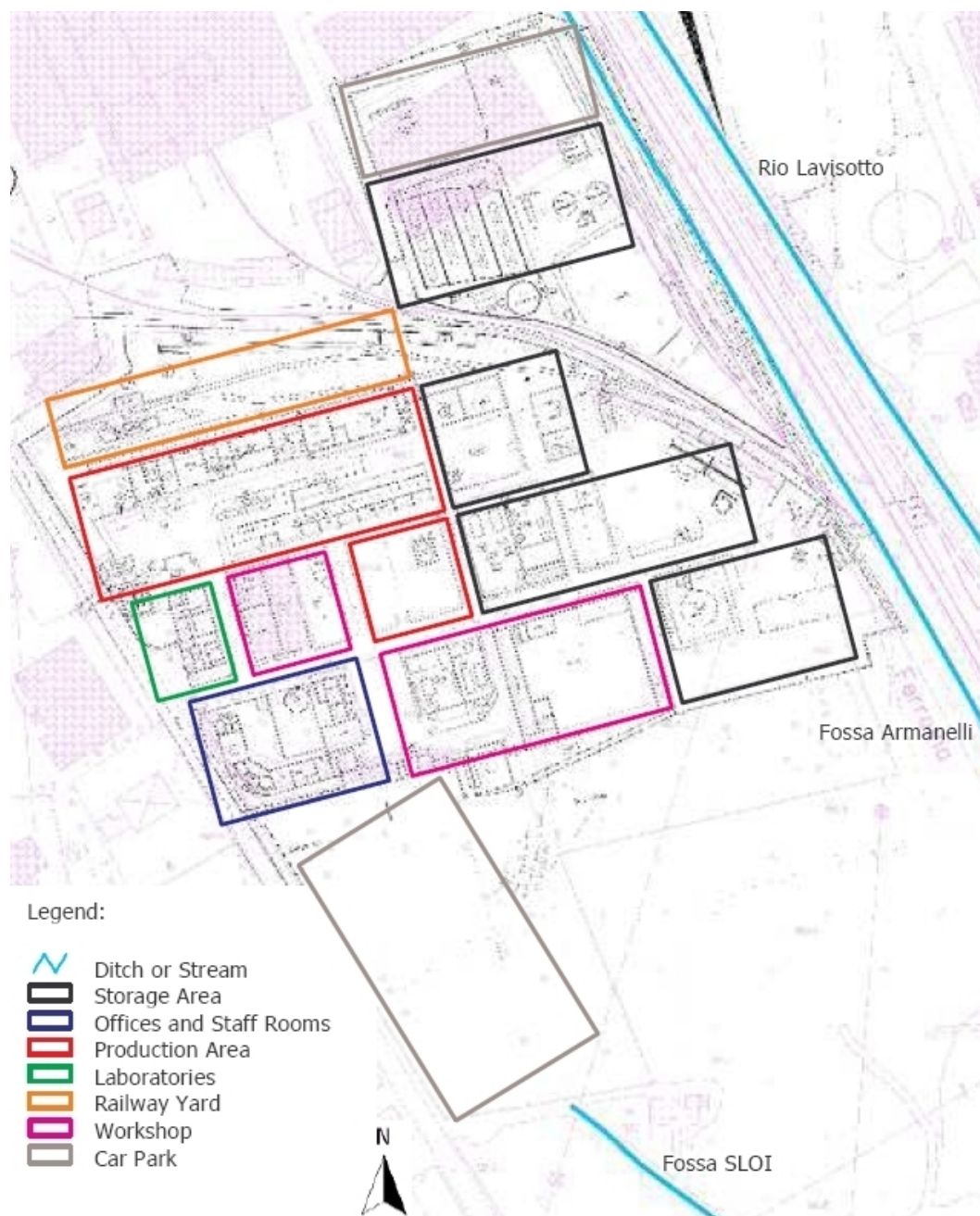


Figure 5.20 – Layout of the SLOI production plant (Collins et al., 2005).

## 5.2.2 Experimental investigation

Two tests, named tests TEL.1 and TEL.2, were performed with Setup 1 using soil samples characterized by different contaminant contents. In both trials, the soil specimens, having a mass about 1 kg, a volume of 0.64 L and a length of 10 cm, were tested under a constant voltage of 15 V (specific voltage 1.5 V/cm) for 14 days.

Since TEL and its degradation by-product are highly photosensitive compounds, during the tests the experimental setups were covered with aluminum foils to avoid their photolytic degradation (Figure 5.21).

The analytical procedures used to determine the contaminant concentrations in the soil samples are reported in Chapter 3.4.



**Figure 5.21 – Experimental setup used for the tests performed on the samples of soil contaminated by organolead compounds.**

### 5.2.3 Results and discussion

The first test (test TEL.1) was performed on a soil sample with a TOL content about 34.7 mg/kg<sub>DW</sub> (TEL 0.1 mg/kg<sub>DW</sub>, TREL 12.9 mg/kg<sub>DW</sub>, DEL 21.7 mg/kg<sub>DW</sub>). The total lead content (including both the organic lead content and the inorganic lead content) was 699.0 mg/kg<sub>DW</sub> and the soil initial pH was about 8.5.

The main features of the soil sample and the results of test TEL.1 are reported in Table 5.18.

**Table 5.17 – Main features of test TEL.1.**

test	TEL.1
sample matrix	silt
contaminants	TEL, TREL, DEL, Pb
sample weight	1 [kg]
sample volume	0.64 [L]
sample density	1.6 [kg/L]
test duration	14 [d]
voltage (constant)	15 [V]
specific voltage (constant)	1.5 [V/cm]
initial current	10 [mA]
final current	1 [mA]
pore fluid collected at cathode compartment	20 [mL]

The initial current flowing was about 10 mA, while at the end of the trial the steady-state current was about 1 mA. Being the current flowing so low, the electroosmotic flow was appreciable only during the first hours of the experimental run.

At the end of the test, a 36% TEL removal was encountered, but the final concentration of TREL did not show a significant decrease. Being TREL a by-product of

TEL degradation, it also tended to accumulate in the treated sample. In fact, as can be seen from Table 5.18, the TREL content in the treated sample was higher than the TREL content in the original sample. This difference is even higher than the TEL removal, which is about 0.04 mg/kg<sub>DW</sub>. This can be considered mainly due to sample heterogeneity, which is a typical feature of soil contamination due to hydrophobic compounds and DNAPLs, like TEL is, or to analytical errors, which may have significantly affected the results, because of the very low concentrations of the organolead compounds in the soil samples used for this test. Taking into account these aspects, the TREL contents in the soil samples before and after the electrochemical treatment can be regarded as equal, and the TREL mineralization can be considered negligible. The DEL content removal was about 23%, stating that, since the TREL was not degraded during the process, DEL did not tend to accumulate in the treated soil sample, as was experienced for other oxidation processes (Andreottola et al., 2008). Overall, the TOL removal was very limited, about 10%.

**Table 5.18 – Results of test TEL.1: contaminant concentrations in the soil samples and removal efficiencies.**

Sample	TEL	TREL	DEL	TOL	Total Pb	pH
Original Untreated Sample [mg/kg <sub>DW</sub> ]	0.11	12.9	21.7	34.7	699	8.5
Final Treated Sample [mg/kg <sub>DW</sub> ]	0.07	14.6	16.6	31.2	690	8.2
Removal [%]	36%	-	23%	10%	1%	-

During this test, the occurrence of the electroosmotic flow caused about 20 mL of pore water to accumulate at the cathode compartment. The catholyte solution showed a TOC content about 385 mg/L and a total lead content about 137.34 mg/L, with a TEL concentration of 1.46 µg/L. Therefore, about the 0.026% of the TEL and the 7.9% of the TOL content in the original soil samples were transported by electrokinetic effects to the cathode compartment.

The soil pH slightly increased near the cathode and decreased near the anode (Figure 5.22); the variations of the soil pH were however very limited, as the soil showed a significant buffer capacity.

Table 5.19, Figure 5.23 and Figure 5.24 indicate the contaminant distribution along the specimen at the end of the electrochemical treatment. It must be pointed out that the content of the organolead compounds derived from the TEL contamination, which is commonly characterized by a heterogeneous distribution, being TEL a hydrophobic DNAPL compound. Therefore, the mean of the contaminant concentrations in the different soil sections (reported in Table 5.19) may be significantly different from the average pollutant content in the soil specimen (indicated in Table 5.18), as the soil heterogeneity can result in important differences in the pollutant concentrations within the soil matrix.

Although the TEL content in the different sections of the soil specimen did not show

a definite trend, the average concentration in the sections near the cathode was overall higher than the average concentration in the sections close to the anode. The same effect was achieved in test TEL.2, and it is discussed as follows.

TREL and DEL, which are cationic compounds, showed the highest concentrations at the cathode side (Figure 5.23b and Figure 5.23c). This suggests that a certain electromigration effect could have affected these two compounds. As a consequence, also TOL (Figure 5.23d) showed the same behavior, being mainly determined by the TREL and DEL contents.

The total lead content in the soil samples slightly decreased during the treatment, varying from 699.0 mg/kg<sub>DW</sub> at the beginning of the test to 690.0 mg/kg<sub>DW</sub> at the end of the treatment. As a result, a few milligrams of lead were found in the water accumulated at the cathode compartment. The total lead content in the soil samples at the end of the test (Figure 5.24) can be considered slightly increasing towards the anode and decreasing towards the cathode, besides some variations due to soil natural heterogeneity. The same result was found for test TEL.2 and it is discussed as follows.

**Table 5.19 – Results of test TEL.1: contaminant and pH distribution along the soil specimen at the end of the experiment.**

Normalized distance from cathode	TEL [mg/kg <sub>DW</sub> ]	TREL [mg/kg <sub>DW</sub> ]	DEL [mg/kg <sub>DW</sub> ]	TOL [mg/kg <sub>DW</sub> ]	Total Pb [mg/kg <sub>DW</sub> ]	pH [-]
0.1	0.23	24.1	33.3	57.6	650.7	8.7
0.3	0.37	19.2	30.2	49.8	702.3	8.8
0.5	0.09	24.1	16.2	40.4	654.4	8.3
0.7	0.26	20.1	31.7	52.0	754.6	8.5
0.9	0.04	9.0	21.1	30.1	764.7	8.4

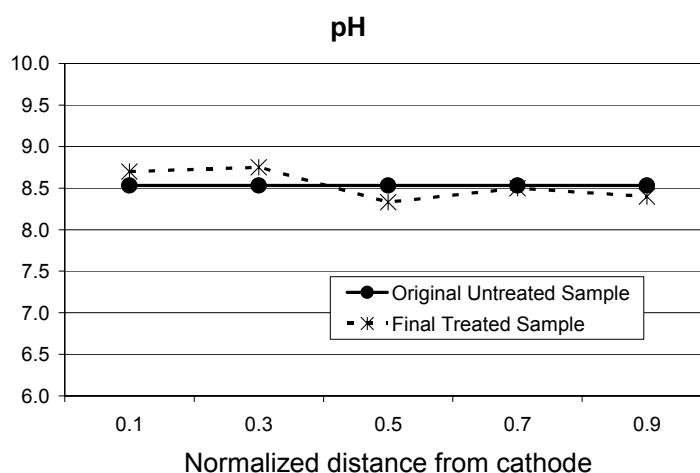


**Figure 5.22 – Results of test TEL.1: pH profile along the soil specimen at the beginning and at the end of the electrochemical treatment.**

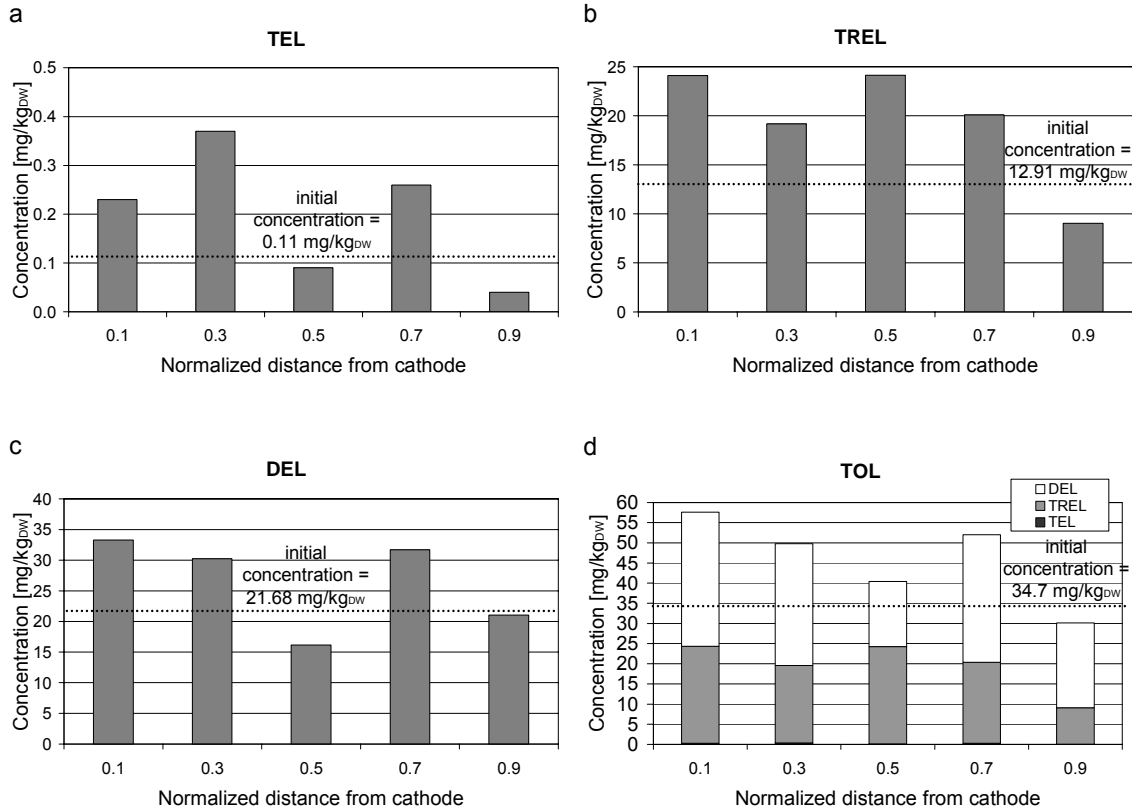


Figure 5.23 – Results of test TEL.1: distribution of TEL (a), TREL (b), DEL (c), TOL (d) along the soil specimen at the end of the electrochemical treatment.

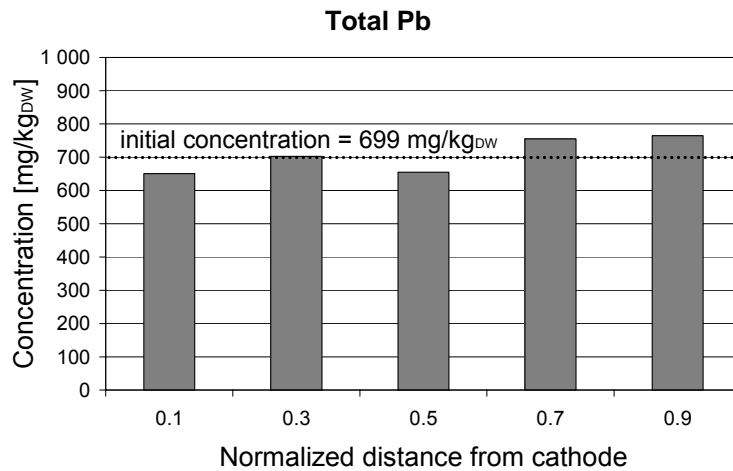


Figure 5.24 – Results of test TEL.1: distribution of total lead along the soil specimen at the end of the electrochemical treatment.

The second test (TEL.2) was performed on a soil sample characterized by a higher contaminant content (TOL about 771 mg/kg<sub>DW</sub>, TEL 213 mg/kg<sub>DW</sub>, TREL 298 mg/kg<sub>DW</sub>, DEL 260 mg/kg<sub>DW</sub>, total lead 56222 mg/kg<sub>DW</sub>) than that used in the previous experiment. During this trial, the TOC removal was also evaluated, the soil showing an initial TOC content about 41.7 g/kg<sub>DW</sub>.



Like in test TEL.1, also during this trial a constant voltage of 15 V was applied to a 10 cm long soil specimen for 14 days. The main features of this test are listed in Table 5.20 and the results are reported in Table 5.21 and in Table 5.22.

The measured currents were higher than in the previous test (the flowing current being about 70 mA at the beginning of the treatment and 14 mA at the end), probably because of a different mineralogical composition of the soil sample used in this test. The electroosmotic flow resulted in the accumulation of about 40 mL of water at the cathode compartment at the end of the trial.

**Table 5.20 – Main features of test TEL.2.**

test	TEL.2	
sample matrix	silt	
contaminants	TEL, TREL, DEL, Pb	
sample weight	1	[kg]
sample volume	0.64	[L]
sample density	1.6	[kg/L]
test duration	14	[d]
voltage (constant)	15	[V]
specific voltage (constant)	1.5	[V/cm]
initial current	70	[mA]
final current	14	[mA]
pore fluid collected at cathode compartment	40	[mL]

During the test, a TOC removal of about 14% was recorded (Table 5.21), thus indicating that a certain mineralization of the organic matter occurred during the electrochemical treatment. A significant TEL removal was also encountered: in this case, the TEL degradation (83%) was even much higher than in the previous tests, probably because of the higher contaminant content in the soil sample resulted in a higher availability of the target pollutants, and enhanced the degradation reactions. As in the previous case, the process was unable to oxidize TREL, which tended to accumulate in the treated sample because of TEL oxidation. Once more, neither significant removals nor accumulations were encountered for DEL. In sum, the TOL removal was about 21%, i.e. it was higher than the removal efficiency measured during test TEL.1 (10%), which were probably affected by the low contaminant concentrations in the original soil samples.

**Table 5.21 – Results of test TEL.2: contaminant concentrations in the soil samples and removal efficiencies.**

Sample	TOC [g/kg <sub>DW</sub> ]	TEL [mg/kg <sub>DW</sub> ]	TREL [mg/kg <sub>DW</sub> ]	DEL [mg/kg <sub>DW</sub> ]	TOL [mg/kg <sub>DW</sub> ]	Total Pb [mg/kg <sub>DW</sub> ]	pH [-]
Original Untreated Sample	41.7	213.0	298.3	260.1	771.4	76222	7.9
Final Treated Sample	35.9	36.4	320.4	254.1	610.9	75685	8.7
Removal	14%	83%	-	2%	21%	1%	-

As expected, during the electrochemical process the soil pH tended to increase at the cathode and decrease at the anode. Like in test TEL.1, the sweeping of the alkaline front was predominant than the acidification effect, therefore the process resulted in the basification of most of the soil specimen (Figure 5.25).

Table 5.22, Figure 5.26, Figure 5.27 and Figure 5.28 indicate the contaminant distribution along the specimen length at the end of test TEL.2.

**Table 5.22 – Results of test TEL.2: contaminant and pH distribution along the soil specimen at the end of the experiment.**

Normalized distance from cathode	TOC [g/kg <sub>DW</sub> ]	TEL [mg/kg <sub>DW</sub> ]	TREL [mg/kg <sub>DW</sub> ]	DEL [mg/kg <sub>DW</sub> ]	TOL [mg/kg <sub>DW</sub> ]	Total Pb [mg/kg <sub>DW</sub> ]	pH [-]
0.1	39.9	123.2	605.5	272.0	1000.7	57907	10.7
0.3	37.6	44.2	360.3	175.1	579.6	63285	9.7
0.5	37.1	4.7	184.9	153.2	342.8	82082	8.4
0.7	40.5	42.4	406.3	194.7	643.4	78857	8.1
0.9	31.7	0.8	294.6	103.0	398.4	92931	7.6

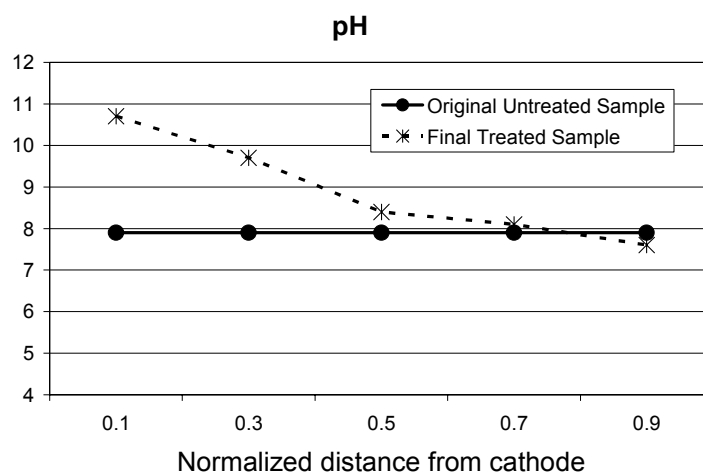


**Figure 5.25 – Results of test TEL.2: pH profile along the soil specimen at the beginning and at the end of the electrochemical treatment.**

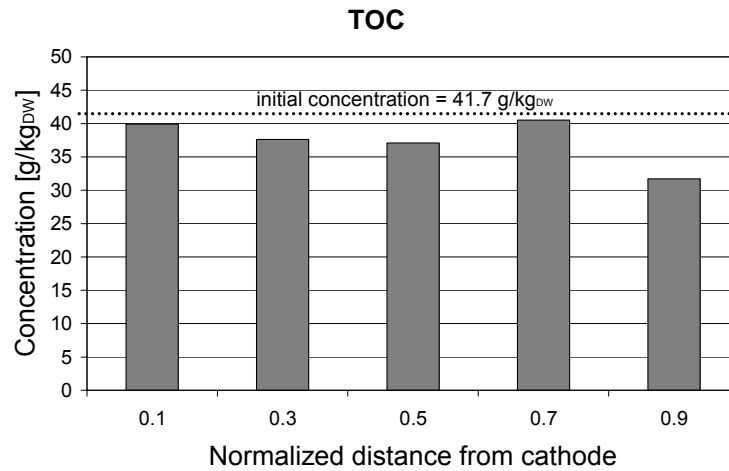


Figure 5.26 – Results of test TEL.2: TOC distribution along the soil specimen at the end of the electrochemical treatment.

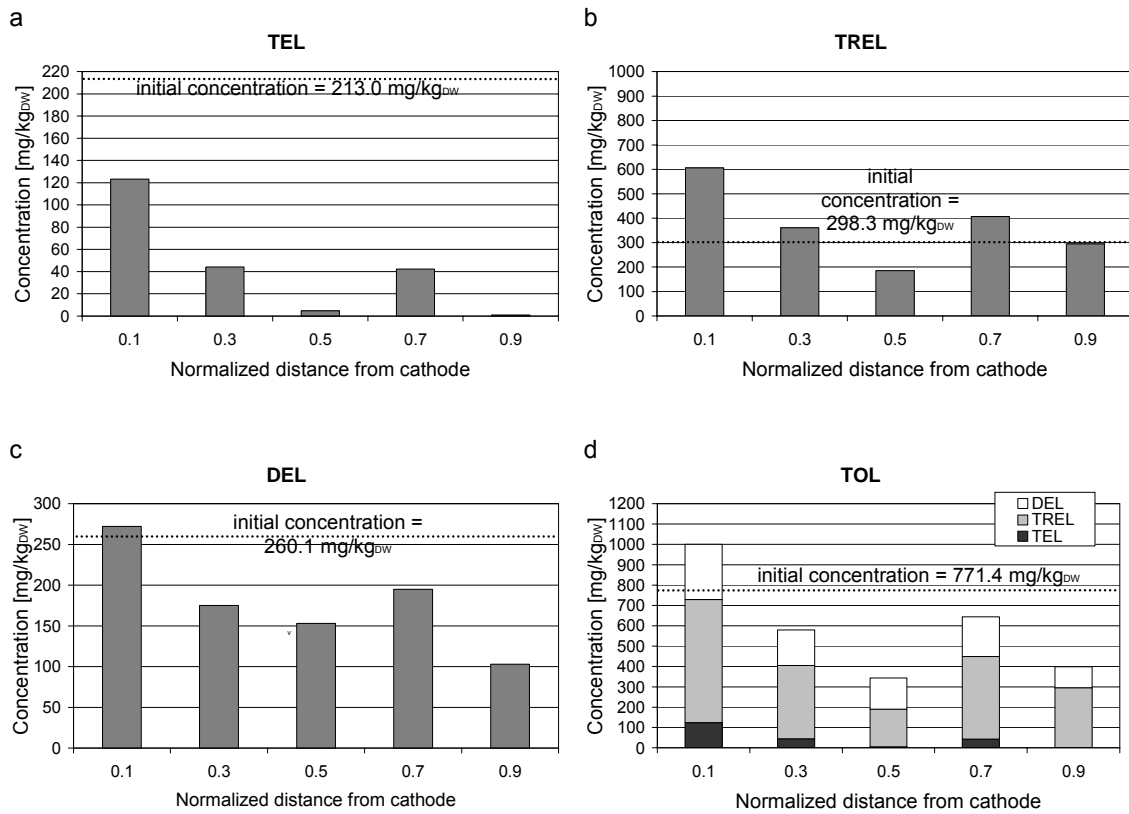
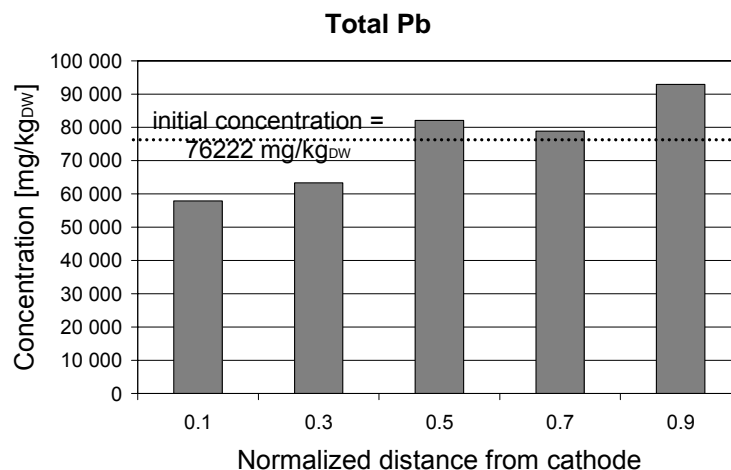


Figure 5.27 – Results of test TEL.2: distribution of TEL (a), TREL (b), DEL (c), TOL (d) along the soil specimen at the end of the electrochemical treatment.



**Figure 5.28 – Results of test TEL.2: distribution of total lead along the soil specimen at the end of the electrochemical treatment.**

The final TOC content (Figure 5.26) can be considered evenly distributed along the soil sample. Figure 5.26 also clearly indicates that the mineralization process occurred within all the soil volume, although it barely affected the target pollutants.

As for the organolead compounds, apart from some variability due to natural sample heterogeneity, the final concentrations of TEL, TREL and DEL seemed to be higher at the cathode side and lower at the anode side (Figure 5.27). As for TEL, which encountered an overall significant removal from the initial content, the final concentrations were found to be lower than the initial values in all the specimen sections. As for TREL and DEL, which experienced a limited or negligible removal, the final concentrations in the sections near the cathode were higher than the initial values. Consequently, also the TOL profile in the soil specimen showed the same behavior as TREL and DEL. It must be observed that these trends were more evident in this test than in the previous experiment because the lower initial pollutant concentrations in the soil sample used for test TEL.1 may have impaired the results.

The results achieved suggest that the electromigration and the electroosmotic transport could have significantly affected the addresses contaminants under the tested conditions. TREL and DEL, which are ions, were probably transported by the electromigration effect.

Being TEL an apolar molecule and a hydrophobic compound, its tendency towards electromigration was expected to be very low. Therefore, its transport is assumed to be mainly due to the electroosmotic advection of the soil particles and the organic matter onto which TEL is sorbed. This effect is also regarded as the main transport phenomenon that causes TEL to migrate in groundwater plumes (Collins et al., 2005).

A previous study (Alshawabkeh et al., 1998), which aimed at investigating the electroosmotic transport of tetraethyl lead and other organolead compounds, had already

indicated that the electrokinetic removal of these compounds was very difficult to achieve. However, since that research only investigated the organolead compound removal in terms of total lead concentration, the results cannot be directly compared with those achieved here, as in the present study the total lead concentrations were only moderately affected by the content of the organolead compounds.

In sum, a certain migration of the organolead compounds toward the cathode was encountered here. However, this effect was too weak for the electrokinetic treatment to be considered effective as sole remediation technique for the removal of these pollutants under the tested conditions.

As expected, the overall total lead content in the soil samples did not vary significantly during the treatment (Table 5.21), with a measured initial concentration of 76222 mg/kg<sub>DW</sub> and a final concentration of 75685 mg/kg<sub>DW</sub>. However, unlike the alkyllead compounds, and as already observed in test TEL.1, the final total lead content in the soil samples proved to be decreasing towards the cathode and increasing towards the anode (Figure 5.28).

During the electrochemical process metals can be mobilized and transported towards the electrode opposite in charge, where they can eventually be removed from the soil and transferred in the water accumulated at the electrode compartment. Most of studies reported the electromigration of metals towards the cathode (Acar et al., 1995; Li et al., 1996; Alshawabkeh, 2001), but the metal migration towards the anode has been reported as well (Acar et al., 1995; Suèr et al., 2003; De Gioannis et al., 2007c). Lead in particular was reported to form both cationic complexes, which tend to migrate toward the cathode, and anionic compounds, which tend to be transported towards the anode (Acar et al., 1995; Suèr et al., 2003). The anionic lead compounds may include lead sulfate or metal hydroxides, as  $\text{Me}(\text{OH})_3^-$  and  $\text{Me}(\text{OH})_4^{2-}$  (Suèr et al., 2003; De Gioannis et al., 2007c), whose formation may be enhanced under alkaline condition, as those existing in the treated soil (the final pH ranging from 7.6 to 10.7). The final distribution of the organolead compound concentrations had a negligible influence on the total lead distribution, being TOL only about the 1% of the total lead concentration.

The overall total lead removal attained during the process was negligible, as confirmed by the low lead concentrations that were found in the pore water accumulated at cathode compartment at the end of test TEL.1. A significant removal of inorganic lead was however not expected, since the metal mobility under basic or neutral conditions is commonly very limited (Acar et al., 1995; Li et al., 1996; Alshawabkeh et al., 1998; Lynch et al., 2007; Mishchuk et al., 2007). Therefore, an important metal transport under the investigated conditions was very difficult to achieve. Moreover, lead compounds have been reported to be strongly attached to the soil during the electrokinetic treatments (Suèr et al., 2003), hence the transport of lead across the soil being very limited unless a strong acid

flushing is performed (Yang and Lin, 1998).

## 5.2.4 Conclusions

This experimental investigation aimed at assessing the effectiveness of electrochemical oxidation for the remediation of a silty soil contaminated by organolead compounds, including TEL, TREL and DEL. The soil samples were collected from two different wells at the site of a former tetraalkyllead producing company in Trento (Italy).

Two laboratory tests were performed for this purpose. In both trials the soil samples were tested under a constant specific voltage of 1.5 V/cm for 14 days.

The first test was performed on a soil sample with a TOL content about 34.7 mg/kg<sub>DW</sub> (TEL 0.11 mg/kg<sub>DW</sub>, TREL 12.9 mg/kg<sub>DW</sub>, DEL 21.7 mg/kg<sub>DW</sub>, total lead 699 mg/kg<sub>DW</sub>). At the end of the test, a 36% TEL removal was encountered, but the final concentration of TREL and DEL did not show a significant decrease. Being TREL a by-product of TEL degradation, it also tended to accumulate in the treated sample. Overall, the TOL removal was very limited, about 10%, while the TOC removal was about 14%.

The second test was performed on a soil sample characterized by a higher contaminant content (TOL about 771.4 mg/kg<sub>DW</sub>, TEL 213.0 mg/kg<sub>DW</sub>, TREL 298.3 mg/kg<sub>DW</sub>, DEL 260.1 mg/kg<sub>DW</sub>, total lead 76222 mg/kg<sub>DW</sub>). As in the previous case, a significant TEL removal was encountered (83%), but the process was unable to oxidize DEL and TREL, which accumulated in the treated soil because of TEL oxidation. TOL removal was about 21%.

The following conclusions can be drawn from all the results achieved:

- A certain TEL oxidation can be attained with the electrochemical methods, but the system seems unable to attack the ionic alkyllead compounds (i.e. TREL and DEL), which proved to be more stable compounds and more recalcitrant to degradation than TEL. Thus, the process is likely to fail in achieving a significant reduction of the TOL content. The TEL partial degradation may also result in an increase in the TREL content in the treated soil samples.
- The TOC removal achieved during the treatments can be considered evenly distributed along the tested specimen, thus indicating that the oxidation process occurred almost homogeneously in the treated soil volume.
- Differently, the final concentrations of organolead compounds were found to be varying along the soil specimen, with higher contaminant contents at the cathode side and lower contaminant contents at the anode side. Therefore, the electrokinetic process seems to have affected the ionic alkyllead compounds (TREL and DEL), which are soluble compounds and which seem

to be easily transported along the treated soil towards the cathode, due to electromigration process and to the electroosmotic transport. Despite the fact that TEL is an apolar pollutant with limited water solubility, also this compound seemed to migrate towards the cathode. This was probably due to the advective transport of the soil and organic matter particles onto which TEL is sorbed, due to the occurrence of the electroosmotic flow towards the cathode.

- The total lead content, which included both the contributions of the organic lead compounds and of inorganic lead compounds (the latter being the major part of the total lead content), proved to be mainly transported towards the anode, probably because of the formation of negatively charged lead compounds, as lead sulphides and lead hydroxides. The migration of such compounds was probably limited by the basic conditions of the treated soil, which usually promote the metal precipitation and constrain the electromigration process.

On the whole, the electrochemical process resulted in a certain oxidation of TEL, but it seemed unable to achieve a complete removal of the organolead pollutants from the soil. The process could be however be used in combination with other remediation processes, to achieve the removal of the most refractory compounds. For example, it could be used to enhance the transformation of TEL, which is an immobile pollutant into TREL and DEL, which are soluble compounds and may be treated by an hydraulic barrier or via pump and treat. Further investigations are needed to assess the effectiveness of such treatment sequences.

## 5.3 Clay contaminated by landfill leachate

The objective of this research was to evaluate the effectiveness of electrooxidation for the removal of organic pollutants and ammonia from a clay contaminated by municipal landfill leachate. If effective, electrooxidation could be of interest either for the recovery of old landfills, in case of a failure of the liner systems, or as a new engineering solution for new landfills.

Several tests were performed during this study. In each experimental trial, a contaminated clay specimen was tested under a constant voltage gradient (ranging from 1 V/cm to 6 V/cm) for a fixed period of time (24-168 h).

### 5.3.1 Contaminants

Landfill leachate poses one of the most important environmental problems of landfill waste disposal. Leachate is produced as a result of water percolating through the landfill waste body and reacting with the products of waste degradation. If the leachate leaks out of the landfill because of improper plant design or of bad landfill management, it can enter into the groundwater and cause severe environmental and health risks.

Leachates from different landfill plants can have different compositions, depending on waste type, landfill conditions (as age, temperature, moisture, pH) and volume of the water entering the landfill. However, leachates are usually a mixture of organic and inorganic contaminants, including humic acids, ammonia nitrogen, heavy metals, microbes and inorganic salts (Lo, 1996; Oman and Rosqvist, 1999 ; Christensen et al., 2001; El-Fadela et al., 2002; Kurniawan et al., 2006).

The environmental risks from landfill leachate are mainly due to high organic contaminant and ammonia nitrogen content (Kurniawan et al., 2006). Because of its high contaminant content, leachate needs to be collected at the base of the landfill and treated in order to allow its safe disposal into the environment.

Existing leachate treatment technologies include biological, chemical and physical methods, or combinations of these techniques. Among the biological treatments, biological nitrification-denitrification is the most common method used to remove nitrogen. In addition, various chemical and physical methods, such as air stripping, coagulation, flocculation, precipitation, filtration, reverse osmosis, active carbon adsorption and advanced oxidation processes, have been used as pre-treatments or as post-treatments, to remove toxic substances or to enhance contaminant removal (Kurniawan et al., 2006;



Wiszniowski et al., 2006; Santamaria and Vagliasindi, 2007; Tizaoui et al., 2007). Leachate is commonly treated in municipal wastewater treatment plants, but, alternatively, it can also be treated in wetlands (Morris et al., 2007; Persson et al., 2007).

Recently, electrochemical processes were also tested for leachate treatment, proving to be effective in reducing organic contaminants, with degradation rates depending on the current intensities (Moraes and Bertazzoli, 2005; Zhabg et al., 2006; Kurniawan T.A., 2006; Cabeza et al., 2007; Deng and Englehardt, 2007). A complete ammonia degradation was also observed during electrochemical treatment, indirect oxidation being regarded as the major degradation process (Cabeza et al., 2007; Deng and Englehardt, 2007).

## **5.3.2 Experimental investigation**

### *5.3.2.1 Research objectives*

This research was carried out to evaluate the effectiveness of electrooxidation for the removal of organic substances and ammonia nitrogen from clayey soils that have been contaminated by municipal landfill leachate. Electrooxidation was expected to be used to remove organic contaminants from clay in the bottom layer of a landfill, when it is contaminated by the leachate.

Possible applications of this technology can include both the remediation of the clay barrier in old landfills, and the introduction of an innovative engineering solution for new landfills. In this latter case, new landfills could be engineered with two parallel conductive nets inside the bottom clay barrier, acting as plate electrodes (Figure 5.29). By creating an electric field between the two electrodes, the clay barrier is expected to be cleaned from the eventual pollution.

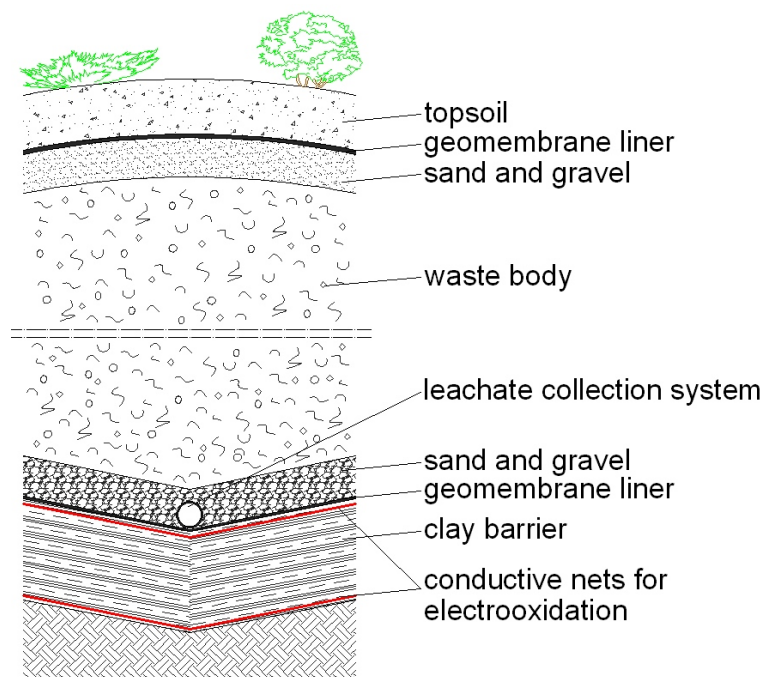


**Figure 5.29 – Possible application of electrooxidation as an innovative engineering solution for landfill bottom barrier.**

### 5.3.2.2 Materials

In order to conduct this investigation, leachate samples were collected from the municipal landfill of Trento (Italy). An old basin, which can be considered stabilized and in the methanogenic phase, was used for the sample collection. In order to complete the experimentation, several samplings were conducted. During each sampling, about 2 L of leachate were collected and immediately used for the tests, to avoid the degradation of ammonia and organic pollutants before the trials.

A clayey soil (main features are presented in

Table 5.23) was collected from a cave near Trento, which also provided the clay for the bottom and lateral barrier of the above-mentioned landfill.

During the experiments, the clay was mixed with the landfill leachate to emulate the pollution of the clay at the bottom barrier of a landfill, deriving by a leakage in the geomembrane liner. For each experiment, 1.1 kg of clay were spiked with 110 mL of leachate. The soil was then carefully mixed to ensure a homogeneous distribution of the pollutants in the sample. Of the resulting soil sample, 100 g were analyzed to assess the initial contaminant concentration, while the remaining soil mass (1 kg) was used for the run.

**Table 5.23 – Characteristics of the clay used in the experiments on leachate-contaminated soils.**

<b>Parameter</b>	<b>Value</b>	
TOC	2.77	[g/kg <sub>DW</sub> ]
Total Nitrogen	96.9	[mg/kg <sub>DW</sub> ]
TKN	95.3	[mg/kg <sub>DW</sub> ]
N-NH <sub>4</sub> <sup>+</sup>	<0.1	[mg/kg <sub>DW</sub> ]
N-NO <sub>3</sub> <sup>-</sup>	1.6	[mg/kg <sub>DW</sub> ]
N-NO <sub>2</sub> <sup>-</sup>	<0.01	[mg/kg <sub>DW</sub> ]
Cation Exchange Capacity	6.5	[meq/100g]
Fe	36350	[mg/kg <sub>DW</sub> ]
Mn	522	[mg/kg <sub>DW</sub> ]
pH	9.1	[-]

### 5.3.2.3 Experimental setup and procedures

To perform this investigation, several tests were performed with a one-dimensional experimental setup for bench scale testing, similar to Setup 2. The setup consisted in an HDPE reactor, including a rectangular reaction cell, a pair of plate electrodes, and a stabilized DC generator. The reaction cell had a volume about 0.53 L, with a length 10 cm, a width 9 cm and a height 7 cm. The electrodes used were rectangular plates (7 cm x 9 cm) made up of stainless steel.

During each experimental run, a leachate contaminated clay specimen, having a mass of about 1 kg and a length of 10 cm, was inserted in the setup and an electric current was generated by applying various constant voltages across the electrodes. Testing was continued for a fixed period of time, after which the soil specimen was removed from the test setup and analyzed. The investigated parameters included soil pH, humidity, TOC (representing the total organic matter in the soil), total nitrogen, ammonia, total Kjehldahl nitrogen (TKN), organic nitrogen, nitrates and nitrites.

All the tests performed are summarized in Table 5.24.

Four tests lasting for one day (24 h) were performed (named as tests LEA.1, LEA.2, LEA.3 and LEA.4). The applied voltages were 10 V, 20 V, 30 V and 60 V, corresponding to specific voltage gradients of 1, 2, 3, 6 V/cm respectively. A further test (test LEA.5), lasting for one week, was performed to assess the trend of contaminant removal with treatment duration. During this last test, a 10 cm long soil specimen was tested under a constant voltage of 30 V (specific voltage of 3 V/cm). This voltage was chosen because it resulted in a good contaminant removal performance during the previous tests performed.

During test LEA.5, samples were collected and analyzed at regular time intervals (i.e. 1, 2, 4 and 7 days after the beginning of the experiment). Moreover, at the end of this

trial, a part of the soil specimen was also sliced into 5 segments, and each segment was analyzed for pH and contaminant concentrations, in order to assess the extent of electrochemical reactions at different distances from the electrodes.

The analytical methods used to determine the contaminant concentrations in the soil samples are described in Chapter 3.4.

**Table 5.24 – List of the tests performed on the leachate-contaminated clay. Each test was performed on a soil specimen having length of 10 cm and a mass about 1 kg.**

Test	Duration [h]	Duration [d]	Applied voltage [V]	Specific voltage [V/cm]
LEA.1	24	1	10	1
LEA.2	24	1	20	2
LEA.3	24	1	30	3
LEA.4	24	1	60	6
LEA.5	168	7	30	3

### 5.3.3 Results and discussion

The clay samples used for the tests, spiked with leachate, showed initial TOC concentrations varying from 6.6 g/kg<sub>DW</sub> to 7.2 g/kg<sub>DW</sub>, while the total nitrogen content ranged from 165.4 mg/kg<sub>DW</sub> to 259.5 mg/kg<sub>DW</sub>, and the ammonia concentration ranged from 32.2 mg/kg<sub>DW</sub> to 90.4 mg/kg<sub>DW</sub>. It must be noticed that a significant part of the TOC and total nitrogen content was due to the soil contribution, because of the natural carbon and nitrogen content of the clay (see

Table 5.23). On the opposite, the ammonia content was entirely given by the leachate. Moreover, the soil used was characterized by a quite high iron content (about 36350 mg/kg<sub>DW</sub>). This was thought to be able to enhance the electrooxidation process, since the iron ions can act as microconductors and enhance the electrooxidation process, as well as catalyze the decomposition of the hydrogen peroxide, which is created by the electrochemical process, into hydroxyl radicals (Fenton's reaction), which can oxidize organic pollutants. Also other transition metals contained in the soil, as manganese, can play the same role as iron and catalyze Fenton-like reactions, as already discussed in Chapter 4.

The results of the one-day tests are reported in Table 5.25, Figure 5.30, Figure 5.31 and Figure 5.32. As can be seen from the data shown, despite some variability in contaminant content, mainly ascribed to the sample heterogeneity, these tests resulted in a significant decrease in contaminant concentration, both for total nitrogen (removals about 15-33%), for ammonia (7-58%) and TOC (26-62%).

Major conclusions can be drawn from the result achieved. Ammonia nitrogen removal showed to improve as the voltage increased from 1 V/cm to 2 V/cm (test LEA.1 and LEA.2), but remained almost constant and independent from the voltage applied afterwards (tests LEA.3 and LEA.4). The same results were evident for total nitrogen and organic nitrogen. As for nitrates and nitrites, nitrates showed to be decreased during the runs (e.g. tests LEA.2 and LEA.3); therefore, the  $\text{NO}_3^-$  reduction to nitrogen gas seemed to occur. However, the denitrification mechanism seems complicated, and the fate of the all forms of nitrogen still needs to be investigated.

In sum, as far as the overall nitrogen removal is concerned, there was certain total nitrogen removal. In particular, the ammonia nitrogen removal, which is of major concern, was assumed to be significantly attained by the electrochemical method proposed and applied here.

The TOC removal improved as the applied voltage increased. However differently than ammonia, the threshold voltage for high removal was quite high, thus leading to higher contaminant removal with higher voltages, as 6 V/cm (test LEA.4).

It is reasoned here that the mineralization of organic macromolecules (with both C and N) and the complete oxidation of carbon can occur in short times only at high voltages, i.e. at very high energy level. In fact, the results achieved for the diesel-fuel contaminated soils (see e.g. Chapter 4) showed that an increase in the applied voltage allowed to attain a good contaminant removal in shorter times than lower voltages. However, long electrochemical processes (e.g. lasting for a few weeks) resulted in a high mineralization effectiveness even for low voltage gradients (e.g. about 1 V/cm). On the whole, it is believed that the mineralization could be significantly improved by increasing treatment duration and that longer processes could result in important contaminant removals even at

lower specific voltages.

**Table 5.25 – Main results of the one-day tests performed on the leachate-contaminated clay: concentration of TOC and nitrogen species in the original soil samples and in the final treated samples.**

Test	Sample	TOC	Total Nitrogen	N-NH <sub>4</sub> <sup>+</sup>	TKN	Organic Nitrogen	N-NO <sub>3</sub> <sup>-</sup>	N-NO <sub>2</sub> <sup>-</sup>
		[g/kg <sub>DW</sub> ]	[mg/kg <sub>DW</sub> ]	[mg/kg <sub>DW</sub> ]	[mg/kg <sub>DW</sub> ]	[mg/kg <sub>DW</sub> ]	[mg/kg <sub>DW</sub> ]	[mg/kg <sub>DW</sub> ]
LEA.1	Original Untreated Sample	7.2	165.4	59.3	-	-	-	-
10 V	Final Treated Sample	4.9 (-32%)	139.8 (-15%)	55.1 (-7%)	-	-	-	-
LEA.2	Original Untreated Sample	6.7	259.5	32.2	132.7	91.2	126.2	0.6
20V	Final Treated Sample	5.0 (-26%)	174.5 (-33%)	13.4 (-58%)	91.8	74.6	82.7	<0.1
LEA.3	Original Untreated Sample	6.7	259.5	32.2	132.7	91.2	126.2	0.6
30 V	Final Treated Sample	4.6 (-32%)	194.1 (-25%)	17.4 (-46%)	83.3	61.0	110.7	0.1
LEA.4	Original Untreated Sample	6.6	191.1	90.4	-	-	-	-
60 V	Final Treated Sample	3.5 (-62%)	134.1 (-30%)	49.7 (-45%)	-	-	-	-

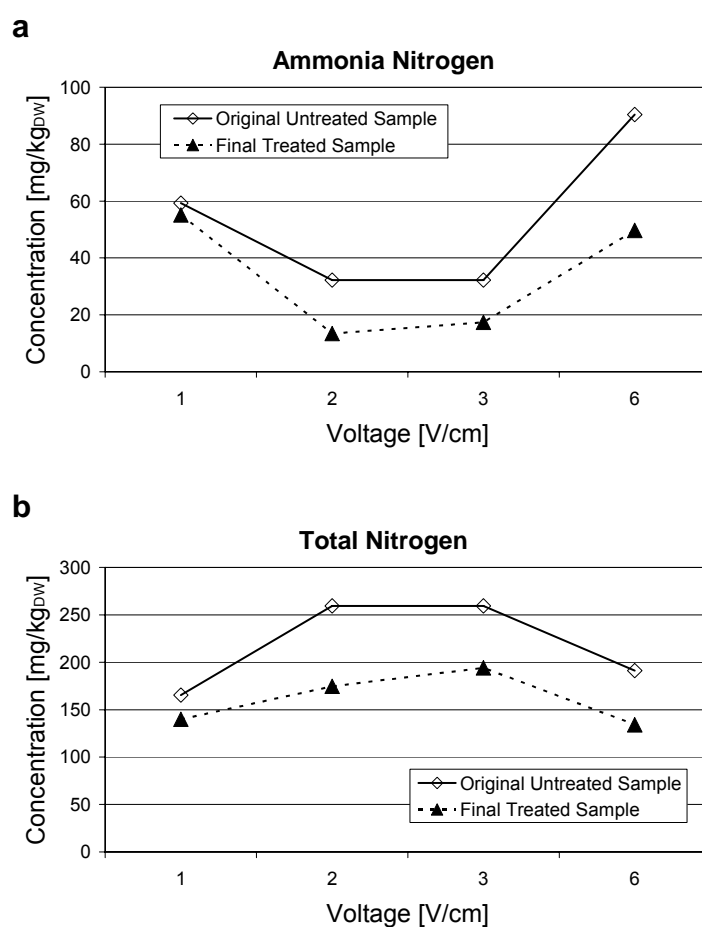


**Figure 5.30 – Results of tests LEA.1, LEA.2, LEA.3 and LEA.4: contaminant concentrations in original and final samples for ammonia nitrogen (a) and total nitrogen (b).**

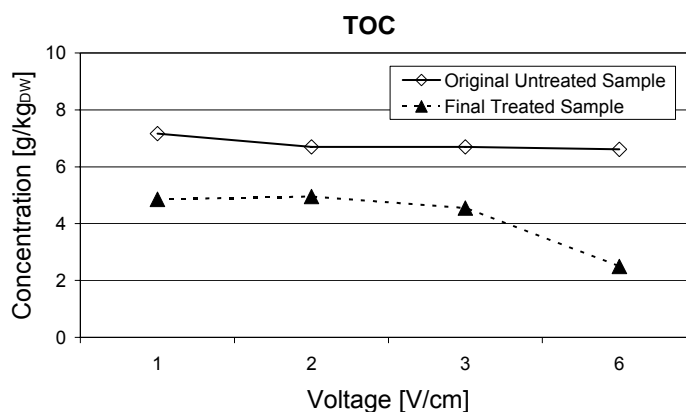


Figure 5.31 – Results of tests LEA.1, LEA.2, LEA.3 and LEA.4: TOC concentrations in original and final samples.

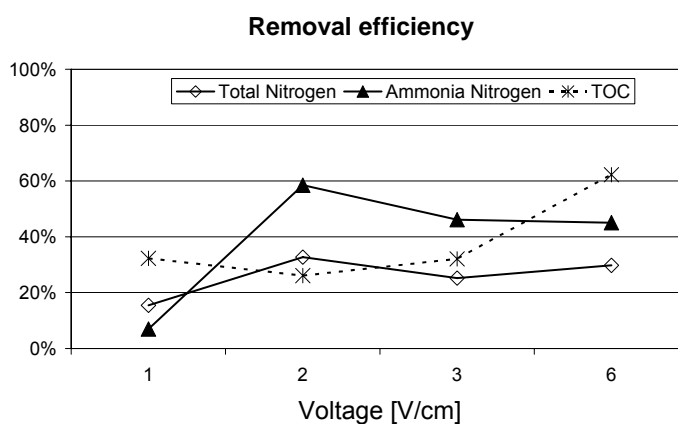


Figure 5.32 – Results of tests LEA.1, LEA.2, LEA.3 and LEA.4: removal efficiencies achieved for total nitrogen, ammonia and TOC during the tests performed.

Test LEA.5, which aimed at investigating the variation of contaminant removal with test duration, was performed with a constant voltage of 30 V (3 V/cm) for 7 days. The current flowing across the soil specimen was 240 mA at the beginning of the test, 250 mA (peak value) after one hour, 8 mA after one day, 3 mA at two days, 1.7 after four days, and was inferior to 1 mA at the end of the tests (Table 5.26).

Table 5.26 – Current flowing across the soil specimen during test LEA.5.

Time [h]	Current [mA]
0	240
0.5	250
24	8
48	3
96	1.7
168	<1

The results attained during test LEA.5 are presented in Table 5.27 and Figure 5.33.



Both for TOC, ammonia nitrogen and total nitrogen, the pollutant concentrations seemed to decrease significantly with time (Figure 5.33). The TOC removal achieved after 1 day was about 9%, but it increased to 42% by the end of the tests, after a 7 day-treatment. Total nitrogen removal ranged similarly from 16% to 36%, and ammonia removal ranged from 13% to 60%.

The TOC removal efficiency can be considered quite satisfactory, as TOC, which represents all organic molecules, decreases only when a certain amount of the organic matter has been completely mineralized. As for nitrogen compounds, the electrooxidation process proved to be able to transform ammonia, while the total nitrogen removal was mainly due to ammonia oxidation. At the end of test LEA.5, in fact, a decrease in the ammonia content of about 86 mg/kg<sub>DW</sub> was encountered, while in the same period the total nitrogen concentration decrease was about 84 mg/kg<sub>DW</sub>. A very limited nitrate formation was observed in the meanwhile.

**Table 5.27 – Results of test LEA.5: concentration of contaminant species and removal efficiencies achieved during the process.**

Elapsed Time [d]	TOC [g/kg <sub>DW</sub> ]	Total Nitrogen [mg/kg <sub>DW</sub> ]	N-NH <sub>4</sub> <sup>+</sup> [mg/kg <sub>DW</sub> ]	TKN [mg/kg <sub>DW</sub> ]	N-NO <sub>3</sub> <sup>-</sup> [mg/kg <sub>DW</sub> ]	N-NO <sub>2</sub> <sup>-</sup> [mg/kg <sub>DW</sub> ]
0	6.6	231.6	142.8	231.0	0.6	0.03
1	6.0 (-9%)	195.1 (-16%)	124.4 (-13%)	194.1	1.0	0.04
2	5.3 (-20%)	199.4 (-14%)	78.1 (-45%)	198.4	0.9	0.09
4	4.7 (-29%)	186.5 (-19%)	-	184.1	2.0	0.41
7	3.8 (-42%)	147.5 (-36%)	56.8 (-60%)	146.2	1.1	0.22

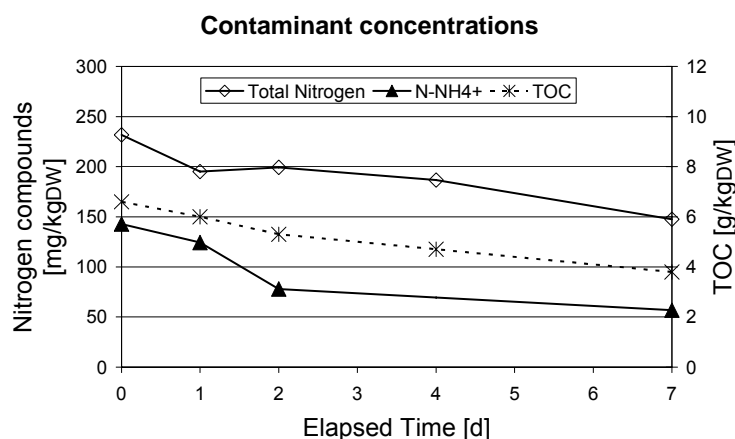


**Figure 5.33 – Results of test LEA.5: concentration of contaminant species (TOC, ammonia nitrogen and total nitrogen) measured during the process.**

Figure 5.34, Figure 5.35 and Figure 5.36 show the results of the investigation about the contaminant distribution along the soil specimen. As can be seen, the electrochemical process induced the pH to change, increasing at the anode side, and decreasing at the cathode side, as a result of water electrolysis. The pH changes were however limited by the soil buffer capacity.

The ammonia nitrogen concentrations showed to be decreasing towards the anode compartment and increasing in the cathode compartment. This suggest that the electrokinetic process significantly affected the ammonium ion ( $\text{NH}_4^+$ ), which seemed to be rapidly transported towards the cathode, thus leading to an accumulation in this area. The ammonia distribution along the soil also influenced the total nitrogen distribution, being ammonia an important part of the total nitrogen content.

As for TOC (Figure 5.36), despite some variability due to sample heterogeneity and uncertainty in chemical analysis, the removal effect can be considered uniform across the treated soil, as the final TOC content was approximately homogeneous along the specimen profile.

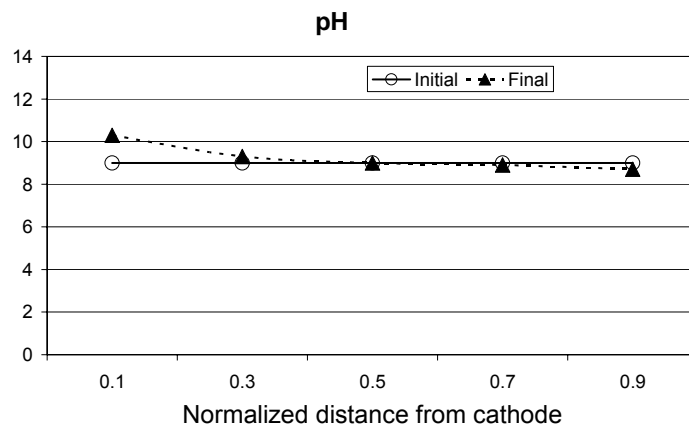
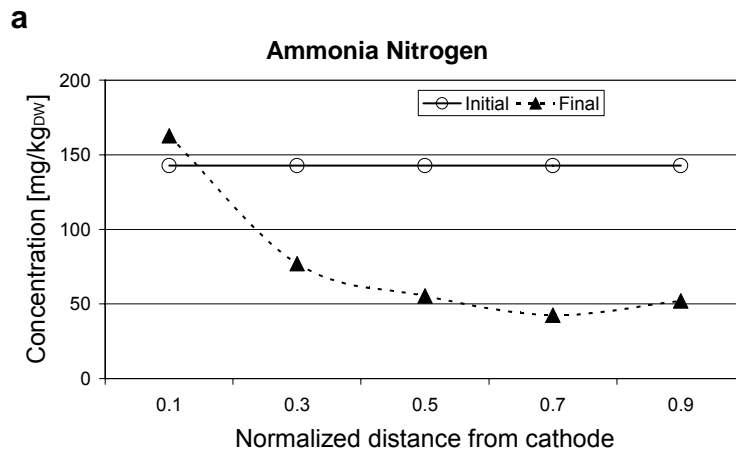
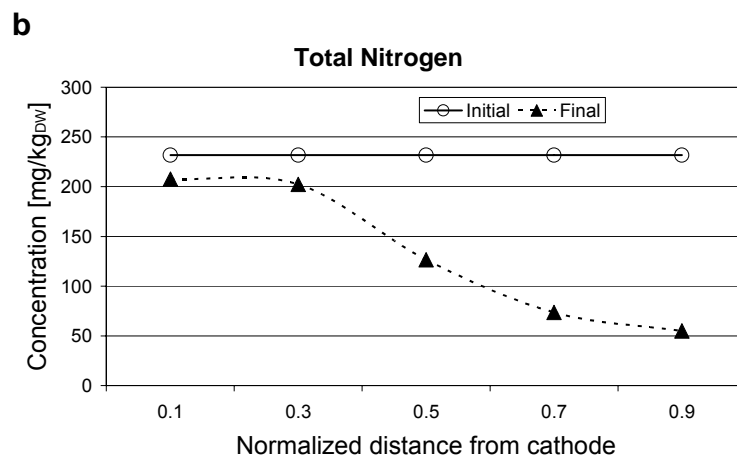
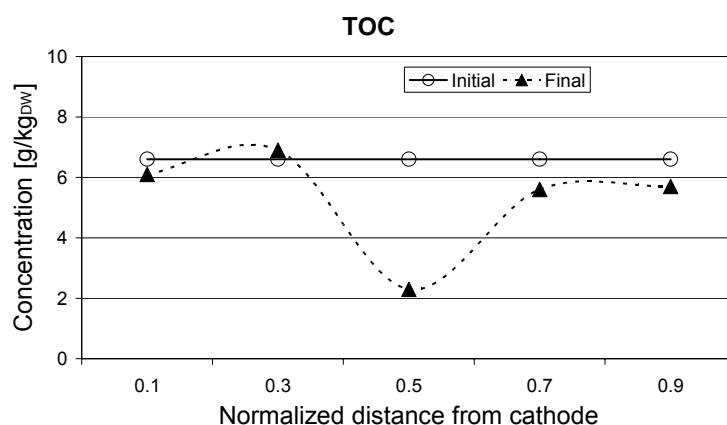


Figure 5.34 – pH profile along the soil specimen achieved at the end of test LEA.5.





**Figure 5.35 – Ammonia nitrogen (a) and total nitrogen (b) concentrations along the soil specimen achieved at the end of test LEA.5.**



**Figure 5.36 – TOC concentrations along the soil specimen achieved at the end of test LEA.5.**

### 5.3.4 Conclusions

This experimental research aimed at evaluating the effectiveness of electrooxidation for the removal of organic substances and ammonia from a clay contaminated by landfill leachate. Several tests were performed with a one-dimensional experimental setup for bench scale testing, with applied voltages ranging from 1 V/cm to 6 V/cm and treatment duration from one to seven days.

Significant removals of both TOC and ammonia nitrogen were achieved after one-day runs, with removal efficiencies up to 62% for TOC and up to 58% for ammonia. The ammonia removals also caused important decreases in the total nitrogen content.

Tests with different specific voltages showed that the ammonia removal increased as the applied voltage arose from 1 V/cm to 2 V/cm, but it remained almost constant for higher voltages. In addition, the TOC removal seemed to increase with increase in the applied voltage, but its threshold voltage for high removal was quite high, i.e. more than 3 V/cm here. It is thought that the mineralization of complex organic macromolecules (with

both C and N) that can occur in short times (e.g. a few days) only at high voltages, i.e. at high energy levels. Nevertheless, it is believed that the mineralization can be significantly improved by increasing treatment duration and that longer processes can allow to achieve important contaminant removals even at low specific voltages. Results from the longest test performed confirmed that the contaminant removals were significantly improved with the treatment duration.

In sum, according to the results achieved, electrooxidation proved to be effective for the remediation of organic pollutants and ammonia from clayey soils contaminated by landfill leachate.

At the end of all tests, ammonia nitrogen concentration was found to be higher near the cathode and lower near the anode. This suggested that the electrokinetic process could highly affect the ammonium ion, which seemed to be rapidly transported towards the cathode, thus leading to an accumulation in this area. Since ammonia proved to be transported very effectively and rapidly towards the cathode, also electrokinesis can be considered a feasible technology to be applied for the removal of ammonia from underground. In this case, the treatment could be enhanced with the addition of conditioning agents (e.g. acid solution to adjust the soil pH or surfactant agents) to promote the contaminant migration and to improve the pollutant recovery. The same processes could also be applied to create an electrokinetic barrier to prevent the contaminant spreading in groundwater plumes.

## Chapter 6

# Conclusions and perspectives

This study was conducted to assess the effectiveness of electrochemical oxidation for the remediation of different organic pollutants from fine-grain soils and sediments. Other aims of the research were to understand the role of different geochemical phenomena, to evaluate the most important design parameters that can affect the system efficiency (as the applied voltage and the treatment duration) and to assess any link between the removal efficiency and the macroscopic electrochemical phenomena, like the the electroosmotic flow and the changes in the soil pH. The influence of the soil mineralogical composition was also investigated.

A systematic study was performed to investigate the effects of electrooxidation on clayey soils contaminated with diesel fuel. Diesel fuel was chosen as soil contaminant to represent the environmental pollution due to spills of oil and of various petroleum products. Oil spills are a frequent source of contamination that may derive from underground fuel leaks, industrial activities, or oil refinery. Due to the high occurrence of these events, these sources of soil contamination pose important environmental concerns. In order to assess the influence of the soil mineralogy on the effectiveness of the electrochemical processes, two types of soils were considered in the study, including a silty clay, mainly composed of kaolin, and a clayey soil, classified as a bentonite and mainly composed of montmorillonite. In order to perform the experiments, the soil samples were spiked with diesel fuel and tested under various constant voltage gradients, ranging from 0.5 to 6 V/cm. The initial TOC concentration in the spiked soil samples ranged from 185.0 g/kg<sub>DW</sub> to 264.8 g/kg<sub>DW</sub>, while the TPH concentration ranged from 131.0 g/kg<sub>DW</sub> to 185.3 g/kg<sub>DW</sub>. These are very high contaminant concentrations, which may represent the soil pollution in the hot spots of underground contaminations due to oil spills and fuel leakages.

The results showed that a high efficiency of organic pollutant degradation could be achieved via electrochemical methods, with about 46-55% TOC removal and 66-85% TPH removal having been attained after four-week treatments on diesel fuel-contaminated

kaolin, without a significant transport of the target pollutants along the treated soil. The recorded initial current densities were about 0.1-1 mA/cm<sup>2</sup> and the flowing current decreased with time after an initial increase. As for the bentonite samples, even higher removal efficiencies were achieved, with 60-69% TOC removals and 73-87% TPH removals.

When an additional oxidant agent (hydrogen peroxide) was dosed at the cathode compartment to promote the contaminant degradation (EK-Fenton process), a more rapid pollutant removal was encountered, but the overall removal efficiencies did not significantly improved if compared to the sole use of the electrochemical process. This was thought to be due to the low permeability of the target soil, which probably constrained the oxidant delivery and caused the chemical oxidation treatment to be ineffective. The mild electric gradient and the lack of conditioning agents also probably limited the occurrence of the electroosmotic flow and hindered the transport of the oxidant agent along the soil specimen.

The main factors influencing the remediation efficiency seemed to be the process duration and the soil mineralogy, especially the iron content, of the treated medium. On the opposite, the applied voltage seemed to have a limited influence on the contaminant removal, good results being attained with specific voltages as low as 1 V/cm.

On the whole, the results achieved suggest that electrooxidation can be effectively used for the mineralization of many organics with low energy expenditure, especially in very fine soils, like clays. This can be of great practical interests, as these soils are often very difficult to treat with conventional chemical methods, because of their low permeability and high sorption capacity. As electrooxidation does not necessarily require a dosage of reactants underground, it also seems to be easily applicable for the in situ recovery of contaminated sites.

Besides the study about the diesel fuel-contaminated soils, three feasibility studies were conducted to assess the applicability of electrooxidation for the remediation of different contaminated soils and sediments. These studies were mainly devoted to evaluate the applicability of electrooxidation to really or potential contamination cases.

The first of these experimental investigations was carried out to evaluate the feasibility of using electrochemical oxidation for the remediation of PAHs from freshwater sediments, in case of old date contamination. The initial total PAH concentration in sediment samples ranged from about 1090 mg/kg<sub>DW</sub> to 1522 mg/kg<sub>DW</sub> (light PAHs about 731-1366 mg/kg<sub>DW</sub>, heavy PAHs about 139-359 mg/kg<sub>DW</sub>) and a 90% degradation was required to meet the remediation goals. Based on the results of this study, electrochemical oxidation proved to be an effective remediation technology, amenably applicable either for the in situ or for the ex situ remediation of the target sediments. A total PAH removal of 90% or more was achieved by this method after a four-week treatment, with a light PAH

removal about 93% and a heavy PAH removal about 77%. Such removal efficiencies were attained for specific voltages as low as 1 V/cm. As expected, the removal efficiencies for light PAHs were higher than for the heavy PAHs, which are commonly found to be sorbed onto soil particles, and often proved to be more recalcitrant to both biological and chemical degradation than light PAH species. Like for the diesel fuel remediation, the final PAH concentrations in the treated samples were found to be evenly distributed across the treated sample, besides some variability due to the natural sediment heterogeneity. The results also indicated that the removal efficiency could be significantly improved by increasing the treatment duration. Moreover, despite the fact that the removal efficiencies achieved for heavier PAH species were always found to be lower than those for light PAHs, longer electrochemical treatments proved to be able to improve the heavy PAH removal significantly. The results achieved were very satisfactory, since a good recovery of these sediments proved to be very difficult to be attained, because of their high contaminant concentrations, low permeability, high sorption capacity and high organic matter content (Ferrarese et al., 2008).

A second feasibility study was conducted to assess the effectiveness of electrooxidation for the remediation of a silty soil contaminated by organolead compounds, including tetraethyl lead (TEL), triethyl lead (TREL) and diethyl lead (DEL). Two laboratory tests were performed on soil samples with different contaminant contents, the total organic lead (TOL) concentration ranging from 34.7 mg/kg<sub>DW</sub> to 771.4 mg/kg<sub>DW</sub>. In both trials, the samples were tested under constant specific voltages of 1.5 V/cm for 14 days. During the tests, a certain TEL oxidation was achieved, but the system seemed unable to attack the ionic alkyllead compounds (i.e. TREL and DEL), which proved to be more stable compounds and more recalcitrant to degradation than TEL. Thus, the process is likely to fail in achieving a significant reduction of the overall TOL content. The TEL partial degradation also resulted in an increase in the TREL content in the treated soil samples. On the whole, the electrochemical process seems unable to achieve a complete recovery of the above-mentioned soil from the organolead pollutants, the electrooxidation being only capable of degrading TEL.

A further experimental research aimed at evaluating the effectiveness of electrooxidation for the remediation of clayey soils contaminated by landfill leachate. The objective of this study was to evaluate the feasibility of using electrooxidation for the removal of organic pollutants and ammonia from the bottom clay barrier on a landfill, in case it has been contaminated by leachate, e.g. because of a failure of the liner system. Several tests were performed with voltages ranging from 1 V/cm to 6 V/cm and treatment duration from one to seven days. Significant removals of both TOC and ammonia nitrogen were achieved, with degradation efficiencies up to 62% for TOC and up to 58% for ammonia after one-day electrochemical processes. The ammonia removals also caused

important decreases in the total nitrogen content. Results from the longest test performed showed that contaminant removals could significantly improve with treatment duration. At the end of all the runs, the residual ammonia nitrogen concentration was found to be higher near the cathode and lower near the anode, thus suggesting that the ammonium ion could be easily transported along the soil towards the cathode by the electrokinetic processes. In sum, the electrochemical methods can be considered effective for the remediation of clayey soils contaminated by landfill leachate. Possible applications of this technology can include both the remediation of the clay barrier and of groundwater plumes for old landfills, and the introduction of an innovative engineering solution for new landfills.

Besides the removal efficiencies attained by the electrochemical methods, some major conclusion can be drawn from the results achieved, and are presented as follows:

- An increase in the applied voltage proved to cause a limited improvement of the hydrocarbon remediation, good removal efficiencies being encountered for specific voltages as low as 1 V/cm, which allowed to conduct the treatment with low energy expenditures. In detail, a certain influence of the applied voltage was encountered during the tests performed on the diesel fuel-contaminated soils, with a quite significant improvement of the treatment efficiency as the voltage increased from 0.5 V/cm to 1 V/cm, but the system effectiveness remained almost constant afterwards. This suggested that there is no need to increase the applied voltage above 1 V/cm to attain a good degree of hydrocarbon mineralization.
- Oppositely, the contaminant removal seemed to increase significantly with the process duration. For example, the application of a constant voltage of 1 V/cm to a bentonite sample led to 30% TOC decrease after a 7-day treatment, but the TOC removal increased to about 69% after a 28-day treatment. However, the time dependency was different for different voltages. In fact, for the diesel-contaminated kaolin, when the lowest voltage was applied (i.e. 0.5 V/cm), the contaminant removal gradually increased, and more than 20 days of treatment were required to achieve a good contaminant removal efficiency (e.g. more than 40% TOC removal and 60% TPH removal). Differently, when higher voltages were applied, high remediation performances could be attained in shorter times, i.e. about 15 days for 1 V/cm and less than 10 days for 3 V/cm. It can be supposed that the higher voltages resulted not only in higher removals of the organic pollutants, but also in a more rapid mineralization process than the lower voltages. An increase in the applied voltage therefore allowed to achieve a good contaminant removal in shorter times than lower voltages, but this advantage is counterbalanced by the fact that higher specific voltages (e.g. 3



V/cm or more) result in higher energy expenditures, and may require more complicated setups for real-scale applications. On the whole, electrochemical treatments with low DC voltages (about 1 V/cm) and durations of a few weeks can be recommended for efficient and cost-effective soil recoveries.

- Tests with specimen having different lengths were performed, the distance across the electrodes ranging from 10 cm to 50 cm. The results indicated that no scale effect significantly affects the electrochemical process, provided that a sufficient voltage gradient (e.g. about 1 V/cm) is created across the electrodes. This conclusion is quite significant as it implies that the results achieved in the laboratory scale tests can be expected also for the real scale applications, where the electrodes are commonly placed one or a few meters apart.
- The soil mineralogy, and in particular the iron content, seems to affect the treatment results significantly. In fact, the removal efficiencies achieved for bentonite (iron content about 10180 mg/kg<sub>DW</sub>, manganese content about 44 mg/kg<sub>DW</sub>) were much higher than those recorded for kaolin, which was characterized by a lower metal content (iron content about 2794 mg/kg<sub>DW</sub> and manganese content about 34 mg/kg<sub>DW</sub>), despite the fact that the two soils showed similar current intensities, which were even lower for the bentonite than for the kaolin. Dissolved iron(II)-species deriving from the corrosion of the steel anodes could also have acted as electron donors, and may have enhanced the electrochemical reactions (Röhrs et al., 2002). The soil iron content was well known to be a key-parameter for Fenton-like reactions in traditional chemical oxidation (Watts et al., 2002; Flotron et al., 2005; Bissey et al., 2006; Rivas, 2006). In fact, it had also been previously reported to be able to promote the EK-Fenton processes, when hydrogen peroxide was used as additional oxidant agent (Yang and Liu, 2001; Kim et al., 2006), but its effectiveness in improving the electrooxidation mechanisms in unenhanced electrochemical treatment had not been previously discussed. The large reservoir of iron that is present in natural occurring iron-containing minerals is supposed to act as a microconductor source, promoting redox reactions and the formation of H<sub>2</sub>O<sub>2</sub>, and also to enhance the Fenton-like reactions that promote the oxidation processes (Rahner et al., 2002; Isosaari et al., 2007). Consequently, significant iron contents in the treated soils are thought to be able to improve the applicability of this remediation method.
- The occurrence of a significant electroosmotic flow was previously considered necessary to provide fresh water for electrolysis and for further redox reactions (Röhrs et al., 2002). During the experiments performed in

this study, an electroosmotic flow occurred when the intensity of the electric current was appreciable (e.g. for currents of the order of magnitude of 5 mA or above). As during the tests the electric current started to decrease within a few hours after the beginning of the tests, the electroosmotic flow, when occurring, was appreciable only in the first days of treatment, and became negligible afterwards. The electroosmotic flow had already been reported to decrease rapidly with time, especially when no ionic solution was added to the soil, and the resulting current was weak (Reddy et al., 2006; Isosaari et al., 2007). However, in this study a very good contaminant removal was obtained even in the tests when the no electroosmotic flow was encountered. This suggests the occurrence of the electroosmotic flux not to be necessary to achieve a significant mineralization of the organic pollutants.

- Moreover, during the tests performed, current densities about 0.1-1 mA/cm<sup>2</sup> were encountered. These values are lower than the current densities usually reported in literature of effective electrochemical processes, i.e. of the order of 1 mA/cm<sup>2</sup> (U.S. AEC, 2000). Thus, the results achieved suggest that the mineralization process can work at lower energy levels than those commonly recommended, allowing moderate energy expenditures.
- For the hydrocarbons, the final contaminant concentrations were found to be evenly distributed across the treated samples. This indicates that the oxidation reactions occurred within all the treated volume and not only close to the electrodes, in agreement with the microconductor principle, according to which the production of radicals occurs diffusely in all the treated soil (Rahner et al., 2002). Moreover, the results show that during the tests performed, that were unenhanced, the electrokinetic transport of the target pollutants was negligible. In fact, for diesel fuel-contaminated soils, even when the electroosmotic flow caused water to accumulate at the cathode compartment, the fraction of the total hydrocarbon content removed from the soil specimen as a result of the electroosmotic transport was unimportant in comparison to the initial pollutant content in the soil samples (e.g. about 0.8% for TOC and 0.7% for TPH). As for PAHs, which are highly hydrophobic species, the concentrations of the target compounds in the water collected at cathode compartment were below the detection limit (<0.1 µg/L). These results were however expected, as the target organic pollutant were apolar molecules, which are known not to be affected by the electromigration process. On the other hand, the electrokinetic transport of apolar organic pollutant was reported to occur only when the electroosmotic flow was significantly improved and the solubilization was enhanced by the used of

surfactants or solvents (Acar et al., 1995; Lee et al., 2005a; Kim et al., 2005a; Wick et al., 2005). Moreover, in the tests performed here, the electroosmotic advection was constrained by the low electroosmotic flow rates encountered during.

- The ecotoxicity of the original and final samples was evaluated for the PAH-contaminated sediment samples, in order to assess any change in the toxic effect of the treated sediments towards the local biota. The results showed that, despite the very high pollutant concentrations, the original samples were characterized by a limited toxic effect (0.23 TU50), probably because of the fact that the PAHs were strongly sorbed onto the sediment particles. In fact, this is thought to have acted as detoxifying effect, constraining the bioavailability of these pollutants (Richnow et al., 1995; Sun and Yan, 2007). No residual toxic effect was detected in the sediment samples treated by electrooxidation. Therefore, the electrochemical treatment proved not to enhance the sole desorption of the target pollutants, hence promoting their mineralization in the sorbed form or oxidizing them as soon as they are desorbed. In fact, if PAHs had been desorbed from environmental matrix, their toxic effect would have significantly increased. Under these conditions, the consequences of a possible remediation process should have been carefully assessed. These results were confirmed by the fact that the PAH concentration in the pore fluid collected at cathode compartment during the tests were below the detection limit (<0.1 mg/L). This evidence suggests that the electrooxidation could be amenably applied for in situ remediation of soils and sediments, without environmental risks due to uncontrolled pollutant mobilization.
- During the tests performed on the leachate-contaminated clay, despite the fact that the experiments were not enhanced by an acid conditioning, the ammonium ion proved to be effectively and rapidly transported along the soil sample towards the cathode, thus tending to accumulate in this area. Therefore, besides the ammonia degradation due to the electrooxidation processes, also electrokinesis can be considered an effective technology for the removal of ammonia from underground. In this case, the treatment could be enhanced with the addition of conditioning agents (e.g. acid solution to adjust the soil pH or surfactant agents) to promote contaminant migration and to improve pollutant recovery. The same processes could also be applied to create an electrokinetic barrier to prevent the contaminant spreading in groundwater plumes.
- Like for ammonia, also the final concentrations of organolead compounds

- were found to be varying along the soil specimen, with higher contaminant contents at the cathode side and lower contents at the anode side. In detail, the electromigration seems to have affected the ionic alkyllead compounds (TREL and DEL), which are soluble cations and which seem to be easily transported along the treated soil towards the cathode. Despite the fact that TEL is an apolar molecule with limited water solubility, also this compound seemed to migrate towards the cathode. This was probably due to the occurrence of the electroosmotic flow towards the cathode, which caused an advective transport of the soil and organic matter particles onto which TEL is sorbed. Apolar organic pollutants can in fact be transported in water attached to dissolved organic material (De Serres and Bloom, 1995). The same pathway is regarded as the main transport mechanism of TEL migration in groundwater plumes (Collins, 2001). The total lead content, which included both the contributions of the organic lead compounds and of the metallic lead compounds (the latter being the major part of the total lead content), proved to be mainly transported towards the anode, probably because of the formation of negatively charged lead compounds, as lead sulphides and lead hydroxides (Acar et al., 1995). The migration of such compounds was probably limited by the basic conditions of the treated soil, which usually promote the metal precipitation and constrain the electromigration process.
- During the electrochemical treatment, the soil pH tended to increase at the cathode and to decrease at the anode because of water hydrolysis, which leads to the production of an acid front moving from the anode towards the cathode and a base front moving from the cathode towards the anode. Important pH changes could be encountered even a few days after the beginning of the tests performed. In most of cases, as the tests continued (e.g. within a few weeks from the beginning of the process), all the soil volume tended to be acidified, as a result of the acid front sweeping along the soil from the anode towards the cathode. This effect was important especially for the highest specific voltages (i.e. 3-6 V/cm) rather than for the lowest voltages (0.5-1 V/cm). However, in soils with a strong buffer capacity, the pH changes were limited. Moreover, in certain soils, the buffer capacity affected the evolution of the soil pH profile, by determining the tendency of the treated medium towards acidification or basification. For example, in certain soils, the electrochemical treatment may result in an increase in the soil pH all along the treated soil specimen (Szpyrkowicz et al., 2007), as occurred here for bentonite and for the organolead contaminated soils.

- The pH changes were expected to influence the system efficiency, since a low pH can enhance the Fenton-like reactions, which lead to the production of hydroxyl radicals, which are regarded as the major oxidant agents responsible of the mineralization process (ITRC, 2005). However, the results achieved here indicated that there was no correlation between the soil pH profile and the final contaminant distributions, which seemed to be independent from the acid or basic conditions created in the soil during the electrochemical process. Therefore, the mineralization process did not seem to be influenced by pH changes, the contaminant removal being of the same order of magnitude both in areas with low and high pH. It is reasoned that the soil natural iron content was sufficient to enhance the Fenton-like reactions, with no need for a strongly acid pH to promote the radical production.
- The enhancement of the electrochemical process with an electrolyte or acidic solution showed not to be necessary for the electrooxidation process to occur. On the other hand, under these conditions, the electrokinetic transport, which is determined by the electroosmotic flow and by the soil pH, was very limited. This probably caused the transport of additional oxidizing agents (EK-Fenton process) to be ineffective. The addition of an electrolyte solution may be useful to keep the soil resistance low and to deliver enough fresh water for electrolysis; moreover, it could be able to allow both the electrooxidation and the EK-Fenton process to contribute to contaminant degradation.

In sum, based on the results achieved, indirect oxidation, due to the production of hydroxyl radicals from electrochemically generated hydrogen peroxide, can be regarded as the major degradation pathway, rather than the direct pollutant oxidation, based on the hydroxyl radical production from water at the electrode surface. In fact, the mineralization processes proved to occur diffusely within all the treated volume, with the residual contaminant content almost evenly distributed along the treated soil. In addition, the EK-Fenton test showed the transport of active species along the soil was very limited under the tested conditions (i.e. without the addition of electrolyte solution as conditioning fluids). This evidence suggests that the mineralization process occurred within all the treated volume, and was not dependent on transport phenomena.

In this framework, the presence of microconductors, as iron minerals (Rahner et al., 2002) is supposed to allow the production of hydrogen peroxide at the pore scale in all the treated soil, while the presence of iron catalysts may enhance its decomposition into hydroxyl radicals, according to the Fenton's process.

The results achieved are very encouraging, since the recovery of fine-grain soils is

often a very challenging technical issue. On the whole, electrochemical oxidation seems to be effectively and amenably applicable for the mineralization of many organics with low energy expenditure, especially in finest soils, like clays, with significant iron contents. The conclusions arisen here could be of interest to define guidelines for the real-scale application of electrochemical remediation methods.

However, until this time, a clear understanding of all the geochemical processes that are involved in the pollutant degradation mechanisms has not been achieved yet, and further research is necessary to understand the nature and kinetics of the chemical reactions induced by electric fields in the treated media. The open questions include the role of the natural iron and other metals contained in soils, and the influence of different iron forms (i.e. exchangeable and bound to carbonate, bound to Fe/Mn oxides, bound to organic matter and sulphides, residual fraction) on the electrooxidation process and on the occurrence of the Fenton-like reactions involved. In addition, also the possibility to enhance the degradation process by adding metals to the soil to be treated should be investigated. Moreover, during the unconditioned electrochemical treatment, the electric current flowing is gradually decreased because of the formation of a high electric resistivity zone near the cathode, due to the precipitation of metal hydroxides under the local basic conditions; hence, the use of the acid conditioning to improve soil conductivity should be evaluated. Furthermore, in this investigation the contaminant degradation was significant but not complete: further work must be done to define how to improve the contaminant removal efficiency. Likewise, the combined use of electrooxidation and of electrokinetically enhanced chemical oxidation needs for additional studies, e.g. in order to define how to improve the reactant transport together with the electrochemical processes.

A better knowledge of these processes will help to design more effective and more efficient remediation actions.

## References

- Acar Y.B., Alshawabkeh A.N. (1993), Principles of electrokinetic remediation. *Environmental Science and Technology*, 27, 2638-2647.
- Acar Y.B., Gale R.J., Alshawabkeh A.N., Marks R.E., Puppala S., Bricka M., Parker R., (1995), Electrokinetic remediation: basics and technology status. *Journal of Hazardous Materials*, 40, 117-137.
- Ahmad H. (2004), Evaluation and enhancement of electro-kinetic technology for remediation of chromium copper arsenic from clayey soil. PhD dissertation, Department of Civil and Environmental Engineering, Florida State University.
- Alshawabkeh A.N. (2001), Basics and Applications of Electrokinetic Remediation. Handouts Prepared for a Short Course. Federal University of Rio de Janeiro, Rio de Janeiro, Brazil, 19-20 November 2001.
- Alshawabkeh A.N., Ozsu-Acar E. Gale R.J. Puppala S.K. (1998), Remediation of soils contaminated with tetraethyl lead by electric fields. *Transportation Research Record*, 1615, 79-85.
- Alshawabkeh A.N., Sheahan T.C., Wu X. (2004), Coupling of electrochemical and mechanical processes in soils under DC fields. *Mechanics of Materials*, 36, 453-465.
- Amrate S., Akretche D.E., Innocent C., Seta P. (2005), Removal of Pb from a calcareous soil during EDTA-enhanced electrokinetic extraction. *Science of the Total Environment*, 349, 56-66.
- Andreottola G. Simonini C. (2004), Test di ozonizzazione in situ di terreni contaminati da IPA. Risultati Preliminari. Proceedings of the conference Nuovi indirizzi nella bonifica dei siti contaminati. La Prassi, la normativa, le nuove tecnologie, 3 December 2004, Milano, Italy.
- Andreottola G., Dallago L., Ferrarese E. (2008), Feasibility study for the remediation of groundwater contaminated by organolead compounds. *Journal of Hazardous Materials*, article in press, doi: 10.1016/j.jhazmat.2007.12.044.
- Antizar-Ladislao B., Lopez-Real J., Beck A.J. (2005), Laboratory studies of the remediation of polycyclic aromatic hydrocarbon contaminated soil by in-vessel composting. *Waste Management*, 25, 281-289.

- Bergmann K., B. Neidhart B. (1996), Speciation of organolead compounds in water samples by GC-AAS after in situ butylation with tetrabutylammonium tetrabutylborate. *Fresenius Journal of Analytical Chemistry*, 356, 57-61.
- Bissey L.L., Smith, J.L., Watts R.J. (2006), Soil organic matter–hydrogen peroxide dynamics in the treatment of contaminated soils and groundwater using catalyzed H<sub>2</sub>O<sub>2</sub> propagations (modified Fenton's reagent). *Water Research*, 40, 2477-2484.
- Borgan B.W., Trbovic V. (2003), Effect of sequestration on PAH degradability with Fenton's reagent: roles of total organic carbon, humin, and soil porosity. *Journal of Hazardous Materials*, 100, 285-300.
- Bossert I.P., Bartha R. (1986), Structure-biodegradability relationships of polycyclic aromatic hydrocarbons in soil. *Bulletin of Environmental Contaminant Toxicology*, 37, 490-495.
- Brillas E., Casado J. (2002), Aniline degradation by Electro-Fenton<sup>®</sup> and peroxi-coagulation processes using a flow reactor for wastewater treatment. *Chemosphere*, 7, 241-248.
- Brown G.S., Barton L.L., Thomson B.M. (2003), Permanganate oxidation of sorbed polycyclic aromatic hydrocarbons. *Waste Management*, 23, 737-740.
- BSI (1999), Code of practice for site investigations. BS 5930, British Standards Institution Standard Sales, London, GB.
- Cabeza A., Ane Urtiaga A., Rivero M.J., Ortiz I. (2007), Ammonium removal from landfill leachate by anodic oxidation. *Journal of Hazardous Materials*, 144, 715-719.
- Cairney S., Maruff P., Burns C., Currie B. (2002), The neurobehavioral consequences of petrol (gasoline) sniffing. *Neuroscience and Biobehavioral Reviews*, 26, 81-89.
- Cairney S., Maruff P., Burns C.B., Currie J., Currie B.J. (2004), Neurological and cognitive impairment associated with leaded gasoline encephalopathy. *Drug and Alcohol Dependence*, 73, 183-188.
- CARB (2001), Risk management guidelines for new, modified and existing sources of lead. California Environmental Protection Agency, California Air Resource Board, Sacramento, CA, USA.
- Carter P., Knowles C., Jackman S., Burton J. (2005), The electrokinetic bioremediation of hydrocarbon contamination from the subsurface. *Proceedings of EREM 2005, 5th Symposium on Electrokinetic Remediation, 22-25 May 2005, Ferrara, Italy.*
- Casagrande L. (1949), Electro-osmosis in soils. *Geotechnique*, 1, 159-177.
- Cerniglia C.E. (1992), Biodegradation of polycyclic aromatic hydrocarbons. *Biodegradation*, 3, 351-368.
- Choi H., Lim H.-N., Kim J., Hwang T.-M., Kang J.-W. (2002), Transport characteristics of gas phase ozone in unsaturated porous media for in-situ chemical oxidation. *Journal of Contaminant Hydrology*, 57, 81-98.



- Christensen T.H., Kjeldsen P., Bjerg P.L., Jensen D.L., Christensen J.B., Baun A., Albrechtsen H.J. Heron G. (2001), Biogeochemistry of landfill leachate plumes. *Applied Geochemistry*, 16, 659-718.
- Chung H.I. (2005), Electrokinetic remediation coupled with permeable reactive barrier for the removal of heavy metal and organic substance in contaminated groundwater. Proceedings of EREM 2005, 5th Symposium on Electrokinetic Remediation, 22-25 May 2005, Ferrara, Italy.
- Chung H.I., Lee Y.S. (2007), Electrokinetic permeable reactive barrier for the removal of heavy metal and organic substance in contaminated soil and groundwater. Proceedings of EREM 2007, 6th Symposium on Electrokinetic Remediation, 12-15 June 2007, Vigo, Spain.
- Chung H.I., Kamon M. (2005), Ultrasonically enhanced electrokinetic remediation for removal of Pb and phenanthrene in contaminated soils. *Engineering Geology*, 77, 233-242.
- Chung H.I., Kang B.H. (1999), Lead removal from contaminated marine clay by electrokinetic soil decontamination. *Engineering Geology*, 53, 139-150.
- Coletta, T.F., Brunell, C.J., Ryan, D.K., Inyang, H.I. (1997), Cation-enhanced removal of lead from kaolinite by electrokinetics. *Journal of Environmental Engineering*, 123, 1227-1233.
- Collins C. Endrizzi M., Shaw G. (2005), Review of the environmental behavior and toxicology of organic lead and proposal for its remediation at the "Trento-Nord" site, Italy. Final report for Provincia Autonoma di Trento, Progetto Speciale Recupero Ambientale e Urbanistico delle Aree Industriali a Nord di Trento. Confidential Report. Imperial College London Consultants, London, GB.
- Cook D.E., Gale S.J. (2005), The curious case of the date of introduction of leaded fuel to Australia: Implications for the history of Southern Hemisphere atmospheric lead pollution. *Atmospheric Environment*, 39, 2553-2557.
- Corwin D.L., Lesch S.M. (2005), Apparent soil electrical conductivity measurements in agriculture. *Computers and Electronics in Agriculture*, 46, 11-43.
- Curtis F., Lammey J. (1998), Intrinsic remediation of a diesel fuel plume in Goose Bay, Labrador, Canada. *Environmental Pollution*, 103, 1998, 203-210.
- Cuypers M.P., Grotenhuis T.C., Rulkens W.H. (1998), Characterization of PAH contaminated sediments in a remediation perspective. *Water Science Technology*, 37, 157-164.
- Da Pozzo A., Merli C., Sirés I., Garrido J.A., Rodriguez R.M., Brillas E. (2005), Removal of the herbicide amitrole from water by anodic oxidation and electro-Fenton. *Environmental Chemistry Letters*, 3, 7-11.
- Dadkhah A.A., Akgerman A. (2002), Hot water extraction with in situ wet oxidation: PAHs

- removal from soil. *Journal of Hazardous Materials*, B93, 307-320.
- De Flaun M.F., Condee C.W. (1997), Electrokinetic transport of bacteria. *Journal of Hazardous Materials*, 55, 263-277.
- De Battisti A. (2006), Electrochemical remediation. Proceedings of the ESSEE 4, 4th European Summer School on Electrochemical Engineering, 17-22 September 2006, Palić, Serbia and Montenegro.
- De Gioannis G., Muntoni A., Poletini A., Pomi R. (2007a), Enhanced electrokinetic treatment of different marine sediments contaminated by heavy metals. Proceedings of EREM 2007, 6th Symposium on Electrokinetic Remediation, 12-15 June 2007, Vigo, Spain.
- De Gioannis G., Muntoni A., Ruggeri R., Zijlstra H. Floris M. (2007b), Chromate adsorption in a transformed red mud permeable reactive barrier using electrokinesis. Proceedings of EREM 2007, 6th Symposium on Electrokinetic Remediation, 12-15 June 2007, Vigo, Spain.
- De Gioannis G., Muntoni A., Poletini A., Pomi R. (2007c), Electrokinetic treatment of marine sediments contaminated by heavy metals. Proceedings of the 23rd Annual Conference on Soils, Sediments and Water, 15-18 October 2007, Amherst, MA, USA.
- Delille D., Pelletier E. (2002), Natural attenuation of diesel-oil contamination in a subAntarctic soil (Crozet Island). *Polar Biology*, 25, 682-687.
- Delille D., Pelletier E., Coulon F. (2007), The influence of temperature on bacterial assemblages during bioremediation of a diesel fuel contaminated subAntarctic soil. *Cold Regions Science and Technology*, 48, 74-83.
- Deng Y., Englehardt J.D. (2007), Electrochemical oxidation for landfill leachate treatment. *Waste Management*, 27, 380-388.
- De Serres F.J., Bloom A.D. (1995), Ecotoxicity and human health – A biological approach to environmental remediation. Lewis Publisher, CRC Press, Boca Raton, FL, USA.
- Di Palma L., Mecozzia R. (2007), Heavy metals mobilization from harbour sediments using EDTA and citric acid as chelating agents. *Journal of Hazardous Materials*, 147, 768-775.
- Doering F., Doering N., Iovenitti J.L., Hill D.G., McIlvride W.A. (2001), Electrochemical remediation technologies for soil, sediment and ground water. Proceedings of the 2001 International Containment & Remediation Technology Conference and Exhibition, 10-13 June 2001, Orlando, FL, USA.
- Doering F., Doering N., Iovenitti J.L., Hill D.G., McIlvride W.A. (2001b), Electrochemical remediation technologies for soil, sediment and ground water. Proceedings of the 17th Annual International Conference on Soils, Sediments and Water, 22-25 October 2001, University of Massachusetts, Amherst, MA, USA.
- Doering F., Doering N., Iovenitti J.L., Hill D.G., McIlvride W.A. (2002), Electrochemical remediation technologies for metals remediation in soil, sediment, and ground water.

- Proceedings of the 3rd International Conference on Remediation of Chlorinated and Recalcitrant Compounds, 20-23 May 2002, Monterey, CA, USA. Paper 2H-12. Battelle Press, Columbus, OH, USA.
- ECP (2003), White Paper: ElectroChemical GeoOxidation (ECGO) - A Synthesis. ECP, Electrochemical Processes, llc, Wayne, PA, USA. [http://www.ecp-int.com/download/white\\_paper\\_on\\_ECGO.pdf](http://www.ecp-int.com/download/white_paper_on_ECGO.pdf).
- El-Fadela M., Bou-Zeida E., Chahineb W., Alaylic B. (2002), Temporal variation of leachate quality from pre-sorted and baled municipal solid waste with high organic and moisture content. *Waste Management*, 22, 269-282.
- Eykholt G.R., Daniel D.E. (1991), Electrokinetic decontamination of soils. *Journal of Hazardous Materials*, 28, 208-209.
- Fauri M., Gnesotto F., Marchesi G., Maschio A. (1999), *Lezioni di elettrotecnica: Volume II, Applicazioni Elettriche*. Società Editrice Esculapio s.r.l., Bologna, Italy.
- Feng D., Aldrich C. (2000), Sonochemical treatment of simulated soil contaminated with diesel. *Advances in Environmental Research*, 4, 103-112.
- Ferguson S.H., Franzmann P.D., Revill A.T., Snape I., Rayner J.L. (2003), The effects of nitrogen and water on mineralization of hydrocarbons in diesel-contaminated terrestrial Antarctic soils. *Cold Regions Science and Technology*, 37, 197-212.
- Ferguson S.H., Woinarski A.Z., Snape I., Morris C.E., Revill A.T. (2007), A field trial of in situ chemical oxidation to remediate long-term diesel contaminated Antarctic soil. *Cold Regions Science and Technology*, 40, 47-60.
- Ferrarese E., Andreottola G., Oprea I.A. (2008), Remediation of PAH-contaminated sediments by chemical oxidation, *Journal of Hazardous Materials*, 152, 128-139.
- Filler D.M., Lindstrom J.E., Braddock J.F., Johnson R.A., Nickalaski R. (2001), Integral biopile components for successful bioremediation in the Arctic. *Cold Regions Science and Technology*, 32, 143-156.
- Flotron V., Delteil C., Padellec Y., Camel V. (2005), Removal of sorbed polycyclic aromatic hydrocarbons from soil, sludge and sediments samples using the Fenton's reagent process. *Chemosphere*, 59, 1427-1437.
- FRTR (2002), Remediation technologies screening matrix and reference guide, fourth edition. Federal Remediation Technologies Roundtable.
- Gallert C., Winter J. (2002) Bioremediation of soil contaminated with alkyllead compounds. *Water Research*. 36, 3130-3140.
- Giannis A., Gidakos E., Skouta A. (2007), Application of sodium dodecyl sulfate and humic acid as surfactants on electrokinetic remediation of cadmium-contaminated soil. *Desalination*, 249-260.
- Godschalk M.S., Lageman R. (2005), Electrokinetic biofence, remediation of VOCs with solar energy and bacteria. *Engineering Geology*, 77, 225-231.

- Gong Z., Alef K., Wilke B.M., Mai M., Li P (2005), Assessment of microbial respiratory activity of a manufactured gas plant soil after remediation using sunflower oil. *Journal of Hazardous Materials*, B124, 217-223.
- Gong Z., Wilke B.M., Alef K., Li P., Zhou Q. (2006), Removal of polycyclic aromatic hydrocarbons from manufactured gas plant-contaminated soils using sunflower oil: Laboratory column experiments. *Chemosphere*, 62, 780-787.
- Haapea P., Tuhkanen T. (2006), Integrated treatment of PAH contaminated soil by soil washing, ozonation and biological treatment. *Journal of Hazardous Materials*, 136, 244-250.
- Halmemies S., Gröndahl S., Arffman M., Nenonen K., Tuhkanen T. (2003), Vacuum extraction based response equipment for recovery of fresh fuel spills from soil *Journal of Hazardous Materials*, 97, 127-143.
- Hamed J.T., Bhadra A. (1997), Influence of current density and pH on electrokinetics. *Journal of Hazardous Materials*, 55, 279-294.
- Haran B.S., Popov B.N., Zheng G., White R.E. (1997), Mathematical modeling of hexavalent chromium decontamination from low surface charged soils. *Journal of Hazardous Materials*, 55, 93-107.
- Harrad S. (2000), *Persistent organic pollutants – Environmental behavior and pathways for human exposure*. Kluwer Academic Publisher, Norwell, MA, USA.
- Harvey R.G. (1997), *Polycyclic Aromatic Hydrocarbons*. Wiley-VCH Publishers, New York, NY, USA.
- Henner P., Schiavon M., Morel J.L., Lichtfouse E. (1997), Polycyclic aromatic hydrocarbon (PAH) occurrence and remediation methods. *Analisis*, 25, M56-M59.
- Ho S.V., Athmer C.J., Sheridan P.W., Shapiro A.P. (1997), Scale-up aspects of the Lasagna<sup>TM</sup> process for in situ soil decontamination. *Journal of Hazardous Materials*, 55, 39-60.
- Höhener P., Hunkeler D., Hess A., Bregnard T., Zeyer J. (1998), Methodology for the evaluation of engineered in situ bioremediation: lessons from a case study. *Journal of Microbiological Methods*, 32, 1998, 179-192.
- Huang J.H., Ilgen G., Matzner E. (2003), Simultaneous extraction of organotin, organolead and organomercury species from soils and litter. *Analytica Chimica Acta*, 493, 23-34.
- Huling S.G., Pivetz B.E. (2006), *In-situ chemical oxidation*. U.S. Environmental Protection Agency, Office of Research and Development, National Risk Management Research Laboratory, Cincinnati, OH, USA. Report EPA 600/R-06/072.
- Hunkeler D., Jörger D., Häberli K., Höhener P., Zeyer J. (1998), Petroleum hydrocarbon mineralization in anaerobic laboratory aquifer columns. *Journal of Contaminant Hydrology*, 32, 1998, 41-61.
- IARC (1983), *Polynuclear aromatic compounds, part 1: chemical, environmental and*

- experimental data. International Agency for Research on Cancer, IARC Monographs on the Evaluation of Carcinogenic Risks to Humans, Volume 32. World Health Organization, Lyon, France.
- IARC (1984), Polynuclear aromatic compounds, part 2: carbon blacks, mineral oils (lubricant base oils and derived products) and some nitroarenes. International Agency for Research on Cancer, IARC Monographs on the Evaluation of Carcinogenic Risks to Humans, Volume 33. World Health Organization, Lyon, France.
- IARC (2006), Inorganic and organic lead compounds. International Agency For Research On Cancer, IARC Monographs on the Evaluation of Carcinogenic Risks to Humans, Volume 87. World Health Organization, Lyon, France.
- Iniesta J., Michaud P.A., Panizza M., Cerisola G., Aldaz A., Comninellis C. (2001), Electrochemical oxidation of phenol at boron-doped diamond electrode. *Electrochimica Acta*, 46, 3573-3578
- Ioannidis T.A., Zouboulis A.I. (2003), Detoxification of a highly toxic lead-loaded industrial solid waste by stabilization using apatites. *Journal of Hazardous Materials*, B97, 173-191.
- ITRC (2005), Technical and regulatory guidance for in situ chemical oxidation of contaminated soil and groundwater, 2nd Edition. Interstate Technology Regulatory Council, ISCO Team, Washington D.C., USA.
- Isosaari P., Piskonen R., Ojala P., Voipio S., Eilola K., Lehmus E., Itävaara M. (2007), Integration of electrokinetics and chemical oxidation for the remediation of creosote-contaminated clay. *Journal of Hazardous Materials*, 144, 538-548.
- Iturbe R., Flores C., Flores R.M., Torres L.G. (2005), Subsoil TPH and other petroleum fractions-contamination levels in an oil storage and distribution station in north-central Mexico. *Chemosphere*, 61, 1618-1631.
- Kakarla P.K., Andrews T., Greenberg R.S., Zervas D. (2002), Modified Fenton's processes for effective in-situ chemical oxidation – Laboratory and Field Evaluation. *Remediation Journal*, 12, 23-36.
- Kechavarzi C., Pettersson K., Leeds-Harrison P., Ritchie L., Ledin S. (2007), Root establishment of perennial ryegrass (*L. perenne*) in diesel contaminated subsurface soil layers. *Environmental Pollution*, 145, 68-74.
- Kim J., Choi H. (2002), Modeling in situ ozonation for the remediation of nonvolatile PAH-contaminated unsaturated soils. *Journal of Contaminant Hydrology*, 55, 261-285.
- Kim J.-H., Han S.-J. Kim S.-S., Yang J.-W. (2006), Effect of soil chemical properties on the remediation of phenanthrene-contaminated soil by electrokinetic-Fenton process. *Chemosphere*, 63, 1667-1676.
- Kim S.-S., Kim J.-H., Han S.-J. (2005a), Application of the electrokinetic-Fenton process for the remediation of kaolinite contaminated with phenanthrene. *Journal of Hazardous*

- Materials, B118, 121-131.
- Kim S.-J., Park J.-K., Lee Y.-J., Lee Y.-C., Yang J.-W. (2005b), Electrokinetic bioremediation of phenanthrene-contaminated soil by *Sphingomonas* sp. 3Y at different current densities. Proceedings of EREM 2005, 5th Symposium on Electrokinetic Remediation, 22-25 May 2005, Ferrara, Italy.
- Kim W.-S., Kim S.-O., Kim K.-W. (2005c), Enhanced electrokinetic extraction of heavy metals from soils assisted by ion exchange membranes. *Journal of Hazardous Materials*, B118, 93-102.
- Kong S., Watts R.J., Choi J. (1998), Treatment of Petroleum-Contaminated Soils Using Iron Mineral Catalyzed Hydrogen Peroxide. *Chemosphere*, 37, 1473-1482.
- Kronholm J., Kuosmanen T., Hartonen K., Riekkola M.L. (2003), Destruction of PAHs from soil by using pressurized hot water extraction coupled with supercritical water oxidation. *Waste Management*, 23, 2003, 253-260.
- Kulik N., Goia A., Trapidoa M., Tuhkanenb T. (2006), Degradation of polycyclic aromatic hydrocarbons by combined chemical pre-oxidation and bioremediation in creosote contaminated soil. *Journal of Environmental Management*, 78, 382-391.
- Kurniawan T.A., Lo W., Chan G.Y.S. (2006), Physico-chemical treatments for removal of recalcitrant contaminants from landfill leachate. *Journal of Hazardous Materials*, B129, 80-100.
- Lageman R., Godschalk B. (2005), Electro-bioreclamation of PCE and TCE contaminated soil at the site of a former silver factory. Proceedings of EREM 2005, 5th Symposium on Electrokinetic Remediation, 22-25 May 2005, Ferrara, Italy.
- Lageman R., Godschalk M.S. (2007), Electro-bioreclamation: a combination of in situ remediation techniques proves successful at a site in Zeist, the Netherlands. *Electrochimica Acta*, 52, 3449-3453.
- Laine D.F., Cheng I.F. (2007), The destruction of organic pollutants under mild reaction conditions: a review. *Microchemical Journal*, 85, 183-193.
- Landrigan P.J. (2002), The worldwide problem of lead in petrol. *Bulletin of the World Health Organization*, 80, 768.
- Lear G., Harbottle M.J., Sills G., Knowles C.J., Semple K.T., Thompson I.P. (2007), Impact of electrokinetic remediation on microbial communities within PCP contaminated soil. *Environmental Pollution*, 146, 139-146.
- Lee Y.-J., Choi J.-Y., Yang J.-W. (2007), Integrated electrokinetic process with bdd electrode for degradation of phenol from contaminated soil. Proceedings of EREM 2007, 6th Symposium on Electrokinetic Remediation, 12-15 June 2007, Vigo, Spain.
- Lee M., Kang H., Do W. (2005a), Application of nonionic surfactant-enhanced in situ flushing to a diesel contaminated site. *Water Research*, 39, 139-146.
- Lee Y.-J., Park J.-K., Kim S.-J., Kim S.-H., Yang J.-W. (2005b), Electrokinetic

- bioremediation of phenanthrene-contaminated soil by *Sphingomonas* sp. 3Y at different current densities. Proceedings of EREM 2005, 5th Symposium on Electrokinetic Remediation, 22-25 May 2005, Ferrara, Italy.
- Li Z., Yu J.-W., Neretnieks I. (1996), A new approach to electrokinetic remediation of soils polluted by heavy metals. *Journal of Contaminant Hydrology*, 22, 241-253.
- Liang C., Bruell C.J., Marley M.C., Sperry K.L. (2004a), Persulfate oxidation for in situ remediation of TCE - I. Activated by ferrous ion with and without a persulfate-thiosulfate redox couple. *Chemosphere*, 55, 1213-1223.
- Liang C., Bruell C.J., Marley M.C., Sperry K.L. (2004b), Persulfate oxidation for in situ remediation of TCE - II. Activated by chelated ferrous ion. *Chemosphere*, 55, 1225-1233.
- Lima A.T., Ribeiro A.B., Castro A., Ottosen L. (2005), A comparative study on the removal of heavy metals from MSWI fly ash by dialytic and electro-dialytic processes. Proceedings of EREM 2005, 5th Symposium on Electrokinetic Remediation, 22-25 May 2005, Ferrara, Italy.
- Liu H., Li X.Z., Leng Y.J., Wang C. (2007), Kinetic modeling of electro-Fenton reaction in aqueous solution. *Water Research*, 41, 1161-1167.
- Lo I.M.C. (1996), Characteristics and treatment of leachates from domestic landfills. *Environmental International*, 22, 433-442.
- Lohner S.T., Tiehm A. (2005), Influence of electric fields on VC dechlorinating microorganisms. Proceedings of EREM 2005, 5th Symposium on Electrokinetic Remediation, 22-25 May 2005, Ferrara, Italy.
- Lovei M. (1998), Phasing out lead from gasoline, worldwide experience and policy implications. The World Bank, World Bank Technical Paper no. 397, Pollution Management Series.
- Lundstedt S., Persson Y., Oberg L. (2006), Transformation of PAHs during ethanol-Fenton treatment of an aged gasworks' soil. *Chemosphere*, 65, 1288-1294.
- Luo Q., Wang H., Zhang X., Fan X., Qian Y. (2006), In situ bioelectrokinetic remediation of phenol-contaminated soil by use of an electrode matrix and a rotational operation mode. *Chemosphere*, 64, 415-422.
- Luthy R.G., Dzombak D.A., Peters C.A., Roy S.B., Ramaswami A., Nakles D.V., Nott B.R. (1994), Remediating tar-contaminated soils at manufactured gas plant sites. *Environmental Science Technology*, 28, 266A-276A.
- Lynch R.J., Muntoni A., Ruggeri R., Winfield K.C. (2007), Preliminary tests of an electrokinetic barrier to prevent heavy metal pollution of soils. *Electrochimica Acta*, 52, 3432-3440.
- Masten S.J., Davies S.H.R. (1997), Efficacy of in-situ ozonation for the remediation of PAH contaminated soils. *Journal of Contaminant Hydrology*, 28, 327-335.

- Maturi K., Reddy K.R. (2006), Simultaneous removal of organic compounds and heavy metals from soils by electrokinetic remediation with a modified cyclodextrin. *Chemosphere*, 63, 1022-1031.
- McCarthy K., Walker L., Vigoren L., Bartel J. (2004), Remediation of spilled petroleum hydrocarbons by in situ landfarming at an arctic site. *Cold Regions Science and Technology* 40, 31-39.
- MECA (2003), The case for banning lead in gasoline. Manufacturers of Emission Controls Association. Washington, DC, USA.
- Meinero S., Zerbinati O. (2006), Oxidative and energetic efficiency of different electrochemical oxidation processes for chloroanilines abatement in aqueous medium. *Chemosphere*, 64, 386-392.
- Milcic-Terzic J., Lopez-Vidal Y., Vrvic M.M., Saval S. (2001), Detection of catabolic genes in indigenous microbial consortia isolated from a diesel-contaminated soil. *Bioresource Technology*, 78, 47-54.
- Mishchuk N., Kornilovich B., Klishchenko R. (2007), pH regulation as a method of intensification of soil electroremediation. *Colloids and Surfaces A: Physicochemical and Engineering Aspects*, 306, 171-179.
- Mitchell J.K. (1991), Conduction phenomena: from theory to geotechnical practice. *Geotechnique*, 41, 299-340.
- Mitchell J.K. (1993), Fundamentals of soil behavior. John Wiley and Sons Inc., New York, NY, USA.
- Mohamed A.M.O. (1996), Remediation of heavy metal contaminated soils via integrated electrochemical processes. *Waste Management*, 16, 741-747.
- Molina-Barahona L., Rodríguez-Vázquez R., Hernández-Velasco M., Vega-Jarquín C., Zapata-Pérez O., Mendoza-Cantú A., Albores A. (2004), Diesel removal from contaminated soils by biostimulation and supplementation with crop residues. *Applied Soil Ecology* 27, 165-175.
- Molson J.W., Frind E.O., Van Stempvoort D.R., Lesage S. (2002), Humic acid enhanced remediation of an emplaced diesel source in groundwater. 2. Numerical model development and application. *Journal of Contaminant Hydrology*, 54, 277-305.
- Moraes P.B., Bertazzoli R. (2005), Electrodegradation of landfill leachate in a flow electrochemical reactor. *Chemosphere*, 58, 41-46.
- Morris J.W.F., Pendleton C.H., Rozema L.R., Howell J., Kocenko L.B., Germain A.M. (2007), Closed-loop leachate management using engineered wetlands and a phyto-cap. *Proceedings of Sardinia 2007, 11th International Waste Management and Landfill Symposium*, 1-5 October 2007, S. Margherita di Pula (CA), Italy.
- Muller P. (2002), Potential for occupational and environmental exposure to ten carcinogens in Toronto. *Tox Probe Inc.*, March 2002.



- Nam, K., Rodriguez, W., Kukor, J.J. (2001), Enhanced degradation of polycyclic aromatic hydrocarbons by biodegradation combined with a modified Fenton reaction. *Chemosphere*, 45, 11-20.
- Namkoong W., Hwang E.Y., Park J.S., Choi J.Y. (2002), Bioremediation of diesel-contaminated soil with composting. *Environmental Pollution*, 119, 2002, 23-31.
- Narasimhan B., Sri Ranjan R. (2000), Electrokinetic barrier to prevent subsurface contaminant migration: theoretical model development and validation. *Journal of Contaminant Hydrology*, 42, 1-17.
- Needleman H.L. (1997), Clamped in a Straitjacket: The Insertion of Lead into Gasoline. *Environmental Research*, 74, 95-103.
- Nor N.M., Ramli A. (2007), Electrical properties of dry soil under high impulse currents. *Journal of Electrostatics*, 65, 500-505.
- Okuda T., Alcántara-Gardun M.E., Suzuki M., Matsui C., Kose T., Nishijima W., Okada M. (2007), Enhancement of biodegradation of oil adsorbed on fine soils in a bioslurry reactor. *Chemosphere*, 68, 281-286.
- O'Mahony M.M., Dobson A.D.W., Barnes J.D., Singleton I. (2006), The use of ozone in the remediation of polycyclic aromatic hydrocarbon contaminated soil. *Chemosphere*, 63, 307-314.
- Oman C., Rosqvist H. (1999), Transport fate of organic compounds with water through landfills. *Water Research*, 33, 2247-2254.
- Oonnittan A., Shrestha, R., Sillanpää, M. (2007), Remediation of hexachlorobenzene in soil by enhanced electrokinetic fenton process. *Proceedings of EREM 2007, 6th Symposium on Electrokinetic Remediation, 12-15 June 2007, Vigo, Spain.*
- Ou L.T., Jing W., Thomas J.E. (1995), Biological and chemical degradation of ionic ethyllead compounds in soil. *Environmental Toxicology and Chemistry*, 1995, Vol.14, No.4, 545-551.
- Ouyang Y., Mansell R.S., Rhue R.D. (1996), A microemulsification approach for removing organolead and gasoline from contaminated soil. *Journal of Hazardous Materials*, 46, 23-35.
- Panizza M., Cerisola G. (2001), Removal of organic pollutants from industrial wastewater by electrogenerated Fenton's reagent, *Water Research*, 35, 3987-3992.
- Panizza M., Cerisola G. (2007), Electrocatalytic materials for the electrochemical oxidation of synthetic dyes. *Applied Catalysis B: Environmental*, 75, 95-101.
- Park J.-Y., Lee H.-H., Kim S.-J., Lee Y.-J., Yang J.-W. (2007), Surfactant-enhanced electrokinetic removal of phenanthrene from kaolinite. *Journal of Hazardous Materials*, 140, 230-236.
- Park J.-Y., Kim S.-J., Lee Y.-J., Baek K., Yang J.-W. (2005), EK-Fenton process for removal of phenanthrene in a two-dimensional soil system. *Engineering Geology*, 77,

217-224.

- Pazos M., Sanromán M.A., Cameselle C. (2006), Improvement in electrokinetic remediation of heavy metal spiked kaolin with the polarity exchange technique. *Chemosphere*, 62, 817-822.
- Pazos M., Ricart M.T., Sanromán M.A., Cameselle C. (2007), Enhanced electrokinetic remediation of polluted kaolinite with an azo dye. *Electrochimica Acta*, 52, 3393-3398.
- Perraudin E., Budzinski H., Villenave E. (2007), Identification and quantification of ozonation products of anthracene and phenanthrene adsorbed on silica particles. *Atmospheric Environment*, 41, 6005-6017.
- Persson K.M., M. Van Praagh, Olsberg E. (2007), Removal of heavy metals from landfill leachate by an artificial wetland during a Nordic autumn. *Proceedings of Sardinia 2007, 11th International Waste Management and Landfill Symposium*, 1-5 October 2007, S. Margherita di Pula (CA), Italy.
- Polettini A., Pomi R., Rolle E., Ceremigna D., De Propris L., Gabellini M., Tornato A. (2006), A kinetic study of chelant-assisted remediation of contaminated dredged sediment. *Journal of Hazardous Materials*, B137, 1458-1465.
- Poppendieck D.G., Loehr R.C., Webster M.T. (1999), Predicting hydrocarbon removal from thermally enhanced soil vapor extraction systems 1. Laboratory studies. *Journal of Hazardous Materials*, B69, 81-93
- Powell S.M., Harvey P.M., Stark J.S., Snape I., Riddle M.J. (2007), Biodegradation of petroleum products in experimental plots in Antarctic marine sediments is location dependent. *Marine Pollution Bulletin*, 54, 2007, 434-440.
- Probstein R.F., Hicks R.E. (1993), Removal of contaminants from soils by electric fields. *Science*, 260:498-503.
- Puppala S.K., Alshawabkeh A.N., Acar Y.B., Gale R.J., Bricka M. (1997), Enhanced electrokinetic remediation of high sorption capacity soil. *Journal of Hazardous Materials*, 55, 203-220.
- Quan H.N., Teel A.L., Watts, R.J. (2003), Effect of contaminant hydrophobicity on hydrogen peroxide dosage requirements in the Fenton-like treatment of soils. *Journal of Hazardous Materials*, 102, 277-289.
- Rahner D., Ludwig G., Röhrs J. (2002), Electrochemically induced reactions in soils - a new approach to the in-situ remediation of contaminated soils? Part 1: The microconductor principle. *Electrochimica Acta*, 47, 1395-1403.
- Rayner J.L., Snape I., Walworth J.L., Harvey P.M., Ferguson S.H. (2007), Petroleum-hydrocarbon contamination and remediation by microbioventing at sub-Antarctic Macquarie Island. *Cold Regions Science and Technology*, 48, 139-153.
- Reddy K.R., Ala P.R., Sharma S., Kumar S.N. (2006), Enhanced electrokinetic remediation of contaminated manufactured gas plant soil. *Engineering Geology*, 85, 132-146.

- Reddy K.R., Chaparro C. (2001), Electrokinetic remediation of mercury-contaminated soils. Proceedings of the 2001 International Containment & Remediation Technology Conference and Exhibition, 10-13 June 2001, Orland, FL, USA.
- Reddy K.R., Chinthamreddy S. (2004), Enhanced electrokinetic remediation of heavy metals in glacial till soils using different electrolyte solutions. *Journal of Environmental Engineering*, 130, 442-455.
- Reddy K.R., Khodadoust A.P., Karri M.R. (2007), Electrokinetic delivery of nanoscale iron particles for remediation of pentachlorophenol in clayey soil. Proceedings of EREM 2007, 6th Symposium on Electrokinetic Remediation, 12-15 June 2007, Vigo, Spain.
- Ribeiro A.B., Rodríguez-Maroto J.M., Mateus E.P., Gomes H. (2005), Removal of organic contaminants from soils by an electrokinetic process: the case of atrazine. *Experimental and modeling. Chemosphere*, 59, 1229-1239.
- Richnow H.H., Seifert R., Kastner M., Mahro B., Horsfield B., Tiedgen U., Bohm S., Michaelis W. (1995), Rapid screening of PAH-residues in bioremediated soils. *Chemosphere*, 31, 3991-3999.
- Rivas F.J. (2006), Polycyclic aromatic hydrocarbons sorbed on soils: A short review of chemical oxidation based treatments. *Journal of Hazardous Materials*, 138, 234-251.
- Rivera-Espinoza Y., Dendooven L. (2004), Dynamics of carbon, nitrogen and hydrocarbons in diesel-contaminated soil amended with biosolids and maize. *Chemosphere*, 54, 379-386.
- Röhrs J., Ludwig G., Rahner D. (2002), Electrochemically induced reactions in soils - a new approach to the in-situ remediation of contaminated soils? Part 2: remediation experiments with a natural soil containing highly chlorinated hydrocarbons. *Electrochimica Acta*, 47, 1405-1414
- Samouëlian A., Cousin I., Tabbagh A., Bruand A., Richard G. (2005), Electrical resistivity survey in soil science: a review. *Soil & Tillage Research*, 83, 173-193.
- Saner M., Bollier D., Schneider K., Bachofen R. (1996), Mass transfer improvement of contaminants and nutrients in soil in a new type of closed soil bioreactor. *Journal of Biotechnology*, 48, 1996, 25-35.
- Sanromán M.A., Pazos M., Ricart M.T., Cameselle C. (2005), Decolourisation of textile indigo dye by DC electric current. *Engineering Geology*, 77, 253-261.
- Santamaria A.E., Vagliasindi F.G.A. (2007), Treatment of MSW landfill leachate laboratory and pilot plant studies. Proceedings of Sardinia 2007, 11th International Waste Management and Landfill Symposium, 1-5 October 2007, S. Margherita di Pula (CA), Italy.
- Sarkar D., Ferguson M., Datta R., Birnbaum S. (2005), Bioremediation of petroleum hydrocarbons in contaminated soils: Comparison of biosolids addition, carbon supplementation, and monitored natural attenuation. *Environmental Pollution*, 136, 187-

195.

- Searle D.E., Mitchell D.J. (2006), The effect of coal and diesel particulates on the weathering loss of Portland Limestone in an urban environment. *Science of the Total Environment*, 370, 207-223.
- Segall B.A., O'Bannon C.E., Mattias J.A. (1980), Electro-osmosis chemistry and water quality. *Journal of Geotechnical Engineering, ASCE*, 106, 1148-1152.
- Seyferth D. (2003a), The Rise and Fall of Tetraethyllead. 1. Discovery and Slow Development in European Universities, 1853-1920. Cover Essay. *Organometallics*, 22, 2346-2357.
- Seyferth D. (2003b), The Rise and Fall of Tetraethyllead. 2. *Organometallics*, 22, 5154-5178.
- Silva A., Delerue-Matos C., Fiúza A. (2005), Use of solvent extraction to remediate soils contaminated with hydrocarbons. *Journal of Hazardous Materials*, B124, 224-229.
- Smargiassi A., Takser L., Masse A., Sergerie M., Mergler D., St-Amour G., Blot P., Hellier G., Huel G. (2002), A comparative study of manganese and lead levels in human umbilical cords and maternal blood from two urban centers exposed to different gasoline additives. *The Science of the Total Environment*, 290, 157-164.
- Sopchak D., Miller B., Avyigal Y., Kalish R. (2002), Rotating ring-disk electrode studies of the oxidation of p-methoxyphenol and hydroquinone at boron-doped diamond electrodes. *Journal of Electroanalytical Chemistry*, 538/539, 39-45.
- Suèr P., Gitye K., Allard B. (2003), Speciation and transport of heavy metals and macroelements during electroremediation, *Environmental Science Technology*, 37, 177-181.
- Sun H.-W., Qi-She Yan Q.-S., Influence of pyrene combination state in soils on its treatment efficiency by Fenton oxidation. *Journal of Environmental Management*, article in press, doi:10.1016/j.jenvman.2007.03.031.
- Sun H.-W., Yan Q.-S. (2007), Influence of Fenton oxidation on soil organic matter and its sorption and desorption of pyrene. *Journal of Hazardous Materials*, 144, 164-170.
- Suni S., Romantschuk M. (2005), Bioaugmentation combined with electrokinetics in remediating oil-contaminated soil. *Proceedings of EREM 2005, 5th Symposium on Electrokinetic Remediation, 22-25 May 2005, Ferrara, Italy*.
- Suthersan S.S. (2001), *Natural and enhanced remediation systems*. Lewis Publisher, CRC Press, Boca Raton, FL, USA.
- Szpyrkowicz L., Radaelli M., Bertini S., Daniele S., Casarin F. (2007), Simultaneous removal of metals and organic compounds from a heavily polluted soil. *Electrochimica Acta*, 52, 3386-3392.
- Szpyrkowicz L., Radaelli M., Daniele S., Casarin F. (2005), Simultaneous removal of metals and organic compounds from a heavily polluted soil. *Proceedings of EREM*

- 2005, 5th Symposium on Electrokinetic Remediation, 22-25 May 2005, Ferrara, Italy.
- Taylor L.T., Jones D.M. (2001), Bioremediation of coal tar PAH in soils using biodiesel. *Chemosphere*, 44, 1131-1136.
- Teeling H., Cypionka H. (1997), Microbial degradation of tetraethyl lead in soil monitored by microcalorimetry, *Applied Microbiology and Biotechnology*, 48, 275-279.
- Tiehm A., Lohner S.T., Diederichs, Weidlich C., Mangold K.-M., Jüttner K.-M. (2005), Feasibility study on chloroethene degradation by a coupled bio-electro process. *Proceedings of EREM 2005, 5th Symposium on Electrokinetic Remediation, 22-25 May 2005, Ferrara, Italy.*
- Tizaoui C., Bouselmi L., Mansouri L., Ghrabi A. (2007), Landfill leachate treatment with ozone and ozone/hydrogen peroxide systems. *Journal of Hazardous Materials*, 140, 316-324.
- Train G., Morselli L., Persano Adorso G. (2005) Electrokinetic remediation of bottom ash from MSWI. *Proceedings of EREM 2005, 5th Symposium on Electrokinetic Remediation, 22-25 May 2005, Ferrara, Italy.*
- Turer D., Genc A. (2005), Assessing effect of electrode configuration on the efficiency of electrokinetic remediation by sequential extraction analysis. *Journal of Hazardous Materials*, B119, 167-174.
- Unob F., Hagège A., Lakkis A., Leroy M. (2003), Degradation of organolead species in aqueous solutions by electron beam irradiation. *Water Research*, 37, 2003, 2113-2117.
- U.S. AEC (2000), In-situ electrokinetic remediation of metal contaminated soils – Technology Status Report. U.S. Army Environmental Center, Report Number: SFIM-AEC-ET-CR-99022.
- U.S. EPA (1991), Guide for conducting treatability studies under CERCLA: soil washing, interim guidance. U.S. Environmental Protection Agency, Office of Solid Waste and Emergency Response, Washington, DC, USA. Report EPA 540-2-91-020A.
- U.S. EPA (1998), Field applications of in situ remediation technologies: chemical oxidation. U.S. Environmental Protection Agency, Office of Solid Waste and Emergency Response, Technology Innovation Office, Washington, DC, USA. Report EPA 542-R-98-008.
- U.S. EPA (1999), Understanding oil spills and oil spill response. U.S. Environmental Protection Agency, Office of Emergency and Remedial Response, Washington, DC, USA. Report EPA 540-K-99-007.
- U.S. EPA (2000), In situ flushing with surfactants and cosolvents. U.S. Environmental Protection Agency, Office of Solid Waste and Emergency Response, Washington, DC, USA.
- U.S. EPA (2001a), A citizen's guide to soil vapor extraction and air sparging. U.S. Environmental Protection Agency, Office of Solid Waste and Emergency Response,

- Washington, DC, USA. Report EPA 542-F-01-006.
- U.S. EPA (2001b), A citizen's guide to air sparging. U.S. Environmental Protection Agency, Office of Solid Waste and Emergency Response, Washington, DC, USA. Report EPA 542-F-01-016.
- U.S. EPA (2001c), A citizen's guide to soil washing. U.S. Environmental Protection Agency, Office of Solid Waste and Emergency Response, Washington, DC, USA. Report EPA 542-F-01-008.
- U.S. EPA (2001d), A citizen's guide to in situ flushing. U.S. Environmental Protection Agency, Office of Solid Waste and Emergency Response, Washington, DC, USA. Report EPA 542-F-01-011.
- U.S. EPA (2002a), Electrochemical remediation technologies remove mercury in soil. Technology News and Trends, U.S. Environmental Protection Agency, National Service for Environmental Publications, Cincinnati, OH, USA. Report EPA 542-N-02-004.
- U.S. EPA (2002b) A citizen's guide to monitored natural attenuation. U.S. Environmental Protection Agency, Office of Solid Waste and Emergency Response, Washington, D.C., USA. Report EPA 542-F-01-004.
- U.S. EPA (2004), Electrochemical remediation technologies (ECRTs) - Demonstration Bulletin. U.S. Environmental Protection Agency, National Risk Management Research Laboratory, Cincinnati, OH, USA. Report EPA 540/MR-04/507.
- U.S. EPA (2006), Off-gas treatment technologies for soil vapor extraction systems: state of the practice. U.S. Environmental Protection Agency, Office of Superfund Remediation and Technology Innovation, Office Solid Waste and Emergency Response, Washington, D.C., USA. Report EPA 542-R-05-028
- Van Cauwenberghe L. (1997) Electrokinetics. Technology Overview Report, GWRTAC (Ground-Water Remediation Technologies Analysis Center), Pittsburgh, PA, USA. Report TO 97-03.
- Ventura A., Jacquet G., Bermond A., Camel V. (2002), Electrochemical generation of the Fenton's reagent: application to atrazine degradation. *Water Research*, 36, 3517-3522.
- Virkutyte J., Sillanpää M., Latostenmaa P. (2002), Electrokinetic soil remediation - critical overview. *The Science of the Total Environment*, 289, 97-121.
- Wadge A. (1999), Lead. *Air Pollution and Health*, 1999, 797-812.
- Wang B., Kong W., Ma H. (1007), Electrochemical treatment of paper mill wastewater using three-dimensional electrodes with Ti/Co/SnO<sub>2</sub>-Sb<sub>2</sub>O<sub>5</sub> anode. *Journal of Hazardous Materials*, 146, 295-301.
- Watts R.J., Asce M., Teel A.L. (2005), Chemistry of modified Fenton's reagent (catalyzed H<sub>2</sub>O<sub>2</sub> propagations - CHP) for in situ soil and groundwater remediation. *Journal of Environmental Engineering*, 131, 612-622.
- Watts R.J., Bottenberg B., Hess T.F., Jensen M.D., Teel A.L. (1999), Role of reductants in

- the enhanced desorption and transformation of chloroaliphatic compounds by modified Fenton's reaction. *Environmental Science Technology*, 33, 3432-3437.
- Watts R.J., Dilly S.E. (1996), Evaluation of iron catalysts for the Fenton-like remediation of diesel-contaminated soils. *Journal of Hazardous Materials*, 51, 209-224.
- Watts R.J., Stanton, P.C., Howsawheng, J., Teel, A.L. (2002), Mineralization of a sorbed polycyclic aromatic hydrocarbon in two soils using catalyzed hydrogen peroxide. *Water Research*, 36, 4283-4292.
- Wick L.Y., Mattle P., Shi L., Wattiau P., Harms H. (2005), Electrokinetic transport of PAH-degrading bacteria in model aquifers and soil. *Proceedings of EREM 2005, 5th Symposium on Electrokinetic Remediation, 22-25 May 2005, Ferrara, Italy*.
- Wild S.R., Jones K.C. (1995), Polynuclear aromatic hydrocarbons in the united kingdom environment: a preliminary source inventory and budget. *Environmental Pollution*, 88, 91-108.
- Wiszniewski J., Robert D., Surmacz-Gorska J., Miksch K., Weber J.V. (2006), Landfill leachate treatment methods: a review. *Environmental Chemistry Letters*, 4, 51-61.
- Wong J.S.H., Hicks R.E., Probst R.F. (1997), EDTA-enhanced electroremediation of metal-contaminated soils. *Journal of Hazardous Materials*, 55, 61-79.
- Yang G.C.C., Lin S.-L. (1998), Removal of lead in a silt loam soil by electrokinetic remediation. *Journal of Hazardous Materials*, 58, 285-299.
- Yang G.C.C., Liu C.-Y. (2001), Remediation of TCE contaminated soils by in situ EK-Fenton process. *Journal of Hazardous Materials*, B85, 317-331.
- Yang G.C.C., Long Y.-W. (1999), Removal and degradation of phenol in a saturated flow by in-situ electrokinetic remediation and Fenton-like process. *Journal of Hazardous Materials*, 69, 259-271.
- Yu D.Y., Kang N., Bae W., Banks M.K. (2007), Characteristics in oxidative degradation by ozone for saturated hydrocarbons in soil contaminated with diesel fuel. *Chemosphere*, 66, 799-807.
- Yu J.-W., Neretnieks I. (1996), Modelling of transport and reaction processes in a porous medium in an electrical field. *Chemical Engineering Science*, 51, 4355-4368.
- Yu J.-W., Neretnieks I. (1997), Theoretical evaluation of a technique for electrokinetic decontamination of soils. *Journal of Contaminant Hydrology*, 26, 291-299.
- Zhang H., Zhang D., Zhou J. (2006), Removal of COD from landfill leachate by electro-Fenton method. *Journal of Hazardous Materials*, B135, 106-111.
- Zheng X.-J., Blais J.-F., Mercier G., Bergeron M., Drogui P. (2007), PAH removal from spiked municipal wastewater sewage sludge using biological, chemical and electrochemical treatments. *Chemosphere*, 68, 1143-1152.
- Zhou D.-M., Deng C.-F., Alshwabkeh A.N., Cang L. (2005), Effects of catholyte conditioning on electrokinetic extraction of copper from mine tailings. *Environmental*

International, 31, 885-890.

Zorn R., Czurda K., Steger H., Borst M. (2005a), Electroremediation models: application possibilities and remediation forecasts. Proceedings of EREM 2005, 5th Symposium on Electrokinetic Remediation, 22-25 May 2005, Ferrara, Italy.

Zorn R., Steger H., Ludwig S., Gregolec G., Borst M., Czurda K. (2005b), Electroosmotic dewatering of high water containing river sludges. Proceedings of EREM 2005, 5th Symposium on Electrokinetic Remediation, 22-25 May 2005, Ferrara, Italy.



# Publications

Some parts of this thesis can be found in:

- Ferrarese E., Andreottola G., Oprea I.A. (2008), Remediation of PAH-contaminated sediments by chemical oxidation. *Journal of Hazardous Materials*, Vol. 152, pp. 128-139, doi:10.1016/j.jhazmat.2007.06.080.
- Andreottola G., Dallago L., Ferrarese E. (2008), Feasibility study for the remediation of groundwater contaminated by organolead compounds. *Journal of Hazardous Materials*, article in press, doi: 10.1016/j.jhazmat.2007.12.044.
- Andreottola G., Ferrarese E. (2007), Tecniche di ossidazione chimica ed elettrochimica in situ di terreni contaminati da idrocarburi. In: Carucci A., Muntoni A., Cappai G., De Gioannis G., “La bonifica dei suoli e delle acque sotterranee contaminati: situazione attuale e prospettive”. Edizioni Lithos Grafiche Collana Didattica e Ricerca. ISBN 978-88-95398-00-6, pp. 47-68.
- Saroj D.P., Guglielmi G., Chiarani D., Ferrarese E., Andreottola G. (2007), Electro-assisted treatment of sludge from membrane bioreactor treating municipal wastewater. Poster presentation at 2nd IWA National Young Water Professionals Conference Membrane Technologies for Wastewater Treatment and Reuse, 4-5 June 2007, Berlin, Germany. Abstract book p. 251.
- Andreottola G., Ferrarese E., Saroj D.P., Oprea I.A. (2007), Feasibility study of electro-oxidation of landfill clay barrier contaminated by leachate. *Proceedings of Sardinia 2007, 11th International Waste Management and Landfill Symposium*, 1-5 October 2007, S. Margherita di Pula (CA), Italy. CISA, Centro di Ingegneria Sanitaria Ambientale, Italy. Abstract book pp. 177-178, full paper on cd.
- Ferrarese E., Andreottola G. (2007), Application of electrochemical techniques for the remediation of soils contaminated with organic pollutants. *Proceedings of Umasssoils, 23rd Annual International Conference on Soils, Sediments and Water*, 15-18 October 2007, University of Massachusetts, Amherst (MA), USA. Abstract book p. 138, full paper available on-line at <http://www.umasssoils.com/proceeding.htm>.

- Oprea I.A., Ferrarese E., Badea A., Ziglio G., Andreottola G., Ragazzi M., Apostol T. (2007), Comparison between chemical and electrochemical techniques for the remediation of PAH contaminated sediments. Proceedings of CIEM 2007, 3rd International Conference on Energy and Environment, 22-23 November 2007, Bucharest, Romania. University Polytechnica of Bucharest Scientific Bulletin, Vol. C 69, pp. 549-556.
- Ferrarese E. (2007), Sperimentazione di tecnologie di bonifica innovative per il Sito di Interesse nazionale di Trento Nord. Proceedings of Sustainable Approaches for Mega-Site Management and Remediation: New Perspectives, 30 November 2007, Venice, Italy. Presentation available on-line at [http://www.apat.gov.it/site/it-IT/Rubriche/Eventi/2007/Novembre/documenti\\_megasiti.html](http://www.apat.gov.it/site/it-IT/Rubriche/Eventi/2007/Novembre/documenti_megasiti.html).
- Oprea I.A., Ferrarese E., Andreottola G., Badea A., Ziglio G., Apostol T. (2008), The remediation of contaminated sites using electrochemical methods. Poster presentation at MGP 2008, Redevelopment, Site Management and Contaminant Issues of former MGP's and other Tar Oil Polluted Sites, 4-6 March 2008, Dresden, Germany.
- Andreottola G., Ferrarese E. (2008), Remediation of polycyclic aromatic hydrocarbons and organolead compounds by electrochemical oxidation. Proceedings of ConSoil 2008, 10th International Conference on Soil-Water System, 3-6 June 2008, Milan, Italy.
- Andreottola G., Ferrarese E., Lorenzoni E., Oprea I.A. (2008), Remediation of hydrocarbon contaminated soils by electrochemical methods. Proceedings of SIDISA 2008, Simposio Internazionale di Ingegneria Sanitaria e Ambientale, 24-27 June 2008, Florence, Italy.
- Oprea I.A., Badea A., Andreottola G., Ziglio G., Ragazzi M., Ferrarese E., Apostol T. (2008), Assessment of electrochemical technology as a remediation treatment for diesel fuel contaminated soils. Proceedings of SIDISA 2008, Simposio Internazionale di Ingegneria Sanitaria e Ambientale, 24-27 June 2008, Florence, Italy.
- Andreottola G., Bonomo L., De Gioannis G., Ferrarese E., Lavagnolo M.C., Muntoni A., Polettini A., Pomi R., Saponaro S. (2008), Marine, lagoon, and river sediment remediation. Proceedings of I2SM, International Symposium on Sediment Management, 9-11 July 2008, Lille, France.
- Andreottola G., Ferrarese E., Application of advanced oxidation processes and electrooxidation for the remediation of river sediments contaminated by PAHs. Submitted for publication to Journal of Environmental Science and Health, Part A.